

Fiscal Year 2015: Third Quarter

Progress Report
**Advanced Battery Materials
Research (BMR) Program**

Released October 2015
for the period of April – June 2015

Approved by

Tien Q. Duong, Advanced Battery Materials Research Program Manager
Vehicle Technologies Office, Energy Efficiency and Renewable Energy

TABLE OF CONTENTS

A Message from the Advanced Battery Materials Research Program Manager.....	1
Task 1 – Advanced Electrode Architectures	3
Task 1.1 – Physical, Chemical, and Electrochemical Failure Analysis of Electrodes and Cells (Vincent Battaglia, Lawrence Berkeley National Laboratory)	4
Task 1.2 – Electrode Architecture-Assembly of Battery Materials and Electrodes (Karim Zaghib, HydroQuebec).....	6
Task 1.3 – Design and Scalable Assembly of High-Density, Low-Tortuosity Electrodes (Yet-Ming Chiang, Massachusetts Institute of Technology)	8
Task 1.4 – Hierarchical Assembly of Inorganic/Organic Hybrid Si Negative Electrodes (Gao Liu, Lawrence Berkeley National Laboratory)	10
Task 1.5 – Studies in Advanced Electrode Fabrication (Vincent Battaglia, Lawrence Berkeley National Laboratory).....	13
Task 2 – Silicon Anode Research.....	15
Task 2.1 – Development of Silicon-Based High Capacity Anodes (Ji-Guang Zhang and Jun Liu, PNNL; Prashant Kumta, University of Pittsburgh; Jim Zheng, PSU)	16
Task 2.2 – Pre-Lithiation of Silicon Anode for High Energy Li Ion Batteries (Yi Cui, Stanford University)	19
Task 3 – High Energy Density Cathodes for Advanced Lithium-ion Batteries	22
Task 3.1 – Studies of High Capacity Cathodes for Advanced Lithium-ion Systems (Jagjit Nanda, Oak Ridge National Laboratory)	23
Task 3.2 – High Energy Density Lithium Battery (Stanley Whittingham, SUNY Binghamton).....	26
Task 3.3 – Development of High-Energy Cathode Materials (Ji-Guang Zhang and Jie Xiao, Pacific Northwest National Laboratory)	29
Task 3.4 – <i>In situ</i> Solvothermal Synthesis of Novel High Capacity Cathodes (Patrick Looney and Feng Wang, Brookhaven National Laboratory)	31
Task 3.5 – Novel Cathode Materials and Processing Methods (Michael M. Thackeray and Jason R. Croy, Argonne National Laboratory)	34
Task 3.6 – High-capacity, High-voltage Cathode Materials for Lithium-ion Batteries (Arumugam Manthiram, University of Texas, Austin)	37
Task 3.7 – Lithium-bearing Mixed Polyanion (LBMP) Glasses as Cathode Materials (Jim Kiggans and Andrew Kercher, Oak Ridge National Laboratory)	40
Task 3.8 – Design of High Performance, High Energy Cathode Materials (Marca Doeff, Lawrence Berkeley National Laboratory).....	42
Task 3.9 – Lithium Batteries with Higher Capacity and Voltage (John B. Goodenough, UT-Austin).....	45
Task 3.10 – Exploiting Co and Ni Spinel in Structurally Integrated Composite Electrodes (Michael M. Thackeray and Jason R. Croy, Argonne National Laboratory).....	47

Task 4 – Electrolytes for High-Voltage, High-Energy Lithium-ion Batteries.....	50
Task 4.1 – Fluorinated Electrolyte for 5-V Li-ion Chemistry (Zhengcheng Zhang, Argonne National Laboratory).....	51
Task 4.2 – Daikin Advanced Lithium Ion Battery Technology – High Voltage Electric (Ron Hendershot, Joe Sunstrom, and Michael Gilmore, Daikin America).....	53
Task 4.3 – Novel Non-Carbonate Based Electrolytes for Silicon Anodes (Dee Strand, Wildcat Discovery Technologies)	55
Task 5 – Diagnostics.....	57
Task 5.1 – Design and Synthesis of Advanced High-Energy Cathode Materials (Guoying Chen, Lawrence Berkeley National Laboratory)	58
Task 5.2 – Interfacial Processes – Diagnostics (Robert Kostecki, Lawrence Berkeley National Laboratory).....	61
Task 5.3 – Advanced <i>in situ</i> Diagnostic Techniques for Battery Materials (Xiao-Qing Yang and Xiqian Yu, Brookhaven National Laboratory)	64
Task 5.4 – NMR and Pulse Field Gradient Studies of SEI and Electrode Structure (Clare Grey, Cambridge University)	67
Task 5.5 – Optimization of Ion Transport in High-Energy Composite Cathodes (Shirley Meng, UC San Diego)	69
Task 5.6 – Analysis of Film Formation Chemistry on Silicon Anodes by Advanced <i>In situ</i> and <i>Operando</i> Vibrational Spectroscopy (Gabor Somorjai, UC Berkeley, and Phil Ross, Lawrence Berkeley National Laboratory)	72
Task 5.7 – Microscopy Investigation on the Fading Mechanism of Electrode Materials (Chongmin Wang, Pacific Northwest National Laboratory).....	74
Task 5.8 – Energy Storage Materials Research using DOE’s User Facilities and Beyond (Michael M. Thackeray and Jason R. Croy, Argonne National Laboratory).....	77
Task 6 – Modeling Advanced Electrode Materials	80
Task 6.1 – Electrode Materials Design and Failure Prediction (Venkat Srinivasan, Lawrence Berkeley National Laboratory)	81
Task 6.2 – Predicting and Understanding Novel Electrode Materials from First-Principles (Kristin Persson, Lawrence Berkeley National Laboratory)	83
Task 6.3 – First Principles Calculations of Existing and Novel Electrode Materials (Gerbrand Ceder, MIT).....	85
Task 6.4 – First Principles Modeling of SEI Formation on Bare and Surface/Additive Modified Silicon Anode (Perla Balbuena, Texas A&M University)	87
Task 6.5 – A Combined Experimental and Modeling Approach for the Design of High Current Efficiency Si Electrodes (Xingcheng Xiao, General Motors, and Yue Qi, Michigan State University)	90
Task 6.6 – Predicting Microstructure and Performance for Optimal Cell Fabrication (Dean Wheeler and Brian Mazzeo, Brigham Young University)	93

Task 7 – Metallic Lithium and Solid Electrolytes	96
Task 7.1 – Mechanical Properties at the Protected Lithium Interface (Nancy Dudney, ORNL; Erik Herbert, UTK; and Jeff Sakamoto, UM)	97
Task 7.2 – Solid Electrolytes for Solid-State and Lithium-Sulfur Batteries (Jeff Sakamoto, University of Michigan)	99
Task 7.3 – Composite Electrolytes to Stabilize Metallic Lithium Anodes (Nancy Dudney and Sergiy Kalnaus, Oak Ridge National Laboratory)	101
Task 7.4 – Overcoming Interfacial Impedance in Solid-State Batteries (Eric Wachsman, University of Maryland, College Park)	104
Task 7.5 – Nanoscale Interfacial Engineering for Stable Lithium Metal Anodes (Yi Cui, Stanford University)	106
Task 7.6 – Lithium Dendrite Suppression for Lithium-Ion Batteries (Wu Xu and Ji-Guang Zhang, Pacific Northwest National Laboratory)	108
Task 8 – Lithium Sulfur Batteries	111
Task 8.1 – New Lamination and Doping Concepts for Enhanced Li – S Battery Performance (Prashant N. Kumta, University of Pittsburgh)	112
Task 8.2 – Simulations and X-ray Spectroscopy of Li-S Chemistry (Nitash Balsara, Lawrence Berkeley National Laboratory)	115
Task 8.3 – Novel Chemistry: Lithium Selenium and Selenium Sulfur Couple (Khalil Amine, Argonne National Laboratory)	118
Task 8.4 – Multi-Functional Cathode Additives (MFCA) for Li-S Battery Technology (Hong Gan, Brookhaven National Laboratory, and Co-PI Esther Takeuchi, Brookhaven National Laboratory and Stony Brook University)	120
Task 8.5 – Development of High-Energy Lithium-Sulfur Batteries (Jie Xiao and Jun Liu, Pacific Northwest National Laboratory)	122
Task 8.6 – Nanostructured Design of Sulfur Cathodes for High Energy Lithium-Sulfur Batteries (Yi Cui, Stanford University)	125
Task 8.7 – Addressing Internal “Shuttle” Effect: Electrolyte Design and Cathode Morphology Evolution in Li-S Batteries (Perla Balbuena, Texas A&M University)	127
Task 9 – Li-Air Batteries	129
Task 9.1 – Rechargeable Lithium-Air Batteries (Ji-Guang Zhang and Wu Xu, PNNL)	130
Task 9.2 – Efficient Rechargeable Li/O ₂ Batteries Utilizing Stable Inorganic Molten Salt Electrolytes (Vincent Giordani, Liox)	133
Task 9.3 – Li-Air Batteries (Khalil Amine, ANL)	136
Task 9.4 – Overcome the Obstacles for the Rechargeable Li-air Batteries (Deyang Qu, University of Massachusetts, Boston and Xiao-Qing Yang, Brookhaven National Laboratory)	139
Task 10 – Na-ion Batteries	142
Task 10.1 – Exploratory Studies of Novel Sodium-Ion Battery Systems (Xiao-Qing Yang and Xiqian Yu, Brookhaven National Laboratory)	143

LIST OF FIGURES

Figure 1. Capacity versus cycle number of a half cell of NCM cycled between 2.8 and 4.5 v with baseline electrolyte.	5
Figure 2. Capacity versus cycle number of a half cell of NCM cycled between 2.8 and 4.5 v with high voltage electrolyte.	5
Figure 3. Superimposed voltage curves for baseline electrolyte.	5
Figure 4. Superimposed voltage curves for high-voltage electrolyte.	5
Figure 5. Cycle life of Li/Si cells with different materials: (a) nano-Si/PAA/C, (b) nano-Si/C simple mixing, and (c) nano-Si/PAA composites made by spray-drying.	7
Figure 6. Photos of anode powders (a) nano-Si, (b) nano-Si/PAA/C composite.	7
Figure 7. Scheme for magnetic alignment of removable pore former followed by pyrolysis and sintering. Lower right image shows end-on view of aligned pores.	9
Figure 8. DST test protocol (top) and comparison of discharge capacity for homogeneous and aligned porosity electrodes of same density and thickness.	9
Figure 9. (a) Chemical structure of PFM conductive polymer binder. (b) Particle size analysis via light scattering for the SiO ₂ pristine particles; embedded is the SEM image of the particles with a scale bar of 1 μ m. (c) Cycling performance of the SiO ₂ /PFM electrode after being calendered into different porosities. (d) Rate performance.	11
Figure 10. Capacity versus cycle number for a Graphite/NCM cell cycled between 2.8 and 4.2 V at different rates.	14
Figure 11. Average voltage on charge and discharge plotted versus cycle number.	14
Figure 12. A full-cell of NCA cathode and porous Si anode with the areal capacity of ~ 1.8 mAh/cm ²	17
Figure 13. Schematic view (a), SEM image (b), and TEM image (c) of graphite/nano-Si/carbon composite.	17
Figure 14. Specific charge/discharge capacity vs cycles of nc-Si/inactive matrix in Li/Li ⁺ system.	17
Figure 15. The first cycle discharge and charge capacities of SLMP-pre-lithiated cells as a function of SLMP to SiNPs-CNTs anode mass ratio.	17
Figure 16. (a) Schematic diagram of the artificial-SEI coating formed by reducing 1-fluorodecane on the surface of Li _x Si NPs in cyclohexane. TEM images of Li _x Si NPs (b) before and (c) after coating.	20
Figure 17. (a) XRD pattern of artificial-SEI coated Li _x Si NPs sealed in Kapton tape. (b) XPS of artificial-SEI coated Li _x Si NPs. Corresponding high-resolution XPS spectrum around F 1s peak region is shown in the inset. (c) High-resolution XPS spectra of C 1s. (d) Raman spectrum reveals the peak near 1762 cm ⁻¹ as the stretching vibration mode of C=O.	20
Figure 18. (Top) 1st charge and discharge plot of Li ₂ Cu _{0.5} Ni _{0.5} O ₂ during the <i>in situ</i> XAS measurements. (Middle) Ni-K edge shift during various charge-discharge regions. (Bottom) Corresponding <i>in situ</i> XAS of Cu K-edge.	24
Figure 19. Cycling behavior of (left) CuF ₂ , (middle) CuF ₂ /MoO ₃ , and (right) CuF ₂ /VOPO ₄	27
Figure 20. The initial cycling behavior of the solid solution Cu _{1-y} Fe _y F ₂ , (a) y= 0.2, (b) 0.5 cathode.	27

Figure 21. (a) The AlF_3 -coated material showed substantially improved cycling stability, exhibiting negligible capacity loss after 100 cycles. (b) The AlF_3 -coated material showed mitigated voltage fade during cycling.	30
Figure 22. Characterization of (a-c) uncoated and (d-f) AlF_3 -coated materials after 100 cycles. (a) TEM image showing a thick SEI layer formation. (b) High resolution Z-contrast image showing the formation of spinel-like/rock-salt phase at particle surface region. (c) Z-contrast images showing corrosion pit formation. (d) Overview Z-contrast image of AlF_3 -coated material after cycling. (e) Z-contrast image showing the spinel-like phase formation at the surface of cycled particle. (f) STEM images showing that the bulk region maintained layered structure.	30
Figure 23. Design of micro-reactors for both <i>in situ</i> and <i>ex-situ</i> combinatorial studies of synthesis reactions, enabling high-throughput synthesis of new cathode materials (an example of $\text{Cu}_x\text{V}_{1-x}\text{O}_y$ being used here).	32
Figure 24. The XRD patterns obtained from powder sample within sub-seconds.	32
Figure 25. (a) ^{27}Al MAS NMR spectra of 10% (blue) and 20% (red) Al-doped Li_3PO_4 ; Inset: illustration of Al octahedral occupancy in $\text{Li}_{3-3x}\text{Al}_{x-2x}\text{PO}_4$. (b) SEM/EDX data of $\text{Li}_{2.7}\text{Al}_{0.1-0.2}\text{PO}_4$ coated $\text{LiNi}_{0.5}\text{Mn}_{1.5}\text{O}_4$. (c) First-cycle discharge profiles of $\text{Li}_{2.7}\text{Al}_{0.1-0.2}\text{PO}_4$ -coated LiCoO_2 for various coating loadings (4.4 – 2.5 V, 20 mA/g).	35
Figure 26. (a) SEM image of the $\alpha\text{-LiVOPO}_4$ /graphene nanocomposite (~ 3 wt.% graphene) and (b) its first charge-discharge profiles at C/20 rate.	38
Figure 27. XRD patterns of the three forms of LiVOPO_4 and their delithiated and lithiated products.	38
Figure 28. XRD patterns and chemical analysis results of the delithiated products of $\alpha\text{-LiVOPO}_4$	38
Figure 29. Lithium copper phosphate glasses with borate and vanadate substitution ($\text{Li}_x\text{Cu}(\text{P-B-V})_y$) showed negligible 1st cycle irreversible capacity.	41
Figure 30. Cyclic voltammetry (CV) of silver metaphosphate glass with 50% vanadate substitution (AgMP-50V) showed excellent cycleability between 3.5 V and 1.5 V after the first cycle, but progressive irreversible loss when further charged to 4 V. Cycling with different maximum charge voltages agreed with the CV result.	41
Figure 31. Elemental association maps of spray pyrolyzed NMC powder after annealing at 850°C. Top: 3D rendering of the elemental associations viewing the particles at different angles. Bottom: 2D slices of the elemental associations. The colors presenting the elemental associations are shown at the bottom.	43
Figure 32. Processing scheme for PETT-Ester polymer coating on a porous PVDF membrane.	46
Figure 33. Charge/discharge voltage curves of 6-bromohexyl ferrocene catholyte with the PETT-Ester-coated PVDF membrane as a separator.	46
Figure 34: (a) XRD patterns and (b) initial discharge profiles of the $\text{LiCo}_{0.9}\text{Ni}_{0.1}\text{O}_2$ samples synthesized at various temperatures between 400 and 800°C.	48
Figure 35. 2D-DOSY NMR spectra of fluorinated carbonate F-EMC and its non-fluorinated counterpart EMC without LiPF_6 (left) and with LiPF_6 (right). (X axis is ppm of the H chemical shift; Y axis is the diffusion coefficient.)	52
Figure 36. Δ OCV vs Δ volume% for several electrolyte/electrode combinations.	54

Figure 37. Cycle life vs capacity for several additive combinations in 1.2 LiPF ₆ FEC/EMC/D ₇ (HFE) (2:6:2).....	54
Figure 38. Optimized salt concentration can achieve 300 cycles in noncarbonate electrolyte formulation	56
Figure 39. EC-free formulation has good performance relative to the control EC/EMC	56
Figure 40. HAADF STEM image of (a) an entire needle-shaped Li _{1.2} Ni _{0.13} Mn _{0.54} Co _{0.13} O ₂ crystal, (b) and (c) zoomed in view of the crystal structure, (d) color-coded HAADF image showing domains of monoclinic variants, and (e) models showing monoclinic structure in [100], [1-10] and [110] directions.	59
Figure 41. (a) HAADF STEM image, (b) EEL spectra collected from surface (top) and the bulk (bottom) corresponding to the HAADF image, and (c) L ₃ /L ₂ ratio of Mn, Co and Ni determined from the EELS data.	59
Figure 42. HAADF STEM images alongside STEM simulation images and models of interface in 3 zone axes: (a) [103]M, (b) [010]M, and (c) [001]M.	59
Figure 43.: Impedance evolution of graphite symmetric cells filled with 1 M LiPF ₆ , EC/DEC (1:2) spiked with 500 ppm of MnII/III compounds, measured at 50% of SOC.	62
Figure 44. XAS spectra of Li ₂ MoO ₃ during the first charge: (a) <i>In situ</i> XANES spectra at Mo K-edge during charging to 4.8 V and (b) <i>Ex-situ</i> FT-EXAFS spectra of Li _{2-x} MoO ₃ at pristine (x=0), half charged (x=0.75) and fully charged (x=1.47) states. The lower panel shows the FT-EXAFS spectra of MoO ₂ and α-MoO ₃ references.....	65
Figure 45. <i>In situ</i> ²³ Na NMR spectra for continuous galvanostatic plating, and galvanostatically cycled samples, at currents of 0.5, 1, and 2 mA cm ⁻² (A-C, and A*-C*, respectively) with the superscript (*) denoting galvanostatically cycled samples. Stack plots vs. time (in min.) are shown. The resonance assigned to Na metal continues to grow until the cell fails (e.g., 3000 mins for B) due to extensive short circuits.	68
Figure 46. Fraction of high surface area (FHSA) Na during galvanostatic cycling at various current densities. A ratio of 1 indicates complete microstructure deposition while 0 indicates smooth deposition.	68
Figure 47. (a) Voltage profiles of the pristine and surface modified Li _{1.133} Ni _{0.3} Mn _{0.567} O ₂ at different cycle numbers (0.1 C, 2 – 4.8 V) and (b) 1st and 2nd charge-discharge voltage profiles of the pristine and surface modified Li _{1.144} Ni _{0.136} Co _{0.136} Mn _{0.544} O ₂ at 0.05 C.	70
Figure 48. ADF-STEM image of (a) pristine Si, (b) lithiated Si after one cycle, (c) lithiated Si with FEC after one cycle, EELS spectra, (d) O-K edge, and (e) Li-K edge.	70
Figure 49. We suggest, according to this SFG spectrum that polyethylene carbonate is the main product of the Si/electrolyte interface layer at reduction potential of 0.5 V.	73
Figure 50. We performed two consecutive SFG measurements on Si-ethoxy wafer. Due to poor signal to noise ratio we are unable at this point to validate that indeed Si-ethoxy forms on the Si(100) surface.	73
Figure 51. Li _{1.2} Ni _{0.13} Co _{0.13} Mn _{0.54} O ₂ (NC-LMR) sample: (a) [010] zone axis STEM-HAADF image showing the EDS mapping region, (b) Surface plot of Mn K map, (c) Surface plot of Co K map, (d) Surface plot of Ni K map, (e) Integrated line scan profile showing x-ray counts distribution across the layered structure, (f) Based on counts ratio that from TM-layer and Li-layer, 4% Co and 41% Ni were estimated to seat in Li-layer due to a interlayer mixing, and (g) Optimized crystal model for NC-LMR based on EDS mapping results.	75

Figure 52. (a) DFT calculations of local structures in Ga-doped LiCoO_2 , (b) XRD patterns of $\text{LiCo}_{1-x}\text{Cr}_x\text{O}_2$ for $x=0.05$ and 0.075 , and (c) First-cycle charge profiles for $\text{LiCo}_{1-x}\text{Cr}_x\text{O}_2$ lithium half-cells.	78
Figure 53. C/12 discharge and charge of custom Li-S cell	82
Figure 54. (a) Structure of layered Li-excess material (inset), and Li-ion migration barrier in Li-layer. (b) Four symmetric hopping paths of Li-ion.	84
Figure 55. Transition metal-deficient off-stoichiometry leads to crystalline the olivine particle with Li-phosphate surface phases	86
Figure 56. Good capacity retention and high rate capability in the mixed olivine cathode driven from off-stoichiometric composition.....	86
Figure 57. SEI nucleation of organic oligomers over LiF. Li: purple; F: light blue; O: red; C: grey; H: white; Si: yellow	88
Figure 58. Disk model and slab model to mimic the experimental design. The disk model shows coating crack along radial direction.	91
Figure 59. Thickness-dependent interfacial sliding and SEI fracture of lithiated Si islands with thicknesses of (a) 50 nm (b) 250 nm.....	91
Figure 60. Photo of new six-line probe.....	94
Figure 61. Indentation of a $3\mu\text{m}$ -thick Li film at strain rates of 1/s and 0.1/s, blue and green respectively.	98
Figure 62. SEM images of LLZO fracture surfaces of varying relative density (RD) from 80.0% to 98.6%.	100
Figure 63. Infrared ATR of polymer and composite electrolytes, both dry (solid lines) and exposed to DMC vapor (dashed lines).	102
Figure 64. DSC scans for dry PEO, polymer and composite electrolytes (solid lines), with one exposed to DMC (dashed).	102
Figure 65. Developed model for garnet-electrode interfaces, which takes input from first principles calculations and experimental condition parameters.....	105
Figure 66. Cyclic voltammogram for Li/polymer gel electrolyte/Ti.....	105
Figure 67. Guided deposition of lithium metal by polymer nanofibers. (a) Formation of dendritic lithium metal when no guiding nanofiber mat existed. (b) When nanofiber mat is applied, lithium metal deposition is guided by the mat, due to the polymer surface where polar groups are affiliated by lithium metal deposition.	107
Figure 68. Stable cycling of lithium metal anode enabled by electrospun nanofibers. Average Coulombic efficiency of 97.4% was achieved for more than 120 cycles, with areal capacity and current density up to 3 mAh/cm^2 and 3 mA/cm^2 , respectively.	107
Figure 69. (a) Charge/discharge voltage profiles of selected electrolytes, and (b) cycling stability of Li NMC-442 coin cells at RT.	109
Figure 70. (a) Voltage curves of graphite charging or Li deposition on graphite anode at four charging current densities. (b, c) SME images of graphite anode charged at 2.0 mA/cm^2 and cutoff at 1.25 mAh/cm^2	109
Figure 71. (a) Voltage curves of graphite charging or Li deposition on graphite anode at four charging current densities. (b, c) SME images of graphite anode charged at 0.5 and 2.0 mA/cm^2 and cutoff at 2.0 mAh/cm^2	109

Figure 72. Activation barriers E_a for different migration paths of Li-ions in pure and doped Li_4SiO_4 .	113
Figure 73. (a) Comparison of cycling behavior of various polymeric LIC electrolyte materials. (b) Effect of oxide filler material in polymer LIC materials.	113
Figure 74. Experimental XAS data of Li_2S_4 and Li_2S_8 dissolved in PEO were obtained at a range of temperatures (a) and concentrations (b); XAS data were also obtained for Li_2S_x ($x = 4, 6$, and 8) dissolved in DMF (c).	116
Figure 75. Raman spectroscopies of typical Se_xS_y samples.	119
Figure 76. (a) <i>In situ</i> XANES of Li/ Se_2S_5 battery using a carbonate-based electrolyte. (b) Capacity retention of Li/ Se_2S_5 battery using a carbonate-based electrolyte.	119
Figure 77. Nano-CuS from Cu_2S +Sulfur	121
Figure 78. S: Cu_2S Coin Cell Cycling	121
Figure 79. Conversion of FeS to FeS_2	121
Figure 80. TiS_2 +S vs. S Control Cycling	121
Figure 81. (a) Charge/discharge curves of lithiated graphite/Sulfur (LG/S) full cell at different C rates in 5M LiTFSI/DOL electrolyte without any additive and (b) their corresponding cycling stability and Coulombic efficiency. (c) Charge/discharge curves of LG/S full cell at 0.1 C in 1M LiTFSI/DOL/DME with 0.1M LiNO_3 as additive and (d) their corresponding cycling performance. Areal capacity of cathode (limiting electrode) is 2 mAh/cm ² .	123
Figure 82. (a) Digital images of the Li_2S_8 trapping by the metal oxide nanoparticles in 1,3-dioxolane (DOL) and dimethoxyethane (DME) (1:1, v:v) solution. (b) Experimental and simulated adsorption amount of Li_2S_8 on different metal oxides. (c) Optimized geometries of most stable Li_2S on $\text{CeO}_2(111)$, $\text{Al}_2\text{O}_3(110)$, $\text{La}_2\text{O}_3(001)$, $\text{MgO}(100)$, and $\text{CaO}(100)$ surfaces.	126
Figure 83. Energy profile of Li_2S (111) layer formation on graphene calculated with DFT/vdW-D3 approach. Green, violet and grey spheres represent S, Li and C atoms, respectively.	128
Figure 84. Voltage profiles of selected cycles for Li-O ₂ cells with (a) 1 M, (b) 2 M and (c) 3 M electrolytes cycled at a discharge capacity limited (100 mAh g ⁻¹) protocol between 2.0 and 4.5 V at a current density of 0.1 mA cm ⁻² . (d) Comparison of cycling stability performance.	131
Figure 85. SEM images of air-electrodes at the charged state (a-c) and Li metal anodes (d-f) after 40 full discharge/charge cycles from LiTFSI-DME electrolytes of 1 M (a,d), 2 M (b,e), and 3 M (c,f).	131
Figure 86. DFT calculations of the Gibbs activation barriers for the C-H bond scission from CH_2 groups in DME, $\text{Li}^+(\text{DME})_2$, and $\text{Li}^{+2}(\text{DME})_3$ by the attack of superoxide radical anion ($\text{O}_2^{\bullet-}$).	131
Figure 87. Voltage/Pressure profile for a Li-O ₂ cell cycling at 150°C using Super P carbon cathode and $\text{LiNO}_3\text{-KNO}_3$ eutectic. 0.25 mA (100 mA per gr of carbon) constant current discharge/charge with 2.65 and 3 V voltage cutoff. E0 based of $2\text{Li} + \text{O}_2 \rightleftharpoons \text{Li}_2\text{O}_2$ equilibrium at 150°C.	134
Figure 88. Voltage profile comparison between (a) B-doped CNT cathode and (b) Super P carbon cathode. T=150°C in $\text{LiNO}_3\text{-KNO}_3$ eutectic. 100 mA per gr of carbon constant current discharge/charge with 2.65 and 3 V voltage cutoff. C loading ~4 mg/cm ² .	134

Figure 89. Results of DFT calculations: (a) The oxidized Mo ₂ C (101)-Mo surface with a MoO ₃ -like portion (the highlighted region shows a MoO ₃ -bulk unit-like configuration in the inset) on top surface layer after the adsorbed O ₂ molecules dissociate. (b) The electronic density of states (e-DOS) around the Fermi-level (E _f). The light-blue region is the Mo 3d projected e-DOS that dominate the e-DOS around the Fermi-level.	137
Figure 90. Cyclic voltammograms at various scan rates in 1 M TEABF ₄ DMSO electrolyte (A) and 1 M LiBF ₄ DMSO electrolyte (B) saturated with O ₂ on a glassy carbon-disc electrode.	140
Figure 91. First 50 cycles for a Li-air flow cell with and without B additive.	140
Figure 92. <i>In situ</i> x-ray diffraction patterns collected during the first charge (up to 3.6 V at C/12 rate) for a NaCrO ₂ /Na cell (The 2 θ angles are calculated to corresponding angles for $\lambda=1.54$ Å for Cu-K α from the real $\lambda=0.7747$ Å wavelength used for synchrotron XRD experiment). Corresponding voltage-composition profile is given on the right of XRD patterns. Oxygen stacking of O ₃ and P ₃ structure is given on the right.	144

LIST OF TABLES

Table 1: Lattice parameters of the LiCo _{1-x} Ni _x O ₂ (x = 0.1 and 0.2) samples synthesized at various temperatures.....	48
Table 2. Ion diffusion coefficient, transference number, and ionic conductivity of FEC-based electrolyte.....	52
Table 3. Structure of F-EMC and EMC (left) and the diffusion coefficient with and without LiPF ₆ salt (right) measured by NMR.....	52
Table 4. Li-ion migration barriers in Li-layer.....	84
Table 5. Results of the elastic (E) and shear moduli (G) from the pulse echol method compared with those obtained by nano-indentation.	98
Table 6. Molten Salt Li-O ₂ cell characteristics: e-/O ₂ and OER/ORR ratios. Analysis done on 1st cycle in (Li/K)NO ₃ melt cycling at 150°C.	134
Table 7. The relative strength of integration between Li ion and various solvents against DMSO.	140

A MESSAGE FROM THE ADVANCED BATTERY MATERIALS RESEARCH PROGRAM MANAGER

This report summarizes the results of research investigations performed in the ten, BMR topic areas, namely cell analysis, silicon anodes, advanced cathodes, liquid electrolytes, diagnostics, electrode modeling, metallic lithium and solid electrolytes, lithium sulfur batteries, lithium air batteries, and sodium ion batteries. The work was performed during the period from April 1, 2015, through June 30, 2015.

A few selected highlights from the BMR projects are summarized below:

- MIT (Ceder's Group) used the concept of designing an off-stoichiometric glassy coating on olivine cathodes to solve the rate problems with $\text{LiFe}_{0.6}\text{Mn}_{0.4}\text{PO}_4$ cathodes. The resulting material shows a capacity of 165mAh/g at low rates with greater than 100 mAh/g at a 60C rate.
- Brigham Young University (Wheeler's Group) is developing methods to measure the electronic conductivity of composite electrodes and has designed a method to measure the anisotropy in conductivity between the in-plane and out-of-plane directions. Using layered material based cathodes, the Group has shown that the out-of-plane conductivity is a factor of two lower than the in-plane directions, suggesting that further electrode improvements are needed.
- Lawrence Berkeley National Laboratory (Chen's Group) identified the crystal structure of Li- and Mn-rich layered oxide crystals by using complementary microscopy and spectroscopy techniques at multi-length scale.
- Lawrence Berkeley National Laboratory (Kostecki's Group) demonstrated that transition metal complexes cause impedance increase of the graphite anode by inhibiting Li^+ transport within the solid electrolyte interface.
- Cambridge University (Grey's Group) developed ^{23}Na *in situ* NMR to study Na metal anode in sodium-ion batteries.
- University of California, San Diego (Meng's Group) showed that FEC additive improves Si anode cycling by forming uniform and stable SEI that covers the Li_xSi particles with a high LiF content.
- Pacific Northwest National Laboratory (Wang's Group) demonstrated atomic-resolution visualization of ion mixing between transition metals (Ni, Co, Mn) and lithium in layered oxide cathodes using aberration corrected STEM imaging and DFT calculations.
- Argonne National Laboratory (Thackeray's Group) developed model systems to investigate the migration mechanisms of cations (M and M') in $\text{Li}_{1+x}(\text{MM}')_{1-x}\text{O}_2$ cathodes and to understand the connection between experiment and theory.
- Oak Ridge National Laboratory (Nanda's Group) stabilized a high-capacity cathode composition, $\text{Li}_2\text{Cu}_{0.5}\text{Ni}_{0.5}\text{O}_2$, and showed that 50 % nickel substitution improved the electrochemical retention and stability compared to Li_2CuO_2 .
- Brookhaven National Laboratory (Patrick Looney, Feng Wang Team) developed a micro-reactor that enables combinatorial screening of a large number of cathode compositions by varying synthesis parameters. The initial investigation was the $\alpha\text{-CuVO}_3$ cathode.
- Argonne National Laboratory (Zhang's Group) developed a fluorinated PC-based high-voltage electrolyte for 5-V $\text{LiNi}_{0.5}\text{Ni}_{1.5}\text{O}_4$ spinel cathode that has high compatibility with graphite and enhanced thermal stability.

Our next BMR quarterly report will cover the progress made during July through September and will be available December 2015.

Sincerely,

Tien Q. Duong

Manager, Advanced Battery Materials Research (BMR) Program

Energy Storage R&D

Office of Vehicle Technologies

Energy Efficiency and Renewable Energy

U.S. Department of Energy

TASK 1 – ADVANCED ELECTRODE ARCHITECTURES

Summary and Highlights

Energy density is a critical characterization parameter for batteries for electric vehicles, given the limited space for the battery and requirements for travel of more than 200 miles. The DOE targets are 500 Wh/L on a system basis and 750 Wh/L on a cell basis. Not only do the batteries have to have high energy density, they must also still deliver 1000 Wh/L for 30 seconds on the system level. To meet these requirements not only entails finding new, high energy density electrochemical couples, but also highly efficient electrode structures that minimize inactive material content, allow for expansion and contraction from one to several thousand cycles, and allow full access to the active materials by the electrolyte during pulse discharges. In that vein, the DOE OVT supports five projects in the BMR Program under Electrode Architectures: (1) Physical, Chemical, and Electrochemical Failure Analysis of Electrodes and Cells at LBNL, (2) Assembly of Battery Materials and Electrodes at HQ, (3) Design and Scalable Assembly of High-density, Low-tortuosity Electrodes at MIT, (4) Hierarchical Assembly of Inorganic/Organic Hybrid Si Negative Electrodes at LBNL, and (5) Studies in Advanced Electrode Fabrication at LBNL.

One of the more promising active materials for higher energy-density Li-ion batteries is Si used as the anode. It has a specific capacity of over 3500 mAh/g and an average voltage during delithiation of 0.4 V vs. the Li/Li⁺ electrode. This material suffers from two major problems both associated with the 300% volume change the material experiences as it goes from a fully delithiated state to a fully lithiated one: (1) the volume change results in a change in exposed surface area to electrolyte during cycling that consumes electrolyte and results in a lithium imbalance between the two electrodes, and (2) the volume change causes the particles to become electrically disconnected (which is further enhanced if particle fracturing also occurs) during cycling. Tasks 2, 4, and 5 are focused on Si to make it a more robust electrode by finding better binders.

Another approach to higher energy density is to make the electrodes thicker. The problem with thicker electrodes is that the salt in the electrolyte has to travel a farther distance to meet the current needs of the entire electrode throughout the discharge. If the salt cannot reach the back of the electrode at the discharge rates required of batteries for automobiles, the battery is said to be running at its limiting current. If the diffusional path through the electrode is tortuous or the volume for electrolyte is too low, the limiting current is reduced. The other problem with thicker electrodes is that they tend to not cycle as well as thinner electrodes and thus reach the end-of-life condition sooner, delivering fewer cycles. Tasks 1, 3, and 5 are focused on increasing the limiting current of thick electrodes while maintaining cycleability through the fabrication of less tortuous electrodes or of electrodes with less binder and more room for electrolyte.

If these projects are successful, they will result in a 25% increase in energy density as a result of replacing graphite with Si, and another 20% increase in energy density by moving from 2 mAh/cm² electrodes to 4 mAh/cm² electrodes. This would result in a net increase of 50% in energy density of the cell, and so a battery that once allowed a vehicle to travel only 200 miles may now allow travel of 300 miles.

Task 1.1 – Physical, Chemical, and Electrochemical Failure Analysis of Electrodes and Cells (Vincent Battaglia, Lawrence Berkeley National Laboratory)

Project Objective. This project investigates failure modes of targeted chemistries as defined by the BMR Program and its Focus Groups. The emphasis of this effort for 2015 will be on the High-Voltage and Si Anode Focus Groups. The objectives are to identify and quantify the chemical and physical aspects of cell cycling and aging that lead to reduced electrochemical performance. Specifically, research will focus on the effects on material stability as a result of increasing the cell voltage of Graphite/NCM cells from 4.2 V to 4.7 V. In addition, differences in performance between Graphite/NCM and Si/NCM will be investigated. Specifically, investigations into the differences in cell performance as a result of Coulombic inefficiencies and the effects of increased electrode loadings on cycleability will be carried out.

Project Impact. Success with understanding and improving the stability of NCM in the presence of electrolyte at voltages greater than 4.3 V vs. Li/Li⁺ will translate to an increase in capacity and voltage and hence a compounding improvement in energy density by as much as 45%. Improvement in the loading of anodes and cathodes from 2 to 5 mAh/cm² could result in larger fractions of active materials in cells and a projected increase in energy density by an additional 20%.

Out-year Goals. Provide a prescription of the physical and structural properties required to increase the accessible capacity of layered oxide materials. Demonstrate high loading cells with an increased energy density of 20% with no change in chemistry or operating parameters.

Collaborations. This project engages in collaborations with many BMR principal investigators.

Milestones

1. Measure and report the difference in capacity fade in mAh/h between LCO and HV-LCO at 4.3 V in mAh/h. (12/31/14 – Complete)
2. Identify and report the electrochemical phenomena responsible for the capacity fade of the LCO and HV-LCO cells at 4.3 V. (3/31/15 – Complete)
3. Measure and report the phenomena responsible for the capacity fade of a 3 mAh/cm² cell in mAh/h. (6/30/15 – Ongoing)
4. Measure and report the self-discharge rate of the baseline Li/S cell in mA/(g of S) and decide if this is an appropriate baseline design. (9/30/15 – Ongoing)

Progress Report

Milestone 3. Measure and report the phenomena responsible for the capacity fade of a 3 mAh/cm² cell in mAh/h.

Research in the area of higher loading electrodes is now set to begin in the October at the beginning of the next fiscal year. For the rest of this fiscal year, research will be focused on completing the bench-marking of cathodes and electrolytes at high voltage. In this quarter, the baseline electrolyte (1M LiPF₆ in EC:DEC 1:2) was tested in a NCM half-cell and compared side-by-side to a “high-voltage” electrolyte from Daikin-America in a cell of the same chemistry. Both cells were cycled to 4.5 upper cut-off voltage. The cycling data of the baseline electrolyte is provided in Figure 1. The cell shows very good capacity retention for the first 100 cycles. Similar cycling data of the high-voltage electrolyte is provided in Figure 2. This cell also shows excellent cycling performance for the first 100 cycles. The difference in capacity is just 1.7%, which is approximately 0.017% per cycle.

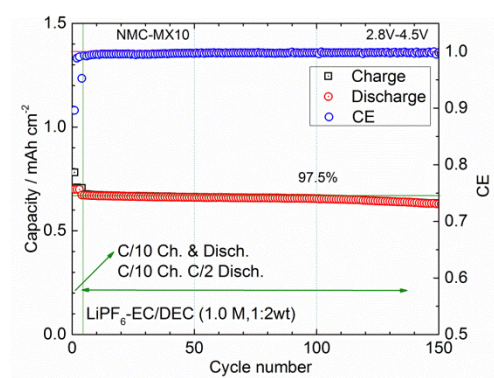


Figure 1. Capacity *versus* cycle number of a half cell of NCM cycled between 2.8 and 4.5 v with baseline electrolyte.

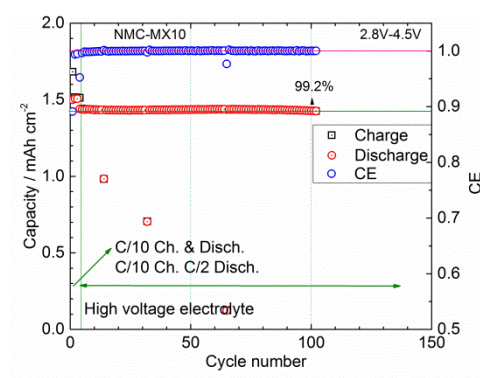


Figure 2. Capacity *versus* cycle number of a half cell of NCM cycled between 2.8 and 4.5 v with high voltage electrolyte.

A bigger difference in the two electrolytes can be observed when the voltage curves versus capacity are superimposed on each other (Figures 3 and 4). Here we see the side reaction in the cell with baseline electrolyte is resulting in an exaggerated sliding to the right of the voltage curves with each cycle. The sliding is at a rate of 0.27% per cycle, which is ca. 15 times greater than the rate of fade of the cell. Next quarter the electrolytes will be tested in full cells. In most full cells, we have seen capacity sliding of the anode at a rate of ca. 0.2% per cycle. It will be interesting to see if the sliding of the cathode, or lack thereof, helps or hurts the capacity fade of the full cell.

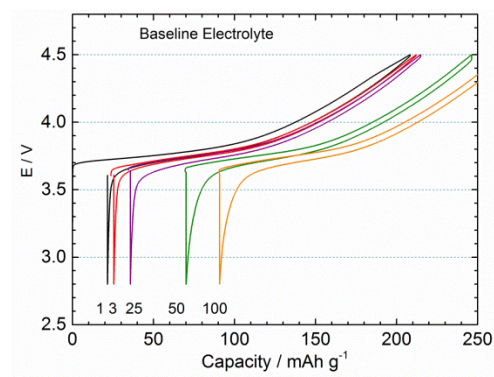


Figure 3. Superimposed voltage curves for baseline electrolyte.

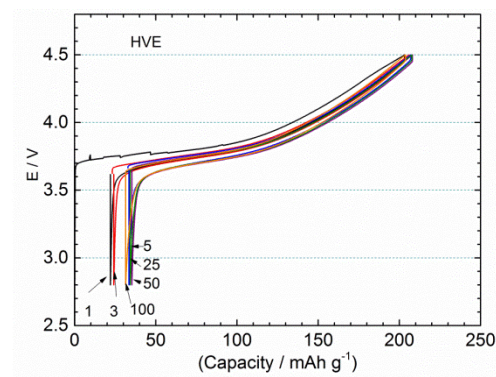


Figure 4. Superimposed voltage curves for high-voltage electrolyte.

Task 1.2 – Electrode Architecture-Assembly of Battery Materials and Electrodes (Karim Zaghib, HydroQuebec)

Project Objective. The project objective is to develop high-capacity, low-cost electrodes with good cycle stability and rate capability to replace graphite in Li-ion batteries.

The aim is to overcome the limit of electrochemical capacity (both gravimetric and volumetric) of conventional carbon anodes. This will be achieved by developing low-cost electrodes that utilize a high-capacity material such as silicon. Controlling the composition (that is, loading of the active material, ratio of binder and carbon additive) of the electrode will yield a more tolerant anode with acceptable volume change, useful cycle life, and low capacity fade. A high-energy, large-format, Li-ion cell will be produced using optimized Si-based anode and high-energy cathode electrodes.

Project Impact. Production of Si nano-powder using commercially scalable and affordable methods will justify replacing the graphite anode without jeopardizing the cost structure of conventional batteries. In addition, the energy density of cells is increased to > 250 Wh/kg by using a high content of Si (> 50%) with reasonable loading (2 mAh/cm²). The results obtained in large-format cells (> 20Ah) will enable us to study the wide spectrum of electrochemical performance under actual vehicle operation conditions.

Out-Year Goals. Out-year goals include the following:

- Complete the optimization of the electrode composition by varying the carbon additive ratio and the type of carbon. In addition to *in situ* SEM analyses, *in situ* impedance spectroscopy will be employed to enhance the understanding of capacity fade of the Si-material. These analyses will clarify the mechanism leading to electrode failure and guide further improvement and design of the electrode architecture.
- Complete optimization of the method to synthesize Si-nano powder developed at HQ.
- As a final goal, the optimized Si-anode and high-energy cathode will be coated in the pilot line and then assembled in large-format cells (> 20Ah) using the new automatic stacking machine at HQ.

Collaborations. This project collaborates with BMR members: V. Battaglia and G. Liu from LBNL, C. Wong and Z. Jiguang from PNNL, and J. Goodenough from the University of Texas.

Milestones

1. Complete optimization of the nano-Si-anode formulation. (12/31/14 – Complete)
2. Complete optimization of the synthesis of nano-size Si developed at HQ. Go/No-Go decision: Terminate the Si synthesis effort if the capacity is less than 1200 mAh/g. (3/31/15 – Complete)
3. Produce and supply laminate films of Si-anode and LMNO-cathode (10 m) to BMR principal investigators. (6/30/15 – Complete)
4. Produce and supply large-format 20 Ah high-energy stacking cells (4) to BMR principal investigators. (9/30/15 – Ongoing)

Progress Report

After the last quarterly report, Hydro-Quebec focused on increasing the loading of the anode to greater than 2 mg/cm^2 of total solids content. This goal was set in order to reach a specific energy density of 250 Wh/kg for a full cell when combined with an NCM cathode. From our extensive studies, it was discovered that at low loading levels ($<0.5 \text{ mg/cm}^2$) the cycle life at 40% DOD cycling in half-cells exceeded 900 cycles. However, if the loading level was increased, the capacity retention decreased dramatically: 260 cycles at 1.0 mg/cm^2 and 120 cycles at 1.26 mg/cm^2 .

In the previous report, we reported that a water-base binder showed a huge amount of gas generated during the mixing and coating processes. To overcome this barrier, the *nano*-Si particles' surface was pre-coated with poly acrylic acid (PAA) by using a spray-dry technique. The gas generation was suppressed; however, the retention of cycle life (Figure 5c) was less than the reference anode without the PAA coating (Figure 5b compared to 5c).

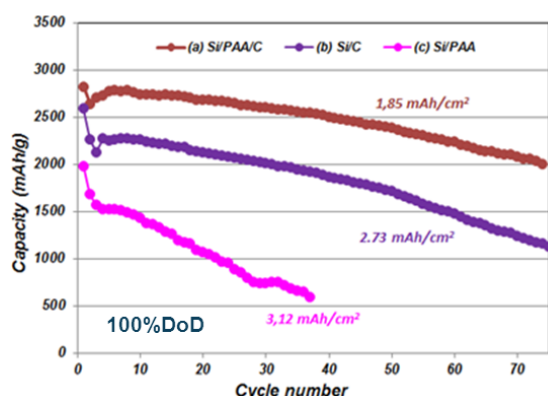


Figure 5. Cycle life of Li/Si cells with different materials: (a) *nano*-Si/PAA/C, (b) *nano*-Si/C simple mixing, and (c) *nano*-Si/PAA composites made by spray-drying.

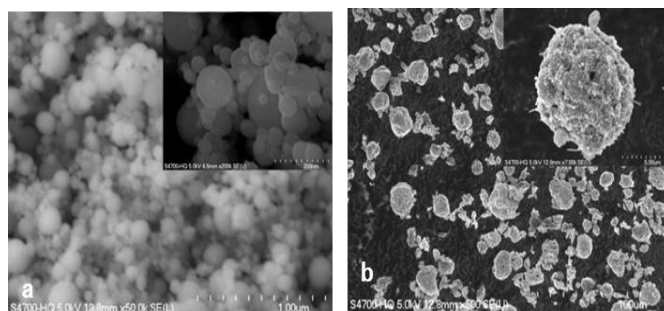


Figure 6. Photos of anode powders (a) *nano*-Si, (b) *nano*-Si/PAA/C composite.

To increase the cycle life of the anode, in a second trial with PAA treatment, the carbon additive was premixed with the *nano*-Si and PAA, and then spray-dried, followed by heat-treatment at 200°C in vacuum for 12 hours. A *nano*-Si/PAA/C composite with a secondary particle size of 1 to $10 \mu\text{m}$ (Figure 6b) was obtained. The Si-anode based on this process demonstrated respectable improvement in cycle life (Figure 5a) and even exceeded the performance of the reference anode, which was obtained by simply mixing the *nano*-Si and carbon additive. The reversible capacity of the *nano*-Si/PAA/C composite increased by nearly a factor of two compared to the Si/PAA composite, and by a factor of 1.25 of the reference *nano*-Si/C. After resolving the problem of gas generation and improving the performance of the Si-anode, efforts were again directed at increasing the loading of the anode. Electrodes with a loading of *ca.* 3 mAh/cm^2 were attempted, but the adhesion strength of the laminate to the current collector was found to be poor. Focus will now turn to increasing the adhesion strength of this *nano*-Si/PAA/C composite electrode. Towards this goal, alternative binders such as polyimide-type will be investigated to increase the anode performance both electrochemically and mechanically.

Deliverable: As our second deliverable, 10 m of *nano*-Si anode containing a polyimide binder was supplied to LBNL for evaluation.

Task 1.3 – Design and Scalable Assembly of High-Density, Low-Tortuosity Electrodes (Yet- Ming Chiang, Massachusetts Institute of Technology)

PROJECT OBJECTIVE: The project objective is to develop scalable, high-density, low-tortuosity electrode designs and fabrication processes enabling increased cell-level energy density compared to conventional Li-ion technology, and to characterize and optimize the electronic and ionic transport properties of controlled porosity and tortuosity cathodes as well as densely-sintered reference samples. Success is measured by the area capacity (mAh/cm²) that is realized at defined C-rates or current densities.

Project Impact. The high cost (\$/kWh) and low energy density of current automotive lithium-ion technology is in part due to the need for thin electrodes and associated high inactive materials content. If successful, this project will enable use of electrodes based on known families of cathode and anode actives but with at least three times the areal capacity (mAh/cm²) of current technology while satisfying the duty cycles of vehicle applications. This will be accomplished via new electrode architectures fabricated by scalable methods with higher active materials density and reduced inactive content; this will in turn enable higher energy density and lower-cost EV cells and packs.

Approach. Two techniques are used to fabricate thick, high density electrodes with low tortuosity porosity oriented normal to the electrode plane: (1) directional freezing of aqueous suspensions; and (2) magnetic alignment. Characterization includes measurement of single-phase material electronic and ionic transport using blocking and non-blocking electrodes with ac and dc techniques, electrokinetic measurements, and drive-cycle tests of electrodes using appropriate battery scaling factors for EVs.

Out-Year Goals. The out-year goals are as follows:

- Identify anodes and fabrication approaches that enable full cells in which both electrodes have high area capacity under EV operating conditions. Anode approach will include identifying compounds amenable to same fabrication approach as cathode, or use of very high capacity anodes, such as stabilized lithium or Si-alloys that in conventional form can capacity-match the cathodes.
- Use data from best performing electrochemical couple in techno-economic modeling of EV cell and pack performance parameters.

Collaborations. Within BMR, this project collaborates with Antoni P. Tomsia (LBNL) in fabrication of low-tortuosity, high-density electrodes by directional freeze-casting, and with Gao Liu (LBNL) in evaluating Si anodes. Outside of BMR, the project collaborates with Randall Erb (Northeastern University) on magnetic alignment fabrication methods for low-tortuosity electrodes.

Milestones

1. Fabricate and test at least one anode compound in an electrode structure having at least a 10 mAh/cm² theoretical capacity. (12/31/14 – Complete)
2. Demonstrate at least 5 mAh/cm² capacity per unit area at 1C continuous cycling rate for at least one candidate anode. (3/31/15 – Complete)
3. Downselect at least one anode composition for follow-on work. Go/No-Go milestone: Demonstrate an electrode with at least 7.5 mAh/cm² that passes the USABC dynamic stress test (DST) with peak discharge C-rate of 2C. (6/30/15 – Complete)
4. Demonstrate an electrode with at least 10 mAh/cm² that passes the USABC dynamic stress test (DST) with peak discharge C-rate of 2C. (9/30/15 – Complete)

Progress Report

Go/No-Go Milestone. Demonstrate an electrode with at least 7.5 mAh/cm² that passes the USABC dynamic stress test (DST) with peak discharge C-rate of 2C. (6/30/15).

This quarter, a new magnetic-alignment approach to fabricating low-tortuosity, high-density electrodes is reported, with results that meet the Go/No-Go Milestone for this year. As schematized in Figure 7, a LiCoO₂ particle suspension was prepared and mixed with short nylon rods that were magnetized by coating with iron oxide nanoparticles. The suspension was placed in a dc magnetic field and the rods aligned upon application of the field for a short period of time (<1 min). The electrode was then pyrolyzed in air to remove the nylon rods, then sintered to *ca.* 60% of theoretical density.

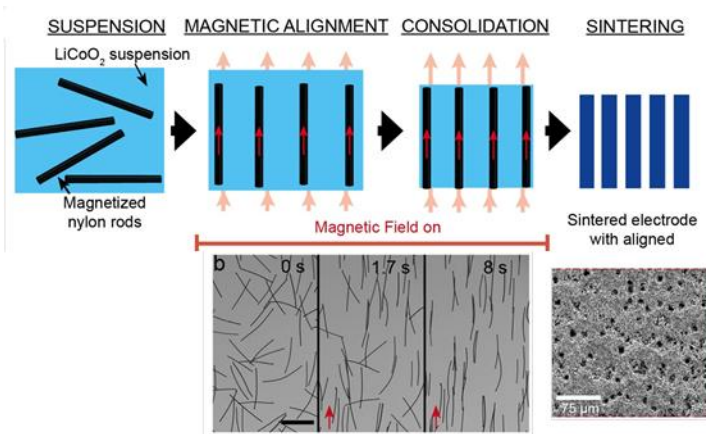


Figure 7. Scheme for magnetic alignment of removable pore former followed by pyrolysis and sintering. Lower right image shows end-on view of aligned pores.

The sintered samples with aligned low-tortuosity porosity were then sectioned into electrodes of 200 to 220 μm thickness and tested in Li half-cells using the DST protocol. This test protocol applies charge and discharge pulses of defined C-rate and duration, as shown in Figure 8 (top). The highest C-rate pulse discharge is 2C for 30 sec. To test the effectiveness of the electrode fabrication technique, a control sample consisting of sintered LiCoO₂ with homogenous porosity and similar sintered density and thickness was prepared for testing *via* the same DST protocol. As shown in Figure 8 (bottom), the DST protocol was run repeatedly on each electrode, beginning with a fully charged cell, until a lower cut-off voltage of 3.0 V was reached during pulse discharge. As shown in Figure 8, the sample with aligned pore channels exhibits more than twice the discharge capacity of the sample with homogeneously distributed pores, and reaches an area capacity of 8.1 mAh/cm². This performance meets the Go/No-Go Milestone of 7.5 mAh/cm² under DST testing.

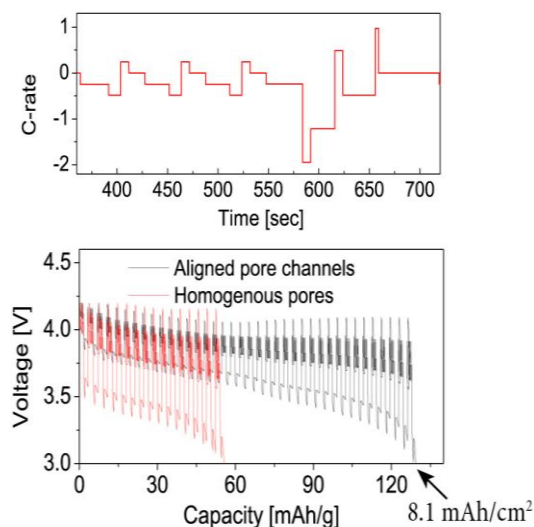


Figure 8. DST test protocol (top) and comparison of discharge capacity for homogeneous and aligned porosity electrodes of same density and thickness.

Based on these promising test results, it is proposed that subsequent milestones also be modified to emphasize drive-cycle testing that more meaningfully reflects real-world EV performance requirements. It is proposed that the fourth quarter Go/No-go Milestone be modified to: “*Demonstrate an electrode with at least 10 mAh/cm² that passes the USABC dynamic stress test (DST) with peak discharge C-rate of 2C.*”

Task 1.4 – Hierarchical Assembly of Inorganic/Organic Hybrid Si Negative Electrodes (Gao Liu, Lawrence Berkeley National Laboratory)

Project Objective. This proposed work aims to enable Si as a high-capacity and long cycle-life material for negative electrode to address two of the barriers of Li-ion chemistry for EV/PHEV application: insufficient energy density and poor cycle life performance. The proposed work will combine material synthesis and composite particle formation with electrode design and engineering to develop high-capacity, long-life, and low-cost hierarchical Si-based electrode. State of the art Li-ion negative electrodes employ graphitic active materials with theoretical capacities of 372 mAh/g. Silicon, a naturally abundant material, possesses the highest capacity of all Li-ion anode materials. It has a theoretical capacity of 4200 mAh/g for full lithiation to the $\text{Li}_{22}\text{Si}_5$ phase. However, Si volume change disrupts the integrity of electrode and induces excessive side reactions, leading to fast capacity fade.

Project Impact. This work addresses the adverse effects of Si volume change and minimizes the side reactions to significantly improve capacity and lifetime to develop negative electrode with Li-ion storage capacity over 2000 mAh/g (electrode level capacity) and significantly improve the Coulombic efficiency to over 99.9%. The research and development activity will provide an in-depth understanding of the challenges associated with assembling large volume change materials into electrodes and will develop a practical hierarchical assembly approach to enable Si materials as negative electrodes in Li-ion batteries.

Out-Year Goals. There are three aspects of this proposed work: bulk assembly, surface stabilization, and Li enrichment; these are formulated into 10 tasks in a four-year period.

- Develop hierarchical electrode structure to maintain electrode mechanical stability and electrical conductivity. (bulk assembly)
- Form *in situ* compliant coating on Si and electrode surface to minimize Si surface reaction (surface stabilization)
- Use prelithiation to compensate first cycle loss of the Si electrode. (Li enrichment)

The goal is to achieve a Si-based electrode at higher mass loading of Si that can be extensively cycled with minimum capacity loss at high Coulombic efficiency to qualify for vehicle application.

Collaborations. This project collaborates with the following: Vince Battaglia and Venkat Srinivasan of LBNL; Xingcheng Xiao of GM; Jason Zhang and Chongmin Wang of PNNL; Yi Cui of Stanford; and the Si-Anode Focus Group.

Milestones

1. Design and synthesize three more PEFM polymers with different ethylene oxide (EO) content to study the adhesion and swelling properties of binder to the Si electrode performance. (Complete)
2. Go/No-Go: Down select Si vs. Si alloy particles and particle sizes (nano vs. micro.) Criteria: Down select based on cycling results. (Complete)
3. Prepare one type of Si/conductive polymer composite particles and test its electrochemical performance. (June – On schedule)
4. Design and synthesize one type of vinylene carbonate (VC) derivative that is targeted to protect Si surface and test it with Si-based electrode. (September – On schedule)

Progress Report

High-capacity and high-density, functional-conductive-polymer-binder/SiO electrodes were fabricated and calendered to various porosities. The effect of calendering on thickness, porosity, and density was investigated. The SiO particle size remained unchanged after calendering. When compressed to an appropriate density, an improved cycling performance was shown compared to the uncalendered electrode and over-calendered electrode. The calendered electrode has a high Si density of *ca.* 1.2 g/cm³. A high-loading electrode with an areal capacity of *ca.* 3.5 mAh/cm² at a C/10 rate is achieved using functional-conductive-polymer-binder and a simple calendering method.

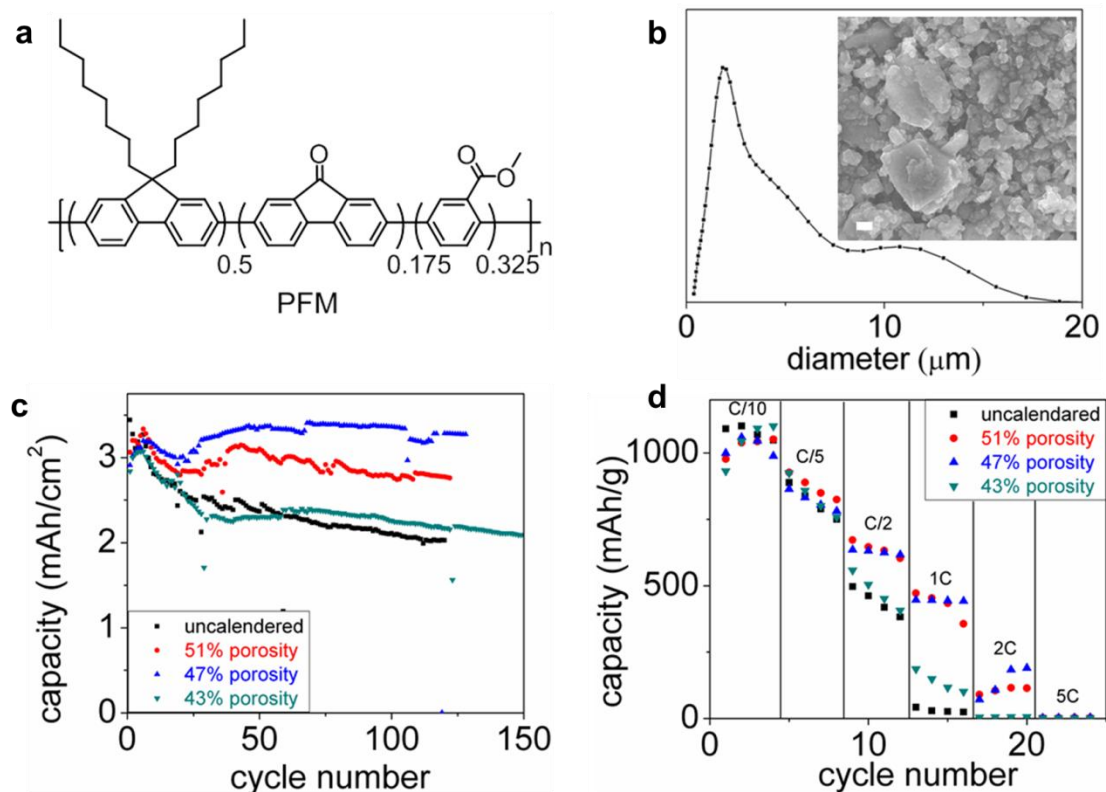


Figure 9. (a) Chemical structure of PFM conductive polymer binder. (b) Particle size analysis via light scattering for the SiO pristine particles; embedded is the SEM image of the particles with a scale bar of 1 μm . (c) Cycling performance of the SiO/PFM electrode after being calendered into different porosities. (d) Rate performance.

Figure 9 (a and b) shows the chemical structure of the PFM conductive-polymer-binder and the morphology of the SiO anode, respectively, used in this work. A 47% porosity was determined to deliver the best cell cycling performance (Figure 9c) among the four options and had a high Coulombic efficiency. Electrodes with 51% porosity may still have too much porosity; the charge transport path is not improved to an ideal case, although the performance is indeed improved compared to the uncalendered electrode. The electrodes with 43% porosity, on the other hand, are over compressed. The improved electrochemical performance is also evident in the rate performance shown in Figure 9d. This high-loading electrode with high density is enabled by the dual strategy of utilizing conductive-polymer-binder and optimized calendering.

Patents/Publications/Presentations

1. Ai, Guo, and Yiling Dai, Yifan Ye, Wenfeng Mao, Zhihui Wang, Hui Zhao, Yulin Chen, Junfa Zhu, Yanbao Fu, Vincent Battaglia, Jinghua Guo, Venkat Srinivasan, and Gao Liu. “Investigation of Surface Effects Through the Application of Functional Binders in Lithium Sulfur Batteries.” *Nano Energy* 16 (2015): 28-37.
2. Ling, Min, and Jingxia Qiu, Sheng Li, Cheng Yan, Milton Kiefei, Gao Liu, and Shanqing Zhang. “Multi-functional SA-PProDOT Binder for Lithium Ion Batteries.” *Nano Letters* 15, no. 7 (2015): 4440-4447.
3. Qiao, Ruimin, and Kehua Dai (**co-first author**), Jing Mao, Tsu-Chien Weng, Dimosthenis Sokaras, Dennis Nordlund, Xiangyun Song, Vince Battaglia, Zahid Hussain, Gao Liu, and Wanli Yang. “Revealing and Suppressing Surface Mn(II) Formation of Na_{0.44}MnO₂ Electrodes for Na-ion Batteries.” *Nano Energy* 16 (2015):186-195.
4. Feng, Caihong, and Le Zhang, Menghuan Yang, Xiangyun Song, Hui Zhao, Zhe Jia, Kening Sun, and Gao Liu. “One Pot Synthesis of Copper Sulfide Nanowires/Reduced Graphene Oxide Nanocomposites with Elithium Storage Properties as Anode Materials for Lithium Ion Batteries.” *ACS Applied Materials & Interfaces* (2015): Article ASAP.
5. Presentations at Electrochemical Society 227th Meeting, 2015 Spring, Chicago (May 24 – 28, 2015):
 - “Toward a Better Understanding of the Surface Effect through the Design of Binders in Lithium Sulfur Battery”; Guo Ai.
 - “Toward Practical Application of Functional Conductive Polymer Binder for a High-Energy Lithium-Ion Battery Design”; Hui Zhao.
 - “Toward a Single-Ion Nanocomposite Electrolyte for Lithium Batteries”; Hui Zhao.

Task 1.5 – Studies in Advanced Electrode Fabrication (Vincent Battaglia, Lawrence Berkeley National Laboratory)

Project Objective. This project supports BMR principal investigators through the supply of electrode materials, laminates, and cells as defined by the BMR Focus Groups. The emphasis of the 2015 effort will be on the High-Voltage Focus Group, the Si-Anode Focus Group, and a nascent Li/S effort. The objectives are to screen sources of materials, define baseline chemistries, and benchmark performance of materials targeted to specific Focus Group topics. This provides a common chemistry and performance metrics that other BMR institutions can use as a benchmark for their own efforts on the subject. In addition, test configurations will be designed and built to identify and isolate problems associated with poor performance. Also, Li/S cells will be designed and tested.

Project Impact. Identification of baseline chemistries and availability of baseline laminates will allow a group of BMR principal investigators to work as a team. Such team work is considered crucial in the acceleration of the advancement of today's Li-ion and Li/S systems. Since all of the focus groups are dedicated to some aspect of increased energy density, all of this work will have an impact on this area.

Out-Year Goals. This framework of a common chemistry will accelerate advancements in energy density and should lead to baseline systems with an increased energy density of at least 40%. It should also provide a recipe for making electrodes of experimental materials that are of high enough performance to allow for critical down select—an important part of the process in advancing any technology.

Collaborations. This project collaborates with many BMR principal investigators.

Milestones

1. Identify and report the source of additional impedance of a symmetric cell. (12/31/14 – Complete)
2. Measure and report the gas composition of a symmetric cathode/cathode cell and an anode/anode cell. (3/31/15 – Complete)
3. Identify the first iteration of the baseline Li/S cell. (6/30/15 – Ongoing)
4. Measure and report gas volume *versus* rate of side reaction at several upper voltage cut-off points. (9/30/15 – Ongoing)

Progress Report

Milestone 3. Identify the first iteration of the baseline Li/S cell.

Work in the area of Li/S cell is gaining less importance as investigations into electrolytes with high solubilities of polysulfides have made little progress. To increase energy density, the DOE is more focused on finding Li-ion cathodes with higher capacities for Li-ions at higher voltages and cell constructions that result in lower fractions of inactive components. Before moving in this direction, it was important to establish good cycleability in pouch cells for the purpose of testing full cells. (It was recently discovered that full cells assembled in coin-cell hardware do not cycle as well as those in pouch cells. A mechanism for the short coming is under investigation.)

Full pouch-cells were made with excess anode capacity of 2.8% and 27% to see if this greatly affects the cycleability of the cells. In these cells, the anode has 9% more superficial area than the cathodes. Cells with excess anode capacity are expected to have less total cell capacity because the side reaction on the anode will require lithium from the cathode, which leads to premature discharge of the anode compared to that expected from a perfectly balanced cell. (Cells with too little anode capacity risk lithium deposition near the top of charge.)

Figure 10 shows the cycling performance of the full cell with just 2.8% more anode capacity than cathode capacity. The cell was cycled between 2.8 and 4.2 V at a C/2 charge and C/1 discharge rate and has reached 700 cycles with a small amount of capacity fade. Figure 11 shows the average voltage of the charge and of the discharge during each cycle.

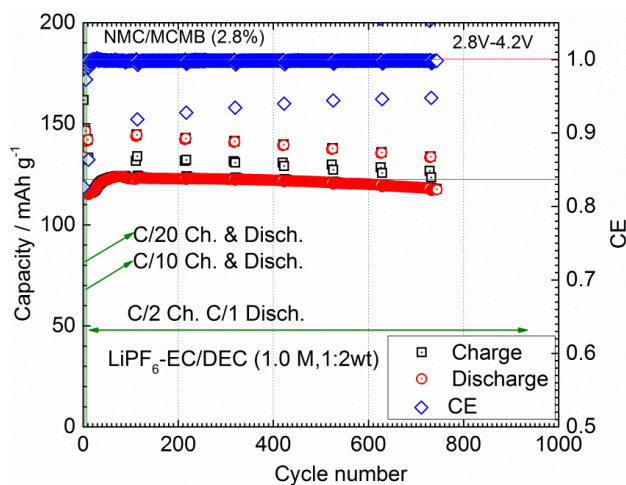


Figure 10. Capacity versus cycle number for a Graphite/NCM cell cycled between 2.8 and 4.2 V at different rates.

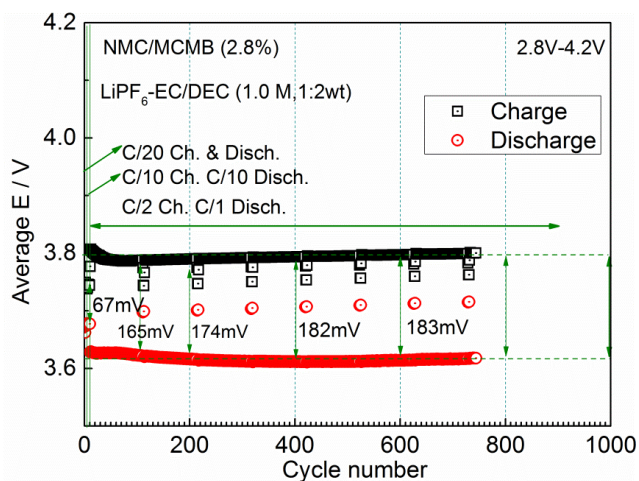


Figure 11. Average voltage on charge and discharge plotted versus cycle number.

The difference between the two is a measure of the average resistance of the cell. One sees that this resistance has increased less than 10% from cycle 100 to cycle 600. The capacity fade appears to accelerate after the first 600 cycles even though the difference in average voltage appears to be leveling off. This could still be an effect of resistance rise, if the resistance rise at the top of charge or end of discharge is accelerating faster than the average.

Task 2 – Silicone Anode Research

Summary and Highlights

Most Li-ion batteries used in the state-of-the-art electric vehicles (EVs) contain graphite as their anode material. Limited capacity of graphite (LiC₆, 372 mAh/g) is one of the barriers that prevent the long range operation of EVs required by the EV Everywhere Grand Challenge proposed by the DOE/EERE. In this regard, Silicon (Si) is one of the most promising candidate as an alternative anode for Li-ion battery applications. Si is environmentally benign and ubiquitous. The theoretical specific capacity of silicon is 4212 mAh/g (Li₂₁Si₅), which is 10 times greater than the specific capacity of graphite. However, the high specific capacity of silicon is associated with large volume changes (more than 300 percent) when alloyed with lithium. These extreme volume changes can cause severe cracking and disintegration of the electrode and can lead to significant capacity loss.

Significant scientific research has been conducted to circumvent the deterioration of silicon-based anode materials during cycling. Various strategies, such as reduction of particle size, generation of active/inactive composites, fabrication of silicon-based thin films, use of alternative binders, and the synthesis of one-dimensional silicon nanostructures have been implemented by a number of research groups. Fundamental mechanistic research also has been performed to better understand the electrochemical lithiation and delithiation processes during cycling in terms of crystal structure, phase transitions, morphological changes, and reaction kinetics. Although significant progress has been made on developing silicon-based anodes, many obstacles still prevent their practical application. Long-term cycling stability remains the foremost challenge for Si based anode, especially for the high loading electrode (> 3mAh/cm²) required for many practical applications. The cyclability of full cells using silicon-based anodes is also complicated by multiple factors, such as diffusion-induced stress and fracture, loss of electrical contact among silicon particles and between silicon and current collector, and the breakdown of SEI layers during volume expansion/contraction processes. The design and engineering of a full cell with a silicon-based anode still needs to be optimized. Critical research remaining in this area includes, but is not limited to, the following:

- The effects of SEI formation and stability on the cyclability of silicon-based anodes need to be further investigated. Electrolytes and additives that can produce a stable SEI layer need to be developed.
- Low cost manufacturing processes have to be found to produce nano-structured silicon with the desired properties.
- A better binder and a conductive matrix need to be developed. They should provide flexible but stable electrical contacts among silicon particles and between particles and the current collector under repeated volume changes during charge/ discharge processes.
- The performances of full cells using silicon-based anode need to be investigated and optimized.

The main goal of the Battery Materials Research Task 2 is to gain a fundamental understanding on the failure mechanism of Si based anode and improve its long term stability, especially for thick electrode operated at full cell conditions. The Stanford group will address the problem of large first cycle loss in Si-based anode by novel prelithiation approaches. Two approaches will be investigated in this study: (1) developing facile and practical methods to increase first-cycle Coulombic efficiency of Si anodes, and (2) synthesizing fully lithiated Si to pair with high capacity lithium-free cathode materials. The PNNL/UP/FSU team will explore new electrode structures using nano Si and SiO_x to enable high-capacity and low-cost Si-based anodes with good cycle stability and rate capability. Nanocomposites of silicon lithium oxide will be prepared by novel *in situ* chemical reduction methods to reduce the first cycle loss. Mechanical and electrochemical stability of the SEI layer formed on the surface of Si particles will be investigated by electrochemical evaluation and *in situ/ex situ* microscopic analysis. Success of this project will accelerate large-scale application of Si based anode and improve the energy density of Li-ion batteries to meet the goal of EV Everywhere.

Task 2.1 – Development of Silicon-Based High Capacity Anodes

(Ji-Guang Zhang/Jun Liu, PNNL; Prashant Kumta, Univ. of Pittsburgh; Jim Zheng, PSU)

Project Objective. The objective of this project is to develop high-capacity and low-cost Si-based anodes with good cycle stability and rate capability to replace graphite in Li-ion batteries. Nanocomposites of silicon and Li-ion conducting lithium oxide will be prepared by novel *in situ* chemical reduction methods to solve the problems associated with large first cycle irreversible capacity loss, while achieving acceptable Coulombic efficiencies. Large irreversible capacity loss in the first cycle will also be minimized by pre-doping Li into the anode using stabilized lithium metal powder or additional sacrificial Li electrode. The optimized materials will be used as the baseline for both thick electrode fabrication and studies to advance our fundamental understanding of the degradation mechanism of Si-based anodes. The electrode structures will be modified to enable high utilization of thick electrode. Mechanical and electrochemical stability of the SEI layer will be investigated by electrochemical method, simulation and *in situ* microscopic analysis to guide their further improvement.

Project Impact. Si-based anodes have much larger specific capacities compared with conventional graphite anodes. However, the cyclability of Si-based anodes is limited because of the large volume expansion characteristic of these anodes. This work will develop a low-cost approach to extend the cycle life of high-capacity, Si-based anodes. The success of this work will further increase the energy density of Li-ion batteries and accelerate market acceptance of electrical vehicles (EV), especially for the plug-in hybrid electrical vehicles (PHEV) required by the EV Everywhere Grand Challenge proposed by the DOE/EERE.

Out-Year Goals. The main goal of the proposed work is to enable Li-ion batteries with a specific energy of >200 Wh/kg (in cell level for PHEVs), 5000 deep-discharge cycles, 15-year calendar life, improved abuse tolerance, and less than 20% capacity fade over a 10-year period.

Collaborations. We will continue to collaborate with the following battery groups on anode development:

- Dr. Karim Zaghib, Hydro Quebec; preparation of nano-Si
- Prof. Michael Sailor, UCSD; preparation of porous Si
- Prof. David Ji, Oregon State University; preparation of porous Si by thermite reactions

Milestones

1. Identify the stability window of SEI formed on Si-based anode. (12/31/2014 – Complete)
2. Optimize the synthesis conditions of the rigid-skeleton supported Si composite. (3/31/2015 – Complete)
3. Demonstrate the operation of full cell using Si anode and selected cathode with >80% capacity retention over 100 cycles. (6/30/2015 – Complete)
4. Achieve >80% capacity retention over 200 cycles of thick electrodes (~3 mAh/cm²) through optimization of the Si electrode structure and binder. (9/30/2015 – Ongoing)

Progress Report

Porous Si made by electrochemical etching was matched with NCA cathode for full cell demonstration. The NCA-Si full cell was tested between 2 and 4.3V at the current density of ~ 0.375 mA/cm². The porous Si electrode was pre-lithiated before full cell assembly. The areal capacity of the full cell is ~ 1.8 mAh/cm², and the capacity retention is $\sim 80\%$ after 100 cycles (Figure 12). In another effort, a new type of ternary core-shell structured graphite/nano-Si/hard carbon composite (SGC) has been developed. Nano-Si and graphite were dispersed into 1.5M carbonhydrate solution and hydrothermally treated after stirring for 1h. It is a low cost, scalable, one-step synthesis. The ratio of graphite, nano-Si, and hard carbon from polymer carbonization can be well controlled. Figure 13 shows the schematic view (a), SEM image (b) and TEM image (c) image of the SGC composite. At a high loading of 2.5 mAh/cm², the optimized sample exhibits a specific capacity of ~ 800 mAh/g based on active materials weight at 0.2C rate with minimal capacity loss in 60 cycles.

In another effort, a nanocomposite comprised of amorphous and/or *nc*-Si and a light weight intermetallic matrix exhibiting excellent mechanical properties has been generated by a single-step mechanochemical reduction of a Si-containing alloy. The nanocomposite comprised of Si and the HEMM-derived, mechanically compliant, electrochemically inactive matrix obtained after milling for 20h shows a reversible capacity of ~ 800 mAh/g, validating the efficacy of the simple approach (Figure 14). The observed reversible capacity, albeit lower than the expected theoretical capacity (~ 1300 mAh/g), is primarily due to the incomplete reduction of the Si alloy. Further experiments continue for inducing complete reduction of the Si-containing alloy with a suitable reducing agent that will likely exhibit higher specific capacity. Results of these studies will be presented in the next report.

The relationship between the SLMP to SiNPs-CNTs anode ratio and the first cycle Coulombic efficiency was systematically investigated as shown in Figure 15. At a SLMP and anode mass ratio of around 0.25, the charge capacity equals to the discharge capacity, or the Coulombic efficiency closes to 100%. At low SLMP loadings, the discharge capacity was greater than the charge capacity, which means that anode would consume Li from the cathode when a Li-ion battery was fully charged; at high SLMP loadings, the discharge capacity was less than the charge capacity, which means that anode would not be able to be fully discharged. The pre-lithiation method has been used to prepare a symmetrical button cell super-capacitor using hierarchical porous carbon (HPC) with a specific capacitance of 107 F/g.

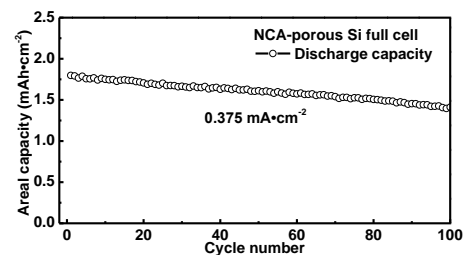


Figure 12. A full-cell of NCA cathode and porous Si anode with the areal capacity of ~ 1.8 mAh/cm².

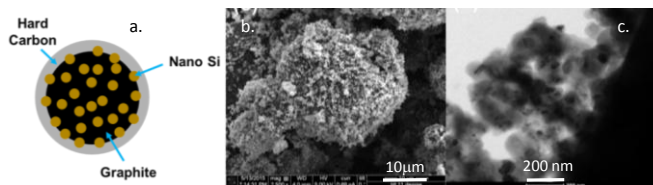


Figure 13. Schematic view (a), SEM image (b), and TEM image (c) of graphite/nano-Si/carbon composite.

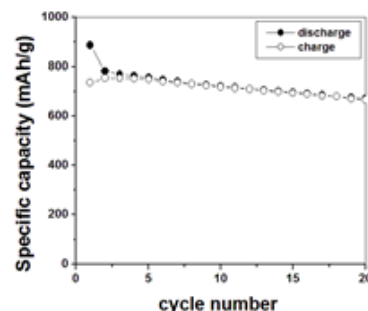


Figure 14. Specific charge/discharge capacity vs cycles of nc-Si/inactive matrix in Li/Li⁺ system.

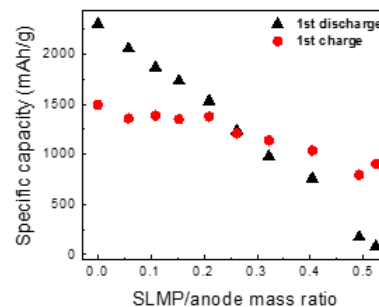


Figure 15. The first cycle discharge and charge capacities of SLMP-pre-lithiated cells as a function of SLMP to SiNPs-CNTs anode mass ratio.

Patents/Publications/Presentations

1. Presentation at MRS Spring 2015, San Francisco (April 8, 2015): “High Loading Si Anode for Practical Li-Ion Batteries”; Xiaolin Li, Sookyung Jeong, Yulin Chen, Pengfei Yan, Chongmin Wang, Xiulei Ji, Wei Luo, Chunlong Chen, Jun Liu, and Ji-Guang Zhang.
2. Presentation at the Symposium on Energy Storage Beyond Li-ion VIII, Oak Ridge, TN (June 3, 2015): “Hierarchically Porous Materials for Energy Storage Applications”; Luis Estevez, Genggeng Qi, Konstantinos Spyrou, Sookyung Jeong, Mark H. Engelhard, Xiaolin Li, Wu Xu, Emmanuel P. Giannelis, and Ji-Guang Zhang.

Task 2.2 – Pre-Lithiation of Silicon Anode for High Energy Li Ion Batteries (Yi Cui, Stanford University)

Project Objective. Prelithiation of high capacity electrode materials such as Si is an important means to enable those materials in high-energy batteries. This study pursues two main directions: (1) developing facile and practical methods to increase first-cycle Coulombic efficiency of Si anodes, and (2) synthesizing fully lithiated Si to pair with high capacity lithium-free cathode materials.

Project Impact. The first-cycle Coulombic efficiency of anode materials will be increased dramatically via prelithiation. Prelithiation of high capacity electrode materials will enable those materials in next-generation high-energy-density lithium ion batteries. This project's success will make high-energy-density lithium ion batteries for electric vehicles.

Out-Year Goals. Compounds containing a large quantity of Li will be synthesized for pre-storing Li ions inside batteries. First-cycle Coulombic efficiency (1st CE) will be improved and optimized (over 95%) by prelithiating anode materials with the synthesized Li-rich compounds.

Collaborations. The Project works with the following collaborators: (1) BMR program principal investigators, (2) SLAC: *in situ* x-ray, Dr. Michael Toney, and (3) Stanford: mechanics, Prof. Nix.

Milestones

1. Prelithiate anode materials by direct contact of Li metal foil to anodes. (January – Complete)
2. Synthesize Li_xSi nanoparticles with high capacity ($>1000\text{mAh/g Si}$). (July – Complete)
3. Prelithiate anode materials with dry-air-stable $\text{Li}_x\text{Si-Li}_2\text{O}$ core-shell nanoparticles. (April – Complete)
4. Synthesize artificial-SEI protected Li_xSi NPs. (July – Complete)

Progress Report

Usually, Li_xSi nanoparticles (NPs) maintain their capacity in air with low humidity only for relatively short durations, which could limit its potential use in large-scale applications. Therefore, nanoscale prelithiation reagents with higher capacity and improved stability should be explored. Here we develop a facile reaction process utilizing the highly reactive nature of Li_xSi NPs to reduce 1-fluorodecane, thereby producing a continuous and dense coating over the NPs (Figure 16a). The synthesis is inspired by the SEI formation process in regular battery anodes. The TEM image (Figure 16b) shows that the surface of synthesized Li_xSi NPs is clean. After modified by 1-fluorodecane in solution, each Li_xSi NP is wrapped in a uniform ~ 13 nm thickness coating, as shown in Figure 16c.

Compositional analysis of the synthesized core-shell NPs was acquired by XRD, XPS, and Raman spectroscopy. All peaks in the XRD pattern (Figure 17a) are indexed as $\text{Li}_{21}\text{Si}_5$ (PDF# 00-018-747), indicating a crystalline Li_xSi core and an amorphous coating layer. XPS analysis (Figure 17b) confirms the chemical composition of the coating layer with the presence of F, O, C and Li. As shown in the inset of Figure 17b, the F 1s spectrum contains a single peak at 684.9 eV, supporting the presence of LiF. Besides the strong hydrocarbon peak, the XPS of C shows two main peaks at 289.8 eV and 286.4 eV, corresponding to two types of C as in $\text{O}(\text{C}=\text{O})\text{O}-$ and $\text{C}-\text{O}-$, respectively (Figure 17c). The peak assignments were further supported by Raman spectroscopy (Figure 17d). The Raman spectrum reveals a strong peak at 1762 cm^{-1} , which corresponds to the $\text{C}=\text{O}$ stretching vibration mode, with a similar peak position to that of Li_2CO_3 . Compositional analysis demonstrates the conformal coating consists of LiF and Li alkyl carbonate with long hydrophobic carbon chains, which effectively suppresses the reactivity of Li_xSi NPs under ambient conditions.

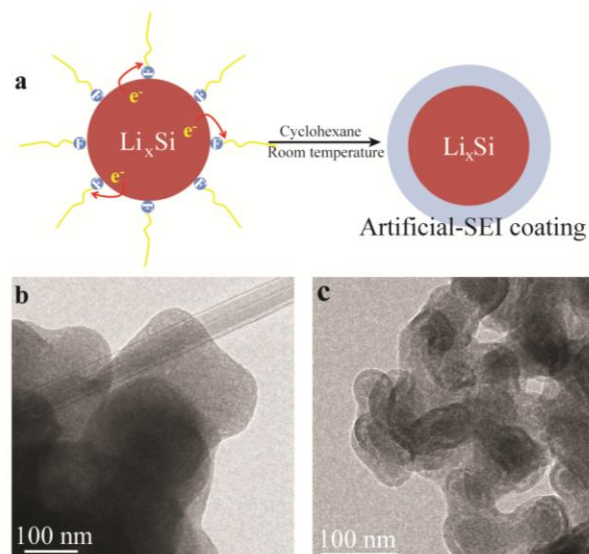


Figure 16. (a) Schematic diagram of the artificial-SEI coating formed by reducing 1-fluorodecane on the surface of Li_xSi NPs in cyclohexane. TEM images of Li_xSi NPs (b) before and (c) after coating.

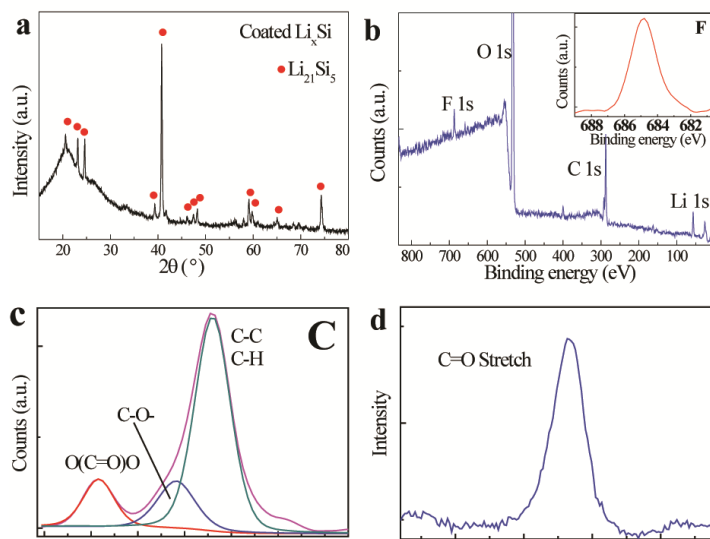


Figure 17. (a) XRD pattern of artificial-SEI coated Li_xSi NPs sealed in Kapton tape. (b) XPS of artificial-SEI coated Li_xSi NPs. Corresponding high-resolution XPS spectrum around F 1s peak region is shown in the inset. (c) High-resolution XPS spectra of C 1s. (d) Raman spectrum reveals the peak near 1762 cm^{-1} as the stretching vibration mode of $\text{C}=\text{O}$.

Patents/Publications/Presentations

1. Patent: S14-109| Dry-air-stable Li_xSi - Li_2O core-shell nanoparticles as high-capacity prelithiation reagents.
2. Zhao, J. et al. “Dry-air-stable Lithium Silicide–lithium Oxide Core–shell Nanoparticles as High-capacity Prelithiation Reagents.” *Nat. Commun.* 5, no. 5088 (2014).
3. Zhao, J. et al. “Artificial Solid Electrolyte Interphase-Protected Li_xSi Nanoparticles: An Efficient and Stable Prelithiation Reagent for Lithium-Ion Batteries.” *J. Am. Chem. Soc.*, 137 (2015).
4. Poster: 2015 MRS Spring Meeting and Exhibit.

TASK 3 – HIGH ENERGY DENSITY CATHODES FOR ADVANCED LITHIUM-ION BATTERIES

Summary and Highlights

Developing high energy density, low-cost, thermally stable, and environmentally safe electrode materials is a key enabler for advanced batteries for transportation. High energy density is synonymous with reducing cost per unit weight or volume. Currently, one major technical barrier toward developing high energy density lithium-ion batteries (LiBs) is the lack of robust, high-capacity cathodes. As an example, the most commonly used anode material for LiBs is graphitic carbon, which has a specific capacity of 372 mAh/g, while even the most advanced cathodes like lithium nickel manganese cobalt oxide (NMC) has a maximum capacity of ~180 mAh/g. This indicates an immediate need to develop high capacity (and voltage) intercalation type cathodes that have stable reversible capacities of 300 mAh/g and beyond. High volumetric density is also critical for transportation applications. Alternative high capacity cathode chemistries such as those based on conversion mechanisms, Li-S, or metal air chemistries still have fundamental issues that must be addressed before integration into cells for automotive use.

During the last decade, many high voltage cathode chemistries have been developed under the BATT (now BMR) program, including Li-rich NMC and Ni-Mn spinels. Current efforts are directed towards new syntheses and modifications to improve stability (both bulk and interfacial) under high-voltage cycling condition (> 4.6 V) for Li-rich NMC [Nanda, ORNL; Zhang & Jie, PNNL; Thackeray and Croy, ANL; Marca Doeff, LBNL]. Three other subtasks are directed toward synthesis and structural stabilization of high capacity, multivalent, polyanionic cathodes, both in crystalline and amorphous phases [Manthiram, UT-Austin; Looney and Wang, BNL; Whittingham, SUNY-Binghamton; and Kercher-Kiggans, ORNL]. Approaches also include aliovalent or isovalent doping to stabilize cathode structures during delithiation, as well as surface coatings to improve interfacial stability. John Goodenough's group at UT-Austin is developing novel separators to enable lithium metal anodes and high capacity cathodes in a flow cell.

The highlights for this quarter are as follows:

- **Task 3.1.** *In situ* XAS of $\text{Li}_2\text{Cu}_{1-x}\text{Ni}_x\text{O}_2$ high capacity cathodes identifies Ni^{2+} to Ni^{3+} redox activity.
- **Task 3.2.** Synthesis of high capacity CuF_2 – MoO_3 and CuF_2 – VOPO_4 composites.
- **Task 3.3.** AlF_3 coated $\text{Li}_{1.2}\text{Ni}_{0.15}\text{Co}_{0.10}\text{Mn}_{0.55}\text{O}_2$ (LMR-NMC) cathodes showed improved capacity retention and suppressed voltage fade.
- **Task 3.4.** Development of micro-reactors for battery materials synthesis using solvothermal.
- **Task 3.5.** LAP-coated $\text{LiNi}_0.5\text{Mn}_1.5\text{O}_4$ electrode exhibited enhanced electrochemical performance compared to the uncoated sample.
- **Task 3.6.** Synthesis of α - and/or β - LiVOPO_4 /graphene nanocomposites with > 200 mAh/g capacity.
- **Task 3.7.** Lithium copper phosphate glasses with borate and vanadate substitution showed negligible first cycle irreversible capacity.
- **Task 3.8.** Optimization of the synthesis condition for Ni-rich NMC cathode (622 & 442) by spray pyrolysis.
- **Task 3.9.** Demonstration of PETT-Ester coated PVDF membrane as a separator for a liquid cathode.
- **Task 3.10.** Synthesis and electrochemical characterization of high-capacity $\text{LiCo}_{1-x}\text{Ni}_x\text{O}_2$ ($x = 0.1$ and 0.2) cathodes.

Task 3.1 – Studies of High Capacity Cathodes for Advanced Lithium-ion Systems (Jagjit Nanda, Oak Ridge National Laboratory)

Project Objective. The overall project goal is to develop high energy density lithium-ion electrodes for EV and PHEV application that meet and/or exceed the DOE energy density and life cycle targets as from the USDRIVE/USABC roadmap. Specifically, this project aims to address and mitigate the technical barriers associated with high-voltage cathode compositions such as lithium-manganese rich NMC (LMR-NMC) and $\text{Li}_2\text{M}^{\text{I}}\text{M}^{\text{II}}\text{O}_2$, where M^{I} and M^{II} are transition metals that do not include Mn or Co. Major emphasis is placed on developing new materials modifications (including synthetic approaches) for high-voltage cathodes that will mitigate issues such as: (i) voltage fade associated with LMR-NMC composition that leads to loss of energy over the cycle life; (ii) transition metal dissolution that leads to capacity and power fade; (iii) thermal and structural stability under the operating SOC range; and (iv) voltage hysteresis associated with multivalent transition metal compositions. Another enabling feature of the project is utilizing (and developing) various advanced characterization and diagnostic methods at the electrode and/or cell level for studying cell and/or electrode degradation under abuse conditions. The techniques include electrochemical impedance spectroscopy, Micro-Raman, aberration corrected electron microscopy combined with EELS, x-ray photoelectron spectroscopy, ICP-AES, Fluorescence, and x-ray and Neutron diffraction.

Project Impact. The project has both short-term and long-term deliverables directed toward VTO Energy Storage 2015 and 2022 goals. Specifically, we are working on advanced electrode couples that have cell-level energy density targets of 400 Wh/kg and 600 Wh/l for 5000 cycles. Increasing the energy density per unit mass or volume ultimately reduces the cost of battery packs consistent with the DOE 2022 EV Everywhere goal of \$125/kWh.

Out-Year Goals. The project is directed toward developing high-capacity cathodes for advanced lithium-ion batteries. The goal is to develop new cathode materials that have high capacity, are based on low-cost materials, and meet the DOE road map in terms of safety and cycle life. Two kinds of high-energy cathode materials are being studied. Over the last few years, the principal investigator has worked on improving cycle life and mitigating energy losses of high-voltage, Li-rich composite cathodes (referred to as LMR-NMC) in collaboration with the voltage fade team at Argonne National Laboratory. The tasks also include working in collaboration with researchers at Stanford Synchrotron Research Laboratory (SSRL) and APS (LBNL) to understand local changes in morphology and microstructure under *in situ* and *ex-situ* conditions.

Collaborations. This project collaborates with Johanna Nelson, SSRL, SLAC: x-ray imaging and XANES; Guoying Chen, LBNL: *in situ* XAS and XRD; Feng Wang, Brookhaven National Lab: x-ray synchrotron spectroscopy and microscopy; and Bryant Polzin, Argonne Research Laboratory: CAMP Facility for electrode fabrication.

Milestones

1. Investigation of surface reactivity, vacancy disorder, and interfacial kinetics of LMR-NMC composite cathodes to mitigate voltage fade and TM dissolution. (12/31/14 – Complete)
2. Stabilize the structure and electrochemical performance of high capacity $\text{Li}_2\text{Cu}_x\text{Ni}_{1-x}\text{O}_2$ cathodes to achieve capacity between 250-300 mAh/g for > 50 charge-discharge cycles at C/3 rate. (03/31/15 – 80% complete)
3. Undertake *in situ* and *ex-situ* x-ray synchrotron and spectroscopic studies to correlate changes in local structure, surface chemistry, and morphology of cycled high energy density electrodes (LMR- NMC and 5V Mn-Ni spinel) and compare the changes with pristine or uncycled electrodes. (06/30/15 – Complete)
4. Investigate the role of Ni in stabilizing the structure of 2-Lithium Cu-Ni phase, and identify the role of oxygen reactivity from gas generation experiments. (09/30/15 – In Progress) [Smart Milestone]

Progress Report

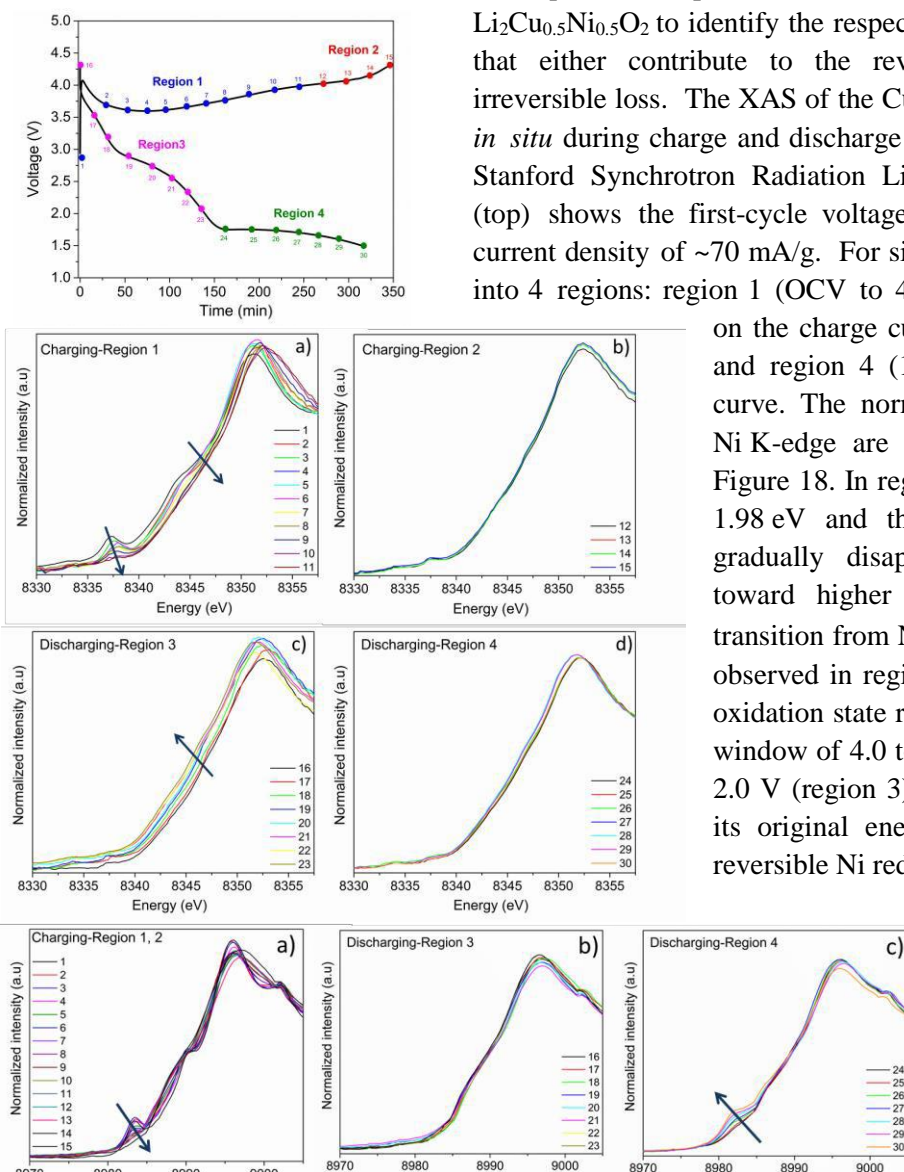


Figure 18. (Top) 1st charge and discharge plot of $\text{Li}_2\text{Cu}_{0.5}\text{Ni}_{0.5}\text{O}_2$ during the *in situ* XAS measurements. (Middle) Ni-K edge shift during various charge-discharge regions. (Bottom) Corresponding *in situ* XAS of Cu K-edge.

Unlike the Ni K-edge, the Cu K-edge did not show any systematic shift during the first charge up to 4.3 V in both region 1 and 2. The strong pre-edge peak at 8983 eV, however, also disappeared during charging, suggesting a change in symmetry or coordination in the Cu environment. No obvious change was observed on the copper oxidation state during discharge to 1.7 V in region 3. Further discharge to 1.5 V (region 4) resulted in the reappearance of the pre-edge feature. The results are consistent with the $\text{Cu}^+/\text{Cu}^{2+}$ transition. Details are being communicated as a journal publication.

This quarter we performed *in situ* x-ray absorption studies on $\text{Li}_2\text{Cu}_{0.5}\text{Ni}_{0.5}\text{O}_2$ to identify the respective Cu and Ni redox processes that either contribute to the reversible capacity or result in irreversible loss. The XAS of the Cu and Ni K-edges were collected *in situ* during charge and discharge (1.5-4.3 V) at beam line 4-1 at Stanford Synchrotron Radiation Lightsource (SSRL). Figure 18 (top) shows the first-cycle voltage profile of $\text{Li}_2\text{Cu}_{0.5}\text{Ni}_{0.5}\text{O}_2$ at a current density of ~70 mA/g. For simplicity, the profile was broken into 4 regions: region 1 (OCV to 4 V) and region 2 (4 to 4.3 V) on the charge curve, with region 3 (4.3 to 2 V) and region 4 (1.7 to 1.5 V) on the discharge curve. The normalized XANES spectra at the Ni K-edge are shown in the middle panel of Figure 18. In region 1, the Ni K-edge shifted by 1.98 eV and the pre-edge peak at 8337 eV gradually disappeared. The continuous shift toward higher energy is likely due to the transition from Ni^{2+} to Ni^{3+} . No further shift was observed in region 2, suggesting that the nickel oxidation state remained the same in the voltage window of 4.0 to 4.3 V. During the discharge to 2.0 V (region 3), the Ni K-edge shifted back to its original energy position which suggests a reversible Ni redox process.

However, the pre-edge feature at 8337 eV present in the pristine sample did not return. This provides clear evidence that permanent structural changes occurred during the charging process. The bottom panel of Figure 18 shows the normalized XANES spectra collected at the Cu K-edge.

Patents/Publications/Presentations

Presentations

- Annual Merit Review, DOE, Washington, D.C. (June 8 – 12, 2015): “Studies on High Capacity Cathodes for Advanced Lithium-ion Systems”; J. Nanda and R. Ruther.
- Indian Institute of Technology, Bhubaneswar, India (June 24, 2015), Invited: “New Frontiers in Electrochemical Energy Storage: Materials and Systems”; J. Nanda.

Publications

- Nanda, J., and S. K. Martha, and R. Kalyanaraman. “High-capacity Electrode Materials for Electrochemical Energy Storage: Role of Nanoscale Effects.” *Pramana – Journal of Physics* 54, no. 6 (2015): 1073. Invited Review.
- Ruther, R., and H. Dixit, A. Pezesheki, R. Sacci, V. Cooper, J. Nanda and G. Veith. “Correlating Local Structure with Electrochemical Activity in Li_2MnO_3 .” *J. Phys. Chem C* (2015). Accepted.
- Ruther, R., and H. Zhou, C. Dhital, K. Saravanan, A. K. Kercher, G. Chen, A. Huq, Frank M. Delnick, and J. Nanda. “Synthesis, Structure, and Electrochemical Performance of High Capacity $\text{Li}_2\text{Cu}_{0.5}\text{Ni}_{0.5}\text{O}_2$ Cathodes.” Manuscript ready for submission.

Task 3.2 – High Energy Density Lithium Battery (Stanley Whittingham, SUNY Binghamton)

Project Objective. The project objective is to develop the anode and cathode materials for high-energy density cells for use in plug-in hybrid electric vehicles (PHEVs) and in electric vehicles (EV) that offer substantially enhanced performance over current batteries used in PHEVs and with reduced cost. Specifically, the primary objectives are to:

- Increase the volumetric capacity of the anode by a factor of 1.5 over today's carbons
 - Using a SnFeC composite conversion reaction anode
- Increase the capacity of the cathode
 - Using a high capacity conversion reaction cathode, CuF_2 , and/or
 - Using a high capacity 2 Li intercalation reaction cathode, VOPO_4
- Enable cells with an energy density exceeding 1 kWh/liter

Project Impact. The volumetric energy density of today's lithium-ion batteries is limited primarily by the low volumetric capacity of the carbon anode. If the volume of the anode could be cut in half, and the capacity of the cathode to over 200 Ah/kg, then the cell energy density can be increased by over 50% to approach 1 kWh/liter (actual cell). This will increase the driving range of vehicles.

Moreover, smaller cells using lower cost manufacturing will lower the cost of tomorrow's batteries.

Out-Year Goals. The long-term stretch goal of this project is to enable cells with an energy density of 1 kWh/liter. This will be accomplished by replacing both the present carbon used in Li-ion batteries with anodes that approach double the volumetric capacity of carbon, and the present intercalation cathodes with materials that significantly exceed 200 Ah/kg. By the end of this project, it is anticipated that cells will be available that can exceed the volumetric energy density of today's Li-ion batteries by 50%.

Collaborations. The Advanced Photon Source (Argonne National Laboratory) and when available the National Synchrotron Light Source II (Brookhaven National Laboratory) will be used to determine the phases formed in both *ex-situ* and *operando* electrochemical cells. University of Colorado, Boulder, will provide some of the electrolytes to be used.

Milestones

1. Demonstrate synthesis and complete characterization of CuF_2 . (December – Complete)
2. Determine discharge product of CuF_2 . (March – Complete)
3. Begin cyclability testing of CuF_2 . (June – Complete)
4. Demonstrate more than 100 cycles on Sn_2Fe at 1.5 times the volumetric energy density of carbon. (September – Ongoing)
5. *Go/No-Go*: Demonstrate cyclability of CuF_2 . Criteria: Capacity of 200 mAh/g over 10 cycles. (September)

Progress Report

The goal of this project is to synthesize tin-based anodes that have 1.5 times the volumetric capacity of the present carbons, and conversion and intercalation cathodes with capacities over 200 Ah/kg.

The major effort in this third quarter was to study the impact of making composites of CuF_2 and several oxides. Studies on the anode are also underway.

Milestone 2. “Using first a CuF_2/C composite, then a $\text{CuF}_2/\text{MoO}_3$ composite, and finally make a $\text{CuF}_2/\text{VOPO}_4$ composite, determine discharge product of CuF_2 .” This milestone has been completed. Composites of CuF_2 with carbon and either MoO_3 or LiVOPO_4 were synthesized; the products of reaction were determined to be merely mixtures of the two materials, with no new compounds formed. This is in contrast to the composites of CuF_2 and FeF_2 , reported last quarter, where a complete solid solution was found. The MoO_3 composite was found to exhibit close to the expected theoretical capacity on the first reaction with lithium in electrochemical cells as shown in Figure 19; the LiVOPO_4 composite was somewhat lower. However, there was a sharp drop-off in capacity on the second and subsequent discharge cycles for the CuF_2 and $\text{CuF}_2/\text{MoO}_3$ composite. In contrast, the solid solution $\text{Cu}_{1-y}\text{Fe}_y\text{F}_2$, retains its capacity for several cycles.

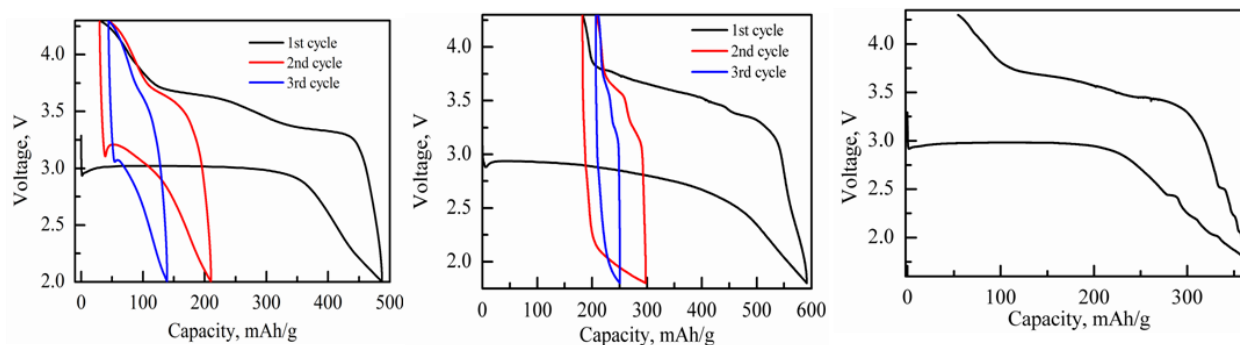


Figure 19. Cycling behavior of (left) CuF_2 , (middle) $\text{CuF}_2/\text{MoO}_3$, and (right) $\text{CuF}_2/\text{VOPO}_4$.

Milestone 3. “Begin cyclability testing of CuF_2 .” Based on the results found for Milestone 2, major effort is focused on the solid solution $\text{Cu}_{1-y}\text{Fe}_y\text{F}_2$ composite with carbon. Initial cycling behavior is showing promising results, as indicated in Figure 20.

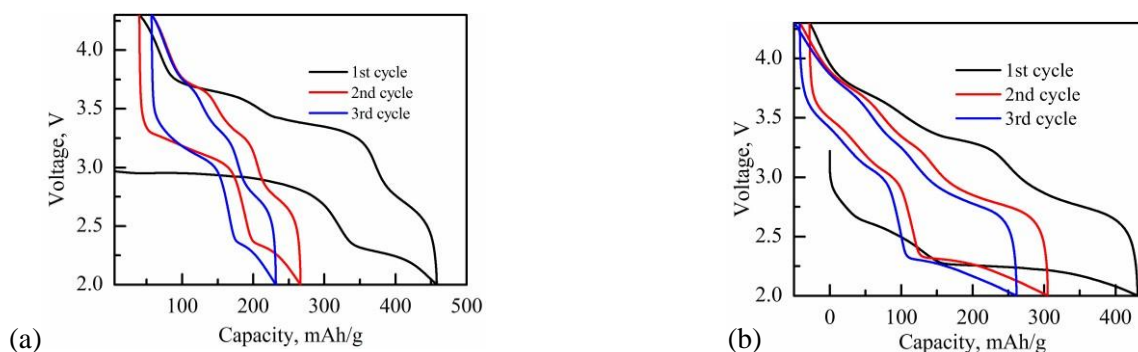


Figure 20. The initial cycling behavior of the solid solution $\text{Cu}_{1-y}\text{Fe}_y\text{F}_2$, (a) $y= 0.2$, (b) 0.5 cathode.

Milestone 4. The extended cyclability of the Sn^{2+}Fe anode composite with carbon is under way, and more than 100 cycles have been achieved (reported at June 2015 Annual Merit Review). The tap density of this composite was determined to be around 1.8 g/cc, much higher than graphitic carbon; tap density of the latter was determined to be much less than half that of the composite, and the best carbons do not exceed 1 g/cc.

Patents/Publications/Presentations

Presentation: DOE-EERE Annual Merit Review, Washington, D.C. (June 10, 2015): “High Energy Density Lithium Battery”; Stanley Whittingham.

Dong, Zhixin. “Tin-Iron Based High Capacity Anodes for Lithium-Ion Batteries.” PhD thesis, Binghamton University (April 28, 2015). *Note:* From this BMR and prior BATT funding.

Jiang, Tianchan. “Synthesis and Characterization of Novel Anode Materials for Lithium Ion Batteries.” PhD thesis, Binghamton University (March 31, 2015) *Note:* From prior BATT funding.

Task 3.3 – Development of High-Energy Cathode Materials (Ji-Guang Zhang and Jie Xiao, Pacific Northwest National Laboratory)

Project Objective. The objective of this project is to develop high-energy, low-cost, cathode materials with long cycle life. Based on the knowledge gathered in FY14 on the failure mechanism of Li-Mn-rich (LMR) cathode, synthesis modification will be pursued to improve distribution of different transition metal cations at the atomic level. Leveraging with PNNL's advanced characterization capabilities, the effects from synthesis alteration and the surface treatment will be monitored and correlated to the electrochemical properties of LMR to guide the rational design of LMR. Extension of the cutoff voltage on traditional layered $\text{LiNi}_{1/3}\text{Mn}_{1/3}\text{Co}_{1/3}\text{O}_2$ (NMC) will be also investigated to increase the usable energy density from NMC while maintaining structural integrity and long lifespan.

Project Impact. Although state-of-the-art cathode materials such as LMR layered composites have very high energy densities, their voltage fade and long-term cycling stability still need to be further improved. In this work, we will investigate the fundamental fading mechanism of LMR cathodes and develop new approaches to reduce the energy loss of these high-energy cathode materials. The success of this work will increase the energy density of Li-ion batteries and accelerate market acceptance of electrical vehicles (EV), especially for plug-in hybrid electrical vehicles (PHEV) required by the EV Everywhere Grand Challenge proposed by the DOE/EERE.

Out-Year Goals. The long-term goal of the proposed work is to enable Li-ion batteries with a specific energy of $> 96 \text{ Wh/kg}$ (for PHEVs), 5000 deep-discharge cycles, 15-year calendar life, improved abuse tolerance, and less than 20% capacity fade over a 10-year period.

Collaborations. This project engages with the following collaborators:

- Dr. Bryant Polzin (ANL)- LMR electrode supply
- Dr. X.Q. Yang (BNL) – *in situ* XRD characterization during cycling
- Dr. Karim Zaghib (Hydro-Quebec) – material synthesis
- Dr. Kang Xu (ARL) – new electrolyte

Milestones

1. Investigate the transition metal migration pathway in LMR during cycling. (12/31/14 – Complete)
2. Identify appropriate synthesis step to enhance the homogenous cation distribution in the lattice and demonstrate 200 stable cycling with less than 10% energy loss. (3/31/15 – Complete)
3. Develop the surface treatment approaches to improve the stability of high-energy cathode at high-voltage conditions. (6/30/2015 – Complete)
4. Demonstrate high-voltage operation of modified NCM with 180 mAh/g capacity and less than 20% capacity fade for 100 cycling. (9/30/2015 – Ongoing)

Progress Report

The third quarter milestone has been completed. Li-rich Mn-rich (LMR) cathode material $\text{Li}_{1.2}\text{Ni}_{0.15}\text{Co}_{0.10}\text{Mn}_{0.55}\text{O}_2$ (HE5050 LMR-NMC) has been coated with AlF_3 , which proved to be an effective coating material in enhancing the performance of LMR cathode materials. The AlF_3 -coated material showed substantially improved cycling stability, exhibiting negligible capacity loss after 100 cycles (Figure 21a). Moreover, the AlF_3 -coated material showed mitigated voltage fade during cycling (Figure 21b-c).

Microstructures of cycled uncoated and AlF_3 -coated materials were characterized in detail by STEM to get insight on the functioning mechanism of AlF_3 coating. For uncoated material, a thick SEI layer (10~20 nm) was formed on the particle surface (Figure 22a) owing to the aggressive side reactions occurring at high voltages, typically > 4.5 V. Spinel-like structure was identified at surface regions over the whole particle of uncoated material after cycling (Figure 22b). A number of corrosion pits with diameters ranging from 10 nm to 100 nm were observed at the particle surface (Figure 22c), ascribed to the continuous attack by the acidic species in the electrolyte. All of these negative effects lead to a rapid increase of the charge transfer resistance and the fast capacity fading.

In contrast, neither a thick SEI layer nor severe corrosion phenomena, such as etched particle surfaces and corrosion pits, was detected in cycled AlF_3 -coated material (Figure 22d). It was found that phase transformation from layered to spinel-like structure still occurred at the surface region of the AlF_3 -coated material (Figure 22e), with a depth of several nanometers. R-3m LiMO_2 -type layered structure was well reserved in the bulk region of the material as projected along the [100] zone of the R-3m phase (Figure 22f).

Although the structural transformation from layered to spinel-like phase was unavoidable, with AlF_3 coating, the structural stability of the spinel-like phase and the electrode/electrolyte interface were significantly enhanced, facilitating the reversible Li^+ ion de/intercalation processes in LMR cathode materials and enabling substantially improved long-term cycle life. The fundamental findings of this work may also be widely applicable to explain the functioning mechanisms of other surface coatings used for LMR cathode materials.

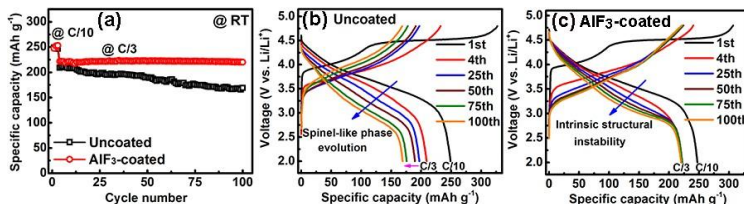


Figure 21. (a) The AlF_3 -coated material showed substantially improved cycling stability, exhibiting negligible capacity loss after 100 cycles. (b) The AlF_3 -coated material showed mitigated voltage fade during cycling.

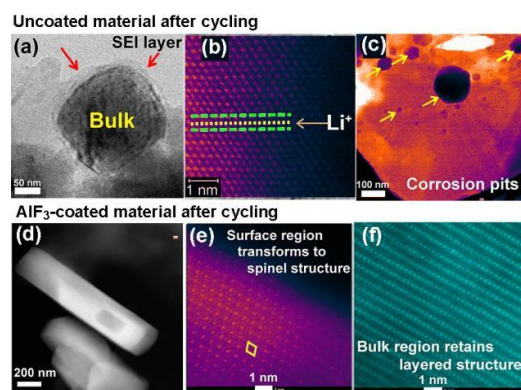


Figure 22. Characterization of (a-c) uncoated and (d-f) AlF_3 -coated materials after 100 cycles. (a) TEM image showing a thick SEI layer formation. (b) High resolution Z-contrast image showing the formation of spinel-like/rock-salt phase at particle surface region. (c) Z-contrast images showing corrosion pit formation. (d) Overview Z-contrast image of AlF_3 -coated material after cycling. (e) Z-contrast image showing the spinel-like phase formation at the surface of cycled particle. (f) STEM images showing that the bulk region maintained layered structure.

Patents/Publications/Presentations

Xiao, Liang, and Jie Xiao, Xiqian Yu, Pengfei Yan, Jianming Zheng, Mark Engelhard, Priyanka Bhattacharya, Chongmin Wang, Xiao-Qing Yang, and Ji-Guang Zhang. "Effects of Structural Defects on the Electrochemical Activation of Li_2MnO_3 ", *Nano Energy* 16 (2015): 143-151.

Task 3.4 – *In situ* Solvothermal Synthesis of Novel High Capacity Cathodes (Patrick Looney and Feng Wang, Brookhaven National Laboratory)

Project Objective. Develop low-cost cathode materials that offer high energy density (≥ 660 Wh/kg) and electrochemical properties (cycle life, power density, safety) consistent with USABC goals.

Project Impact. Present-day Li-ion batteries are incapable of meeting the 40-mile all-electric- range within the weight and volume constraints established for PHEVs by the DOE and USABC. Higher energy density cathodes are needed for Li-ion batteries to be widely commercialized for PHEV applications. This effort will focus on increasing energy density (while maintaining the other performance characteristics of current cathodes) using synthesis methods that have the potential to lower cost. The primary deliverable for this project is a reversible cathode with an energy density of about 660 Wh/kg or higher.

Out-Year Goals. In FY15, we will continue work on *in situ* solvothermal synthesis, structural and electrochemical characterization of V-based (fluoro)phosphates and other high-capacity cathodes. We will also work on technique development for *in situ* synthesis. Out-year goals include:

- Determining the reaction pathway during ion-exchange of $\text{Li}(\text{Na})\text{VPO}_5\text{F}_x$
- Optimizing the ion-exchange procedures to maximize the Li-exchange content in $\text{Li}(\text{Na})\text{VPO}_5\text{F}_x$
- Characterizing the structure of the intermediate and final exchanged products of $\text{Li}(\text{Na})\text{VPO}_5\text{F}_x$ and their electrochemical properties
- Identifying at least one cathode material, with reversible specific capacity higher than 200 mAh/g under moderate cycling conditions
- Developing new *in situ* reactors that may be applied for different types of synthesis methods (beyond solvothermal) in making phase-pure cathodes
- Building new capabilities for simultaneous *in situ* measurements of multiple synthesis reactions in the newly built beamlines at NSLS II

Collaborations. This project engages with the following collaborators: Jianming Bai, Lijun Wu, Yimei Zhu, (Brookhaven Nat. Lab), Peter Khalifha (Stony Brook U.), Kirsuk Kang (Seoul Nat. U.), Nitash Balsara, Wei Tong (Lawrence Berkeley Nat. Lab), Jagjit Nanda (Oak Ridge Nat. Lab), Arumugam Manthiram (U. Texas at Austin), Brett Lucht (U. Rhode Island), Zaghbi Karim (Hydro-Quebec), Jason Graetz (HRL).

Milestones

1. Determine the reaction pathways and phase evolution during hydrothermal ion exchange synthesis of $\text{Li}(\text{Na})\text{VPO}_5\text{F}_x$ cathodes via *in situ* studies. (12/01/14 – Complete)
2. Optimize ion exchange synthesis for preparing $\text{Li}(\text{Na})\text{VPO}_5\text{F}_x$ with maximized Li content, and characterize its structural and electrochemical properties. (3/01/15 – Complete)
3. Develop new reactor design to enable high-throughput synthesis of phase-pure cathode materials. (6/01/15 – Complete)
4. Obtain good cycling stability of one high-capacity cathode in a prototype cell with specific capacity higher than 200 mAh/g. No-Go if 80% capacity retention after 50 cycles cannot be achieved. (9/01/15 – On Schedule)

Progress Report

In previous quarters, we reported the development and utilization of *in situ* reactors for real-time probing of reactions involved with solvothermal synthesis of cathode materials. These reactors give access to the study of intermediate and short-lived phases, and enable deep insights as to how temperature, pressure, time, and precursor concentration affect the kinetic reaction pathways. In this quarter, we report the development of micro-reactors of a more flexible design that accommodates different types of synthesis (*e.g.*, solvothermal, ion-exchange, solid-state reactions), and their applications in both *in situ* and *ex-situ* studies of kinetics and pathways of a particular reaction. These micro-reactors enable combinatorial screening of a large number of synthesis parameters, thereby opening new avenues in the search for high-capacity cathodes. This approach requires only small amounts of precursor materials for synthesis studies, and fast post-synthesis phase identification by XRD can be undertaken directly to the products within the reactors.

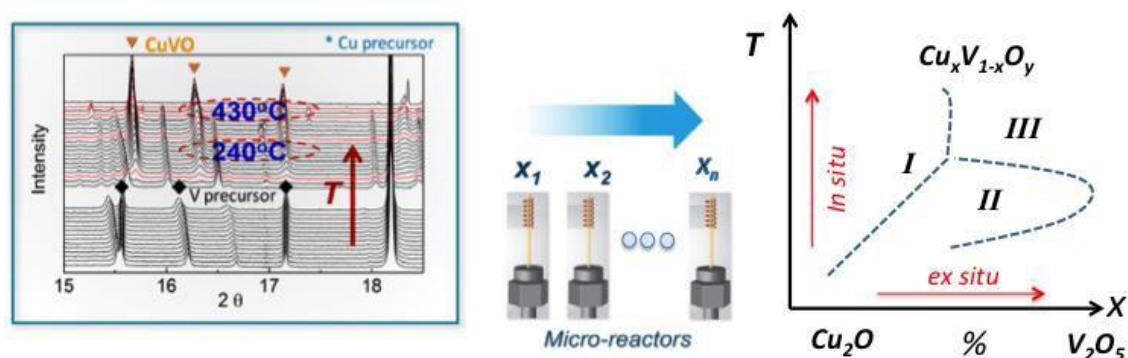


Figure 23. Design of micro-reactors for both *in situ* and *ex-situ* combinatorial studies of synthesis reactions, enabling high-throughput synthesis of new cathode materials (an example of $Cu_xV_{1-x}O_y$ being used here).

Application of these micro-reactors was demonstrated in the synthesis of Cu-V-O (Figure 23). Using *in situ* XRD to track phase formation in the micro-reactor, we found that the α - $CuVO_3$ phase started to form at temperatures as low as 240°C, and the pure phase was obtained at 430°C within one hour; this contrasts with tens of hours of solid-state reaction at $\sim 700^\circ\text{C}$ or above (as is commonly done). Further, *in situ* studies can now be coupled with combinatorial studies of different reactions by using multiple micro-reactors that contain precursors (Cu_2O and V_2O_5 in this case) of varying concentration, to cover wide composition-temperature space (as illustrated in Figure 23).

Coupled with the dramatic advances in beamline design at NSLS-II, where high-quality XRD patterns (wide collection angle along with high angular resolution) can be acquired in less than a second (Figure 24), these micro-reactors enable high throughput synthesis. It is estimated that tens of samples may be studied in minutes, thereby greatly reducing the time for optimizing synthesis procedures in preparing new phase-pure cathode materials.

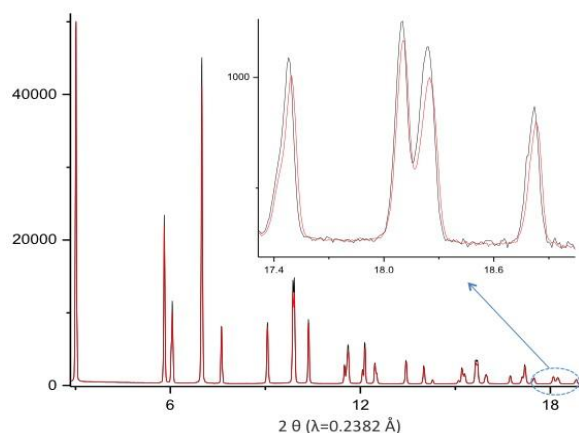


Figure 24. The XRD patterns obtained from powder sample within sub-seconds.

Patents/Publications/Presentations

Presentation: SRI Meeting, New York (July 6 – 12, 2015): “Tracking the Crystalline Phases in Solution-based Syntheses of Battery Materials with *In situ* Time-re-solved Synchrotron X-ray Powder Diffraction”; J. Bai and F. Wang.

Task 3.5 – Novel Cathode Materials and Processing Methods (Michael M. Thackeray and Jason R. Croy, Argonne National Laboratory)

Project Objective. The goal of this project is to develop low-cost, high-energy and high-power Mn-oxide-based cathodes for lithium-ion batteries that will meet the performance requirements of PHEV and EV vehicles. Improving the design, composition and performance of advanced electrodes with stable architectures and surfaces, facilitated by an atomic-scale understanding of electrochemical and degradation processes, is a key objective of this work.

Project Impact. Standard lithium-ion battery technologies are currently unable to meet the demands of next-generation PHEV and EV vehicles. Battery developers and scientists alike will take advantage of the knowledge generated from this project, both applied and fundamental, to further advance the field. In particular, it is expected that this knowledge will enable progress toward meeting the DOE goals for 40-mile, all-electric range PHEVs.

Approach. Exploit the concept and optimize the performance of structurally integrated “composite” electrode structures with a prime focus on “layered-layered-spinel” materials. Alternative processing routes will be investigated; the Argonne National Laboratory comprehensive characterization facilities will be used to explore novel surface and bulk structures by both *in situ* and *ex-situ* techniques in the pursuit of advancing the properties of state-of-the-art cathode materials. A theoretical component will complement the experimental work of this project.

Out-Year Goals. Identify high-capacity (‘layered-layered’ and ‘layered-spinel’) composite electrode structures and compositions that are stable to electrochemical cycling at high potentials (~4.5 V).

Identify and characterize surface chemistries and architectures that allow fast Li-ion transport and mitigate or eliminate transition-metal dissolution.

Use complementary theoretical approaches to further the understanding of electrode structures and electrochemical processes to accelerate progress of materials development.

Scale-up, evaluate, and verify promising cathode materials using Argonne National Laboratory scale-up and cell fabrication facilities.

Collaborators. This project engages with the following collaborators: Joong Sun Park, Arturo Gutierrez, Christopher Johnson, Fulya Dogan, Vic Maroni, Roy Benedek (CSE), and Mali Balasubramanian (APS).

Milestones

1. Optimize the capacity and cycling stability of composite cathode structures with a low (~10%) Li_2MnO_3 content. Target capacity = 190-200 mAh/g (baseline electrode). (September 2015 – In Progress)
2. Scale up the most promising materials to 1 kg batch size at the Argonne Materials Engineering Research Facility (MERF). (April 2015 – Delayed due to limited availability of MERF)
3. Synthesize and characterize unique surface architectures that enable >200 mAh/g at a >1C rate with complementary theoretical studies of surface structures. (September 2015 – In Progress, see text)
4. Optimize capacity and cycling stability of composite cathode structures with a medium (~20%) Li_2MnO_3 content. Target capacity = 200-220 mAh/g (advanced electrode). (September 2015 – In Progress)

Progress Report

As part of our objective to design unique surface structures that allow high capacities above 200 mAh/g at a 1C rate from composite electrode structures, aliovalent cation doping in Li_3PO_4 coatings was further investigated. Previous reports showed that Ni^{2+} substitution for Li^+ in Li_3PO_4 [$\text{Li}_{3-2x}\text{Ni}_x\text{PO}_4$; \square = lithium vacancy; $x = 0.01$ - 0.02)] enhances the electrical conductivity by about an order of magnitude at room temperature. Trivalent cation dopants, such as Al^{3+} , have an advantage over divalent dopants because twice the number of vacancies can be created in the structure. A microwave-assisted hydrothermal (MW-HT) process is being used to coat $\text{Li}_{3-3x}\text{Al}_x\text{PO}_4$ ($0 \leq x \leq 0.2$) on underlying cathode materials and to explore the consequent electrochemical properties of the coated electrodes. The MW-HT process is a low-temperature ($<300^\circ\text{C}$) approach that allows for rapid processing of inorganic materials with unique morphologies. A series of Al-doped Li_3PO_4 materials was synthesized at 125°C in just five minutes with this technique. The XRD patterns of $\text{Li}_{3-3x}\text{Al}_x\text{PO}_4$ ($0 \leq x \leq 0.2$) showed a single phase β - Li_3PO_4 product without detectable impurities (for example, AlPO_4), suggesting that Li^+ had been substituted by Al^{3+} in the structure. Figure 25a shows the ^{27}Al magic-angle-spinning nuclear magnetic resonance (MAS NMR) spectra of $\text{Li}_{2.7}\text{Al}_{0.1}\text{PO}_4$ and $\text{Li}_{2.4}\text{Al}_{0.2}\text{PO}_4$ powders synthesized by the MW-HT method. The chemical shift at ~ 45 ppm corresponds to 4-coordinated Al^{3+} (substitution in the tetrahedral Li sites), while the shift at -9 ppm corresponds to 6-coordinated Al^{3+} in the octahedral sites of the structure. Note that the octahedral sites share faces with the tetrahedral sites (as indicated by the green arrow in Figure 25(a-inset)). A weak chemical shift at ~ 15 ppm suggests some 5-fold coordination of the Al^{3+} ions in the structure. The occupation of Al^{3+} in tetrahedral, octahedral, and 5-fold coordinated positions therefore distributes the higher charge density of Al^{3+} over three sites. NMR experiments, combined with Raman spectroscopy and structural simulations are currently being explored to better understand these substituted structures.

Evaluation of 10% Al-doped Li_3PO_4 , i.e. $\text{Li}_{2.7}\text{Al}_{0.1}\text{PO}_4$, as a coating material for two model systems, namely the spinel phase $\text{LiNi}_{0.5}\text{Mn}_{1.5}\text{O}_4$ and layered LiCoO_2 , has been completed. It is well known that these cathodes suffer from transition metal migration and/or surface degradation at high potentials ($>4.4\text{V}$ vs. Li/Li^+). Scanning electron microscopy and energy dispersive x-ray spectroscopy (SEM/EDX) data of a $\text{LiNi}_{0.5}\text{Mn}_{1.5}\text{O}_4$ sample, coated with 2 wt% $\text{Li}_{2.7}\text{Al}_{0.1}\text{PO}_4$ (LAP), showed that the coating was homogenous (Figure 25b). The LAP-coated $\text{LiNi}_{0.5}\text{Mn}_{1.5}\text{O}_4$ electrode exhibited enhanced electrochemical performance compared to the uncoated sample in lithium half cells at room temperature (data not shown). Figure 25c shows the first discharge (4.4-2.5V at 20 mA/g) of a standard LiCoO_2 electrode and those coated with 2, 5, and 10 wt% LAP. As expected, higher concentrations of the coating increased the overpotential during discharge. Further studies are underway on samples to determine the effect of the Al concentration on Li-diffusion through $\text{Li}_{3-3x}\text{Al}_x\text{PO}_4$ coatings.

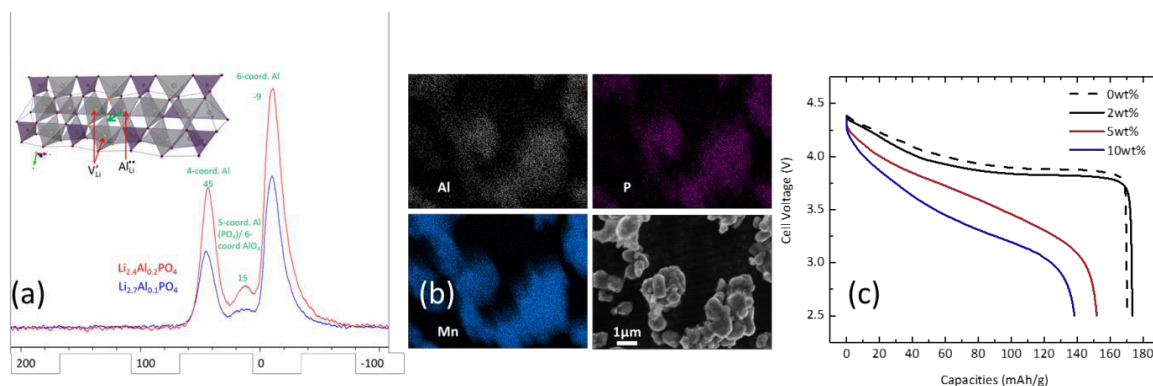


Figure 25. (a) ^{27}Al MAS NMR spectra of 10% (blue) and 20% (red) Al-doped Li_3PO_4 ; Inset: illustration of Al octahedral occupancy in $\text{Li}_{3-3x}\text{Al}_x\text{PO}_4$. (b) SEM/EDX data of $\text{Li}_{2.7}\text{Al}_{0.1}\text{PO}_4$ coated $\text{LiNi}_{0.5}\text{Mn}_{1.5}\text{O}_4$. (c) First-cycle discharge profiles of $\text{Li}_{2.7}\text{Al}_{0.1}\text{PO}_4$ -coated LiCoO_2 for various coating loadings (4.4 – 2.5 V, 20mA/g).

Patents/Publications/Presentations

Patent Applications

- M. M. Thackeray, J. R. Croy and B. R. Long, *Cobalt-Stabilized Lithium Metal Oxide Electrodes for Lithium Batteries*, U.S. Pat. Appl. 20150180032, 25 June 2015.
- A. U. Mane, J. S. Park, J. R. Croy, J. W. Elam, *Metal Fluoride Passivation Coatings Prepared by Atomic Layer Deposition for Li-Ion Batteries*, Filed at USPTO (2015).

Publication

- Park, J. S., and A. U. Mane, J. W. Elam, and J. R. Croy. “Amorphous Metal Fluoride Passivation Coatings Prepared by Atomic Layer Deposition on LiCoO₂ for Li-Ion Batteries.” *Chem Mater.* 27, no. 6 (2015): 117.

Presentations

- MRS Meeting, San Francisco, (April 6 – 10, 2015): “Ultrathin Metal Fluoride Coatings for High Energy Li-Ion Batteries”; J. S. Park, A. U. Mane, J. W. Elam, and J. R. Croy.
- ECS Meeting, Chicago, (May 24 – 28, 2015): “Amorphous Metal Fluorides Coatings by Atomic Layer Deposition for Stable Li-Ion Batteries”; A. U. Mane, J. S. Park, J. R. Croy, and J. W. Elam.
- Annual Merit Review, DOE Vehicle Technologies Program, Arlington, VA (June 8 – 12, 2015): “and Evaluation of High Capacity Cathodes”; M. M. Thackeray.
- Annual Merit Review, DOE Vehicle Technologies Program, Arlington VA, (June 8 – 12, 2015): “User Facilities for Energy Storage Materials Research”; J. R. Croy.
- Annual Meeting of the STFC Global Challenge Network in Batteries and Electrochemical Energy Devices, Abingdon, (June 30 – July 1, 2015): “Electrical Energy Storage: Looking Back – Looking Forward”; M. M. Thackeray.

Task 3.6 – High-capacity, High-voltage Cathode Materials for Lithium-ion Batteries (Arumugam Manthiram, University of Texas, Austin)

Project Objective. A significant increase in capacity and/or operating voltage is needed to make the lithium-ion technology viable for vehicle applications. This project addresses this issue by focusing on the design and development of cathode materials based on polyanions that have the possibility for reversibly inserting/extracting more than one lithium ion per transition-metal ion and/or operating above 4.3 V. Specifically, high-capacity and/or high-voltage lithium transition-metal phosphate, silicate, and carbonophosphate cathodes are investigated. The major issue with the phosphate and silicate cathodes is the poor electronic and ionic transport, which limits the practical capacity, energy density, and power density. To overcome these difficulties, novel microwave-assisted solvothermal, microwave-assisted hydrothermal, and template-assisted synthesis approaches are pursued to realize controlled morphology with smaller particle size and to integrate conductive additives like graphene in a single synthesis step.

Project Impact. The critical requirements for the widespread adoption of lithium-ion batteries for vehicle applications are high energy, high power, long cycle life, low cost, and acceptable safety. The currently available cathode materials do not adequately fulfill these requirements. The polyanion cathodes with the novel synthesis approaches pursued in this project have the potential to significantly increase the energy and power. More importantly, the covalently bonded polyanion groups can offer excellent thermal stability and enhanced safety. The microwave-assisted synthesis approaches pursued also lower the manufacturing cost of the cathodes through a significant reduction in reaction time and temperature.

Out-Year Goals. The overall goal is to enhance the electrochemical performances of high-capacity, high-voltage polyanion cathode systems and to develop a fundamental understanding of their structure-composition-performance relationships. Specifically, the project is focused on enhancing the electrochemical performance of systems such as LiMPO_4 , $\text{Li}_2\text{MP}_2\text{O}_7$, LiYMSiO_4 , $\text{Li}_3\text{V}_2(\text{PO}_4)_3$, $\text{Li}_9\text{V}_3(\text{P}_2\text{O}_7)_3(\text{PO}_4)_2$, $\text{Li}_3\text{M}(\text{CO}_3)(\text{PO}_4)$, and their solid solutions with $\text{M} = \text{Mn, Fe, Co, Ni, and VO}$. Advanced structural, chemical, surface, and electrochemical characterizations of the materials synthesized by novel approaches are anticipated to provide in-depth understanding of the factors that control the electrochemical properties of the polyanion cathodes. For example, the possible segregation of certain cations to the surface in solid solution cathodes consisting of multiple transition-metal ions as well as the role of conductive graphene integrated into the polyanion cathodes can help design better-performing cathodes.

Collaborations. Please list current collaborations in this section, whether inside or outside the BMR Program.

Milestones

1. Demonstrate the synthesis of LiVOPO_4 nanoparticles with $> 200 \text{ mAh/g}$ capacity by employing ordered macroporous carbon as a hard-template. (December 2014 – Complete)
2. Demonstrate aliovalent doping with Ti^{4+} in $\text{LiM}_{1-2x}\text{Ti}_x\text{PO}_4$ with enhanced electrochemical properties by the microwave-assisted solvothermal synthesis. (March 2015 – Complete)
3. Demonstrate the synthesis of α - and/or β - LiVOPO_4 /graphene nanocomposites with $> 200 \text{ mAh/g}$ capacity by the microwave-assisted process. (June 2015 – Complete)
4. *Go/No-Go*: Demonstrate the extraction of more than one lithium ($> 110 \text{ mAh/g}$) through aliovalent doping in $\text{Li}_2\text{M}_{1-3/2x}\text{V}_x\text{P}_{x/2}\text{P}_2\text{O}_7$ by low-temperature synthesis approaches. (September 2015 – Ongoing)

Progress Report

Our previous work on the layered α_1 -LiVOPO₄ (tetragonal) demonstrated the importance of incorporating graphene nanosheets to enhance the electrical conductivity of the cathodes. In this quarter, this strategy has been extended to the α -LiVOPO₄ (triclinic) and β -LiVOPO₄ (orthorhombic) by the microwave-assisted solvothermal (MW-ST) method. The bare triclinic α -LiVOPO₄ without graphene was first synthesized by the MW-ST process reported by us at 230°C in water/ethanol medium. The α -LiVOPO₄/graphene nanocomposite was then synthesized by the same procedure with the addition of different amounts of graphene oxide (GO) to the reaction mixture. During the MW-ST process, GO is reduced to graphene. X-ray diffraction (XRD) data indicated that phase-pure α -LiVOPO₄ in the composite could be obtained only when the GO concentration is $< 0.4 \text{ mg mL}^{-1}$ in the reaction mixture, which resulted in a rather low graphene content of $< 3 \text{ wt.}\%$ in the α -LiVOPO₄/graphene nanocomposite. This result differs from that of the tetragonal α_1 -LiVOPO₄/graphene system, where a graphene content of up to 10 wt.% could be realized. On the other hand, no phase-pure β -LiVOPO₄ could be formed at all in the presence of GO. Optimization of synthesis conditions, such as increasing the reaction temperatures/pressures or varying the water/ethanol ratios, was not successful. These results imply that the known conditions to prepare pure phases of bare α - and β -LiVOPO₄ are not suitable when GO is present. The incorporation of graphene in the α -LiVOPO₄/graphene (3 wt.%) sample was confirmed by scanning electron microscopy (SEM, Figure 26a), in which LiVOPO₄ spheres are partially wrapped by graphene sheets. This composite cathode shows a high initial discharge capacity of 210 mA h g^{-1} at C/20 rate (Figure 26b), but with some capacity fade.

In addition, we have systematically investigated the phase evolution (Figure 27) with the three forms of LiVOPO₄ by chemical lithiation with n-butyllithium and delithiation with NO₂BF₄. The delithiated product from α_1 -LiVOPO₄ is a new phase of VOPO₄ that is isostructural with α_1 -LiVOPO₄ (tetragonal). The phase change with β -Li₂VOPO₄ is being investigated with neutron diffraction at ORNL. Moreover, it was found that complete delithiation of α -LiVOPO₄ could only be achieved by treating the sample with at least two times excess NO₂BF₄ (Figure 28).

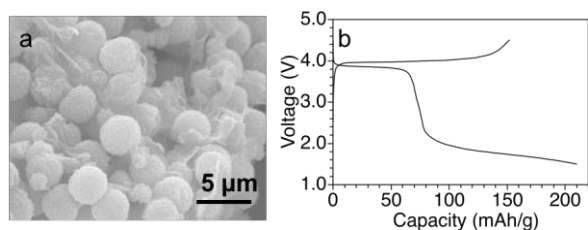


Figure 26. (a) SEM image of the α -LiVOPO₄/graphene nanocomposite ($\sim 3 \text{ wt.}\%$ graphene) and (b) its first charge-discharge profiles at C/20 rate.

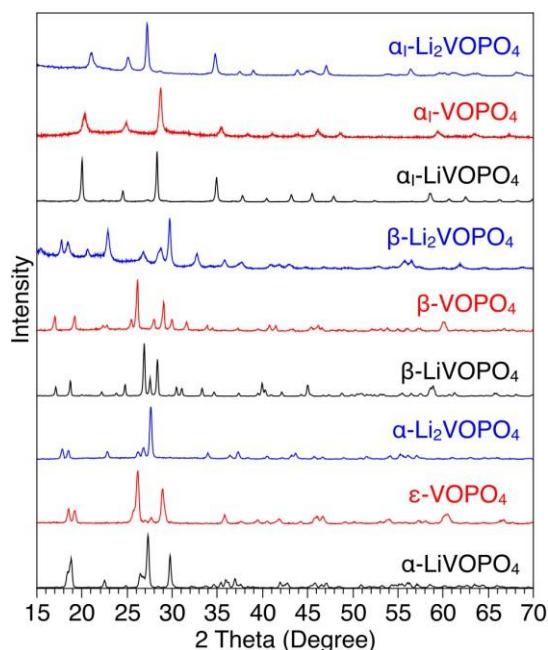


Figure 27. XRD patterns of the three forms of LiVOPO₄ and their delithiated and lithiated products.

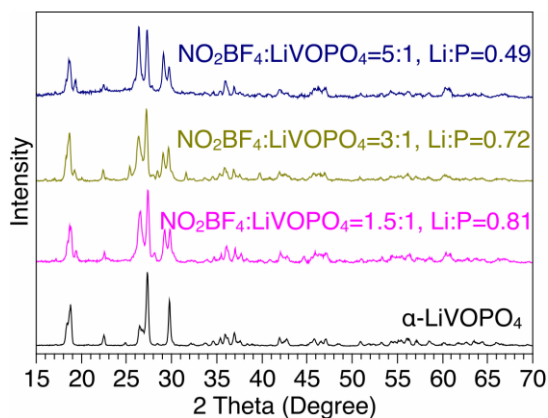


Figure 28. XRD patterns and chemical analysis results of the delithiated products of α -LiVOPO₄.

Patents/Publications/Presentations

Publications

- He, G., and L. Li, and A. Manthiram. “VO₂/rGO Nanorods as a Potential Anode for Sodium- and Lithium- ion Batteries.” *Journal of Materials Chemistry A* 3 (2015): 14750-14758.
- Xiang, X., and J. C. Knight, W. Li, and A. Manthiram. “Sensitivity and Intricacy of Cationic Substitutions on the First Charge/Discharge Cycle of Lithium-rich Layered Oxide Cathodes.” *Journal of the Electrochemical Society* 162 (2015): A1662-A1666.

Presentations

- Hanyang University, Seoul, South Korea, (May 19, 2015) Invited: “High Energy Density Rechargeable Batteries”; A. Manthiram.
- Institute of Chemistry, Beijing, China, (June 1, 2015) Invited: “Next Generation Rechargeable Battery Chemistries”; A. Manthiram.

Task 3.7 – Lithium-bearing Mixed Polyanion (LBMP) Glasses as Cathode Materials (Jim Kiggans and Andrew Kercher, Oak Ridge National Laboratory)

Project Objective. Develop mixed polyanion (MP) glasses as potential cathode materials for lithium ion batteries with superior performance to lithium iron phosphate for use in electric vehicle applications. Modify MP glass compositions to provide higher electrical conductivities, specific capacities, and specific energies than similar crystalline polyanionic materials. Test MP glasses in coin cells for electrochemical performance and cycleability. The final goal is to develop MP glass compositions for cathodes with specific energies up to near 1,000 Wh/kg.

Project Impact. The projected performance of MP glass cathode materials addresses the Vehicle Technology Multi-Year Plan goals of higher energy densities, excellent cycle life, and low cost. MP glasses offer the potential of exceptional cathode energy density up to 1,000 Wh/kg, excellent cycle life from a rigid polyanionic framework, and low-cost, conventional glass processing.

Out-Year Goals. MP glass development will focus on compositions with expected multi-valent intercalation reactions within a desirable voltage window and/or expected high-energy glass-state conversion reactions.

Polyanion substitution will be further adjusted to improve glass properties to potentially enable multi-valent intercalation reactions and to improve the discharge voltage and cycleability of glass-state conversion reactions. Cathode processing of the most promising mixed polyanion glasses will be refined to obtain desired cycling and rate performance. These optimized glasses will be disseminated to BMR collaborators for further electrochemical testing and validation.

Collaborations. No collaborations this quarter.

Milestones

1. Perform electron microscopy on mixed polyanion glass cathodes at key states of charge. (December 2014 – Completed 12/04/14)
2. Produce and electrochemically test MP glasses designed to have enhanced ionic diffusivity. (March 2015 – Completed 3/31/15)
3. Produce and electrochemically test an MP glass designed to have enhanced ionic diffusivity and theoretically capable of a multi-valent intercalation reaction. (June 2015 – Completed 6/30/15)
4. Determine the polyanion substitution effect on a series of non-phosphate glasses. (September 2015 – In Progress)

Progress Report

Lithium copper phosphate glasses were produced with excess lithium and polyanion content and substituted with borate and vanadate with the goal of enabling a multi-valent intercalation reaction. However, only a limited intercalation reaction (3.4 - 2.4V) was observed in these glasses, and the intercalation capacity increased with polyanion content of the glass.

The conversion reaction (2.4 - 1V) had a high capacity. Interestingly, the first cycle irreversible loss, which is commonly fairly large in MP glass cathodes, was nearly eliminated, and the voltage hysteresis decreased substantially with increasing polyanion content. Fundamental compositional changes that established desirable changes in physical properties will continue to be explored to improve the electrochemical performance of MP glass cathodes.

MP glass cathode materials have amorphous structures that can have complicated compositions and can undergo both intercalation and conversion reactions. Establishing an appropriate voltage window for cycling can be important for obtaining maximum capacity while avoiding deleterious irreversible reactions that promote cycling fade. Cyclic voltammetry is now being used to identify key voltages of electrochemical reactions, to establish optimal voltage windows for cycling, and to determine common reaction features among families of glasses. For example, using cyclic voltammetry results, a key voltage limit for cycling of silver phosphate vanadate (AgMP-50V) was identified, which significantly affected the cycling performance (Figure 30).

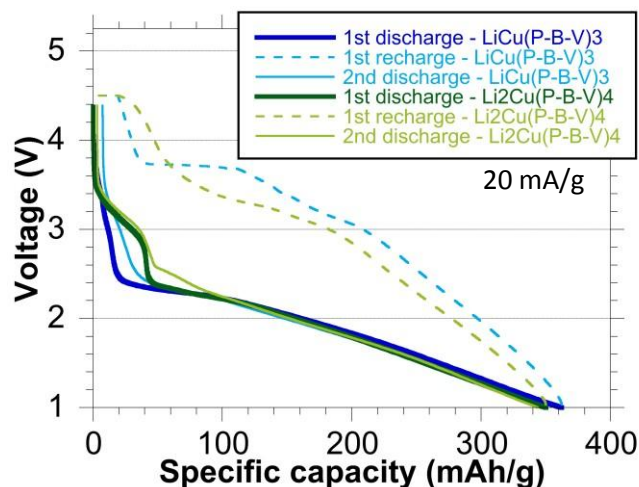


Figure 29. Lithium copper phosphate glasses with borate and vanadate substitution ($\text{Li}_x\text{Cu}(\text{P-B-V})_y$) showed negligible 1st cycle irreversible capacity.

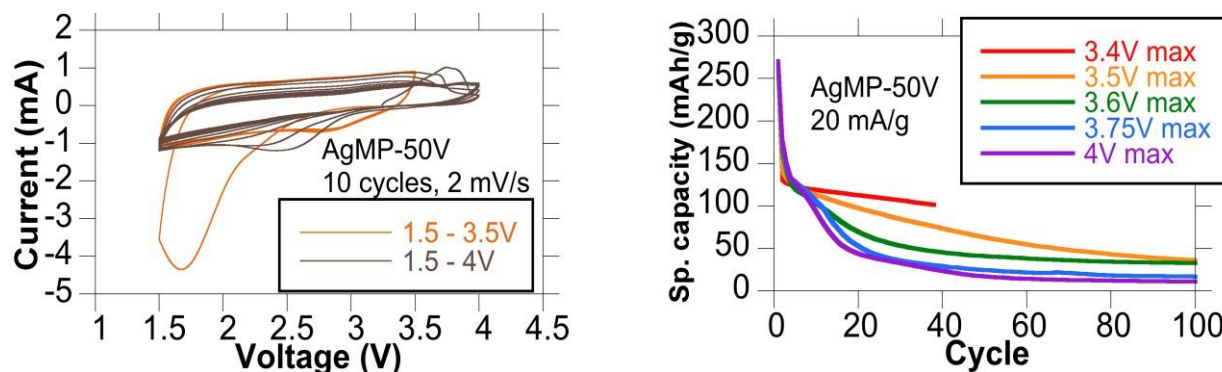


Figure 30. Cyclic voltammetry (CV) of silver metaphosphate glass with 50% vanadate substitution (AgMP-50V) showed excellent cycleability between 3.5 V and 1.5 V after the first cycle, but progressive irreversible loss when further charged to 4 V. Cycling with different maximum charge voltages agreed with the CV result.

Task 3.8 – Design of High Performance, High Energy Cathode Materials (Marca Doeff, Lawrence Berkeley National Laboratory)

Project Objective. The objective of the project is to develop high-energy, high-performance cathode materials including composites and coated powders, using spray pyrolysis and other synthesis techniques. The emphasis is on high-voltage systems including NMCs designed for higher voltage operation. Experiments are directed toward optimizing the synthesis, improving cycle life, and understanding the behavior of NMCs subjected to high voltage cycling. Particle size and morphology are controlled during spray pyrolysis synthesis by varying residence time, temperature, precursors and other synthetic parameters. By exploiting differences in precursor reactivity, coated materials can be produced, and composites can be prepared by post-processing techniques such as infiltration. These approaches are expected to improve cycling due to reduced side reactions with electrolytes.

Project Impact. To increase the energy density of Li ion batteries, cathode materials with higher voltages and/or higher capacities are required, but safety and cycle life cannot be compromised. In the short term, the most promising materials are based on NMCs modified to undergo high-voltage cycling that do not require formation cycles or undergo structural transformations during cycling. Spray pyrolysis synthesis results in high quality materials that can be coated (solid particles) or used as the basis for composites (hollow particles) designed to withstand high-voltage cycling.

Out-Year Goals. The objective is to design high-capacity NMC cathodes that can withstand high-voltage cycling without bulk structural transformation. Materials will be synthesized by a simple, low-cost spray pyrolysis method, which has potential for commercialization. This technique produces phase-pure, unagglomerated powders and allows for excellent control over particle morphologies, sizes, and distributions. Coated materials will also be produced in either one or two simple steps by exploiting differing precursor reactivities during the spray pyrolysis procedure, or by first preparing hollow spheres of an electroactive material, infiltrating the spheres with precursors of a second phase (for example, high voltage spinel), and subsequent thermal treatment. The final result is expected to be a high energy density cathode material with good safety and cycling characteristics suitable for use in vehicular applications, which can be made by a low-cost process that is easily scalable.

Collaborations. TXM has also been used this quarter to characterize NMC materials, work done in collaboration with Yijin Liu (SSRL). Synchrotron and computational efforts are continued in collaboration with Professor M. Asta (UCB), Dr. Dennis Nordlund (SSRL), Dr. Yijin Liu (SSRL), Dr. Tsu-Chien Weng (SSRL) and Dr. Dimosthenis Sokaras (SSRL). Atomic layer deposition was performed in collaboration with Dr. Chunmei Ban (NREL). The TEM effort is continued in collaboration with Dr. Huolin Xin (BNL). We are also collaborating with Professor Shirley Meng (UCSD), Dr. Chunmei Ban (NREL), and Dr. Wei Tong (LBNL) on soft XAS and x-ray Raman characterization of materials.

Milestones

1. Complete synchrotron x-ray Raman experiments on representative NMC samples. (12/31/14 – Experiments and Analysis Completed; Paper in Preparation)
2. Finish survey of composites made with spray pyrolyzed NMC hollow particles. (3/31/15 – Postponed due to equipment and space issues)
3. *Go/no go decision:* Feasibility of coating processes using spray pyrolysis methods or molecular layer deposition. (6/30/15 – On Track)
4. Select best-performing coated or composite material based on capacities and high-voltage cycling results. (9/30/15 – On Track)

Progress Report

Spray pyrolysis synthesis of cathode materials continued this quarter with more electrochemical measurements and characterization. In particular, nickel rich NMC (NR-NMC) materials, such as 622, were targeted. Previously, we encountered several challenges in preparing NR-NMC materials by spray pyrolysis. Different annealing atmospheres, temperature and excess lithium content were examined. This quarter, we focused on the lithium content. The most important parameter seems to be the excess lithium content. The best synthesis conditions are with 20% excess lithium and 800 °C; this product yielded first cycle discharge capacity of over 200 mAh/g. However, cycling stability needs to be further improved.

As for NMC-442 materials, this quarter, we performed in-depth characterization of these using full-field transmission x-ray microscopy (TXM) to elucidate the elemental distribution of both the as-pyrolyzed NMC442 precursor and the annealed NMC442 powder. We analyzed the elemental association throughout the 3D volume by performing a correlation analysis of the absorption coefficient as a function of the x-ray energies (above and below the K-edges of all the three transition metal elements). The Mn-Co-Ni association was only 70% for both the lithium-containing precursor powder and the annealed NMC-442 product. 10% of the total voxels contain a single transition metal in the precursor, which reduced to 5% after annealing at 850°C. This observation indicates the migration of transition metals during thermal annealing. Direct visualization was achieved by color mapping individual elemental associations in 3D, as shown in Figure 31. A large number of nanodomains showed significant deviation from the global NMC-442 composition. The interior elemental associations were visualized by slicing through the particles and are shown in the bottom of Figure 31. While the bulks of these particles also deviated from the global NMC-442 composition in parts, there are more three-element domains than on the surfaces. These 3D and 2D elemental association maps clearly show that there segregation of transition metals throughout the hierarchically structured materials.

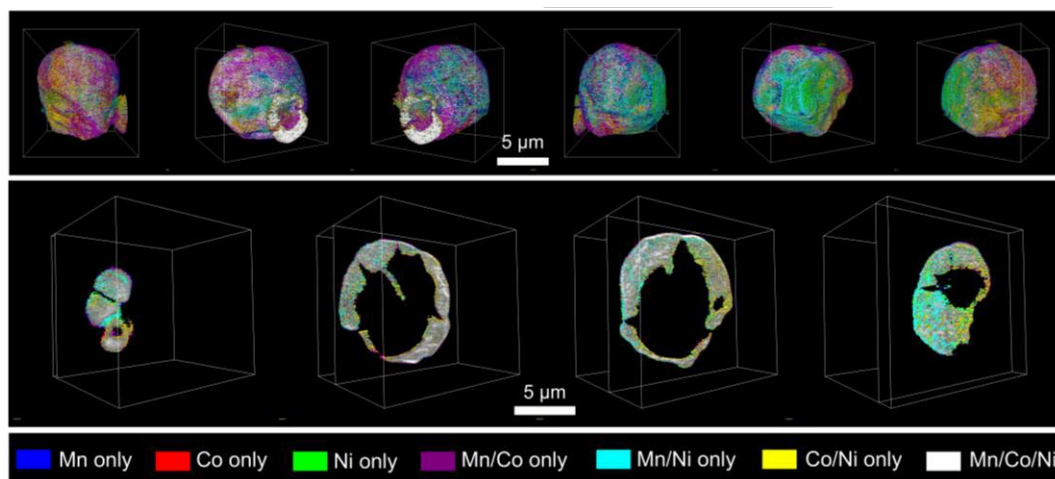


Figure 31. Elemental association maps of spray pyrolyzed NMC powder after annealing at 850°C. Top: 3D rendering of the elemental associations viewing the particles at different angles. Bottom: 2D slices of the elemental associations. The colors presenting the elemental associations are shown at the bottom.

Patents/Publications/Presentations

1. Iturrondobeitia, A., and A. Goñi, I. Oruc, I. Gil de Muro, L. Lezama, M. M. Doeff, and T. Rojo. “Effect of Carbon Coating on the Physico-chemical and Electrochemical Properties of Fe_2O_3 Nanoparticles.” *Inorg. Chem.* 54 (2015): 5239.
2. Lin, Feng, and Yuyi Li, Dennis Nordlund, Tsu-Chien Weng, Huolin Xin, and Marca Doeff. “Layered Cathode Materials Prepared by Spray Pyrolysis for High-Energy Lithium-Ion Batteries.” 20th International Conference on Solid State Ionics, Keystone, Colorado (June 14 – 19, 2015).
3. Cheng, Lei, and Guoying Chen, and Marca M. Doeff. “Probing Interfaces of Garnet Solid Electrolytes in Lithium Batteries.” 20th International Conference on Solid State Ionics, Keystone, Colorado (June 14 – 19, 2015).
4. Shirpour, Mona, and Marca Doeff. “Sodium-Ion Batteries: Beyond Lithium-Ion.” Tech Connect World Innovation Conference, Washington D.C. (June 14 – 17, 2015).
5. Markus, Isaac, and Mona Shirpour, Simon Engelke, Mark Asta, and Marca Doeff. “First Principles Investigation of Sodium Intercalation Mechanisms into Corrugated Titanate Structures for Sodium-Ion Battery Anodes.” 227th meeting of the Electrochemical Society, Chicago, Illinois (May 2015).
6. Shirpour, Mona, and Dhruv Seshadri, and Marca Doeff. “Electrochemistry of Nonatitanates in Lithium and Sodium Ion Batteries.” 227th meeting of the Electrochemical Society, Chicago, Illinois (May 2015).

Task 3.9 – Lithium Batteries with Higher Capacity and Voltage (John B. Goodenough, UT – Austin)

Project Objective. The objectives of this project are to increase cell energy density for a given cathode and to allow low-cost rechargeable batteries with cathodes other than insertion compounds.

Project Impact. A solid Na^+ or Li^+ -electrolyte separator would permit use of a Li^0 anode, thus maximizing energy density for a given cathode, and liquid flow-through and air cathodes of high capacity as well as high-voltage solid cathodes given two liquid electrolytes having different windows.

Out-Year Goals. The out-year goals are to increase cell energy density for a given cathode and to allow low-cost, high-capacity rechargeable batteries with cathodes other than insertion compounds.

Collaborations. This project collaborates with A. Manthiram at UT Austin and with Karim Zaghib at Hydro Quebec.

Milestones

1. Fabricate oxide/polymer composite membrane as a separator in an alkali-ion (Li^+ , Na^+) battery and optimization of pore size, oxide loading, and thickness for blocking anode dendrites with fast alkali-ion transport. (3/31/15 – Complete)
2. Investigate membranes that can block a customized soluble redox couple in a flow-through cathode. (6/30/15 – Complete)
3. Evaluate Li-ion and Na-ion cells with a metallic Li or Na anode, oxide/polymer membrane as separator, and a flow-through liquid cathode. (9/30/15 – Complete).
4. Measure performance of cells with a metallic Li or Na anode, oxide/polymer composite membrane as separator, and an insertion compound as cathode. (12/31/15)

Progress Report

In the previous quarter, we fabricated a PETT-Ester membrane (PETT is a tetrathiol crosslinker and Ester stands for divinyl adipate) via thiol-ene polymerization and characterized it with FTIR and DSC. For the study, we had made free-standing solid electrolyte membranes, so controlling the membrane thickness was limited by the thickness of a spacer. Here we adopt a porous PVDF membrane as a support and coated the desired polymer layer on it. Figure 32 shows the processing scheme. The PVDF membrane was treated to make its surface hydrophilic, so the PETT-Ester monomer solution could wet the surface homogeneously. In this way, we were able to control the membrane thickness and to eliminate rolling of the membrane after the coating or electrolyte soaking.

The fabricated PETT-Ester on PVDF membrane was used as a separator in a cell with a liquid cathode. The redox molecule in the catholyte is 6-bromohexyl ferrocene, and lithium metal was used as the anode. Figure 33 shows initial charge/discharge voltage curves of the half-cell. Electrochemical activity of the Fe(III)/Fe(II) redox couple was clearly observed, so the membrane is permeable to the charge carrier, Li^+ ions. However, the voltage curves show notable polarization. We attribute the cell impedance to the trapping of the Li^+ ions by the electron-donating nature of the ester groups in the separator. The ester group can transfer electronic charges to Li^+ to bind, which hinders fast Li^+ transport through the separator membrane. We could understand from the experiment that controlling the chemical nature of the membrane is also an important factor to control ionic transport kinetics.

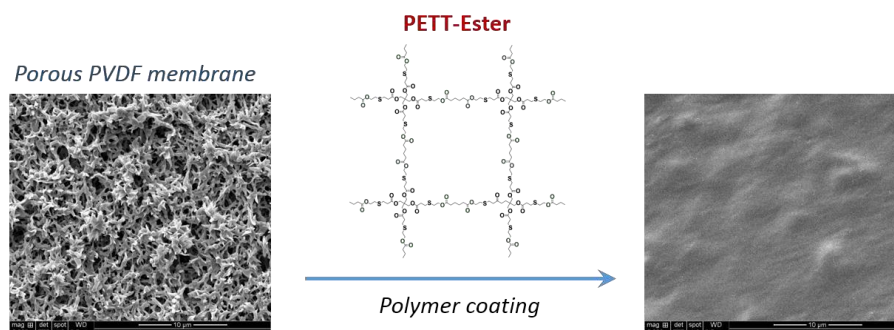


Figure 32. Processing scheme for PETT-Ester polymer coating on a porous PVDF membrane.

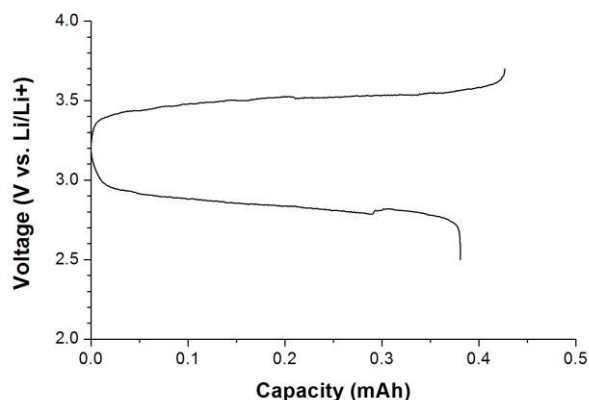


Figure 33. Charge/discharge voltage curves of 6-bromohexyl ferrocene catholyte with the PETT-Ester-coated PVDF membrane as a separator.

Task 3.10 – Exploiting Co and Ni Spinel in Structurally Integrated Composite Electrodes (Michael M. Thackeray and Jason R. Croy, Argonne National Laboratory)

Project Objective. This is a new project, the goal of which is to stabilize high capacity, composite ‘layered-layered’ electrode structures with lithium-cobalt-oxide and lithium-nickel-oxide spinel components (referred to as LCO-S and LNO-S, respectively), or solid solutions thereof (LCNO-S), which can accommodate lithium at approximately 3.5 V vs. metallic lithium. This approach and the motivation to use LCO-S and LNO-S spinel components, about which relatively little is known, is novel.

Project Impact. State-of-the-art lithium-ion batteries are currently unable to satisfy the performance goals for plug-in hybrid- (PHEV) and all-electric (EV) vehicles. If successful, this project will impact the advance of energy storage for electrified transportation as well as other applications, such as portable electronic devices and the electrical grid.

Approach. Focus on the design and synthesis of new spinel compositions and structures that operate above 3 V and below 4 V and to determine their structural and electrochemical properties through advanced characterization. This information will subsequently be used to select the most promising spinel materials for integration as stabilizers into high-capacity composite electrode structures.

Out-Year Goals. The electrochemical capacity of most high-potential lithium-metal oxide insertion electrodes is generally severely compromised by their structural instability and surface reactivity with the electrolyte at low lithium loadings (that is, at highly charged states). Although some progress has been made by cation substitution and structural modification, the practical capacity of these electrodes is still restricted to approximately 160-170 mAh/g. This project proposes a new structural and compositional approach with the goal of producing electrode materials that can provide 200-220 mAh/g without significant structural or voltage decay for 500 cycles. If successful, the materials processing technology will be transferred to the Argonne Materials Engineering and Research Facility (MERF) for scale up and further evaluation.

Collaborations. This project collaborates with Eungje Lee, Joong Sun Park (CSE, ANL), Mali Balasubramanian (APS, ANL), and V. Dravid and C. Wolverton (Northwestern University).

Milestones

1. Synthesize and optimize LCO-S, LNO-S and LCNO-S spinel compositions and structures and determine their structural and electrochemical properties. (September 2015 – In Progress, see text)
2. Devise synthesis techniques to embed the most promising spinel compositions into layered structures. (September 2015 – In Progress)
3. Determine the impact of embedding LCO-S or LNO-S components on the electrochemical properties and cycling stability of composite ‘layered-spinel’ or ‘layered-layered-spinel’ structures. (September 2015 – In Progress)
4. Use complementary theoretical approaches to further the understanding of the structural and electrochemical properties of LCO-S, LNO-S and LCNO-S electrodes and protective surface layers. (September 2015)

Progress Report

Past reports have shown successful preparation of the lithiated spinel phase $\text{Li}_2[\text{Co}_2]\text{O}_4$ by a ‘low temperature’ (LT) solid-state synthesis method. The electrochemical performance of this phase was further enhanced by Ni-substitution for Co (for example, $\text{LT-LiCo}_{0.9}\text{Ni}_{0.1}\text{O}_2$). In this mild synthesis route, precise control of the synthesis temperature and time is of critical importance to the properties of the final product. In this report, a systematic study of the effects of synthesis temperature and time on the crystal structure and electrochemical performance of $\text{LiCo}_{1-x}\text{Ni}_x\text{O}_2$ electrode materials is described.

$\text{LiCo}_{1-x}\text{Ni}_x\text{O}_2$ ($x = 0.1$ and 0.2) compounds were produced by solid-state synthesis at various temperatures ($400 - 800^\circ\text{C}$) for different furnace dwelling times. As previously reported, the spinel $\text{LiCo}_{0.9}\text{Ni}_{0.1}\text{O}_2$ (Fd-3m, $a = 8.0 \text{ \AA}$) is obtained at 400°C . When indexed to the layered structure (R-3m), the a - and c -axis parameters are 2.827 \AA and 13.850 \AA , respectively, where the c/a ratio of 4.90 indicates, within experimental error, an ideal cubic-close-packed oxygen-ion lattice ($c/a=4.89$) as shown in Table 1. An impurity, $\text{Li}_x\text{Ni}_{1-x}\text{O}$, rock-salt phase was observed in the 400°C -3d sample but disappeared after 6 days of annealing. The XRD patterns of the 500°C -6d and 600°C -4d samples could also be indexed to a spinel phase with similar lattice parameters. However, a detailed examination of the 600°C -4d sample reveals asymmetric broadening of the (044) peak at lower 2θ (Figure 34a), revealing the onset of layered ordering between the lithium and cobalt/nickel ions at 600°C . The XRD patterns of the samples synthesized at 700°C and above clearly show the development of a layered structure. For example, the (044) peak in the spinel phase (Fd-3m) splits into the (018) and (110) peaks of a layered component (R3-m), increasing the c/a ratio to 4.99; it indicates the significant enhancement of an ordered layered structure. The XRD patterns of the $\text{LiCo}_{0.8}\text{Ni}_{0.2}\text{O}_2$ samples, prepared at various temperatures, show the same trends as a function of synthesis temperature.

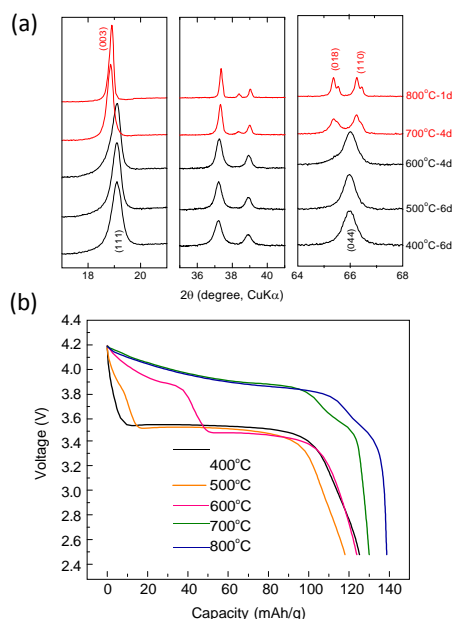


Figure 34: (a) XRD patterns and (b) initial discharge profiles of the $\text{LiCo}_{0.9}\text{Ni}_{0.1}\text{O}_2$ samples synthesized at various temperatures between 400 and 800°C .

The electrochemical data of the $\text{LiCo}_{1-x}\text{Ni}_x\text{O}_2$ ($x = 0.1$ and 0.2) compounds exhibit voltage profiles expected for spinel, layered and composite structures and their corresponding synthesis temperatures. Figure 34b shows initial voltage response of $\text{LiCo}_{0.9}\text{Ni}_{0.1}\text{O}_2$ electrodes ($2.5 - 4.2 \text{ V}$). For higher synthesis temperatures, the sloping voltage response at $\sim 4.0 \text{ V}$ is characteristic of the ‘high-temperature’ (HT) layered LiCoO_2 structure, while for the lower synthesis temperatures the reaction at $\sim 3.5 \text{ V}$ is characteristic of ‘low-temperature’ (LT) spinel LiCoO_2 . The significant contribution from the 3.5 V plateau and the 4.0 V slope in the 600°C sample confirms its intermediate structure between the LT-spinel and HT-layered phases. Further synthesis, structural and electrochemical characterization studies of these spinel-related compositions in structurally integrated composite electrodes are in progress.

Table 1: Lattice parameters of the $\text{LiCo}_{1-x}\text{Ni}_x\text{O}_2$ ($x = 0.1$ and 0.2) samples synthesized at various temperatures.

$\text{LiCo}_{0.9}\text{Ni}_{0.1}\text{O}_2$				$\text{LiCo}_{0.8}\text{Ni}_{0.2}\text{O}_2$			
Sample	$a [\text{\AA}]$	$c [\text{\AA}]$	c/a	Sample	$a [\text{\AA}]$	$c [\text{\AA}]$	c/a
$400^\circ\text{C} - 6\text{d}$	2.827	13.850	4.90	$400^\circ\text{C} - 6\text{d}$	-	-	-
$500^\circ\text{C} - 6\text{d}$	2.826	13.846	4.90	$500^\circ\text{C} - 6\text{d}$	2.830	13.864	4.90
$600^\circ\text{C} - 4\text{d}$	2.825	13.838	4.90	$600^\circ\text{C} - 4\text{d}$	2.830	13.866	4.90
$700^\circ\text{C} - 4\text{d}$	2.817	14.05	4.99	$700^\circ\text{C} - 4\text{d}$	2.823	14.066	4.98
$800^\circ\text{C} - 1\text{d}$	2.817	14.056	4.99	$800^\circ\text{C} - 1\text{d}$	2.822	14.069	4.99

Patents/Publications/Presentations

Patent Applications

- M. M. Thackeray, J. R. Croy and B. R. Long, Lithium Metal Oxide Electrodes for Lithium Batteries, U.S. Pat. Appl. 20150180031, 25 June 2015.

Presentations

- Perspectives on Catalysis and Energy Workshop, Pontificia Universidad Catolica de Chile, Santiago, Chile (April 28 – 29, 2015): “Progress in Designing High Capacity Cathodes for Lithium Cells: Challenges and Opportunities in an Evolving Lithium Economy”; M. M. Thackeray.
- Materials Science and Engineering Department, Northwestern University, Evanston, Illinois (May 7, 2015) Invited seminar presentation: “Structure-Property Relationship of 2D Layered Materials for Sodium- and Lithium-ion Batteries”; Eungje Lee.

TASK 4 – ELECTROLYTES FOR HIGH-VOLTAGE, HIGH-ENERGY LITHIUM-ION BATTERIES

Summary and Highlights

The current lithium-ion electrolyte technology is based on LiPF_6 solutions in organic carbonate mixtures with one or more functional additives. Lithium-ion battery chemistries with energy density of 175~250 Wh/Kg are the most promising choice. To further increase the energy density, the most efficient way is to raise either the voltage and/or the capacity of the positive materials. Several high energy materials including high-capacity composite cathode $x\text{Li}_2\text{MnO}_3 \bullet (1-x)\text{LiMO}_2$ and high-voltage cathode materials such as $\text{LiNi}_{0.5}\text{Mn}_{1.5}\text{O}_4$ (4.8 V) and LiCoPO_4 (5.1 V) have been developed. However, their increased operating voltage during activation and charging poses great challenges to the conventional electrolytes, whose organic carbonate-based components tend to oxidatively decompose at the threshold beyond 4.5 V vs Li^+/Li .

Other candidate positive materials for PHEV application that have potential of providing high capacity are the layered Ni-rich NCM materials. When charged to a voltage higher than 4.5 V, they can deliver a much higher capacity. For example, $\text{LiNi}_{0.8}\text{Co}_{0.1}\text{Mn}_{0.1}\text{O}_2$ (NCM 811) only utilizes 50% of its theoretical capacity of 275 mAh/g when operating in a voltage window of 4.2 V-3.0 V. Operating voltage higher than 4.4 V would significantly increase the capacity to 220 mAh/g; however, the cell cycle life becomes significantly shortened mainly due to the interfacial reactivity of the charged cathode with the conventional electrolyte. The oxidative voltage instability of the conventional electrolyte essentially prevents the practicality to access the extra capacities of these materials.

To address the above challenges, new electrolytes that have substantial high-voltage tolerance at high temperature with improved safety are needed urgently. Organic compounds with low HOMO (highest occupied molecular orbital) energy level are suitable candidates for high-voltage application. An alternative approach to address the electrolyte challenges is to mitigate the surface reactivity of high-voltage cathodes by developing cathode passivating additives. Like the indispensable role of SEI on the carbonaceous anodes, cathode electrolyte interphase (CEI) formation additives could kinetically suppress the thermodynamic reaction of the delithiated cathode and electrolyte, thus significantly improving the cycle life and calendar life of the high energy density lithium-ion battery.

An ideal electrolyte for high-voltage, high-energy cathodes also requires high compatibility with anode materials (graphite or silicon). New anode SEI formation additives tailored for the new high-voltage electrolyte are equally critical for the high-energy lithium-ion battery system. Such an electrolyte should have the following properties: high stability against 4.5-5.0 V charging state, particularly with cathodes exhibiting high surface oxygen activity; high compatibility with a strongly reducing anode under high-voltage charging; high Li salt solubility (>1.0 M) and ionic conductivity ($> 6 \times 10^{-3}$ S/cm @ room temperature); and non-flammability (no flash point) for improved safety and excellent low-temperature performance (-30°C).

Task 4.1 – Fluorinated Electrolyte for 5-V Li-ion Chemistry (Zhengcheng Zhang, Argonne National Laboratory)

Project Objective. The objective of this project is to develop a new advanced electrolyte system with outstanding stability at high voltage and high temperature and improved safety characteristic for an electrochemical couple consisting of the high-voltage $\text{LiNi}_{0.5}\text{Mn}_{1.5}\text{O}_4$ (LNMO) cathode and graphite anode. The specific objectives of this proposal are the design, synthesis, and evaluation of (1) non-flammable, high-voltage solvents to render intrinsic voltage and thermal stability in the entire electrochemical window of the high-voltage cathode materials, and (2) electrolyte additives to enhance the formation of a compact and robust solid electrolyte interphase (SEI) on the surface of the high-voltage cathode. A third objective is to gain fundamental understanding of the interaction between electrolyte and high-voltage electrode materials, the dependence of SEI functionality on electrolyte composition, and the effect of high temperature on the full Li-ion cells using the advanced electrolyte system.

Project Impact. This innovative fluorinated electrolyte is intrinsically more stable in electrochemical oxidation due to the fluorine substitution; therefore, it would be also applicable to cathode chemistries based on TM oxides other than LNMO. The results of this project can be further applied to a wide spectrum of high-energy battery systems oriented for PHEVs that operate at high potentials, such as LiMPO_4 ($\text{M}=\text{Co}, \text{Ni}, \text{Mn}$), or battery systems that require a high-voltage activation process, such as the high-capacity Li-Mn-rich $\text{xLi}_2\text{MnO}_3 \cdot (1-\text{x})\text{Li}[\text{Ni}_\text{x}\text{Mn}_\text{y}\text{Co}_\text{z}]\text{O}_2$. This electrolyte innovation will push the U.S. supply base of batteries and battery materials past the technological and cost advantages of foreign competitors, thereby increasing economic value to the USA. ANL's new fluorinated electrolyte material will enable the demand for more PHEVs and EVs, which directly transforms to greatly reduced gasoline consumption and pollutant emissions.

Out-Year Goals. The goal of this project is to deliver a new fluorinated electrolyte system with outstanding stability at high voltage and high temperature with improved safety characteristic for an electrochemical couple consisting of 5-V Ni-Mn spinel $\text{LiNi}_{0.5}\text{Mn}_{1.5}\text{O}_4$ (LNMO) cathode and graphite anode. The specific objectives of this proposal are the design, synthesis, and evaluation of (1) non-flammable high voltage fluorinated solvents to attain intrinsic voltage stability in the entire electrochemical window of the high-voltage cathode material and (2) effective electrolyte additives that form a compact and robust solid-electrolyte interphase (SEI) on the surfaces of the high voltage cathode and graphitic anode.

Collaborations. This project collaborates with Dr. Kang Xu, U.S. Army Research Laboratory; Dr. Xiao-Qing Yang, Brookhaven National Laboratory; Dr. Brett Lucht, University of Rhode Island; and Dr. Andrew Jansen and Dr. Gregory Krumdick, Argonne National Laboratory.

Milestones

1. Complete theoretical calculation of electrolyte solvents; Validate the electrochemical properties of the available fluorinated solvents by CV and leakage current experiment. (March 2014 – Complete)
2. Synthesize and characterize the Gen-1 electrolyte. (June 2014 – Complete)
3. Evaluate the LNMO/graphite cell performance of Gen-1 F-electrolyte. (September 2014 – Complete)
4. Design and build interim cells and baseline pouch cells. (January 2015 – Complete)
5. Synthesize and evaluate Gen-2 F-electrolyte based on TF-PC. (March 2015 – Complete)
6. Develop optimized F-electrolyte containing multinary F-solvents. (June 2015 – Complete)
7. Design and build final cells. (September 2015 – On Track)

Progress Report

The current phase of the research focuses on the fundamental understanding of the Li^+ solvation, Li^+ transference number (t_{Li^+}) and ion diffusion kinetics for the new fluorinated electrolytes developed in the previous phases by 2D diffusion-ordered NMR spectroscopy (DOSY). The first studied system is FEC-based electrolyte with the formulation of 1.0 M LiPF_6 dissolved in 30% FEC, 50% F-EMC and 20% FEPE mixture solvent. For SOA electrolyte, Li^+ preferably interacts with the nucleophilic site of the selected solvent molecule with an optimal coordination number between 4~6. Spectroscopy and computation method also predict that Li^+ -EC solvates diffuse much slower compared with other species including PF_6^- . However, the Li^+ solvation in the fluorinated electrolyte is quite different from the state of the art. As shown in Table 2, at each temperature, the diffusion coefficient of Li^+ (D_{Li^+}) is slightly higher than that of the anion PF_6^- , indicating the weak coordination between the Li^+ and the fluorinated solvent, which promotes the transference number (t_{Li^+}) more than half.

Table 2. Ion diffusion coefficient, transference number, and ionic conductivity of FEC-based electrolyte.

T (K)	D_{Li^+} (m^2/s)	$D_{\text{PF}_6^-}$ (m^2/s)	t_{Li^+}	Λ_{NMR} (mS cm^{-1})	$\Lambda_{\text{impedance}}$ (mS cm^{-1})	$\Lambda_{\text{imp}}/\Lambda_{\text{NMR}}$
283	1.94e-10	1.66e-10	0.54	4.92	1.22	0.25
293	2.37e-10	2.23e-10	0.51	6.08	1.39	0.23
303	3.13e-10	2.83e-10	0.53	7.61	1.55	0.20
313	5.07e-10	3.64e-10	0.58	10.8	1.69	0.16

To further understand the Li^+ interaction with the individual fluorinated solvent, new DOSY NMR experiments have been performed; the data are shown in Table 3. Without LiPF_6 salt, the diffusion coefficient for FEMC in the FEMC/EMC mixture is slightly lower than that of EMC, mainly due to the larger molecular size and weight. Surprisingly, when the salt is added, the results are the opposite. The faster kinetics of the FEMC- Li^+ than EMC- Li^+ clearly (Figure 35) confirm weak interaction between Li^+ and the fluorinated carbonate solvent.

Table 3. Structure of F-EMC and EMC (left) and the diffusion coefficient with and without LiPF_6 salt (right) measured by NMR.

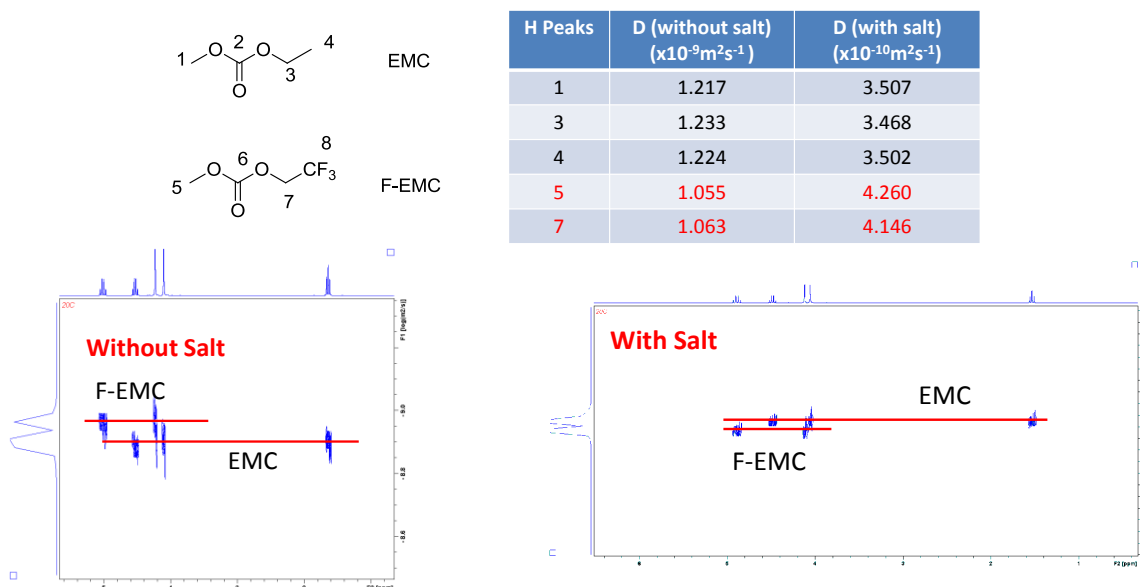


Figure 35. 2D-DOSY NMR spectra of fluorinated carbonate F-EMC and its non-fluorinated counterpart EMC without LiPF_6 (left) and with LiPF_6 (right). (X axis is ppm of the H chemical shift; Y axis is the diffusion coefficient.)

Further work on understanding the second fluorinated electrolyte is planned for next quarter.

Task 4.2 – Daikin Advanced Lithium Ion Battery Technology – High-Voltage Electrolyte (R. Hendershot/J. Sunstrom/Michael Gilmore, Daikin America)

Project Objective. The project objective is to develop a stable (300 – 1000 cycles), high-voltage (at 4.6 V), and safe (self-extinguishing) formulated electrolyte.

- Exploratory Development (Budget Period #1 – October 1, 2013 to January 31, 2015)
 - Identify promising electrolyte compositions for high-voltage (4.6 V) electrolytes via the initial experimental screening and testing of selected compositions
- Advanced Development (Budget Period #2 – February 1, 2015 to September 31, 2015)
 - Detailed studies and testing of the selected high-voltage electrolyte formulations and the fabrication of final demonstration cells

Project Impact. Fluorinated small molecules offer the advantage of low viscosity along with high chemical stability due to the strength of the C-F bond. Due to this bond strength, Daikin fluorochemical materials are among the most electrochemical stable materials that still have the needed performance attributes for a practical electrolyte. Such an electrolyte will allow routine operating voltages to be increased to 4.6 V. This technological advance would allow significant cost reduction by reducing the number of cells needed in a particular application and/or allow for greater driving range in PHEV applications.

Out-Year Goals. This project has a clearly defined goals for both temperature and voltage performance which are consistent with the deliverables of this proposal. Those goals are to deliver an electrolyte capable of 300 - 1000 cycles at 3.2 - 4.6 V at nominal rate with stable performance. An additional goal is to have improved high temperature (> 60°C) performance. An additional safety goal is to have this electrolyte be self-extinguishing.

Collaborations. Daikin is continuing a limited testing agreement with Coulometrics. Surface studies that may include Auger spectroscopy, x-ray photoelectron spectroscopy, and TOF-SIMS mass spectrometry have been contracted to Materials Research Laboratory in Struthers, Ohio.

Milestones

Budget Period #1 – Oct. 1, 2013 to Jan. 31, 2015

1. Complete identification of promising electrolyte formulations. Experimental design completed with consistent data sufficient to build models. Promising electrolyte formulations are identified that are suitable for high-voltage battery testing. (Complete)
2. Successful fabrication of 10 interim cells and delivery of cells to a DOE laboratory (to be specified). (Initiated February 2015 – first report from ANL received)
3. Electrochemical and battery cycle tests are completed, and promising results are obtained that demonstrate stable performance at 4.6 V. (Ongoing)

Progress Report

The technical approach to achieve the milestones is based on an iterative plan following a sound scientific method, also sometimes referred to as a Plan-Do-Check-Act (PDCA) cycle, which has been described in detail in previous reports.

Status: Last quarter, we proposed that FEC-based electrolytes while giving excellent cycle life performance actually do poorly in calendar life tests due to increased gassing. A clear correlation with FEC concentration and voltage was also shown.

The current work is focused on understanding the mechanism of FEC composition on different surfaces and at different conditions. Figure 36 is an example of the data now being collected. It shows 3 electrolytes with or without FEC and/or D7 HFE shown at 2 voltage groups (below/above 4.35 V) and on 3 separate cathodes (NMC-111, NMC-532, and NCA). The data shows a dependence on cathode material with respect to gassing. The NCA/graphite cell has higher gassing than the NMC-532/graphite cell. Further work is centered on formulating electrolytes with lower FEC amounts and trying to understand the critical components and triggers to gas formation.

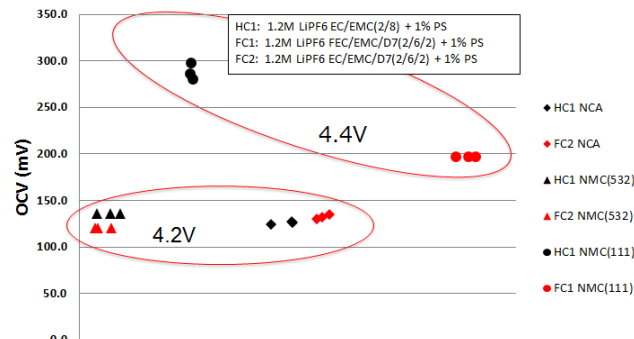


Figure 36. Δ OCV vs Δ volume% for several electrolyte/electrode combinations.

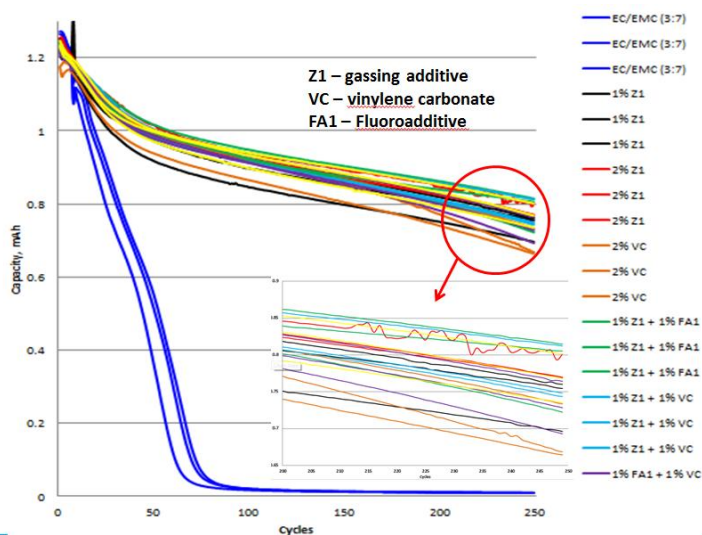


Figure 37. Cycle life vs capacity for several additive combinations in 1.2 LiPF₆ FEC/EMC/D7(HFE) (2:6:2).

chemistry, and usage parameters (voltage, current, impedance).

The cell data on the interim cells provided to the DOE and tested by Argonne indicate that the 4.6 V target has not yet been achieved. The interim cells were filled with electrolytes containing 20% FEC and no additional fluorinate SEI additives. Electrode samples have been sent to Materials Research Laboratory for surface analysis. The electrolytes chosen contain various combinations of FEC, HFE, and fluorinated additives, with the goal being to understand the nature of film formation on both the anode and cathode surfaces for NMC/graphite batteries. This will then be correlated with battery performance.

For the interim cells, the electrolyte solvent formulation proposed was 1.2 M LiPF₆ in FEC/EMC/FE(D7) (2:6:2) with 1% gassing additive. Recent work has concentrated on optimizing an additive package to complement the solvent mixture. The main goal is to minimize the slope of the cycle life curve. Figure 37 shows cycle life data shown for several additive combinations. Selection of these additive groups was accomplished by first evaluating many promising candidates by High Precision Coulometry techniques that have been proposed by J. Dahn. This was completed with our collaborator Coulometrics. The preferred combination for this solvent formulation in NMC111/graphite was 1% Z1 (gassing additive) and 1% FA1 (fluorinated SEI additive). This optimization will most likely need to be repeated based on solvent formulation, battery

Task 4.3 – Novel Non-Carbonate Based Electrolytes for Silicon Anodes (Dee Strand, Wildcat Discovery Technologies)

Project Objective. The objective of this project is to develop non-carbonate electrolytes that form a stable solid electrolyte interphase (SEI) on silicon alloy anodes, enabling substantial improvements in energy density and cost relative to current lithium ion batteries (LIBs). These improvements are vital for mass market adoption of electric vehicles. At present, commercial vehicle batteries employ cells based on LiMO_2 ($\text{M} = \text{Mn, Ni, Co}$), LiMn_2O_4 , and/or LiFePO_4 coupled with graphite anodes. Next generation cathode candidates include materials with higher specific capacity or higher operating voltage, with a goal of improving overall cell energy density. However, to achieve substantial increases in cell energy density, a higher energy density anode material is also required. Silicon anodes demonstrate very high specific capacities, with a theoretical limit of 4200 mAh/g and state-of-the-art electrodes exhibiting capacities greater than 1000 mAh/g. While these types of anodes can help achieve target energy densities, their current cycle life is inadequate for automotive applications. In graphite anodes, carbonate electrolyte formulations reductively decompose during the first-cycle lithiation, forming a passivation layer that allows lithium transport, yet is electrically insulating to prevent further reduction of bulk electrolyte. However, the volumetric changes in silicon upon cycling are substantially larger than graphite, requiring a much more mechanically robust SEI film.

Project Impact. Silicon alloy anodes enable substantial improvements in energy density and cost relative to current lithium ion batteries. These improvements are vital for mass market adoption of electric vehicles, which would significantly reduce CO_2 emissions as well as eliminate U.S. dependence on energy imports.

Out-Year Goals. Development of non-carbonate electrolyte formulations that:

- form stable SEIs on 3M silicon alloy anode, enabling Coulombic efficiency > 99.9% and cycle life > 500 cycles (80% capacity) with NMC cathodes;
- have comparable ionic conductivity to carbonate formulations, enabling high power at room temperature and low temperature;
- are oxidatively stable to 4.6V, enabling the use of high energy NMC cathodes in the future; and
- do not increase cell costs over today's carbonate formulations.

Collaborations. Wildcat is working with 3M on this project. To date, 3M is supplying the silicon alloy anode films and NMC cathode films for use in Wildcat cells.

Milestones

1. Assemble materials, establish baseline performance with 3M materials. (December 2013 – Complete)
2. Develop initial additive package using non-SEI forming solvent. (March 2014 – Complete)
3. Screen initial solvents with initial additive package. (June 2014 –Complete)
4. Design/build interim cells for DOE (September 2014 –Complete)
5. Improve performance with noncarbonate solvents and new SEI additives (March 2015 – On Track; continuous to end of project)
6. Optimize formulations (August 2015 –On Track)
7. Design/build final cells for DOE (December 2015)

Progress Report

The current phase of the project focuses on optimization of the promising solvent formulations found in previous phases. This includes optimization of (1) salt content and concentration, (2) solvent combinations and ratios, and (3) additive type, concentrations, and combinations. Wildcat is systematically screening these variables to identify formulations with target cycle life, as well as promising leads to hit other key metrics.

The first screens were completed on salt content and concentration. We started from the most promising salts identified previously, and screened all of these in combinations and at varying concentrations in a variety of promising noncarbonate or EC-free electrolyte formulations. Figure 38 shows some of the best results from optimization of salt concentration, with a capacity retention of about 80% at 300 cycles. We followed up on this by testing binary combinations of salts to identify the most promising combinations.

After optimization of salts, we designed experiments to look at different combinations and ratios of the novel solvents previously identified in the project. This included multiple approaches such as changing the ratio of the high dielectric to low viscosity solvent and investigating ternary solvents systems. From this effort, a number of promising systems were identified for further investigation.

In parallel to these studies, we have designed and assembled cells to follow up on and optimize electrolyte additives that were identified very early in this project. This also includes additional work on EC containing formulations, as several additive categories showed benefit in the presence of EC. We continue to test the best formulations on Argonne NMC//Si electrodes and have identified several other sources of materials for testing.

We have also started testing electrolyte formulations at voltage higher than 4.2V, which was used for all studies to date. The most promising formulations were tested at 4.35V, 4.45V, and 4.55V. Results at the highest voltage (4.55V) are shown in Figure 39, indicating that high-voltage solutions are possible. Further work on achieving high-voltage stability is planned for next quarter.

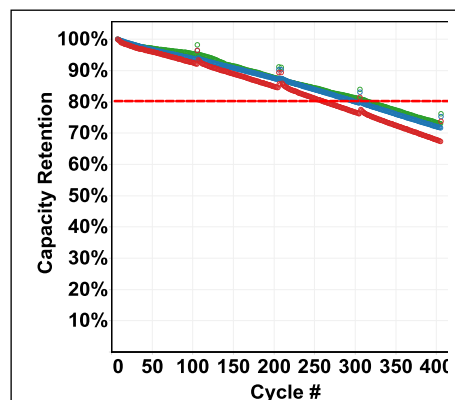


Figure 38. Optimized salt concentration can achieve 300 cycles in noncarbonate electrolyte formulation

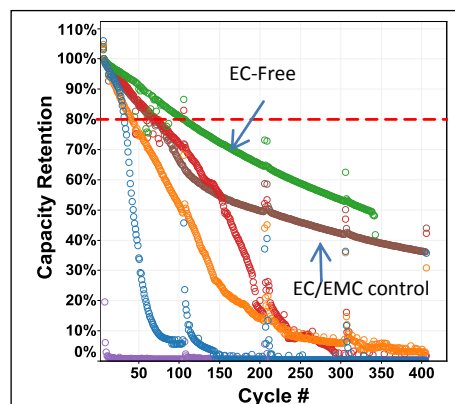


Figure 39. EC-free formulation has good performance relative to the control EC/EMC

TASK 5 – DIAGNOSTICS

Summary and Highlights

To meet the goals of Vehicle Technology Program (VTP) Multi Year Program Plan (MYPP) and develop lower-cost, abuse-tolerant batteries with higher energy density, higher power, better low-temperature operation and longer lifetimes suitable for the next-generation of HEVs, PHEVs and EVs, there is a strong need to identify and understand structure-property-electrochemical performance relationships in materials, life-limiting and performance-limiting processes, and various failure modes to guide battery development activities and scale-up efforts. In the pursuit of batteries with high energy density, high cell operating voltages and demanding cycling requirements lead to unprecedented chemical and mechanical instabilities in cell components. Successful implementation of newer materials such as Si anode and high voltage cathodes also requires better understanding of fundamental processes, especially those at the solid/electrolyte interface of both anode and cathode.

The Battery Materials Research Task 5 takes on these challenges by combining model system, *ex situ*, *in situ* and *operando* approaches with an array of the start-of-the-art analytical and computational tools. Four subtasks are tackling the chemical processes and reactions at the electrode/electrolyte interface. Researchers at LBNL use *in situ* and *ex situ* vibrational spectroscopy, far- and near-field scanning probe spectroscopy and laser-induced breakdown spectroscopy (LIBS) to understand the composition, structure, and formation/degradation mechanisms of the solid electrolyte interface at Si anode and high voltage cathodes. UCSD combines scanning transmission electron microscopy (STEM)/electron energy loss spectroscopy (EELS), x-ray photoelectron spectroscopy (XPS) and *Ab Initio* computation for surface and interface characterization and identification of instability causes at both electrodes. At Cambridge, nuclear magnetic resonance (NMR) is being used to identify major SEI components, their spatial proximity, and how they change with cycling. Subtasks at BNL and PNNL focus on the understanding of fading mechanisms in electrode materials, with the help of synchrotron based x-ray techniques (diffraction and hard/soft x-ray absorption) at BNL and high-resolution transmission electron microscopy (HRTEM) and spectroscopy techniques at PNNL. At LBNL, model systems of electrode materials with well-defined physical attributes are being developed and used for advanced diagnostic and mechanistic studies at both bulk and single-crystal levels. These controlled studies remove the ambiguity in correlating material's physical properties and reaction mechanisms to its performance and stability, which is critical for further optimization. The final subtask takes advantage of the user facilities at ANL that bring together x-ray and neutron diffraction, x-ray absorption, emission and scattering, HRTEM, Raman spectroscopy and theory to look into the structural, electrochemical, and chemical mechanisms in the complex electrode/electrolyte systems. The diagnostics team not only produces a wealth of knowledge that is key to developing next-generation batteries, it also advances analytical techniques and instrumentation that have a far-reaching effect on material and device development in a range of fields.

The highlights for this quarter are as follows:

- Chen's group revealed the crystal structure of Li- and Mn-rich layered oxide crystals by using complementary microscopy and spectroscopy techniques at multi-length scale.
- Kostecki's group demonstrated that transition metal complexes cause impedance increase of the graphite anode by inhibiting Li^+ transport within the SEI.
- Grey's group developed ^{23}Na *in situ* NMR to study Na metal anode in sodium-ion batteries.
- Meng's group reports that FEC additive improves Si anode cycling by forming uniform and stable SEI that covers the Li_xSi particles with a high LiF content.
- Wang's group demonstrated atomic-resolution visualization of ion mixing between transition metals (Ni, Co, Mn) and lithium in layered oxide cathodes using aberration corrected STEM imaging and DFT calculations.
- Thackeray's group developed model systems to investigate the migration mechanisms of cations (M and M') in $\text{Li}_{1+x}(\text{MM}')_{1-x}\text{O}_2$ cathodes and understand the connection between experiment and theory.

Task 5.1 – Design and Synthesis of Advanced High-Energy Cathode Materials (Guoying Chen, Lawrence Berkeley National Laboratory)

Project Objective. The successful development of next-generation electrode materials requires particle-level knowledge of the relationships between materials' specific physical properties and reaction mechanisms to their performance and stability. This single-crystal-based project was developed specifically for this purpose, and it has the following objectives: (1) obtain new insights into electrode materials by utilizing state-of-the-art analytical techniques that are mostly inapplicable on conventional, aggregated secondary particles, (2) gain fundamental understanding on structural, chemical, and morphological instabilities during Li extraction/insertion and prolonged cycling, (3) establish and control the interfacial chemistry between the cathode and electrolyte at high-operating voltages, (4) determine transport limitations at both particle and electrode levels, and (5) develop next-generation electrode materials based on rational design as opposed to more conventional empirical approaches.

Project Impact. This project will reveal performance-limiting physical properties, phase-transition mechanisms, parasitic reactions, and transport processes based on the advanced diagnostic studies on well-formed single crystals. The findings will establish rational, non-empirical design methods that will improve the commercial viability of next-generation $\text{Li}_{1+x}\text{M}_{1-x}\text{O}_2$ ($\text{M}=\text{Mn}, \text{Ni}$ and Co) and spinel $\text{LiNi}_x\text{Mn}_{2-x}\text{O}_4$ cathode materials.

Approach. Prepare crystal samples of Li-rich layered oxides and high-voltage Ni/Mn spinels with well-defined physical attributes. Perform advanced diagnostic and mechanistic studies at both bulk and single-crystal levels. Global properties and performance of the samples will be established from the bulk analyses, while the single-crystal based studies will utilize time- and spatial-resolved analytical techniques to probe material's redox transformation and failure mechanisms.

Out-Year Goals. This project aims to determine performance and stability limiting fundamental properties and processes in high-energy cathode materials and to outline mitigating approaches. Improved electrode materials will be designed and synthesized.

Collaborations. This project collaborates with Drs. R. Kostecki, M. Doeff, K. Persson, V. Zorba, T. Tyliszczak and Z. Liu (LBNL); Prof. C. Grey (Cambridge); Prof. B. Lucht (URI); and Prof. Y.-M. Chiang (MIT).

Milestones

1. Characterize Ni/Mn spinel solid solutions and determine the impact of phase transformation and phase boundary on rate capability. (December 2014 – Complete)
2. Complete the investigation on crystal-plane specific reactivity between Li-rich layered oxides and the electrolyte. Determine morphology effect in side reactions. (March 2015 – Complete)
3. Develop new techniques to characterize reactions and processes at the cathode-electrolyte interface. Evaluate the effect of surface compositions and modifications on side reactions and interface stability (June 2015 – Complete)
4. *Go/No-Go*: Continue the approach of using synthesis conditions to vary surface composition if significant structural and performance differences are observed. (September 2015 – On Schedule)

Progress Report

This quarter, complementary microscopy and spectroscopy techniques at multi-length scale, including aberration corrected (scanning) transmission electron microscopy (STEM), electron energy loss spectroscopy (EELS) and x-ray energy dispersive spectroscopy (EDS), were used to characterize the bulk and surface structures of the $\text{Li}_{1.2}\text{Mn}_{0.13}\text{Mn}_{0.54}\text{Co}_{0.13}\text{O}_2$ crystals reported previously.

In Figure 40a-c, the high angle angular dark field (HAADF) STEM images collected on the needle-shaped crystals are shown. The bright columns correspond to the transition metals (Mn, Ni, and Co), and the atomic arrangements in the bulk of the crystal can be assigned to [100], [1-10] and [110] directions of monoclinic phase, as shown in the structural models in Figure 40e. The study revealed the random distribution of domains of three monoclinic variants (Figure 40d) in the entire bulk of $\text{Li}_{1.2}\text{Mn}_{0.13}\text{Mn}_{0.54}\text{Co}_{0.13}\text{O}_2$ crystal and the lack of composite structure with R-3m and C2/m nano-domains as typically reported on this class of oxides made by the co-precipitation method. The observation of single-phase crystal structure was found to be independent of particle morphology.

EELS imaging was used to examine the chemical changes between the bulk and the surface. Figure 41b shows a series of spectra covering EELS edges from O to Ni, transitioning from the bulk (bottom) to the surface (top). Compared to the bulk, the Mn and Ni L3 edges collected on the surface showed a lower energy loss, indicating a decrease in oxidation state. The L3/L2 ratios for the TMs are shown in Figure 41c.

Although the exact valence is difficult to quantify, the trend clearly shows the reduction in oxidation state of Mn and Co from the bulk to the surface. As expected, the oxidation state of Ni remains constant at 2+. The reduction in the TM oxidation state is also supported by the lower O pre-peak intensity observed on the surface, where the O profile resembles that of a spinel. EELS Li K-edge imaging in the low-loss region further confirmed the presence of Li in the surface region where Mn and Co are reduced.

The presence of surface spinel with reduced TMs was further supported by careful STEM imaging in multiple zone axes. Figure 42a shows the HAADF image in bulk [103]_M orientation, where only one variant of the monoclinic structure is predominantly present. A different structure with filled lower intensity rows was observed on the surface layer of ~ 2 nm. Modeling of the interface suggests surface spinel structure with a [111]_S orientation. The change from monoclinic bulk to spinel surface was also observed in other orientations (Figure 42b-c). However, spinel formation on pristine surface is directional and morphology dependent, with minimal spinel found in the TM layer stacking direction.

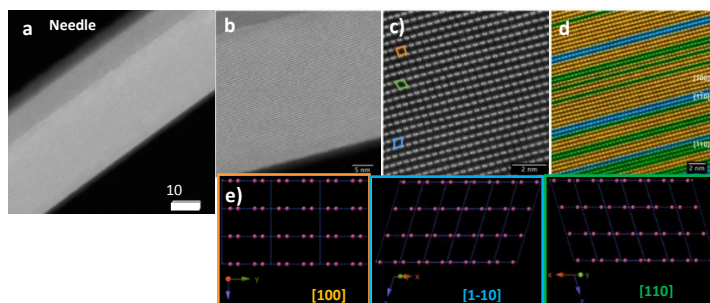


Figure 40. HAADF STEM image of (a) an entire needle-shaped $\text{Li}_{1.2}\text{Ni}_{0.13}\text{Mn}_{0.54}\text{Co}_{0.13}\text{O}_2$ crystal, (b) and (c) zoomed-in view of the crystal structure, (d) color-coded HAADF image showing domains of monoclinic variants, and (e) models showing monoclinic structure in [100], [1-10] and [110] directions.

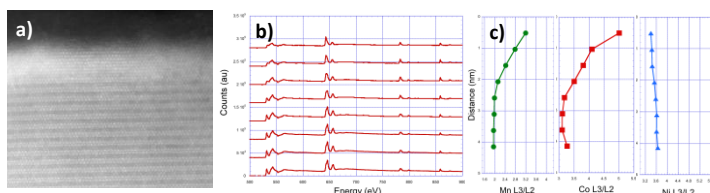


Figure 41. (a) HAADF STEM image, (b) EEL spectra collected from surface (top) and the bulk (bottom) corresponding to the HAADF image, and (c) L3/L2 ratio of Mn, Co and Ni determined from the EELS data.

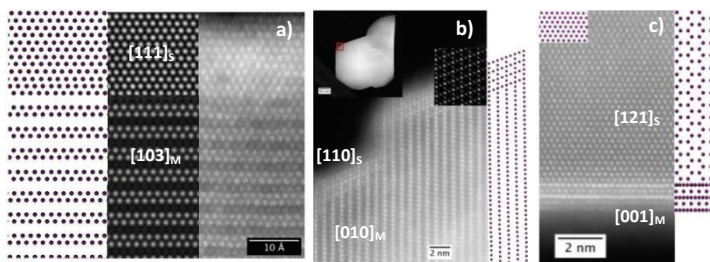


Figure 42. HAADF STEM images alongside STEM simulation images and models of interface in 3 zone axes: (a) [103]_M, (b) [010]_M, and (c) [001]_M.

Patents/Publications/Presentations

Publications

- Yan, P., and D. Lv, J. Zheng, Z. Wang, S. Kuppan, J. Yu, L. Luo, D. Edwards, M. Olszta, K. Amine, J. Liu, J. Xiao, G. Chen, J.-G. Zhang, and C.-M. Wang. “Atomic-resolution Visualization of Distinctive Chemical Mixing Behavior of Ni, Co and Mn with Li in Layered Lithium Transition Metal Oxide Cathode Materials,” *Chemistry of Materials*, DOI: 10.1021 (2015).
- Cheng, L., and W. Chen, M. Kunz, K. Persson, N. Tamura, G. Chen, and M. M. Doeff. “Interrelationships among Grain Size, Surface Composition, Air Stability and Interfacial Resistance of Al-substituted $\text{Li}_7\text{La}_3\text{Zr}_2\text{O}_{12}$ Solid Electrolytes.” *ACS Applied Materials & Interfaces*, DOI: 10.1021/acsami.5b02528 (2015).
- Hou, H., and L. Cheng, T. Richardson, G. Chen, M. M. Doeff, R. Zheng, R. Russo, and V. Zorba. “Three-Dimensional Elemental Imaging of Li-ion Solid-State Electrolytes Using fs-Laser Induced Breakdown Spectroscopy (LIBS).” *Journal of Analytical Atomic Spectrometry*, in press (2015).
- Shukla, A. K., and Q. Ramasse, C. Ophus, H. Duncan, and G. Chen. “Unraveling Structural Ambiguities in Li and Mn Rich Transition Metal Oxides.” Submitted to *Nature Communications* (2015).

Presentations

- DOE Hydrogen Program and Vehicle Technologies Program Annual Merit Review and Peer Evaluation Meeting, Arlington, Virginia (June 2015): “Design and Synthesis of Advanced High-Energy Cathode Materials”; G. Chen.
- CalCharge Open House, Berkeley, California (April 2015): “Surface Facet Dependent Self-discharge in High-voltage Spinel Cathodes”; S. Kuppan and G. Chen.
- 2015 MRS Spring Meeting & Exhibit, San Francisco (April 2015): “Thermal Behavior of $\text{Li}_x\text{Mn}_{1.5}\text{Ni}_{0.5}\text{O}_4$ ($0 \leq x \leq 1$) and Isolation of Room-Temperature Solid Solutions”; S. Kuppan and G. Chen.

Task 5.2 – Interfacial Processes – Diagnostics (Robert Kostecki, Lawrence Berkeley National Laboratory)

Project Objective. The main objective of this task is to obtain detailed insight into the dynamic behavior of molecules, atoms, and electrons at electrode/electrolyte interfaces of intermetallic anodes (Si) and high voltage Ni/Mn-based materials at a spatial resolution that corresponds to the size of basic chemical or structural building blocks. The aim of these studies is to unveil the structure and reactivity at hidden or buried interfaces and interphases that determine battery performance and failure modes. To accomplish these goals, novel far- and near-field optical multifunctional probes must be developed and deployed *in situ*. The work constitutes an integral part of the concerted effort within the BMR Program, and it attempts to establish clear connections between diagnostics, theory/modelling, materials synthesis, and cell development efforts.

Project Impact. This project provides better understanding of the underlying principles that govern the function and operation of battery materials, interfaces, and interphases, which is inextricably linked with successful implementation of high energy density materials such as Si and high-voltage cathodes in Li-ion cells for PHEVs and EVs. This task also involves the development and application of novel innovative experimental methodologies to study and understand the basic function and mechanism of operation of materials, composite electrodes, and Li-ion battery systems for PHEV and EV applications.

Approach. Design and employ novel and sophisticated *in situ* analytical methods to address the key problems of the BMR baseline chemistries. Experimental strategies combine imaging with spectroscopy aimed at probing electrodes at an atom, molecular, or nanoparticulate level to unveil structure and reactivity at hidden or buried interfaces and determine electrode performance and failure modes in baseline Li_xSi -anodes and high-voltage LMNO cathodes. The proposed methodologies include *in situ* and *ex-situ* Raman, FTIR and LIBS far- and near-field spectroscopy/microscopy, scanning probe microscopy (SPM), spectroscopic ellipsometry, electron microscopy (SEM, HRTEM), and standard electrochemical techniques and model single particle and/or monocrystal model electrodes to probe and characterize bulk and surface processes in Si anodes, and high-energy cathodes.

Out-Year Goals. The main goal is to gain insight into the mechanism of surface phenomena on thin-film and monocrystal Sn and Si intermetallic anodes and evaluate their impact on the electrode long-term electrochemical behavior. Comprehensive fundamental study of the early stages of SEI layer formation on polycrystalline and single crystal face Sn and Si electrodes will be carried out. *In situ* and *ex situ* far- and near-field scanning probe spectroscopy and LIBS will be employed to detect and monitor surface phenomena at the intermetallic anodes and high-voltage (>4.3V) model and composite cathodes.

Collaborations. This project collaborates with Vincent Battaglia, Ban Chunmei, Vassilia Zorba, and Bryan D. McCloskey.

Milestones

1. Determine the mechanism of formation of the metal complexes species that are produced at high-energy Li-ion cathodes. (December 2014 –Complete)
2. Resolve SEI layer chemistry of coated Si single crystal and thin film anodes (collaboration with Chunmei Ban). (March 2015 –Complete)
3. Determine the mechanism of SEI layer poisoning by Ni and Mn coordination compounds (collaboration with Bryan D. McCloskey). (June 2015 – On Schedule)
4. *Go/No-Go*: Demonstrate feasibility of *in situ* near-field and LIBS techniques at Li-ion electrodes (collaboration with Vassilia Zorba). Criteria: Stop development of near-field and LIBS techniques, if the experiments fail to deliver adequate sensitivity. (September 2015 – On Schedule)

Progress Report

Previously, we have shown that contrary to the disproportionation mechanism proposed 30 years ago, transition metal dissolution from $\text{LiNi}_{0.5}\text{Mn}_{1.5}\text{O}_4$ occurs via surface oxidation of DEC and EC and formation of Ni(II) and Mn(II) coordination complexes at potentials > 4.2 V. This leads to subsequent incorporation of Mn(II)(acac)_2 complexes in the SEI at the graphite electrode. This quarter, the effect of $\text{Mn(II/III)(}\beta\text{-diketone)}$ complexes on the Li^+ transport in the SEI layer was investigated.

The influence of the transition metal complexes on the Li^+ transport was tested using graphite symmetric coin cells (prelithiated graphite/graphite) filled with 1 M LiPF_6 , EC/DEC (1:2) electrolyte spiked with 500 ppm Ni(II) and Mn(II) compounds. The cells were cycled galvanostatically at C/10 during the initial four cycles and at C/3 for the following 270 cycles. Electrochemical impedance spectra were measured at 50% of state of charge every 10 cycles. To analyze the anode impedance spectra, we used standard equivalent circuit models consisting of a resistance of the electrolyte (R_1) in series with a second resistance that represents transport processes in the SEI layer and charge transfer resistance (R_2), and constant phase element (CPE_2), which corresponds to the double-layer capacitance. Figure 43 shows the dependence of the SEI ionic resistance (R_2) vs. cell cycle number in the baseline electrolyte and electrolyte containing 500 ppm of different transition metal species observed by XANES experiments at the graphite surface in an aged LMNO/graphite cell (Figure 43).

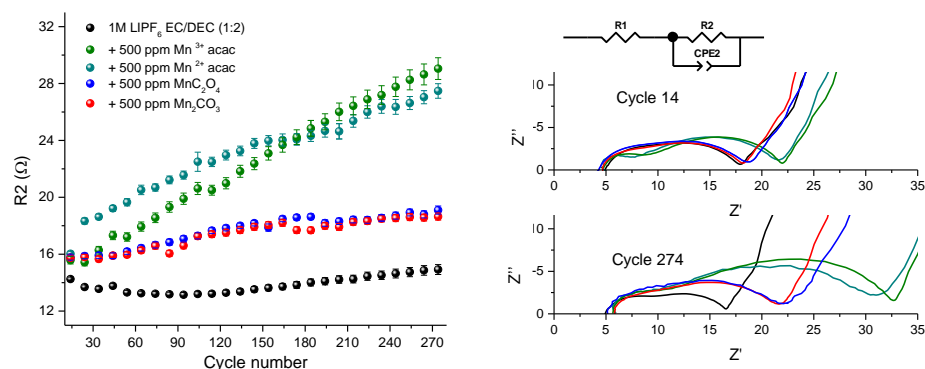


Figure 43. Impedance evolution of graphite symmetric cells filled with 1 M LiPF_6 , EC/DEC (1:2) spiked with 500 ppm of MnII/III compounds, measured at 50% of SOC.

Contrary to the cell cycled with the baseline electrolyte, the presence of transition metal species leads to a rapid increase of the impedance with cycling. Interestingly, while only a moderate impedance rise is observed in the presence of Mn(II) carbonate and Mn(II) oxalate, the presence of Mn(II)(acac)_2 and Mn(III)(acac)_3 results in a steep increase of R_2 during cycling. β -diketone complexes are responsible for the observed impedance increase of the graphite anode by inhibiting Li^+ transport within the SEI. Although the exact mechanism of these Li^+ - $\text{Mn(III/II)(acac)}_3$ interactions in the SEI layer is still unknown, fluorescent β -diketone complexes produced on the cathode may and will be used as a unique probe into the mechanism of Li^+ transport across the solid electrolyte interphases in Li-ion anodes. This completes our efforts toward Milestone 3.

Near-field IR imaging and spectroscopy investigations also continued to elucidate the nanoscale structure and functionality specific compounds in the SEI layer. Key components of the SEI were identified by taking advantage of the near-field microscope's ability to selectively probe individual compounds without convolution. Further investigations on the interaction between fluorescent compounds and SEI components as well as *ex-situ* and *in situ* LIBS and near-field IR techniques are under way to identify the SEI components function (Milestone 4).

Patents/Publications/Presentations

Publications

- Winter, Martin, and Ulrike Vogl, Simon Lux, Adam Weber, Prodib Das, and Robert Kostecki. “The Mechanism of SEI Formation on/at Single Crystal Si (110) and (111) Electrodes.” *Journal of Electrochemical Society*, submitted.
- Cheng, L., and W.H. Wu, A. Jarry, W. Chen, Y. Ye, J. Zhu, R. Kostecki, K. Persson, J. Guo, M. Salmeron. G. Chen, and M. Doeff. “Interrelationships among Grain Size, Surface Composition, Air Stability and Interfacial Resistance of Al-substituted $\text{Li}_7\text{La}_3\text{Zr}_2\text{O}_{12}$ Solid Electrolytes.” *ACS Applied Materials and Interfaces*, submitted.

Presentations

- 227th ECS Meeting, Chicago (May 24 – 28, 2015): “Advanced X-Ray Transmission Microscopy for Chemical and Fracture Imaging of Single Li_xFePO_4 Particles at High Resolution”; Y. S. Yu, C. Kim, D. Shapiro, M. Farmand, R. Kostecki, D. Qian, S. Meng, and J. Cabana.
- 227th ECS Meeting, Chicago (May 24 – 28, 2015): “Mechanism of Formation of Metal Acetylacetonates at the $\text{Li}_x\text{Ni}_{0.5}\text{Mn}_{1.5}\text{O}_{4-\text{S}}$ /Carbonate Ester Electrolyte Interface”; R. Kostecki, A. Jarry, S. Gottis, and J. B. Kerr.
- 227th ECS Meeting, Chicago (May 24 – 28, 2015): “Interfacial Reactivity of a High Capacity Manganese Rich (HCMRTM) Li-ion Positive Electrode”; L. Terborg, Y. Park, S. Venkatachalam, P. Hernandez, and R. Kostecki.
- 227th ECS Meeting, Chicago (May 24 – 28, 2015): “Nanoscale IR Near-Field Imaging of the SEI Layer on an HOPG Electrode”; M. Ayache, D. Jang, and R. Kostecki.

Task 5.3 – Advanced *in situ* Diagnostic Techniques for Battery Materials (Xiao-Qing Yang and Xiqian Yu, Brookhaven National Laboratory)

Project Objective. The primary objective of this project is to develop new advanced *in situ* material characterization techniques and to apply these techniques to support the development of new cathode and anode materials for the next generation of lithium-ion batteries (LIBs) for plug-in hybrid electric vehicles (PHEV). To meet the challenges of powering the PHEV, LIBs with high energy and power density, low cost, good abuse tolerance, and long calendar and cycle life must be developed.

Project Impact. The Multi Year Program Plan (MYPP) of the Vehicle Technology Program (VTP) describes the goals for battery: “Specifically, lower-cost, abuse-tolerant batteries with higher energy density, higher power, better low-temperature operation, and longer lifetimes are needed for the development of the next-generation of HEVs, PHEVs, and EVs.” The knowledge gained from diagnostic studies through this project will help U.S. industries develop new materials and processes for new generation LIBs in the effort to reach these VTP goals.

Approach. This project will use the combined synchrotron based *in situ* x-ray techniques (x-ray diffraction, and hard and soft x-ray absorption) with other imaging and spectroscopic tools such as high-resolution transmission electron microscopy (HRTEM) and mass spectroscopy (MS) to study the mechanisms governing the performance of electrode materials and provide guidance for new material and new technology development regarding Li-ion battery systems.

Out-Year Goals. For the high-voltage spinel $\text{LiMn}_{1.5}\text{Ni}_{0.5}\text{O}_4$, the high-voltage charge and discharge cycling is a serious challenge for the electrolyte oxidation decomposition. Studies on improvement of thermal stability are important for better safety characteristics. For high energy density $\text{Li}(\text{NiMnCo})\text{O}_2$ composite materials, the problem of poor rate capability during charge and discharge and performance degradation during charge-discharge cycling are issues to be addressed.

Collaborations. The BNL team will work closely with material synthesis groups at ANL (Drs. Thackeray and Amine) for the high-energy composite; at UT Austin for the high-voltage spinel; and at PNNL for the Si-based anode materials. Such interaction between the diagnostic team at BNL and synthesis groups of these other BMR members will catalyze innovative design and synthesis of advanced cathode and anode materials. We will also collaborate with industrial partners at General Motor, Duracell, and Johnson Controls to obtain feedback information from battery end users.

Milestones

1. Complete the thermal stability studies of a series of blended LiMn_2O_4 (LMO) - $\text{LiNi}_{1/3}\text{Co}_{1/3}\text{Mn}_{1/3}\text{O}_2$ (NCM) cathode materials with different weight ratios using *in situ* time-resolved x-ray diffraction (XRD) and mass spectroscopy techniques in the temperature range of 25°C to 580°C. (December 2014 – Complete)
2. Complete the *in situ* XRD studies of the structural evolution of $\text{Li}_{2-x}\text{MoO}_3$ ($0 \leq x \leq 2$) high energy density cathode material during charge-discharge cycling between 2.0 and 4.8 V. (March 2015 – Complete)
3. Complete the x-ray absorption near edge structure (XANES) and extended x-ray absorption fine structure (EXAFS) studies at Mo K-edge of Li_2MoO_3 at different charge-discharge states. (June 2015 – Complete)
4. Complete the preliminary studies of elemental distribution of Fe substituted high-voltage spinel cathode materials using transmission x-ray microscopy (TXM). (September 2015 –In Progress)

Progress Report

This quarter, the third milestones for FY15 have been completed.

BNL has been focused on studies of a new cathode material, lithium molybdenum trioxide (Li_2MoO_3). Through a systematic study, a new “unit-cell-breathing” mechanism is introduced based on both crystal and electronic structural changes of transition metal oxide cathode materials during charge-discharge. These results open a new strategy for designing and engineering layered cathode materials for high-energy-density lithium-ion batteries. To understand the abnormal structural changes of Li_2MoO_3 during lithium extraction, *in situ* x-ray absorption spectroscopy (XAS) at Mo K-edge was applied to monitor the valence state changes of Mo and local structure changes of Li_2MoO_3 during charge process. Figure 44a shows the x-ray absorption near edge structure (XANES) spectra of the Mo K-edge during charge. A continuous increase of the pre-edge intensity indicates the increased distortion of MoO_6 octahedra. Such pre-edge structure is originated from a quadruple excitation, which is forbidden under perfect octahedral symmetry. This MoO_6 octahedra distortion caused pre-edge structure is the typical feature of $\alpha\text{-MoO}_3$ with Mo^{6+} oxidation state. The observation of the increased pre-edge structure and the shifting of white line to higher energy positions suggest that Mo ions are oxidized to higher than Mo^{4+} states upon charging. Compared with the Mo K-edge XANES data of the MoO_2 and $\alpha\text{-MoO}_3$ references, it can be estimated that the Mo ions were oxidized from Mo^{4+} to a higher oxidation state between Mo^{5+} to Mo^{6+} . As shown in the enlarged inset of Figure 44a, we can see that the intersection is not exactly an “isosbestic point.” It should be due to the charge process of Li_2MoO_3 not being a simple two-phase reaction, but also including two solid-solution regions. This is confirmed by the *in situ* XRD data. Figure 44b shows the magnitude plot of Fourier transformed extended x-ray absorption fine structure (FT-EXAFS) spectra for Mo K-edge (k^3 -weighted in k -space) of pristine ($x = 0$), half charged ($x = 0.75$) and fully charged ($x = 1.47$) $\text{Li}_{2-x}\text{MoO}_3$. The FT magnitudes of MoO_2 and $\alpha\text{-MoO}_3$ are also plotted in the bottom panels as references.

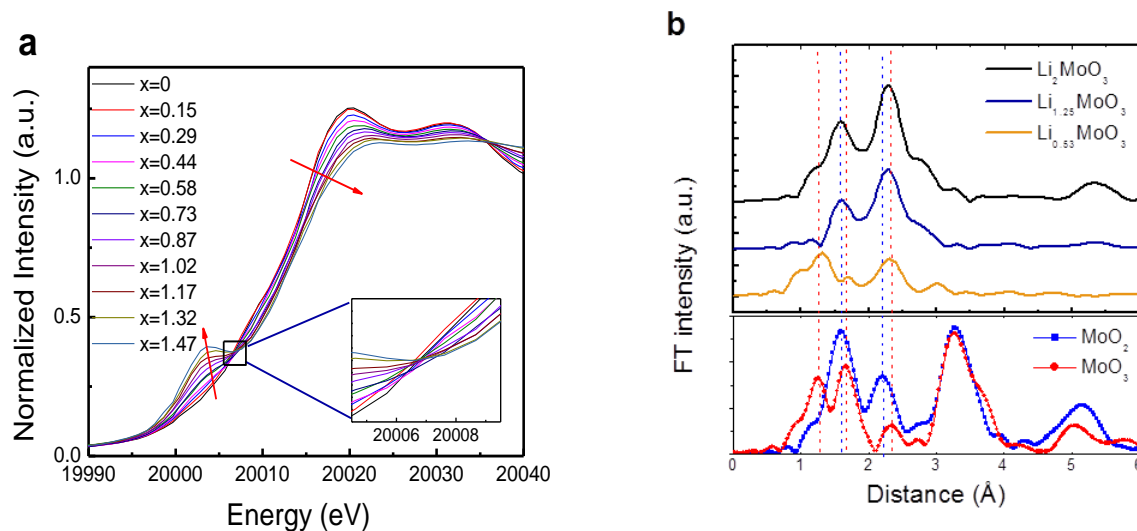


Figure 44. XAS spectra of Li_2MoO_3 during the first charge: (a) *In situ* XANES spectra at Mo K-edge during charging to 4.8 V and (b) *Ex-situ* FT-EXAFS spectra of $\text{Li}_{2-x}\text{MoO}_3$ at pristine ($x=0$), half charged ($x=0.75$) and fully charged ($x=1.47$) states. The lower panel shows the FT-EXAFS spectra of MoO_2 and $\alpha\text{-MoO}_3$ references.

Patents/Publications/Presentations

Publications

- Xiao, Liang, and Jie Xiao,* Xiqian Yu, Pengfei Yan, Jianming Zheng, Mark Engelhard, Priyanka Bhattacharya, Chongmin Wang, Xiao-Qing Yang, and Ji-Guang Zhang*. “Effects of Structural Defects on the Electrochemical Activation of Li_2MnO_3 .” *Nano Energy*, Available online June 27, 2015, doi:10.1016/j.nanoen.2015.06.011.
- Youn, Hee-Chang, and Seong-Min Bak, Myeong-Seong Kim, Chernoo Jaye, Daniel A. Fischer, Chang-Wook Lee, Xiao-Qing Yang, Kwang Chul Roh*, and Kwang-Bum Kim*. “High-Surface-Area Nitrogen-Doped Reduced Graphene Oxide for Electric Double-Layer Capacitors.” *ChemSusChem*, Article first published online: 27 APR 2015 DOI: 10.1002/cssc.201500122.

Presentation:

- MRS 2015 Spring Meeting, San Francisco (April 8, 2015) Invited: “Combined *In situ* Synchrotron Based X-rays and Mass Spectroscopy Study on Thermal Stability of Cathode Materials for Li-ion Batteries during Heating”; Seongmin Bak and Enyuan Hu, Yongning Zhou, Xiqian Yu, Xiao-Qing Yang,* and Kyung-Wan Nam*.

Task 5.4 – NMR and Pulse Field Gradient Studies of SEI and Electrode Structure (Clare Grey, Cambridge University)

Project Objective. The formation of a stable surface electrode interphase (SEI) is critical to the long-term performance of a battery, since the continued growth of the SEI on cycling/aging results in capacity fade (due to Li consumption) and reduced rate performance due to increased interfacial resistance. Although arguably a (largely) solved problem with graphitic anodes/lower voltage cathodes, this is not the case for newer, much higher capacity anodes such as silicon, which suffer from large volume expansions on lithiation, and for cathodes operating above 4.3 V. Thus it is essential to identify how to design a stable SEI. The objectives are to identify major SEI components, and their spatial proximity, and how they change with cycling. SEI formation on Si vs. graphite and high-voltage cathodes will be contrasted. Li⁺ diffusivity in particles and composite electrodes will be correlated with rate. The SEI study will be complemented by investigations of local structural changes of high-voltage/high-capacity electrodes on cycling.

Project Impact. The first impact of this project will be an improved, molecular based understanding of the surface passivation (SEI) layers that form on electrode materials, which are critical to the operation of the battery. Second, we will provide direct evidence for how additives to the electrolyte modify the SEI. Third, we will provide insight to guide and optimize the design of more stable SEIs on electrodes beyond LiCoO₂/graphite.

Out-Year Goals. The goals of this project are to identify the major components of the SEI as a function of state of charge and cycle number different forms of silicon. We will determine how the surface oxide coating affects the SEI structure and establish how the SEI on Si differs from that on graphite and high-voltage cathodes. We will determine how the additives that have been shown to improve SEI stability affect the SEI structure and explore the effect of different additives that react directly with exposed fresh silicon surfaces on SEI structure. Via this program, we will develop new NMR-based methods for identifying different components in the SEI and their spatial proximities within the SEI, which will be broadly applicable to the study of SEI formation on a much wider range of electrodes. These studies will be complemented by studies of electrode bulk and surface structure to develop a fuller model with which to describe how these electrodes function.

Collaborations. This project collaborates with B. Lucht (Rhode Island); E. McCord, W. Holstein (DuPont); J. Cabana, (UIC); G. Chen, K. Persson (LBNL); S. Whittingham (Binghamton); P. Bruce (St. Andrews), R. Seshadri, A. Van der Ven (UCSB), S. Hoffman, A. Morris (U. Cam), N. Brandon (Imperial), and P. Shearing (UCL).

Milestones

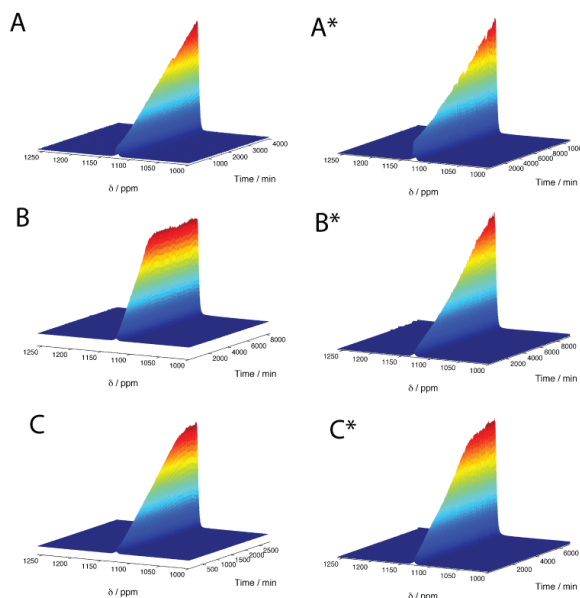
1. Complete initial Si SEI work and submit for publication. Complete 4V spinel work (*in situ* NMR) and submit for publication. (12/31/14 – Complete; papers in prep.)
2. Identify differences in Si SEI after one and multiple cycles. (¹H NMR complete)
3. Identify major organic components on the SEIs formed on high surface area carbons by NMR.
4. Complete initial carbon-SEI interfacial studies. *Go/No-Go*: Determine whether NMR has the sensitivity to probe organics on the cathode side in paramagnetic systems.

Progress Report

^{23}Na *in situ* NMR has been used to study sodium-ion batteries, focusing initially on Na metal anodes and Na anode symmetrical cells. By analogy to Li-anodes and $^6,7\text{Li}$ NMR¹ the limited penetration of the radio frequency field (quantified via the “skin-depth”: 12.3 μm under the conditions used here) used to excite the Na-spins means that we are sensitive to only the surface and the first few microns below the surface of the Na-metal anode. By contrast, Na-metal dendrites can be detected in their entirety as their thickness is less than the skin-depth. On galvanostatic plating (Figure 45) the ^{23}Na NMR resonance assigned to Na metal grows steadily and linearly with time. Since the total mass of Na metal is constant in a symmetric Na-Na cell,

this intensity increase is associated with an increase in Na metal surface (and thus volume of Na excited); this indicates that Na microstructures are formed even at the lowest current studied. Quantification of the NMR signal shows that Na metal deposits are formed, with a morphology associated with an extremely high surface area. In the case of galvanostatic cycling, the Na deposits are partially removed at low currents, on reversing the current, while at high currents there is essentially no removal of the deposits in the initial stages.

High currents show a significantly greater accumulation of deposits during cycling, indicating a much lower efficiency of removal of these structures when the current is reversed (Figure 46). Applying the Scarifker and Hills model,² analysis of chronoamperometry and NMR results are interpreted as a change from progressive to instantaneous nucleation of new Na deposits as the current density is



increased.

Figure 45. *In situ* ^{23}Na NMR spectra for continuous galvanostatic plating, and galvanostatically cycled samples, at currents of 0.5, 1, and 2 mA cm^{-2} (A-C, and A*-C*, respectively) with the superscript (*) denoting galvanostatically cycled samples. Stack plots vs. time (in min.) are shown. The resonance assigned to Na metal continues to grow until the cell fails (e.g., 3000 mins for B) due to extensive short circuits.

Measurement of the ^{23}Na and ^{19}F diffusion coefficients in the electrolyte by the pulsed field-gradient NMR method reveal a surprisingly high mobility for the Na^+ cation (compared to dilute NaCl and lithium electrolytes) in the NaTFSI/PC electrolyte used here. Furthermore, analysis of the diffusion data within the context of the Chazalviel model³ for lithium dendrite formation suggests that this Na system is operating well away from this regime.

¹Bhattacharyya, R., Key, B., Chen, H., Best, A. S., Hollenkamp, A. F., Grey, C.P. *Nat Mater* (2010), 9, 504–510.

²Scharifker, B., & Hills, G. (1983). *Electrochimica Acta*, 28(7), 879–889.

³Chazalviel, J. N. (1990). *Physical Review A*, 42(12), 7355–7367.

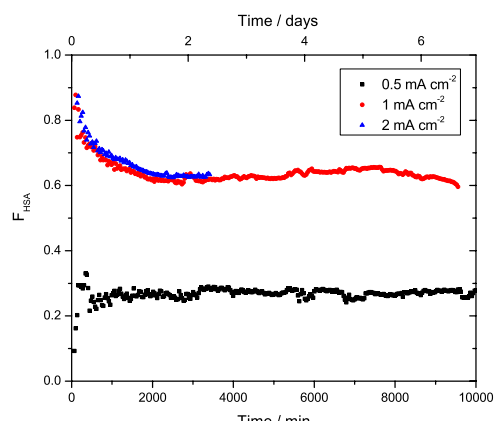


Figure 46. Fraction of high surface area (FHSA) Na during galvanostatic cycling at various current densities. A ratio of 1 indicates complete microstructure deposition while 0 indicates smooth deposition.

Task 5.5 – Optimization of Ion Transport in High-Energy Composite Cathodes (Shirley Meng, UC – San Diego)

Project Objective. This project aims to probe and control the atomic-level kinetic processes that govern the performance limitations (rate capability and voltage stability) in a class of high-energy composite electrodes. A systematic study with powerful suite of analytical tools [including atomic resolution scanning transmission electron microscopy (a-STEM) and Electron energy loss spectroscopy (EELS), X-ray photoelectron spectroscopy (XPS) and first principles (FP) computation] will be used to pin down the mechanism and determine the optimum bulk compositions and surface characteristics for high rate and long life. Moreover, it will help the synthesis efforts to produce materials at large scale with consistently good performance. It is also aimed to extend the suite of surface-sensitive tools to diagnose the silicon anodes types.

Project Impact. If successful, this research will provide a major breakthrough in commercial applications of the class of high energy density cathode material for lithium ion batteries. Additionally, it will provide in-depth understanding of the role of surface modifications and bulk substitution in the high voltage composite materials. The diagnostic tools developed here can also be leveraged to study a wide variety of cathode and anode materials for rechargeable batteries.

Approach. Unique approach that combines STEM/EELS, XPS and *Ab Initio* computation as quantities diagnostic tools for surface and interface characterization and to enable quick identification of causes of surface instability (or stability) in various types of electrode materials including both high-voltage cathodes and low voltage anodes.

Out-Year Goals. The goal is to control and optimize Li-ion transport, TM migration, and oxygen activity in the high-energy composite cathodes and to optimize electrode/electrolyte interface in silicon anodes so that their power performance and cycle life can be significantly improved.

Collaborations. This project engages in collaborations with the following:

- Michael Sailor (UCSD) – porous silicon and carbonization of silicon based anodes
- Keith Stevenson (UT Austin) – XPS and TOF-SIMS
- Nancy Dudney and Juchuan Li (Oak Ridge National Lab) – silicon thin film fabrication
- Chunmei Ban (National Renewable Energy Laboratory) – Molecular Layer Deposition
- Zhaoping Liu and Yonggao Xia [Ningbo Institute of Materials Technology and Engineering (NIMTE), Chinese Academy of Sciences]

Milestones

1. Identify ways to extend the STEM/EELS and XPS techniques for anode materials, such as silicon anode. (9/30/14 –Complete)
2. Identify at least two high-voltage cathode materials that deliver 200mAh/g reversible capacity when charged to high voltages. (12/31/14 – Complete)
3. Obtain the optimum surface coating and substitution compositions in lithium rich layered oxides when charged up to 4.8V (or 5.0 V). (3/31/15 –Complete)
4. Identify the appropriate SEI characteristics and microstructure for improving first-cycle irreversible capacity of silicon anode. (Improve to 85-95%; 6/30/15 – Complete)
5. Identify the mechanisms of ALD and MLD coated silicon anode for their improved chemical stability upon long cycling. (9/30/15 – On Track)

Progress Report

Surface modifications of Li-rich Mn-rich oxide cathode. Two different surface modification methods were applied to improve the first cycle efficiency, the capacity and voltage retention of Li-rich Mn-rich oxide materials upon high-voltage cycling. Firstly, it was determined that 1 wt.% LLTO (Lithium Lanthanum Titanium Oxide) coating can improve the capacity and voltage retention of $\text{Li}_{1.133}\text{Ni}_{0.3}\text{Mn}_{0.567}\text{O}_2$. Figure 47a compares the voltage profile of pristine and coated samples with LLTO at different coating conditions (batch1 and batch2), where they were cycled at low current density (0.1C). After 110 cycles, the coated samples show a significant improvement in capacity retention compared to the pristine sample. Secondly, the surface modification strategy manipulating gas-solid interface between Li-rich Mn-rich oxide and a type of common gas has been explored. The process yielded an increased specific capacity of 306 mAh g^{-1} compared to 276 mAh g^{-1} for the pristine electrode (Figure 47b). It also increased the initial Coulombic efficiency from 83.8% to 90.6%. These increased electrochemical performances are highly related to the surface characteristics of particles after the surface modification process.

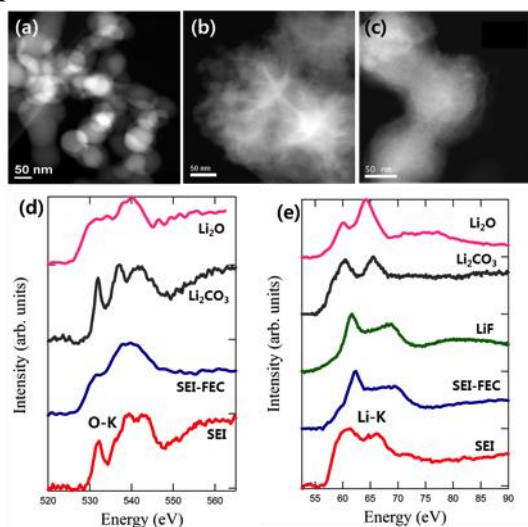


Figure 48. ADF-STEM image of (a) pristine Si, (b) lithiated Si after one cycle, (c) lithiated Si with FEC after one cycle, EELS spectra, (d) O-K edge, and (e) Li-K edge.

FEC. Figure 48(d-e) compares the O-K and Li-K edges of the SEI with the reference samples. The electrode cycled without FEC has an SEI layer that thickens upon cycling and mainly contains Li_2CO_3 (Figure 48d-e). However, the addition of FEC in the electrolyte suppresses the formation of Li_xSiO_y . More importantly, FEC leads to the formation of uniform and stable SEI that covers the Li_xSi particles (Figure 48c) with high LiF content (Figure 48d-e).

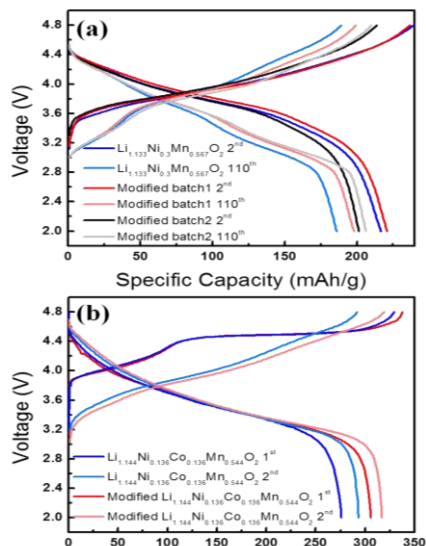


Figure 47. (a) Voltage profiles of the pristine and surface modified $\text{Li}_{1.133}\text{Ni}_{0.3}\text{Mn}_{0.567}\text{O}_2$ at different cycle numbers (0.1 C, 2-4.8V) and (b) 1st and 2nd charge-discharge voltage profiles of the pristine and surface modified $\text{Li}_{1.144}\text{Ni}_{0.136}\text{Co}_{0.136}\text{Mn}_{0.544}\text{O}_2$ at 0.05 C.

Effect of FEC additive on the SEI evolution of Si.

Silicon (Si) electrode optimization has been vigorously conducted, where silicon nanoparticles, various binders, and conductive additives have been tested. The Si electrode has an active mass loading of 0.5 mg cm^{-2} and cycled with the traditional electrolyte. The cycled electrode has an initial Coulombic efficiency of 88.8% with a charge capacity of 1.46 mAh cm^{-2} . The chemical and morphology evolution of both Si and SEI upon progressive cycling was investigated using electron microscopy techniques. Lithiated silicon (Li_xSi) and the SEI layer are extremely beam sensitive. Therefore, the electron dose and spatial resolution were optimized to prevent beam damage. Upon lithiation, crystalline Si (Figure 48a) transformed into the amorphous Li_xSi , and two layers formed on the outermost surface of the electrode including SEI and Li_xSiO_y . Based on Figure 48b, an uneven SEI layer formed at the edge of the particles in the electrode cycled without

Patents/Publications/Presentations

1. Liu, H.D., and D. Qian, M.G. Verde, M. Zhang, L. Baggetto, K. An, Y. Chen, K.J. Carroll, D. Lau, M. Chi, G.M. Veith, and Y.S. Meng. “Understanding the Role of NH_4F and Al_2O_3 Surface Co-Modification on Lithium-excess Layered Oxide $\text{Li}_{1.2}\text{Ni}_{0.2}\text{Mn}_{0.6}\text{O}_2$.” *ACS Applied Materials and Interfaces* (2015) Accepted.
2. Shroder, K.J., and J. Alvarado, T.A Yersak, J. Li, N. Dudney, L. Webb, Y.S Meng, and K.J Stevenson. “The Effect of Fluoroethylene Carbonate as an Additive on the Solid Electrolyte Interphase on Silicon Lithium-ion Electrodes.” *Chemistry of Materials* (2015) Accepted.
3. Invited oral presentation: The Second International Forum on Cathode & Anode Materials for Advanced Batteries, Xiaoshan, China (April 2015): “Probing and Controlling Interface Stability and Oxygen Activities in High Voltage Cathode Materials in Li-ion Batteries”; Shirley Meng.
4. Poster presentation: Jacobs School's Council of Advisors Board, University of California – San Diego, (May 2015): “Understanding the Role of ‘ AlF_3 ’ Surface Modification on Lithium-excess Layered Oxide $\text{Li}_{1.2}\text{Ni}_{0.2}\text{Mn}_{0.6}\text{O}_2$ ”; H.D. Liu, D. Qian, M. Zhang, and Y.S. Meng.
5. Poster presentation: Joint NSRC Workshop, ORNL (June 2015): “STEM Characterization for Oxygen Activities in Li-rich Layered Oxides for High Energy Li-ion Batteries”; Minghao Zhang, Bao Qiu, Danna Qian, Haodong Liu, Ying Shirley Meng.

Task 5.6 – Analysis of Film Formation Chemistry on Silicon Anodes by Advanced *In situ* and *Operando* Vibrational Spectroscopy

(Gabor Somorjai, UC – Berkeley; Phil Ross, Lawrence Berkeley National Laboratory)

Project Objective. Understand the composition, structure, and formation/degradation mechanisms of the solid electrolyte interface (SEI) on the surfaces of Si anodes during charge/discharge cycles by applying advanced *in situ* vibrational spectroscopies. Determine how the properties of the SEI contribute to failure of Si anodes in Li-ion batteries in vehicular applications. Use this understanding to develop electrolyte additives and/or surface modification methods to improve Si anode capacity loss and cycling behavior.

Project Impact. A high-capacity alternative to graphitic carbon anodes is Si, which stores 3.75 Li per Si versus 1 Li per 6 C yielding a theoretical capacity of 4008 mAh/g versus 372 mAh/g for C. But Si anodes suffer from large first cycle irreversible capacity loss and continued parasitic capacity loss upon cycling leading to battery failure. Electrolyte additives and/or surface modification developed from new understanding of failure modes will be applied to reduce irreversible capacity loss, and to improve long-term stability and cyclability of Si anodes for vehicular applications.

Approach. Model Si anode materials including single crystals, e-beam deposited polycrystalline films, and nanostructures are studied using baseline electrolyte and promising electrolyte variations. A combination of *in situ* and *operando* Fourier Transform Infrared (FTIR), Sum Frequency Generation (SFG), and UV-Raman vibrational spectroscopies are used to directly monitor the composition and structure of electrolyte reduction compounds formed on the Si anodes. Pre-natal and post-mortem chemical composition is identified using x-ray photoelectron spectroscopy. The Si films and nanostructures are imaged using scanning electron microscopies.

Out-Year Goals. Extend the study of interfacial processes with advanced vibrational spectroscopies to high-voltage oxide cathode materials. The particular oxide to study will be chosen based on materials of interest at that time and availability of the material in a form suitable for these studies (for example, sufficiently large crystals or sufficiently smooth/reflective thin films). The effect of electrolyte composition, electrolyte additives, and surface coatings will be determined, and new strategies for improving cycle life developed.

Collaborations. This project collaborates with Chunmei Ban (NREL), Functionalization of Si by Atomic Layer Deposition (ALD): Effect of functionalization on electrolyte reduction.

Milestones

1. Determine the reduction products of the electrolyte additive FEC on a characteristic Si electrode and relate composition to the function in cycling. (December 2014 – Complete)
2. Determine the role of $-O_x$ and $-OR$ ($R = H, CH_3, C_2H_5$, etc.) surface functional groups on baseline electrolyte reduction chemistry. (March 2015 – On Schedule)
3. Determine role of the Si surface morphology (for example, roughness) on the SEI formation structure and cycling properties. (June 2015 – On Schedule)
4. *Go/No-Go*: Feasibility of surface functionalization to improve SEI structure and properties. Criteria: Functionalize a model Si anode surface, and determine how SEI formation is changed. (September 2015 – On Schedule)

Progress Report

In Q3, the surface of a Si(100) wafer (anode) was investigated by sum frequency generation vibrational spectroscopy while under constant potential (Chronoamperometry). The potential that we chose was 0.5 V (vs. Li/Li+) corresponding to known electrolyte reduction reactions at the surface.

These preliminary SFG studies performed in our group on anodic half-cell have led us to believe that polyethylene carbonate (poly-EC) is formed on the Si anode surface under working conditions. Under working conditions at a constant reduction potential of 0.5 V (vs. Li/Li+) in contact with 1 M LiPF₆ EC:DEC (1:2 v/v) electrolyte solution, we can assume that poly-EC forms on Si electrodes (Figure 49).

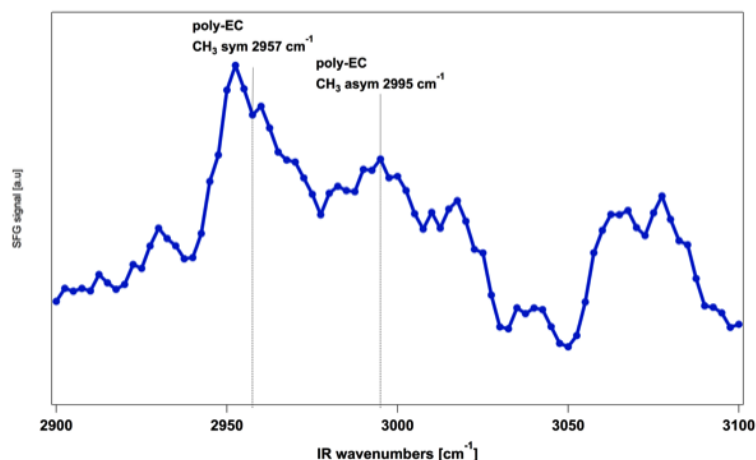
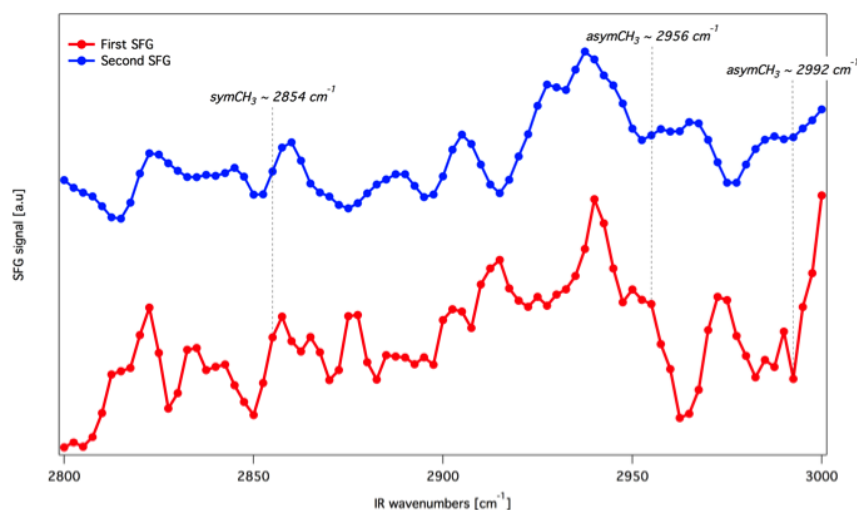


Figure 49. We suggest, according to this SFG spectrum that polyethylene carbonate is the main product of the Si/electrolyte interface layer at reduction potential of 0.5 V.

The appearance of peaks around 2956 cm⁻¹ and 2992 cm⁻¹ had led us to investigate whether the surface of the Si wafer (Si-O_x) undergoes electrochemical substitution with a DEC derivative, radical ethoxy (CH₃CH₂[•]). We have therefore modified the surface of both amorphous and crystalline Si anodes from native Si-O_x

termination to Si-CH₂CH₃ (Si-ethoxy) by boiling them in ethanol for 24 h under inert conditions. The Si-ethoxy surface was probed by SFG and micro-FTIR (beam line 1.4.4 at the advanced light source). However, due to sample contamination the micro-FTIR results are inconclusive, and we are refining our ethoxy substitution procedure.

SFG spectra of Si-ethoxy were also inconclusive since we could not obtain clear symmetric CH₃ vibrations at around 2855 cm⁻¹ and two symmetric CH₃ vibrations at ~ 2955 cm⁻¹ and ~ 2992 cm⁻¹ (Figure 50). The main



reason for this is poor signal to noise ratio due to rapid deterioration of our pump laser. We are upgrading our pump laser to achieve better signal stability.

Figure 50. We performed two consecutive SFG measurements on Si-ethoxy wafer. Due to poor signal to noise ratio we are unable at this point to validate that indeed Si-ethoxy forms on the Si(100) surface.

Task 5.7 – Microscopy Investigation on the Fading Mechanism of Electrode Materials (Chongmin Wang, Pacific Northwest National Laboratory)

Project Objective. The objective of this work is to use *ex-situ*, *in situ*, and *operando* high-resolution transmission electron microscopy (TEM) and spectroscopy to probe the fading mechanism of electrode materials. The focus of the work will be on using *in situ* TEM under real battery operating conditions to probe the structural evolution of electrodes and interfaces between the electrode and electrolyte and correlate this structural and chemical evolution with battery performance. The following three questions will be addressed:

- How do the structure and chemistry of electrode materials evolve at a dimension ranging from atomic-scale to meso-scale during the charge and discharge cycles?
- What is the correlation of the structural and chemical change to the fading and failure of lithium (Li)-ion batteries?
- How does the interface evolve between the electrode and the electrolyte and their dependence on the chemistry of electrolytes?

Project Impact. Most previous microscopic investigations on solid-electrolyte interphase (SEI) layer formation and morphology evolution on electrodes are either *ex situ* studies or used low-vapor-pressure electrolytes so they cannot reveal the details of the dynamic information under practical conditions. We have developed new *operando* characterization tools to characterize SEI formation and electrode/electrolyte interaction using practical electrolyte that are critical for making new breakthroughs in this field. The success of this work will increase the energy density of Li-ion batteries and accelerate market acceptance of electrical vehicles (EV), especially for plug-in hybrid electrical vehicles (PHEV) required by the EV Everywhere Grand Challenge proposed by the DOE/EERE.

Approach. Extend and enhance the unique *ex situ* and *in situ* TEM methods for probing the structure of Li-ion batteries, especially for developing a biasing liquid electrochemical cell that uses a real electrolyte in a nano-battery configuration. Use various microscopic techniques, including *ex situ*, *in situ*, and especially the *operando* TEM system, to study the fading mechanism of electrode materials in batteries. This project will be closely integrated with other research and development efforts on high-capacity cathode and anode projects in the BMR Program to 1) discover the origins of voltage and capacity fading in high-capacity layered cathodes and 2) provide guidance for overcoming barriers to long cycle stability of silicon (Si)-based anode materials.

Out-year goals: The out-year goals are as follows:

- Extended the *in situ* TEM capability for energy storage technology beyond Li ions, such as Li-S, Li-air, Li-metal, sodium ions, and multi-valence ions.
- Multi-scale (that is, ranging from atomic-scale to meso-scale) *in situ* TEM investigation of failure mechanisms for energy-storage materials and devices (both cathode and anode).
- Integration of the *in situ* TEM capability with other microscopy and spectroscopy methods to study energy-storage materials, such as *in situ* SEM, *in situ* SIMS, and *in situ* x-ray diffraction.
- Atomic-level *in situ* TEM and scanning transmission electron microscopy (STEM) imaging to help develop a fundamental understanding of electrochemical energy-storage processes and kinetics of both cathodes and anode.

Collaborations: We are collaborating with the following principal investigators: Dr. Chunmei Ban (NREL); Dr. Gao Liu (LBNL); Dr. Khalil Amine (ANL); Professor Yi Cui (Stanford); Dr. Jason Zhang (PNNL); Dr. Jun Liu (PNNL); Dr. Guoying Chen (LBNL); and Dr. Xingcheng Xiao (GM).

Milestones

1. Establish the methodology that enables reliably positioning a nanowire on the chip to assembly the closed liquid cell. Complete the *in situ* TEM study of the behavior of native oxide layer during lithiation and delithiation. (12/31/2014 – Complete)
2. Complete quantitative measurement of coating layer and SEI layer thickness as a function of cycle number on a Si anode in a liquid cell with a practical electrolyte. (03/31/2015 – Complete)
3. Complete the *operando* TEM study of cathode materials with/without coating layer and the SEI layer formation. (9/30/2015 – Ongoing)

Progress Report

Capacity and voltage fading of layer structured cathode based on lithium transition metal oxide is closely related to the lattice position and migration behavior of the transition metal ions. However, the behavior of each of these transition metal ions in this category of cathode material is scarcely clear.

Using chemical imaging with aberration corrected scanning transmission electron microscope (STEM) and DFT calculations, we directly visualize at atomic resolution on the interatomic layer mixing of transition metal (Ni, Co, Mn) and lithium ions in layer structured oxide cathodes for lithium ion batteries.

As typically illustrated in Figure 51, we discovered that in the layered cathodes, Mn and Co tend to reside almost exclusively at the lattice site of transition metal (TM) layer in the structure or little interlayer mixing with Li. In contrast, Ni shows high degree of interlayer mixing with Li. The fraction of Ni ions residing in the Li layer followed a near linear dependence on total Ni concentration before reaching saturation. The general trend observed by EDS is consistent with the result based on XRD and neutron diffraction analysis, but only the EDS yields atomic level spatial resolution.

The experimental observation is consistent with the density functional theory (DFT) calculations using NMC-442 cathode as

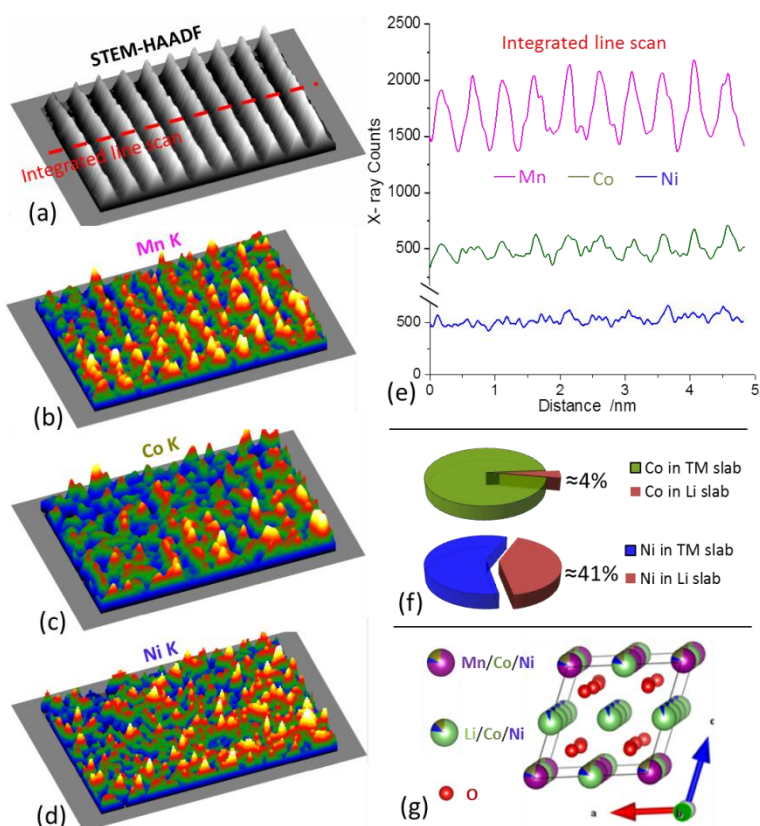


Figure 51. $\text{Li}_{1.2}\text{Ni}_{0.13}\text{Co}_{0.13}\text{Mn}_{0.54}\text{O}_2$ (NC-LMR) sample: (a) [010] zone axis STEM-HAADF image showing the EDS mapping region, (b) Surface plot of Mn K map, (c) Surface plot of Co K map, (d) Surface plot of Ni K map, (e) Integrated line scan profile showing x-ray counts distribution across the layered structure, (f) Based on counts ratio that from TM-layer and Li-layer, 4% Co and 41% Ni were estimated to seat in Li-layer due to an interlayer mixing, and (g) Optimized crystal model for NC-LMR based on EDS mapping results.

an example. According to the DFT calculation, Li/Ni antisite defect pairs show much lower total energy increase than that of Li/Co and Li/Mn ones, which indicates Li/Ni interlayer mixing is the easiest one to happen while Li/Co and Li/Mn interlayer mixing are unlikely to happen.

It has been demonstrated that upon cycling of $\text{Li}_{1.2}\text{Ni}_{0.2}\text{Mn}_{0.6}\text{O}_2$ (20N-LMR) cathode, Ni gradually migrates to the particle surface, leading to Ni depletion in the bulk, structure instability, and consequently cathode voltage and capacity fade. DFT calculation indicated that when Ni resides in the Li layer, migration barrier for Ni is even lower than Li. Apparently, to reduce the migration of Ni to the particle surface during battery operation, the interlayer mixing of Ni into the Li layer should be minimized, which should be taken into consideration during material processing. Furthermore, previous studies indicated that Ni could migrate from TM-layer into Li-layer and resulted in structure instability. However, direct evidence is lacking, and its mechanism is also unclear, even though considerable computational work has been carried out. Cation migration is the fundamental science for LIBs and demands more effort in this direction. The present work using atomic resolution EDS chemical imaging provides a new approach. The observation on the drastically different behavior of Ni, Co, and Mn in terms of atomic level mixing indicates that regulating or guiding Ni behavior constitutes a crucial step for mitigating capacity and voltage fade in this class of layer cathode oxides.

Patents/Publications/Presentations

1. Luo, Langli, and Hui Yang, Pengfei Yan, Jonathan J. Travis, Younghee Lee, Nian Liu, Daniela Molina Piper, Se-Hee Lee, Peng Zhao, Steven M. George, Ji-Guang Zhang, Yi Cui, Sulin Zhang, Chunmei Ban, and Chong-Min Wang. “Surface-Coating Regulated Lithiation Kinetics and Degradation in Silicon Nanowires for Lithium Ion Battery.” *ACS Nano* 9 (2015):5559–5566.
2. Presentation at MRS 2015 Spring Meeting, San Francisco (April 2015): “*In Situ* TEM Study of Native Oxide Layer and Artificial Coating Layer on the Lithiation Kinetics of Si as Anode for Lithium Ion Batteries”; Chong-Min Wang, Langli Luo, Yang He, Hui Yang, Nian Liu, Chunmei Ban, Scott X. Mao, Jun Liu, Sulin Zhang, Yi Cui, and Ji-Guang Zhang.

Task 5.8 – Energy Storage Materials Research Using DOE's User Facilities and Beyond (Michael M. Thackeray and Jason R. Croy, Argonne National Laboratory)

Project Objective. The primary objective of this project is to explore the fundamental, atomic-scale processes that are most relevant to the challenges of next-generation, energy-storage technologies. A deeper understanding of these systems will rely on novel and challenging experiments that are only possible through unique facilities and resources. The goal of this project is to capitalize on a broad range of facilities to advance the field through cutting-edge science, collaborations, and multi-disciplinary efforts.

Project Impact. This project is being implemented to capitalize on and exploit DOE's user facilities and other accessible national and international facilities (including skilled and trained personnel) in order to produce knowledge to advance energy-storage technologies. Specifically, furthering the understanding of structure-electrochemical property relationships and degradation mechanisms will contribute significantly to meeting the near-to-long term goals of EV and PHEV battery technologies.

Approach. A wide array of unique capabilities including x-ray and neutron diffraction, x-ray absorption, emission and scattering, high-resolution transmission electron microscopy, Raman spectroscopy, and theory will be brought together to focus on challenging experimental problems. Combined, these resources promise an unparalleled look into the structural, electrochemical, and chemical mechanisms at play in novel, complex electrode/electrolyte systems being explored at Argonne National Laboratory.

Out-Year Goals. The out-year goals are as follows:

- Gain new, fundamental insights into complex structures and degradation mechanisms of composite cathode materials from novel, probing experiments carried out at user facilities and beyond.
- Investigate structure-property relationships that will provide insight into the design of improved cathode materials.
- Use the knowledge and understanding gained from this project to develop and scale up advanced cathode materials in practical lithium-ion prototype cells,

Collaborators. This project engages in collaboration with Mahalingam Balasubramanian, Joong Sun Park, and Hakim Iddir.

Milestones

1. Evaluation of lithium-ion battery electrodes using DOE User Facilities at Argonne (APS, EMC, and ALCF) and facilities elsewhere, e.g., neutron spallation sources at SNS (Oak Ridge). Other facilities include the neutron facility ISIS, Rutherford Laboratory (UK) and the NUANCE characterization center (Northwestern University). (September 2015 – In Progress)
2. Evaluation of Li_2MnO_3 end member and composite $\text{Li}_2\text{MnO}_3 \bullet (1-x)\text{LiMO}_2$ ($M = \text{Mn, Ni, Co}$) structures by combined neutron/x-ray diffraction. (September 2015 – In Progress)
3. Evaluation of transition metal migration in lithium-metal-oxide insertion electrodes. (September 2015 – In Progress; see text)
4. Analysis, interpretation, and dissemination of collected data for publication and presentation. (September 2015 – In Progress)

Progress Report

The migration of cations M and M' in $\text{Li}_{1-x}(\text{MM}')_{1-x}\text{O}_2$ cathodes (M=Mn, Ni, Co...; M'=Mg, Ga, Al...) is a subject of significant importance. The stability of cations in the octahedral sites of the transition metal (TM) layers, for example, affects the tendencies of phase transformation (for example, layered to spinel) as well as the mechanisms of voltage fade in layered-layered compositions. Non-redox active elements such as Al have also been cited as enhancing oxygen stability and possibly affecting working voltages. Although the stabilities of many elements have been studied both experimentally and theoretically, it is not clear that the underlying mechanisms of migration are well understood. For example, most calculations consider highly delithiated structures (e.g., $\text{Li}_{1-x}\text{MO}_2$, $x \geq 0.5$) and thermodynamic stabilities from which Cr, well-known from experiment to favor migration, has been found to be relatively stable. In addition, the effect of oxygen activity and oxygen loss, as well the changing oxidation of migrating cations (for example, changing U parameter), are not well accounted for. To better understand the connection between experiment and theory, an investigation of several model systems has been undertaken.

A recent report has shown that non-redox active Ga, substituted in $\text{LiCo}_{1-x}\text{Ga}_x\text{O}_2$ ($x=0.05, 0.075$), begins migrating from the octahedral sites of the TM layers immediately upon delithiation with significant migration at just 10% state-of-charge. Secondly, although this migration was found to be ~100% reversible, significant bond disorder was observed by EXAFS analysis after just 1 cycle of charge/discharge to 150 mAh/g (that is, just ~54% of the theoretical capacity). Figure 52a shows recently initiated DFT calculations on Ga-doped LiCoO_2 . In agreement with experiment, Ga prefers to be situated in the octahedral sites of the Co layers. Furthermore, Ga-O bond distances are slightly larger than Co-O distances, in agreement with EXAFS. Calculations on Ga migration as a function of lithium content are in progress.

As a second model system, redox-active Cr substitution is also under study in $\text{LiCo}_{1-x}\text{Cr}_x\text{O}_2$ ($x=0.05, 0.075$). Figure 52b shows x-ray diffraction data of the Cr-containing samples showing well-layered structures for both compositions. Figure 52c shows the initial portion of the first-charge profile for $x=0, 0.05$, and 0.075 . As in the non-redox case of Ga, Cr substitution clearly alters the voltage profiles when substituted in the LiCoO_2 matrix even at very low lithium removal, although the voltage profiles are altered in completely different ways where the redox active Cr shows several features, possibly due to $\text{Cr}^{3+/6+}$ activity (oxidation/migration). Detailed EXAFS, NMR, and DFT studies are currently underway to elucidate the structural and chemical nature of $\text{LiCo}_{1-x}\text{Cr}_x\text{O}_2$ as a function of lithium content. Future reports will focus on the differences and similarities of these non-active and active redox substitutions.

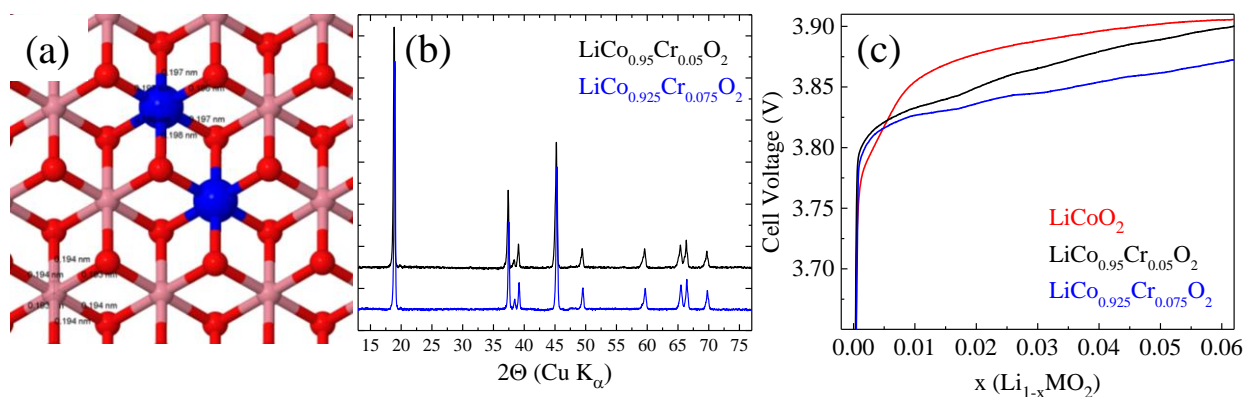


Figure 52. (a) DFT calculations of local structures in Ga-doped LiCoO_2 , (b) XRD patterns of $\text{LiCo}_{1-x}\text{Cr}_x\text{O}_2$ for $x=0.05$ and 0.075 , and (c) First-cycle charge profiles for $\text{LiCo}_{1-x}\text{Cr}_x\text{O}_2$ lithium half-cells.

Patents/Publications/Presentations

1. Presentation at the Annual Merit Review, DOE Vehicle Technologies Program, Arlington, Virginia (June 8 – 12, 2015): “User Facilities for Energy Storage Materials Research”; J. R. Croy.
2. Presentation at Advanced Automotive Battery Conference, Detroit (June 13 – 17, 2015): “Current Research on High-energy Li-Ion Batteries at Argonne National Laboratory”; J. R. Croy.

TASK 6 – MODELING ADVANCED ELECTRODE MATERIALS

Summary and Highlights

Achieving the performance, life, and cost targets outlined in the EV Everywhere Grand Challenge will require moving to next generation chemistries, such as higher capacity Li-ion intercalation cathodes, silicon and other alloy-based anodes, lithium metal anode, sulfur cathodes, and Na-ion systems. However, numerous problems plague development of these systems, from material level challenges in ensuring reversibility to electrode-level issues in accommodating volume changes, to cell-level challenges in preventing cross talk between the electrodes. In this task, a mathematical perspective is applied to these challenges to provide an understanding of the underlying phenomenon and to suggest solutions that can be implemented by the material synthesis and electrode architecture groups.

The effort spans multiple length scales from *ab initio* methods to continuum-scale techniques. Models are combined with experiments, and extensive collaborations are established with experimental groups to ensure that the predictions match reality. Efforts are also focused on obtaining the parameters needed for the models either from lower length scale methods or from experiments. Projects also emphasize pushing the boundaries of the modeling techniques used, to ensure that the task stays at the cutting edge.

In the area of intercalation cathodes, the effort focuses on understanding the working principles of the high Ni layered materials with an aim of understanding structural changes and the associated changes in transport properties. In addition, focus is paid to the assembling of porous electrodes with particles to predict the conduction behavior and developing tools to measure electronic conduction. In this quarter, efforts were focused on Li diffusion mechanisms in the end-member Li-excess Li_2MnO_3 material and on controlling off-stoichiometry to create an electrically conductive glassy coating on olivine cathodes to improve the rate capability of Mn-based olivines. The method yielded high Mn olivines with excellent rate capability above 5C rate with the off-stoichiometry, much improved compared to the base material. Finally, porous electrode conductivity measurements were obtained using micro-probe techniques developed as part of the program using NCM-532 as candidate cathodes. The out-of-plane conductivity was found to be lower than in-plane conductivity, suggesting ways to improve cathode laminate preparation.

In the area of silicon anodes, the effort is in trying to understand the interfacial instability and suggest ways to improve the cycleability of the system. In addition, effort is focused on designing artificial SEI layers that can accommodate the volume change, and in understanding the ideal properties for a binder to accommodate the volume change without delamination. This quarter, a method has been established to simulate the growth and predict the products of the SEI with FEC. In addition, models that mimic the stress in coatings on Si anodes with the coating being either continuous or in islands, shows that island coatings can lead to cracking. In addition, simulations suggest that Al_2O_3 coating is more protective than the native SiO_2 layer.

In the area of sulfur cathodes, the focus is on developing better models for the chemistry with the aim of describing the precipitation reactions accurately. Efforts are focused on performing the necessary experiments to obtain a physical picture of the phase transformations in the system and in measuring the relevant thermodynamic, transport, and kinetic properties. In addition, changes in the morphology of the electrode are described and tested experimentally. Cells that incorporate a single ion conducting ceramic with small electrolyte volume have been fabricated and tested in the lab. In this quarter, these cells were shown to have acceptable rate capability, allowing data with elimination of the polysulfide shuttle.

Finally, microstructure models are an area of focus to ensure that the predictions move away from average techniques to more sophisticated descriptions of processes inside electrodes. Efforts are focused on understanding conduction within the electrode and also on simulating the full electrode that describe the intricate physics inside the battery electrode. These efforts are combined with tomography information as input into the models. This quarter, efforts were focused on identifying various phases in candidate cathode materials so that the relevant information could be fed into mathematical models.

Task 6.1 – Electrode Materials Design and Failure Prediction (Venkat Srinivasan, Lawrence Berkeley National Laboratory)

Project Objective: The goal of this project is to use continuum-level mathematical models along with controlled experiments on model cells to (i) understand the performance and failure models associated with next-generation battery materials, and (ii) design battery materials and electrodes to alleviate these challenges. The research will focus on the Li-S battery chemistry and on microscale modeling of electrodes. Initial work on the Li-S system will develop a mathematical model for the chemistry along with obtaining the necessary experimental data, using a single ion conductor (SIC) as a protective layer to prevent polysulfide migration to the Li anode. The initial work on microscale modeling will use the well-understood Li(NiMnCo)_{1/3}O₂ (NMC) electrode to establish a baseline for modeling next-generation electrodes.

Project Impact: Li-S cells promise to increase the energy density and decrease the cost of batteries compared to the state of the art. If the performance and cycling challenges can be alleviated, these systems hold the promise for meeting the EV-Everywhere targets.

Out-Year Goals: At the end of this project, a mathematical model will be developed that can address the power and cycling performance of next-generation battery systems. The present focus is on microscale modeling of electrodes and Li-S cells, although the project will adapt to newer systems, if appropriate. The models will serve as a guide for better design of materials, such as in the kinetics and solubility needed to decrease the morphological changes in sulfur cells and increase the power performance.

Collaborations: This project collaborates with Gao Liu (LBNL) and CD Adapco.

Milestones

1. Develop a model of a Li-S cell incorporating concentration solution framework. (12/31/14 – Complete)
2. Develop a custom Li-S electrochemical cell with small (~200 μm) catholyte layer incorporating a SIC. (Due 3/31/15) Stop custom cell development if unable to prevent SIC damage during cell assembly.
Status: Go
3. Use custom cell to perform rate experiments. If unsuccessful in developing custom cell, develop cell without SIC and measure shuttle current. (6/30/15 – Complete)
4. Compare microscale and macroscale simulation results and experimental data to determine the importance of microstructural detail. (9/30/15 – In Progress)

Progress Report

Custom Li-S cell with small catholyte layer: “Protected” Li-S cells, wherein the Li electrode is protected by a ceramic single-ion conductor enables measurements of transport and rate data without the complexity of the polysulfide shuttle. Further, the catholyte layer has to be of limited volume to ensure that the experiments are conducted under conditions where practical devices need to be built. To this end, the design of the novel Li-S cell originally developed in Q1 was further refined, and preliminary tests were conducted to eliminate chemically incompatible materials and to improve the seal between the positive and negative chambers, while continuing to provide mechanical protection to the fragile SIC. Rate experiments were performed with the fully assembled cell, including the SIC, using a lithium metal anode a cathode consisting of elemental sulfur, poly(3,4-ethylenedioxythiophene) (PEDOT), and conductive additive on an aluminum foil current collector, and an electrolyte solution consisting of 1M bis(trifluoromethane) sulfonimide lithium (LiTFSI) in 1:1 dioxolane (DOL) / dimethoxyethane (DME). The cell showed an acceptably small ohmic drop—a marked improvement over results from the previous quarter. The catholyte layer is guaranteed to be thinner (and likely significantly thinner) than 140 μm , smaller than the 200 μm target, with a total catholyte volume of approximately 60 microliters. It was found that charging at a rate of C/10 or lower reliably produced the two characteristic plateaus during subsequent discharge. Discharging at C/3 yielded a capacity of about 80% (based on capacity determined from a C/12 discharge). Higher currents lead to impedance growth, due to the resistive ceramic layer. Figure 53 shows results from one of the rate experiments: a discharge and charge at a rate of approximately C/12. These achievements satisfy the third quarter milestone.

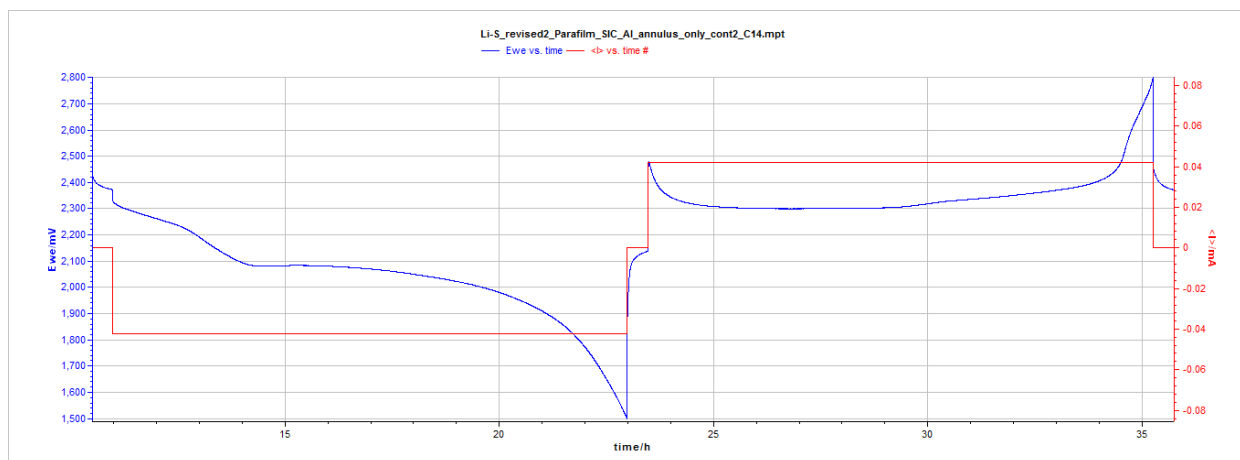


Figure 53. C/12 discharge and charge of custom Li-S cell

Microscale simulation. Progress toward the fourth quarter milestone continued. Advances were made in distinguishing the pore space, binder and conductive material matrix, and active material in the tomography data.

Patents/Publications/Presentations

1. Presentation at Annual Merit Review (2015): “Continuum Modeling as a Guide to Developing New Battery Materials.”
2. Presentation at Beyond Lithium Ion VII (2015): “Understanding Limitations in the Li-S System Using Macro-Modeling and Experimentation.”

Task 6.2 – Predicting and Understanding Novel Electrode Materials from First-Principles (Kristin Persson, Lawrence Berkeley National Laboratory)

Project Objective. The project aim is to model and predict novel electrode materials from first-principles focusing on (1) understanding the atomistic interactions behind the behavior and performance of the high-capacity lithium excess and related composite cathode materials, and (2) predicting new materials using the recently developed Materials Project high-throughput computational capabilities at LBNL. More materials and new capabilities will be added to the Materials Project Lithium Battery Explorer App (www.materialsproject.org/apps/battery_explorer/).

Project Impact. The project will result in a profound understanding of the atomistic mechanisms underlying the behavior and performance of the Li-excess as well as related composite cathode materials. The models of the composite materials will result in prediction of voltage profiles and structural stability—the ultimate goal being to suggest improvements based on the fundamental understanding that will increase the life and safety of these materials. The Materials Project aspect of the work will result in improved data and electrode properties being calculated to aid predictions of new materials for target chemistries relevant for ongoing BMR experimental research.

Out-Year Goals. During year 1-2, the bulk phase diagram will be established, including bulk defect phases in layered Li_2MnO_3 , layered LiMO_2 ($\text{M} = \text{Co}, \text{Ni}, \text{and Mn}$) and LiMn_2O_4 spinel to map out the stable defect intermediate phases as a function of possible transition metal rearrangements. Modeling of defect materials (mainly Li_2MnO_3) under stress/strain will be undertaken to simulate effect of composite nano-domains. The composite voltage profiles as function of structural change and Li content will be obtained. In years two to four, the project will focus on obtaining Li activation barriers for the most favorable TM migration paths as a function of Li content as well as electronic DOS as a function of Li content for the most stable defect structures identified in years one to two. Furthermore, stable crystal facets of the layered and spinel phases will be explored, as a function of O_2 release from surface and oxygen chemical potential. Within the Materials Project, hundreds of novel Li intercalation materials will be calculated and made available.

Collaborations. This project engages in collaboration with Gerbrand Ceder (MIT), Clare Grey (U Cambridge, UK), Mike Thackeray (ANL), and Guoying Chen (LBNL).

Milestones

1. Mn mobilities as a function of Li content in layered Li_xMnO_3 and related defect spinel and layered phases. (3/31/15 – Complete)
2. Surface facets calculated and validated for Li_2MnO_3 . (3/31/15 – Delayed)
3. Calculate stable crystal facets. Determine whether facet stabilization is possible through morphology tuning. (6/30/15 – Delayed)
4. *Go/No-Go*: Stop this approach if facet stabilization cannot be achieved. (6/30/15 – Delayed)
5. Li mobilities as a function of Li content in layered Li_xMnO_3 and related defect spinel and layered phases. (9/30/15 – Ongoing)

Progress Report

The project has experienced some delay due to change in staffing as of August 2014. A new postdoc was hired in November and arrived early 2015.

To meet our milestones, we have continued performing first-principle calculations to explore Li diffusion mechanisms in the end-member Li-excess Li_2MnO_3 material. Here we present the Li-ion migration patterns of intra Li-layer mobility in the high Li content region. The migration energy barriers were calculated with the Nudged Elastic Band method. The inset in Figure 54a shows each layer of Li_2MnO_3 , for which there are two symmetrically different stable octahedral sites in the Li-layer. The Li-ion can migrate to any one of the six nearest neighbors of each stable site. Among the possible migration paths, two distinguishable migration paths exist in each symmetric site for intra-layer Li migration. The list of kinetically resolved migration energy barriers and migration distances is listed in Table 4. One of the representative Li-ion migration paths presented in Figure 54a shows Li-ions migrate from the 4h site to 2c site. Here, the Li-ion located at 2c site is more stable; in other words, the single vacancy located at the 4h site is more stable.

Table 4. Li-ion migration barriers in Li-layer.

Direction (Fig.54-b)	Energy barrier	Distance
4h-4h(red)	0.60 eV	2.92 Å
4h-4h(black)	0.78 eV	2.86 Å
2c-4h(yellow)	0.56 eV	2.92 Å
2c-4h(blue)	0.80 eV	2.86 Å

In spite of their crystal symmetry, the first neighbor migration barriers between each symmetrical site have two different paths. For instance, the 4h site to 4h site migrations have 2 possible paths, which are marked with red and black arrows in Figure 54b. Similarly, 2c site to 4h site hopping also has 2 different paths, which are marked with yellow and blue arrows in Figure 54b. The energy barrier dissimilarity originates from the difference in local environment of saddle point.

Surface calculations to study the morphology of Li_2MnO_3 are under way and will be reported next quarter.

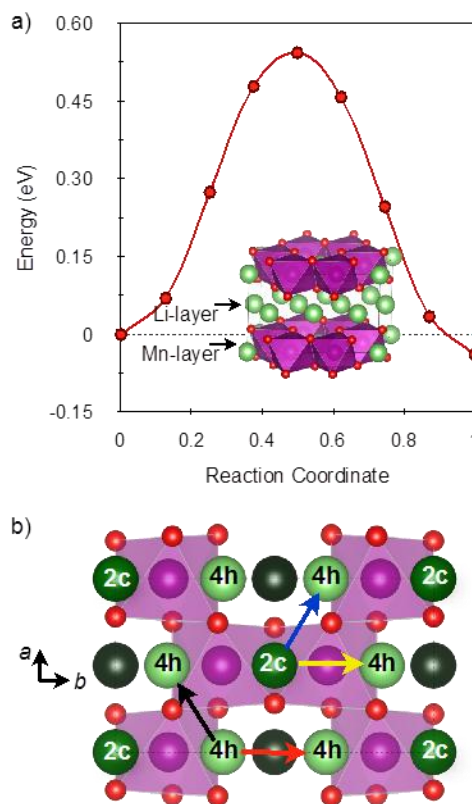


Figure 54. (a) Structure of layered Li-excess material (inset), and Li-ion migration barrier in Li-layer. (b) Four symmetric hopping paths of Li-ion.

Patents/Publications/Presentations

- Annual Merit Review Presentation 2015: “Predicting and Understanding Novel Electrode Materials from First-principles Calculations.”

Task 6.3 – First Principles Calculations of Existing and Novel Electrode Materials (Gerbrand Ceder, MIT)

Project Objective. Develop a mixed olivine cathode that leads to superior energy density compared to the conventional olivine cathodes ($> 600 \text{ Wh kg}^{-1}$). Develop a mixed olivine composition that results in a high-power output ($> 60 \text{ W kg}^{-1}$). Establish synthesis methods of mixed olivine compounds that can make simultaneous formation of glassy surface phases. Give insight into the role of the glassy surface layer that enables high-power performance of mixed olivine cathodes.

Project Impact. The project will lead to insight in how mixed olivine cathodes can cycle at high rates. The project will help in the design of mixed olivine cathode materials with off-stoichiometry that are capable to store more energy or to deliver higher power.

Out-Year Goals. Higher power Li-ion cathode materials, and novel chemistries for higher energy density storage devices. Guide the field in the search for high-power mixed olivine materials.

Collaborations. This project collaborates with K. Persson at LBNL and C. Grey at Cambridge U.

Milestones

1. Demonstrate energy density higher than 600 Wh kg^{-1} in a mixed olivine cathode. (5/31/15 – Complete)
2. Demonstrate high-power density higher than 60 W kg^{-1} in a mixed olivine cathode. (5/31/15 – Complete)
3. Established synthesis methods for high power mixed olivine cathodes using off-stoichiometric compositional design. (4/31/15 – Complete)
4. Develop other mixed olivine compositions that can lead to higher energy density or higher power. (Ongoing)

Progress Report

Higher theoretical energy density for LiFePO_4 can be achieved by mixing Mn with Fe, taking advantage of the $\text{Mn}^{2+/3+}$ redox potential at 4.1 V over $\text{Fe}^{2+/3+}$ at 3.4 V. Compositions with large Mn content, however, tend to lack reasonable rate performance.

In this project, we develop a simple and efficient method to enable high-rate capability of the mixed olivine cathode, $\text{LiFe}_{0.6}\text{Mn}_{0.4}\text{PO}_4$, by controlling off-stoichiometry to create an electrically conductive glassy coating. The molar ratio of the off-stoichiometric composition is 1 : 0.9 : 0.95 for Li : ($\text{Fe}_{0.6} + \text{Mn}_{0.4}$) : P, which maintains transition metal deficiency. The product is obtained with a simple solid-state method.

The obtained particle shows that the $\text{LiFe}_{0.54}\text{Mn}_{0.36}\text{P}_{0.95}\text{O}_{4-\delta}$ particle comprises the crystalline $\text{LiFe}_{0.6}\text{Mn}_{0.4}\text{PO}_4$ particle with the non-crystalline surface of phosphates; balancing the off-stoichiometric ratio: $\text{LiFe}_{0.54}\text{Mn}_{0.36}\text{P}_{0.95}\text{O}_{4-\delta}$ is basically

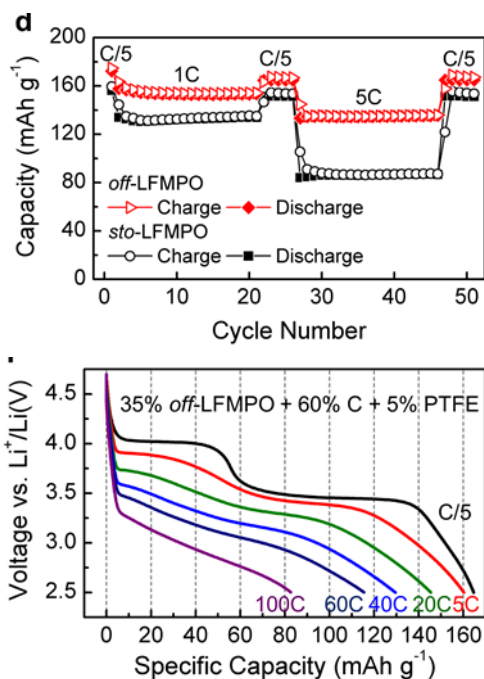


Figure 56. Good capacity retention and high rate capability in the mixed olivine cathode driven from off-stoichiometric composition

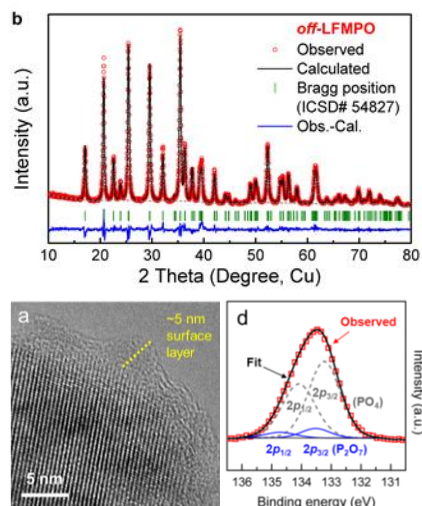


Figure 55. Transition metal-deficient off-stoichiometry leads to crystalline the olivine particle with Li-phosphate surface phases

identical to $\text{LiFe}_{0.6}\text{Mn}_{0.4}\text{PO}_4$ with a compositionally different surface phase. The material achieved a theoretical capacity of 165 mA h g⁻¹ at C/5 cycling (about 605 Wh kg⁻¹) and 135 mA h g⁻¹ at 5C cycling with good capacity retention. It is also capable of very fast discharging, 115 mA h g⁻¹ at 60C and 83 mA h g⁻¹ at 100C between 4.7 and 2.5 V, through diluting the cathode active mass. At 100C, the discharge power density is equivalent to 70 W kg⁻¹. This superior performance likely originates from the phosphate surface layer, which promotes effective electrical wiring for Li⁺ transport throughout the cathode. Our off-stoichiometric design strategy is a simple approach to achieve high-rate performance, applicable to other mixed olivine compositions.

We are investigating more mixed olivine composition that can adopt this off-stoichiometry so that very high rate systems can be developed.

Task 6.4 – First Principles Modeling of SEI Formation on Bare and Surface/Additive Modified Silicon Anode (Perla Balbuena, Texas A&M University)

Project Objective. This project aims to develop fundamental understanding of the molecular processes that lead to the formation of a solid electrolyte interphase (SEI) layer due to electrolyte decomposition on Si anodes, and to use such new knowledge in a rational selection of additives and/or coatings. The focus is on SEI layer formation and evolution during cycling and subsequent effects on capacity fade through two concatenated problems: (1) SEI layers formed on lithiated Si surfaces, and (2) SEI layers formed on coated surfaces. Key issues being addressed include the dynamic evolution of the system and electron transfer through solid-liquid interfaces.

Project Impact. Finding the correspondence between electrolyte molecular properties and SEI formation mechanism, structure, and properties will allow the identification of new/improved additives. Studies of SEI layer formation on modified surfaces will allow the identification of effective coatings able to overcome the intrinsic deficiencies of SEI layers on bare surfaces.

Approach. Investigating the SEI layer formed on modified Si surfaces involves analysis of the interfacial structure and properties of specific coating(s) deposited over the Si anode surface, characterization of the corresponding surface properties before and after lithiation, especially how such modified surfaces may interact with electrolyte systems (solvent/salt/additive), and what SEI layer structure, composition, and properties may result from such interaction. This study will allow identification of effective additives and coatings able to overcome the intrinsic deficiencies of SEI layers on bare surfaces. Once the SEI layer is formed on bare or modified surfaces, it is exposed to cycling effects that influence its overall structure (including the anode), chemical, and mechanical stability.

Out-Year Goals. Elucidating SEI nucleation and electron transfer mechanisms leading to growth processes using a molecular level approach will help establish their relationship with capacity fading, which will lead to revisiting additive and/or coating design.

Collaborations. Work with Chunmei Ban (NREL) consists in modeling the deposition-reaction of alucon coating on Si surfaces and their reactivity. Work with B. Lucht (URI) relates to finding the best additives for optimum SEI formation on Si anodes. Reduction of solvents and additives on Si surfaces were studied in collaboration with K. Leung and S. Rempe (Sandia National Labs). Collaborated with Prof. Jorge Seminario (TAMU) on electron transfer reactions, and Dr. Partha Mukherjee (TAMU) on development of a multi-scale model to describe SEI growth on Si anodes.

Milestones

1. Identification of lithiation and SEI formation mechanisms through alucon coatings on Si surfaces. (Q1 – Complete)
2. Clarify role of additives (VC, FEC) vs. electrolyte without additive on SEI properties. (Q2 – Complete)
3. Characterization of SEI mosaic formation from building blocks. (Q3 – Complete)
4. *Go/No-Go*: Prediction of irreversible capacity loss and electron transfer mechanisms through the SEI layer. (Q4 – In Progress)

Progress Report

Characterization of SEI formation from building blocks. DFT analysis showed that the main dimer products Li_2EDC and Li_2VDC are both susceptible to nucleophilic attack by the surface or by other radical species thus transferring electrons and resulting in SEI growth. In addition, polymerization reactions derived from VC and EC were thoroughly investigated. It was found that competition between polymerization vs. aggregation reactions of the initial radical anion products influence the stability of the SEI layer formed and is different in each case. A manuscript is in preparation. To complement these new insights, and to help integrate them into

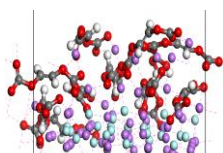


Figure 57. SEI nucleation of organic oligomers over LiF. Li: purple; F: light blue; O: red; C: grey; H: white; Si: yellow.

a mesoscopic level model, new DFT study of the adsorption energies of individual decomposition fragments to the lithiated Si surface have been conducted. The aggregation of these species over the surface was investigated (Figure 57). The main conclusions are: (1) radical species (including polymers) attach very strongly to the bare surface (energies in the order of 2-3 to 8-9 eV depending on the structure and chemical composition); (2) organic oligomer species (for example, Li_2EDC and Li_2VDC) tend to aggregate over the bare anode or over the anode covered with fragments of decomposition. Aggregates of Li_2EDC and Li_2VDC grow based on $\text{Li}\dots\text{O}\dots\text{Li}$ interactions; (3) the same species are also susceptible to reductive

decomposition becoming fragmented; (4) CO_3^- radical anions act as glue in between small agglomerates or in small openings on the surface; (5) LiF islands are very stable on the anode and for monolayer thicknesses solvent/additive/salt molecules are able to reduce over their surfaces and preferentially at the anode/LiF island interface; and (6) the configuration of the organic phase depends on the structure of the inorganic layer: more linear oligomer species aggregate on crystalline layers, whereas more bent configurations grow on amorphous inorganic phases.

FEC reactivity over model SEI. Leung (Sandia), in collaboration with the Balbuena group, performed AIMD simulations on liquid electrolyte decomposition on amorphous LiF-coated $\text{Li}(x)\text{Si}$, $1 < x < 3$, as lithium insertion proceeds. The model electrodes mimic fluoroethylene carbonate (FEC)-treated, partially lithiated Si anodes. Li addition takes place in several stages, each of which is accompanied by manual expansion of the lattice dimensions, forcing the thin LiF surface layer to crack. This exposes bare $\text{Li}(x)\text{Si}$ surfaces that rapidly react with ethylene carbonate (EC) molecules in the liquid layer. The electronic voltage is monitored periodically over the AIMD trajectories via the work function method. These simulations are continued until the instantaneous voltage exceeds EC electrochemical reduction potential due to loss of electrons from and build-up of positive charges on $\text{Li}(x)\text{Si}$ surfaces. At this point the next stage of Li insertion is initiated, and the AIMD protocol is repeated. The resultant surface layer is therefore a physically motivated SEI layer with mixed LiF and EC-product domains unique to FEC-based liquid electrolyte. Future work will analyze the transport properties of such SEI films, modify the film formation conditions, and switch to LiF-free, lithium carbonate-coated $\text{Li}(x)\text{Si}$ electrode surfaces so as to pinpoint the difference between SEI with/without FEC additives.

Dielectric properties of EC and PC. The study of dielectric properties of ethylene carbonate (EC) and propylene carbonate (PC) solvents using a classical MD force field (OPLS-AA) was completed. The effectivity of the force field was determined by computations of the static dielectric constants and dielectric relaxation times over a range of temperatures, and comparison with experiment. A manuscript is in preparation. The solvation free energy of Li ion in EC and PC using the classical force field is in progress, as well as electronic structure methods coupled with continuum solvation models. By decomposing the free energy into components, new insights are gained about the relative importance of local chemical interactions, packing contributions, and the distant solvation environment. A comparison with the same properties computed in aqueous solution highlights fundamental differences between ion hydration in water versus organic solvents. Those studies are important for understanding the fundamental physical chemical properties of organic solvents, ion solvation in organic solvents, and validating a classical force field in preparation for large time-scale studies of ion transport and diffusion in SEI layers.

Patents/Publications/Presentations

- Perez-Beltrán, S., and G. E. Ramirez-Caballero, and P. B. Balbuena. “First Principles Calculations of Lithiation of a Hydroxylated Surface of Amorphous Silicon Dioxide.” *J. Phys. Chem. C*, in press, DOI 10.1021/acs.jpcc.5b02992.
- Ma, Y., and J. M. Martinez de la Hoz, I. Angarita, J. M. Berrio-Sanchez, L. Benitez, J. M. Seminario, S.-B. Son, S.-H. Lee, S. M. George, C. M. Ban, and P. B. Balbuena. “Structure and Reactivity of Alucone-Coated Films on Si and Li_xSi_y Surfaces.” *ACS Appl. Mater. Inter.* 7 (2015): 11948-11955.
- Martinez de la Hoz, J. M., and F. A. Soto, and P. B. Balbuena. “Effect of the electrolyte composition on SEI reactions at Si anodes of Li-ion batteries.” *J. Phys. Chem. C* 119 (2015): 7060-7068, DOI: 10.1021/acs.jpcc.5b01228.
- Martinez de la Hoz, J. M., and P. B. Balbuena. “Reduction Mechanisms of Additives on Si Anodes of Li-Ion Batteries.” *Phys. Chem. Chem. Phys.* 16 (2014): 17091-17098.

Task 6.5 – A Combined Experimental and Modeling Approach for the Design of High Current Efficiency Si Electrodes (Xingcheng Xiao, General Motors; Yue Qi, Michigan State University)

Project Objective. The use of high-capacity, Si-based electrode has been hampered by its mechanical degradation due to the large volume expansion/contraction during cycling. Nanostructured Si can effectively avoid Si cracking/fracture. Unfortunately, the high surface to volume ratio in nanostructures leads to unacceptable amount of solid-electrolyte interphase (SEI) formation and growth, thereby low current/Coulombic efficiency and short life. Based on mechanics models we demonstrate that the artificial SEI coating can be mechanically stable despite the volume change in Si, if the material properties, thickness of the SEI, and the size/shape of Si are optimized. Therefore, the objective of this project is to develop an integrated modeling and experimental approach to understand, design, and make coated Si anode structures with high current efficiency and stability.

Project Impact. The validated model will ultimately be used to guide the synthesis of surface coatings and the optimization of Si size/geometry that can mitigate SEI breakdown. The optimized structures will eventually enable a negative electrode with a 10x improvement in capacity (compared to graphite) while providing a >99.99% Coulombic efficiency, which could significantly improve the energy/power density of current LIB.

Out-Year Goals. The out-year goal is to develop a well validated mechanics model that directly import material properties either measured from experiments or computed from atomic simulations. The predicted SEI induced stress evolution and other critical phenomena will be validated against *in situ* experiments in a simplified thin-film system. This comparison will also allow fundamental understanding of the mechanical and chemical stability of artificial SEI in electrochemical environments and the correlation between the Coulombic efficiency and the dynamic process of SEI evolution. Thus, the size and geometry of coated Si nanostructures can be optimized to mitigate SEI breakdown, thus providing high current efficiency.

Collaborations. This project engages in collaboration with LBNL, PNNL, and NREL.

Milestones

5. Identify SEI failure mode by using combined *in situ* electrochemical experiments and modeling techniques developed in 2014. (12/31/14 – Identified some failure modes; continue comparing individual SEI components)
6. Reveal detailed SEI failure mode by using MD simulations with ReaxFF for Li-Si-Al-O-C system to model the deformation of SEI on a Si as it undergoes large strain. (3/31/15 – Complete)
7. Correlate and determine the desirable material properties for stable SEI, by applying the continuum model and experimental nanomechanics. Establish the material property design methodology for stabilizing SEI on Si. (6/30/15 – Complete)
8. *Go/No-Go*: Determine whether to select oxide, fluoridated, or carbon artificial SEI chemistry based on comparisons of their mechanical stability and transport properties. (9/30/15)

Progress Report

Reactive MD simulations were performed with disk model and slab models of amorphous Si covered with or without Al_2O_3 or SiO_2 . The slab model mimics the continuum thin film geometry in experiment. The disk model mimics the sliding island geometry in experiment. Figure 58 shows the configurations after lithiation. Coating cracking was observed in the disk model, validating the design of the experiment. It was also found that Si atoms initially in the Si electrode diffused through the SiO_2 layer to the surface of the slab, while no such behavior was observed in Al_2O_3 coated Si. This means the Al_2O_3 coating is more protective than the native SiO_2 layer. One of the reasons may be the Li concentration gradient generated in the lithiated Al_2O_3 .

Thickness-dependent interfacial sliding and SEI fracture in lithiated Si thin film islands on Cu substrate. Recent experiments have shown that the extent of sliding of a lithiated Si island on a Cu substrate depends on the thickness of the island, which has been used as a model system to investigate the SEI failure mechanism. To understand this phenomenon, we performed a finite element simulation of the sliding of two Si thin film islands with different thicknesses, 50nm and 250nm, and a layer of SEI was on top of each island. It was observed that the fully-lithiated thinner island consisted of two zones (see Figure 58a), the locked zone in the center of the island where lithiated Si remained adhered to the substrate and the sliding zone where swelling island slid on the substrate. For the thicker island, sliding occurred over the entire interface, leading to a larger lateral expansion compared to that of the thinner island (see Figure 58b), in agreement with the experimental observations. It was further observed that the SEI layer on top of the sliding zone fractured due to the large tensile stress while that on top of the locked zone remained stable. This work attempted to build clear connections between island thickness, lateral expansion, SEI fracture, and irreversible capacity of Si islands on substrate.

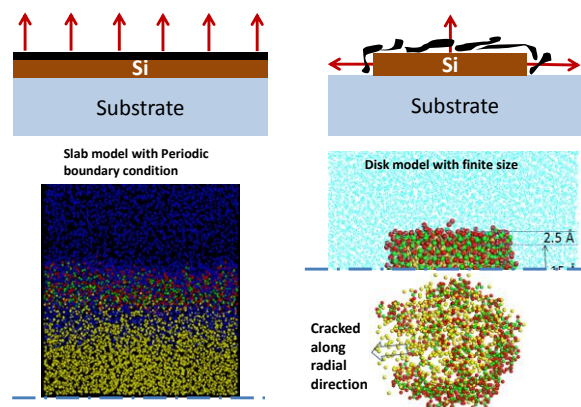


Figure 58. Disk model and slab model to mimic the experimental design. The disk model shows coating crack along radial direction.

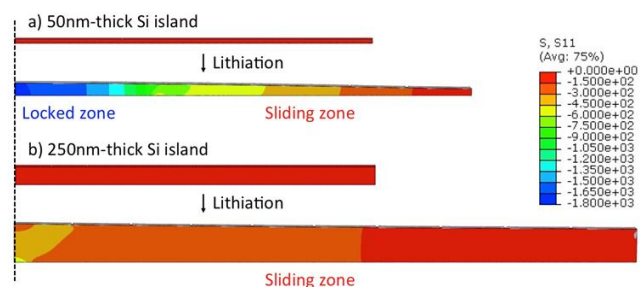


Figure 59. Thickness-dependent interfacial sliding and SEI fracture of lithiated Si islands with thicknesses of (a) 50 nm (b) 250 nm.

Patents/Publications/Presentations

Publications

- Zhang, Q., and X. Xiao, W. Zhou, Y. T. Cheng, and M. W. Verbrugge. “Toward High Cycle Efficiency of Silicon-Based Negative Electrodes by Designing the Solid Electrolyte Interphase.” *Advanced Energy Materials* 5, no. 5 (2015).
- Pan, J., and Y. T. Cheng, and Y. Qi. “General Method to Predict Voltage-dependent Ionic Conduction in a Solid Electrolyte Coating on Electrodes.” *Physical Review B* 91, no. 13 (2015): 134116.
- Kumar, R., and X. Xiao, P. Lu, and B. W. Sheldon. “A Novel Approach to Study the Chemo-Mechanical Stability of the Solid Electrolyte Interphase (SEI) in Lithium-Ion Batteries.” *Meeting Abstracts* 232-232 (2015).

Presentations

- TMS Annual Meeting, Orlando (March 18, 2015): “Stress Evolution and Degradation Mechanisms in the Solid Electrolyte Interphase”; Brian W. Sheldon.
- École polytechnique fédérale de Lausanne, Lausanne, Switzerland, FL (June 26, 2015): “Stress Evolution and Degradation Mechanisms in Energy Storage Materials”; Brian W. Sheldon.

Task 6.6 – Predicting Microstructure and Performance for Optimal Cell Fabrication (Dean Wheeler and Brian Mazzeo, Brigham Young University)

Project Objective. This work uses microstructural modeling coupled with extensive experimental validation and diagnostics to understand and optimize fabrication processes for composite particle-based electrodes. The first main outcome will be revolutionary methods to assess electronic and ionic conductivities of porous electrodes attached to current collectors, including heterogeneities and anisotropic effects. The second main outcome is a particle-dynamics model parameterized with fundamental physical properties that can predict electrode morphology and transport pathways resulting from particular fabrication steps. These two outcomes will enable the third, which is an understanding of the effects of processing conditions on microscopic and macroscopic properties of electrodes.

Project Impact. This work will result in new diagnostic tools for rapidly and conveniently interrogating electronic and ionic pathways in porous electrodes. A new mesoscale 3D microstructure prediction model, validated by experimental structures and electrode-performance metrics, will be developed. The model will enable virtual exploration of process improvements that currently can only be explored empirically.

Out-Year Goals. This project was initiated April 2013 and concludes March 2017. Goals by fiscal year are as follows.

- 2013: Fabricate first-generation micro-four-line probe, and complete associated computer model.
- 2014: Assess conductivity variability in electrodes; characterize microstructures of multiple electrodes.
- 2015: Fabricate first-gen ionic conductivity probe, N-line probe, and dynamic particle packing (DPP) model.
- 2016: Fabricate second-gen N-line probe and DPP model; assess effect of processing variables.
- 2017: Use conductivity predictions in full electrochemical model; evaluate effect of innovative processing conditions.

Collaborations. Bryant Polzin (ANL) and Karim Zaghbi (Hydro-Québec) provided battery materials. Transfer of our technology to A123 to improve their electrode production process is in process. There are ongoing collaborations with Simon Thiele (IMTEK, University of Freiburg) and Mårten Behm (KTH, Sweden).

Milestones

1. Develop localized ionic conductivity probe and demonstrate method by testing two candidate electrode materials. (December 2014 – Complete)
2. Use dynamic particle-packing (DPP) model to predict electrode morphology of Toda 523 material. (March 2014 – Complete)
3. Develop fabrication process of micro-N-line probe and demonstrate method by testing two candidate electrode materials (June 2015 – Complete)
4. *Go/No-Go*: Discontinue DPP model if predictions are not suitable match to real electrode materials (September 2015 – Ongoing)

Progress Report

Milestone 3 (Complete). The third milestone of FY2015 was to extend and adapt the micro-four-line probe (μ 4LP) apparatus to measure anisotropic electronic conductivity of thin-film battery electrodes. In other words, the apparatus must determine three separate conductive parameters: σ_x , σ_y , and R_c'' , where x is an in-plane direction, y is the out-of-plane direction, and R_c'' is a contact resistance at the current collector. This requires a minimum of three orthogonal experiments completed on a particular volume of the sample. These experiments are made possible with a new six-line probe developed in our group, as shown in Figure 60.

With six lines plus the current collector, the user can choose one pair of connections to deliver a perturbing current and another pair of connections to measure an imposed voltage difference, enabling current to flow in different directions. The sampling window of the new six-line probe has similar dimensions as the old one, namely $130\ \mu\text{m} \times 500\ \mu\text{m}$. To independently and rapidly access each connection on the probe, a computer-controlled multiplexer based on solid-state relays was incorporated into the apparatus.

As before, a detailed computer model is required to invert the experiments and compute the conductive properties. Significant effort was expended this quarter to upgrade the model to make it faster, to make it compatible with the six-line-probe, and to incorporate anisotropy.

The probe and inversion routine were tested on two electrode sample films. Both samples in this initial stage were Toda NCM 523 cathodes prepared at Argonne National Lab. A total of six locations were tested on the two films. The average degree of anisotropy was determined to be $\frac{\sigma_x}{\sigma_y} = 2.9 \pm 0.7$, though wide variations in this ratio were observed, ranging from 2 to 7. A large part of the variations are likely due to measurement uncertainty, which will be reduced by optimizing the measurement protocol and weighting factors used in the model. These conductivity results are consistent with the predictive microstructure model developed at BYU in Milestone 2, which suggests an anisotropic conductivity ratio of around 2. This means that conductivity in the out-of-plane direction, which is most needed for electron transport during battery operation, is significantly lower than the in-plane conductivity. This suggests an opportunity for electrode improvement.

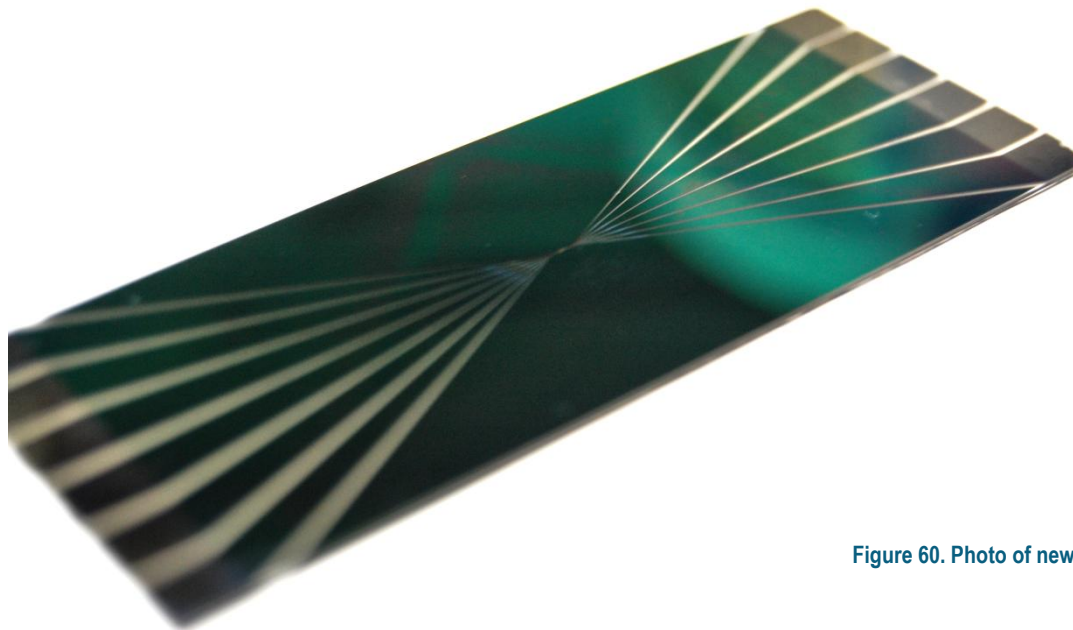


Figure 60. Photo of new six-line probe.

Patents/Publications/Presentations

Presentations:

- 227th Meeting of the Electrochemical Society, Chicago (2015): “Predictive Particle-based Simulation of the Fabrication of Li-ion Battery Electrodes”; M.M. Forouzan, C.-W. Chao, D. Bustamante, W. Lange, B.A. Mazzeo, and D.R. Wheeler.
- 12th Symposium on Fuel Cell and Battery Modeling and Experimental Validation (ModVal 12), Freiburg, Germany (2015): “Modeling the Missing Carbon Phase in x-ray Tomographic Reconstructions of a Metal-based Battery Cathode”; L. Zielke, T. Hutzenlaub, D.R. Wheeler, C.-W. Chao, I. Manke, A. Hilger, N. Paust, R. Zengerle, and S. Thiele,

Publications under review:

- Lanterman, B.J., and A.A. Riet, N.S. Gates, J.D. Flygare, A.D. Cutler, J.E. Vogel, D.R. Wheeler, and B.A. Mazzeo. “Micro-four-line probe to measure electronic conductivity and contact resistance of thin-film battery electrodes.” *J. Electrochem. Soc.*, submitted (2015).
- Flygare, J.D., and A.A. Riet, B.A. Mazzeo, and D.R. Wheeler. “Mathematical Model of Four-Line Probe to Determine Conductive Properties of Thin-film Battery Electrodes.” *J. Electrochem. Soc.*, submitted (2015).

TASK 7 – METALLIC LITHIUM AND SOLID ELECTROLYTES

Summary and Highlights

The use of a metallic lithium anode is required for advanced battery chemistries like Li-air and Li-S to realize dramatic improvements in energy density, vehicle range, cost economy, and safety.

However, the use of metallic Li with liquid and polymer electrolytes has been so far limited due to parasitic SEI reactions and dendrite formation. Adding excess lithium to compensate for such losses effectively negates the high energy density for lithium in the first place. For a long lifetime and safe anode, it is essential that no lithium capacity is lost to physical isolation from roughening, to dendrites or delamination processes, or to chemical isolation from side reactions. The key risk and current limitation for this technology is the gradual loss of lithium over the cycle life of the battery.

To date there are no examples of battery materials and architectures that realize such highly efficient cycling of metallic lithium anodes for a lifetime of 1,000 cycles due to degradation of the Li-electrolyte interface. A much deeper analysis of the degradation processes is needed, so that materials can be engineered to fulfill the target level of performance for EV, namely 1,000 cycles and a 15 year lifetime, with adequate pulse power. Projecting the performance required in terms of just the Li anode, this requires a high rate of lithium deposition and stripping reactions, specifically about 40 μ m Li per cycle, with pulse rates up to 10 and 20 nm/s charge and discharge, respectively. This is a conservative estimate, yet daunting in the total mass and rate of material transport. While such cycling has been achieved for state-of-the-art batteries using *molten* Na in Na-S and zebra cells, solid Na and Li anodes are proving more difficult.

The efficient and safe use of metallic lithium for rechargeable batteries is then a great challenge, and one that has eluded R&D efforts for many years. The Battery Materials Research Task 7, takes a broad look at this challenge for both solid state batteries and batteries continuing to use liquid electrolytes. Four of the projects are new endeavors; two are ongoing. For the liquid electrolyte batteries, PNNL researchers are examining the use of cesium salts and organic additives to the typical organic carbonate electrolytes to impede dendrite formation at both the lithium and graphite anodes. If successful, this is the simplest approach to implement. At Stanford, novel coatings of carbon and boron nitride with a 3D structure are applied to the lithium surface and appear to suppress roughening and lengthen cycle life. A relatively new family of solid electrolytes with a garnet crystal structure shows superionic conductivity and good electrochemical stability. Four programs chose this family of solid electrolytes for investigation. Aspects of the processing of this ceramic garnet electrolyte are addressed at the University of Maryland and at the University of Michigan with attention to effect of flaws and composition. Computational models will complement their experiments to better understand interfaces and reduce the electrode area specific resistance (ASR). At Oak Ridge National Laboratory, composite electrolytes composed of ceramic and polymer phases are being investigated, anticipating that the mixed phase structures may provide additional means to adjust the mechanical and transport properties. The last project takes on the challenge to used nanoindentation methods to measure the mechanical properties of the solid electrolyte, the lithium metal anode, and the interface of an active electrode. Each of these projects involve a collaborative team of experts with the skills needed to address the challenging materials studies of this dynamic electrochemical system.

Task 7.1 – Mechanical Properties at the Protected Lithium Interface (Nancy Dudney, ORNL; Erik Herbert, UT – Knoxville; Jeff Sakamoto UM)

Project Objective. This project will develop the understanding of the Li metal-solid electrolyte interface through state-of-the-art mechanical nanoindentation methods coupled with solid electrolyte fabrication and electrochemical cycling. Our goal is to provide the critical information that will enable transformative insights into the complex coupling between the microstructure, its defects, and the mechanical behavior of Li metal anodes.

Project Impact. Instability and/or high resistance at the interface of lithium metal with various solid electrolytes limit the use of the metallic anode for batteries with high energy density batteries, such as Li-air and Li-S. The critical impact of this endeavor will be a much deeper analysis of the degradation, so that materials can be engineered to fulfill the target level of performance for EV batteries, namely 1000 cycles and a 15-year lifetime, with adequate pulse power.

Approach. Mechanical properties studies through state-of-the-art nanoindentation techniques will be used to probe the surface properties of the solid electrolyte and the changes to the lithium that result from prolonged electrodeposition and dissolution at the interface. An understanding of the degradation processes will guide future electrolyte and anode designs for robust performance. In the first year, the team will address the two critical and poorly understood aspects of the protected Li metal anode assembly: (1) the mechanical properties of the solid electrolyte and (2) the morphology of the cycled Li metal.

Out-Year Goals. Work will progress toward study of the electrode assembly during electrochemical cycling of the anode. We hope to capture the formation and annealing of vacancies and other defects in the lithium and correlate this with the properties of the solid electrolyte and the interface.

Collaborations. This project funds work at Oak Ridge National Laboratory, University of Tennessee at Knoxville, and University of Michigan. Asma Sharafi (UM Ph. D. student), Dr. Robert Schmidt (UM) also contribute to the project. Steve Visco (PolyPlus) will serve as a technical advisor.

Milestones

1. Four nano-indentation maps showing grain boundary regions of the crystalline LLZO and the glass ceramic material from Ohara. (Q1 – Complete)
2. Two or three indentation studies with as-fabricated, air reacted and polished surfaces. (Q2 – Complete)
3. Demonstrate capability to transfer and then map viscoelastic properties of Li films and rolled lithium foils in vacuum system of sem. (Q3; go/no-go – Completed using glove box rather than SEM)
4. Determine elastic properties of battery grade lithium from different sources and preparation, comparing to values from the reference literature. (Q4 – Initiated)

Progress Report

This quarter, we report initial nanoindentation studies of lithium metal (milestone 3). The fixture was set up and successfully operated in an inert atmosphere glove box. Being extremely plastic, the measurements of lithium require a low strain rate and hence thermal stability of the system may need attention. The figure illustrates results for thin film lithium on a glass substrate at high (blue) and low (green) strain rate. The strain was applied for 7s (blue) and 32s (green) followed by a 40s hold. During the hold, substantially more creep was induced by the higher strain rate. The phase angle for the 100Hz modulation, which is an indication of energy dissipation, is surprisingly high for both tests. Rough values for the elastic modulus and hardness agree with values reported in the literature, but more analysis is required. Continuing work will examine thicker films on different substrates, as well as rolled and commercial foils.

Erik Herbert has recently moved to Michigan Technological University and is setting up a glove box and an optical microscope to continue these studies at (MTU). The microscope will be used to examine the structure of the indent and correct results for pile up of material around the tip. Setting up equipment at MTU may delay indentation tests for the next quarter.

An alternative pulse echo technique (not included in the task list) is being investigated for measuring the salient mechanical properties. In the table, results of the elastic (E) and shear moduli (G) from the pulse echo method are compared with those obtained by nano-indentation. In addition we show values predicted using density functional theory (Siegel group in Task 7.2).

The ceramic electrolytes samples are Al and Ta stabilized lithium lanthanum zirconate (LLZO) samples prepared by hot pressing to achieve a high relative density (> 98 %). The predicted and measured values are in good agreement, in general within 10% accuracy. Additionally, the Al-doped pulse echo elastic modulus is within 4 % of the value determined by Ni, et al. [*J. of Mater. Sci.*, 47, 7978-7985 (2012)] using Resonant Ultrasound Spectroscopy for the same composition and comparable density. Because pulse echo is simple, and thus can be integrated with solid-state cell hardware, we believe this capability will provide another means to establish *in situ* measurement of the solid electrolyte - Li interface properties while cycling.

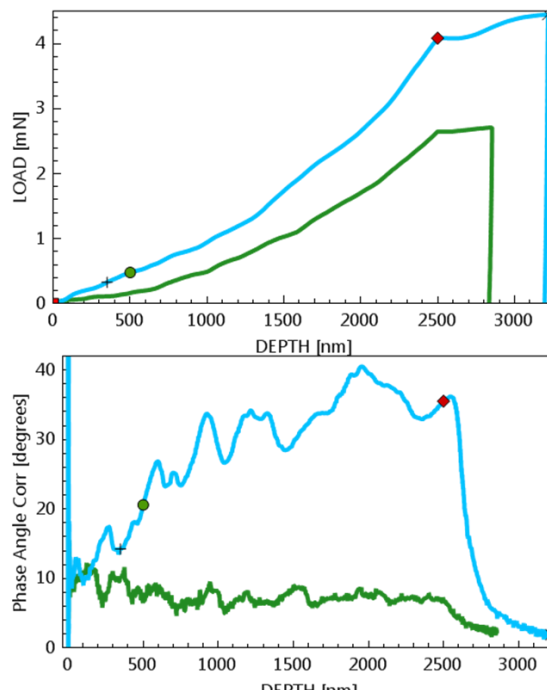


Figure 61. Indentation of a 3 μ m-thick Li film at strain rates of 1/s and 0.1/s, blue and green respectively.

Table 5. Results of the elastic (E) and shear moduli (G) from the pulse echo method compared with those obtained by nano-indentation.

Samples at 298K	E (GPa)	G(GPa)
Al-doped LLZO (calc.)	154	61.7
Al-doped LLZO (pulse echo)	143.5	56.7
Ta-doped LLZO (calc.)	147	59.4
Ta-doped LLZO (pulse echo)	136.8	54.1
Ta-doped LLZO* (indent.)	105-141	
* Range of dopant content. Others Al _{0.25} and Ta _{0.5} per nominal Li ₇ La ₃ Zr ₂ O ₁₂		

Task 7.2 – Solid Electrolytes for Solid-State and Lithium-Sulfur Batteries (Jeff Sakamoto, University of Michigan)

Project Objectives. Enable advanced Li-ion solid-state and lithium-sulfur EV batteries using LLZO solid-electrolyte membrane technology. Owing to its combination of fast ion conductivity, stability, and high elastic modulus, LLZO exhibits promise as an advanced solid-state electrolyte. To demonstrate relevance in EV battery technology, several objectives must be met. First, LLZO membranes must withstand current densities approaching ~ 1 mA/cm² (commensurate with EV battery charging and discharging rates). Second, low area specific resistance (ASR) between Li and LLZO must be achieved to achieve cell impedance comparable to conventional Li-ion technology (~ 10 Ohms/cm²). Third, low ASR and stability between LLZO and sulfur cathodes must be demonstrated.

Project Impact. The expected outcomes will: (i) enable Li metal protection, (ii) augment DOE access to fast ion conductors and/or hybrid electrolytes, (iii) mitigate Li-polysulfide dissolution and deleterious passivation of Li metal anodes, and (iv) prevent dendrite formation. Demonstrating these aspects could enable Li-S batteries with unprecedented end-of-life, cell-level performance: > 500 Wh/kg, > 1080 Wh/l, > 1000 cycles, lasting > 15 years.

Approach. Our effort will focus on the promising new electrolyte known as LLZO (Li₇La₃Zr₂O₁₂). LLZO is the first bulk-scale ceramic electrolyte to simultaneously exhibit the favorable combination of high conductivity (~ 1 mS/cm at 298K), high shear modulus (61 GPa) to suppress Li dendrite penetration, and apparent electrochemical stability (0-6V vs Li/Li⁺). While these attributes are encouraging, additional R&D is needed to demonstrate that LLZO can tolerate current densities in excess of 1mA/cm², thereby establishing its relevance for PHEV/EV applications. We hypothesize that defects and the polycrystalline nature of realistic LLZO membranes can limit the critical current density. However, the relative importance of the many possible defect types (porosity, grain boundaries, interfaces, surface & bulk impurities), and the mechanisms by which they impact current density, have not been identified. Using our experience with the synthesis and processing of LLZO (Sakamoto and Wolfenstine), combined with sophisticated materials characterization (Nanda), we will precisely control atomic and microstructural defects and correlate their concentration with the critical current density. These data will inform multi-scale computation models (Siegel and Monroe) which will isolate and quantify the role(s) that each defect plays in controlling the current density. By bridging the knowledge gap between composition, structure, and performance we will determine if LLZO can achieve the current densities required for vehicle applications.

Collaborations. This project collaborates with Don Siegel (UM atomistic modeling), Chuck Monroe (UM, continuum scale modeling), Jagjit Nanda (ORNL sulfur chemical and electrochemical spectroscopy), and Jeff Wolfenstine (ARL atomic force microscopy of Li-LLZO interfaces).

Milestones

1. *MI.1:* Demonstrate ability to vary porosity from 1 to 15 volume %. Correlate critical current density with scale and volume of porosity. (Q2 after Jan 2015 start; Not complete, see report)
2. *MI.2:* Establish baseline atomistic and continuum theory to predict the maximum critical current density based on pore size and volume. (Q3 after start; Possible delay, see report)

Progress Report

M1.1 Milestone 1.1

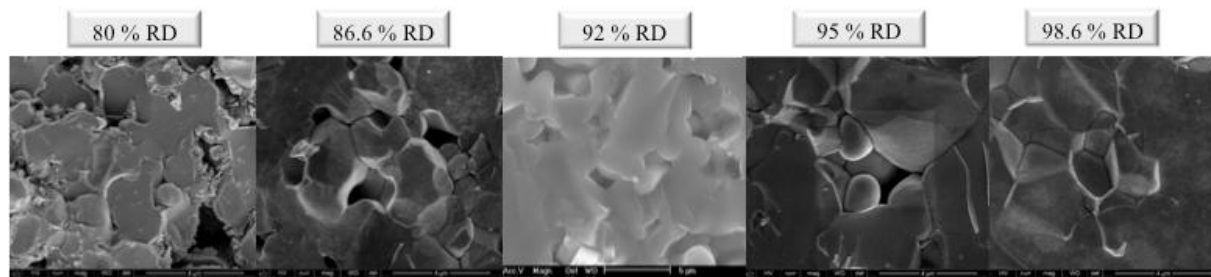


Figure 62. SEM images of LLZO fracture surfaces of varying relative density (RD) from 80.0% to 98.6%.

The Sakamoto group demonstrated the ability to control the porosity between 1% and 20% in cubic LLZO (Task 1, Figure 62). The % porosity ($100 - \%RD$), was controlled by varying the densification temperature. To control the % porosity, while minimizing change in the grain size, pressure was applied during densification. Efforts to correlate the critical current density (CCD) with porosity were postponed due to experiments suggesting that the Li-LLZO interfacial resistance should be reduced first. Thus, it was decided that activity Task 1.7 should be initiated before 1.1 is completed: “Task 1.7: Demonstrate the ability to control surface cleanliness and surface roughness. Correlate the critical current density as a function of surface contamination and roughness.” *We determined that a better understanding of the LLZO surface cleanliness is needed before conducting critical current density measurements. Thus, work on Milestone 1.7 was initiated.*

ORNL and ARL initiated work on Task 1.7 to assist in the completion of M 1.1. The Nanda group at ORNL conducted XPS-LLZO depth profiling to determine the depth of penetration of surface contaminants. The data indicate that a surface contamination layer in the hundred nanometer range was present. ARL conducted surface topographic analysis of LLZO samples using AFM. The AFM data indicate that, despite polishing, ~ 1 microns surface features were detected. Thus, based on the XPS and ARL surface analyses, UM-ORNL-ARL will conduct a matrix of experiments to study the effect of surface preparation techniques on surface cleanliness and roughness. Once this relationship is understood, a correlation between surface preparation and CCD will be conducted. The results of this study may reduce the Li-LLZO interfacial resistance to allow the correlation of CCD vs porosity in Task 1.1.

Some progress made, but UM Prof. C. Monroe is moving to Oxford, UK. Because this Milestone heavily relies on Dr. Monroe’s continuum-scale input, this Milestone may be delayed. Efforts to continue collaboration with Dr. Monroe are under way.

Patents/Publications/Presentations

Patent: J. Sakamoto, E. Rangasamy, H. Kim, R. Maloney, and Y. Kim. “Methods of making and using oxide ceramic solids and products and devices related thereto.” US Patent Issued: 9093717, July 15, 2015.

Task 7.3 – Composite Electrolytes to Stabilize Metallic Lithium Anodes (Nancy Dudney and Sergiy Kalnaus, Oak Ridge National Laboratory)

Project Objective. Prepare composites of representative polymer and ceramic electrolyte materials to achieve thin membranes that have the unique combination of electrochemical and mechanical properties required to stabilize the metallic lithium anode while providing for good power performance and long cycle life. Understand the lithium ion transport at the interface between polymer and ceramic solid electrolytes, which is critical to the effective conductivity of the composite membrane. Identify key features of the composite composition, architecture, and fabrication that optimize the performance. Fabricate thin electrolyte membranes to use with a thin metallic lithium anode to provide good power performance and long cycle life.

Project Impact. A stable lithium anode is critical to achieve high energy density with excellent safety, lifetime, and cycling efficiency. This study will identify the key design strategies that should be used to prepare composite electrolytes to meet the challenging combination of physical and chemical and manufacturing requirements to protect and stabilize the lithium metal anode for advanced batteries. By utilizing well characterized and controlled component phases, the design rules developed for the composite structures will be generally applicable toward the substitution of alternative and improved solid electrolyte component phases as they become available. Success in this program will enable these specific DOE technical targets: 500-700Wh/kg, 3000-5000 deep discharge cycles, and robust operation.

Approach. This program seeks to develop practical solid electrolytes that will provide stable and long-lived protection for the lithium metal anode. Current electrolytes all have serious challenges when used alone: oxide ceramics are brittle, sulfide ceramics are air sensitive, polymers are too resistive and soft, and many electrolytes react with lithium. Composites provide a clear route to address these issues. This program does not seek discovery of new electrolytes; rather, the goal is to study combinations of current well known electrolytes. The program emphasizes the investigation of polymer-ceramic interfaces formed as bilayers and as simple composite mixtures where the effects of the interface properties can be readily isolated. In general, the ceramic phase is several orders of magnitude more conductive than the polymer electrolyte, and interfaces can contribute an additional source of resistance. Using finite element simulations as a guide, composites with promising compositions and architectures are fabricated and evaluated for lithium transport properties using AC impedance and DC cycling with lithium in symmetric or half cells. General design rules will be determined that can be widely applied to other combinations of solid electrolytes.

Out-Year Goal. Use advanced manufacturing processes where the architecture of the composite membrane can be developed and tailored to maximize performance and cost-effective manufacturing.

Collaborations. Electrolytes under investigation include a garnet electrolyte from Jeff Sakamoto (University of Michigan) and ceramic powder from Ohara. Staff at Corning Corporation will serve as our industrial consultant. Student intern, Cara Herwig, from Virginia Tech. Univ. assisted this quarter.

Milestones

1. Compare the vapor absorption (rate and equilibrium) of small molecules in a single-phase polymer and a corresponding ceramic/polymer composite electrolyte. (Q1 – Complete)
2. Compare Li cycling, contacting Li with a buried Ni tab versus a surface metal contact. (Q2 – Complete)
3. By generating a database with at least 5 compositions, determine if the presence of trace solvent molecules that enhance the ionic conductivity are also detrimental to the stability and cycleability of a lithium metal electrode, and if the effect can be altered by adding an overlayer film. (Q3 – SMART, Ongoing)
4. Demonstrate a practical processing route to a thin, dense membrane 100 μ m x 50cm². (Q4 – On Schedule)

Progress Report

The dramatic increase in the conductivity of both polymer and ceramic composite electrolytes upon exposure to dimethylcarbonate (DMC) and water vapor is being completed for publication (milestone 3). This includes quantifying the amount of adsorbed molecules, their stability under vacuum, and effect on the density of the composite. In addition we probed how both molecules and ceramic particles alter the extent and temperature of crystallization. Special holders were employed to protect samples from air exposure for these tests.

For measures of the density, a special fixture was designed to use our BET surface analyzer as a gas pycnometer. The first generation of the multichamber sample holder did not provide sufficient precision and modifications are under way. An example of the infrared attenuated total reflectance is shown in Figure 63.

The spectrum is complicated and requires correction for the index of refraction, but two frequency windows allow clear identification of DMC vibrational modes that we can follow through the electrolyte processing. Figure 64 shows examples of the differential scanning calorimetry results normalized by the total mass of the samples. The endotherm at 60-70°C reflects the PEO transition from semi-crystalline to amorphous. It is surprising to see this persist for large addition of Ohara ceramic particles and also DMC, as the crystallization is no longer apparent in the Arrhenius plot of conductivity.

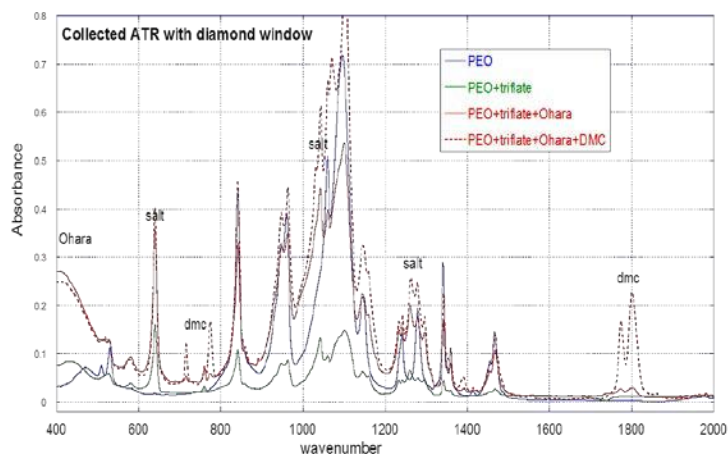


Figure 63. Infrared ATR of polymer and composite electrolytes, both dry (solid lines) and exposed to DMC vapor (dashed lines).

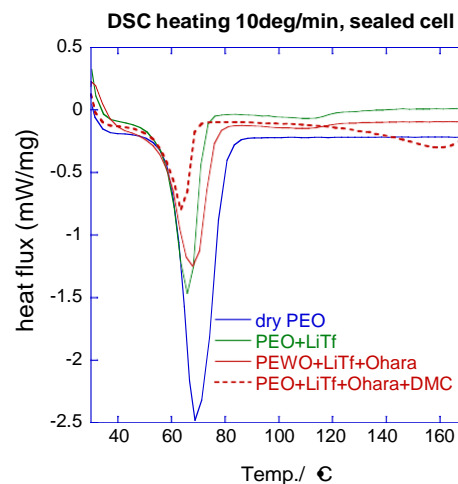


Figure 64. DSC scans for dry PEO, polymer and composite electrolytes (solid lines), with one exposed to DMC (dashed).

Two paths are being investigated to fabricate larger and thinner sheet of the electrolyte (milestone 4). New presses are being used for solvent-free melt processing, so far to 7cm². The challenge for scaling to larger area using this method is to evenly distribute the powder mixture across the platen, as given the large volume fraction of ceramic powder, the material does not flow well when melt-pressed. As an alternative, slurries have been prepared with several solvents. Achieving a good viscosity in a well dispersed and concentrated suspension required trial and error, but to date an aqueous suspension is giving the best quality polymer-ceramic composite films when dried in air and heated to remove residual water. Initial attempts to measure the conductivity of such a membrane were unsuccessful because the thin films shorted. The ceramic-polymer interface formed by solution casting will be compared to that from solvent-free melt-processing.

Patents/Publications/Presentations

Presentations

- Advanced Automotive Battery Conference (AABC), Detroit (June 2015) Invited: “Solid Electrolytes for High Energy Density Batteries”; Nancy Dudney, Sergiy Kalnaus, and Jeff Sakamoto.
- Annual Merit Review, Washington, DC (June 2015): “Composite Electrolyte to Stabilize Metallic Lithium Anodes”; Nancy Dudney.

Task 7.4 – Overcoming Interfacial Impedance in Solid-State Batteries (Eric Wachsman, University of Maryland – College Park)

Project Objective. Develop a multifaceted and integrated (experimental and computational) approach to solve the key issue in solid-state Li-ion batteries (SSLiBs), interfacial impedance, with a focus on Garnet-based solid-state electrolytes (SSEs), the knowledge of which can be applied to other SSE chemistries. The focus is to develop methods to decrease the impedance across interfaces with the solid electrolyte, and ultimately demonstrate a high power/energy density battery employing the best of these methods.

Project Impact. Garnet electrolytes have shown great promises for safer and higher energy density batteries due to their stability to both high-voltage cathodes and Li metal anodes, as well as their inherent non-flammability. The success of the proposed research can lead to dramatic progress on the development of SSLiBs based on Garnet electrolytes. With regard to the fundamental science, our methodology by combining computations and experiments can lead to an understanding of the thermodynamics, kinetics, and structural stability and evolution of SSLiBs with the Garnet electrolytes. Due to the ceramic nature of Garnet electrolyte, being brittle and hard, Garnet electrolyte particles intrinsically lead to poor contacts among themselves or with electrode materials. A fundamental understanding at the nanoscale and through computations, especially with interface layers, can guide improvements to their design and eventually lead to the commercial use of such technologies.

Approach. SSLiB interfaces are typically planar resulting in high impedance due to low specific surface area; attempts to make 3D high surface area interfaces can also result in high impedance due to poor contact at the electrode-electrolyte interface that hinders ion transport or degradation due to expansion/contraction with voltage cycling. We will experimentally and computationally determine the interfacial structure-impedance relationship in SSLiBs to obtain fundamental insight into design parameters to overcome this issue. Furthermore, we will investigate interfacial modification (layers between SSE and electrode) to see if we can extend these structure-property relationships to higher performance.

Collaborations. We are in collaboration with Dr. Venkataraman Thangadurai on garnet synthesis. We will collaborate with Dr. Leonid A. Bendersky and Dr. Howard Wang at NIST to use Neutron scattering to investigate the lithium profile across the bilayer interface with different charge-discharge rates.

Milestones

1. Synthesize garnet and electrode materials. (Complete)
2. Determine frequency dependence of garnet and electrode impedances. (Complete)
3. Develop computation models for garnet based interfaces. (Complete)
4. Identify gel or PFPE based electrolyte with a stable voltage window (0V-4.2 V). (Complete)

Progress Report

In this quarter, we developed a computational model for garnet-electrode interfaces (Figure 65, milestone 3). The comprehensive interface model is based on a large variety of inputs provided by a range of first principles computation and by actual experimental parameters to model the interface properties. The interface model has been developed and demonstrated for garnet materials with electrode materials, such as LiCoO_2 . The interphase layers between the garnet and the electrode were determined using grand potential phase diagram at the applied voltage of the battery at the input for the model. The formation of the interphase was found to be thermodynamically favorable for the interfaces of garnet with anode and cathode. In addition, the properties of the materials comprising the interphase, such as defect and migration energy, were also evaluated in first principles calculations. The effects of the space-charge layer were incorporated as a part of the interface model. Using all these predicted input parameters, the conductivity and interfacial resistance of the interfacial layer was determined. The model is now ready to be applied to any composition of garnet solid electrolyte in contacting interface with any electrode materials. The inputs for the interface model are generated by the first principles computation and experimental parameters. The model was able to demonstrate that poor interfacial layer causes high interfacial resistance in all-solid-state batteries.

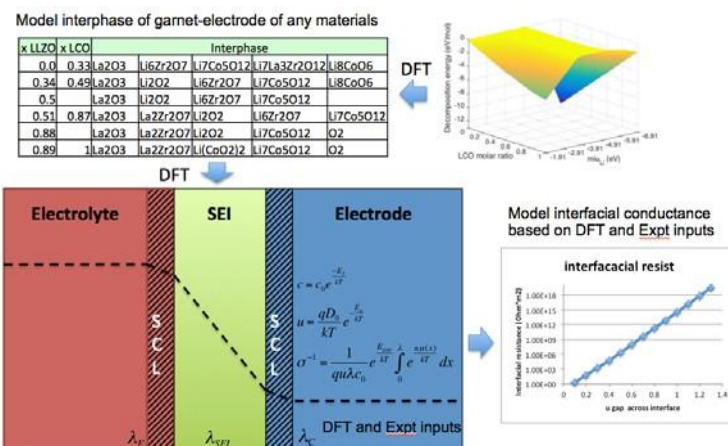


Figure 65. Developed model for garnet-electrode interfaces, which takes input from first principles calculations and experimental condition parameters.

A PVDF-HFP based gel polymer was prepared and characterized. 0.25 g PVDF-HFP was dissolved in a mixture of 4.75 g acetone and 0.25 g distilled water (95:5, m/m) with stirring for 1 h. The solution was cast on a Al foil, and the solvent was evaporated at ambient temperature. After drying under vacuum at 100°C for 2 h, a homogeneous free-standing membrane was obtained. The as-prepared porous membrane was immersed in 1 M LiTFSI solution of 1:1 (vol) tetraethylene glycol dimethyl ether and n-methyl-(n-butyl)pyrrolidinium bis(trifluoromethanesulfonyl)imide (Py14TFSI) in the room temperature for 30 mins in an argon-filled glovebox. A cyclic voltammogram testing cell was set up by sandwiching the polymer gel electrolyte membrane between lithium and titanium disks and sealing into a coin cell. As shown in Figure 66, the cyclic voltammogram with a scan rate of 1 mV/s suggests that the stable electrochemical window of such a polymer gel electrolyte is up to 4.2 V (milestone 4). The peaks at -0.2 V and 0.1 V correspond to the Li plating / stripping.

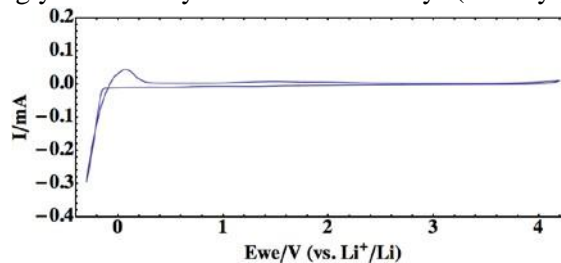


Figure 66. Cyclic voltammogram for Li/polymer gel electrolyte/Ti.

Task 7.5 – Nanoscale Interfacial Engineering for Stable Lithium Metal Anodes (Yi Cui, Stanford University)

Project Objective. This study aims to render lithium metal anode with high capacity and reliability by developing chemically and mechanically stable interfacial layers between lithium metal and electrolytes, which is essential to couple with sulfur cathode for high-energy lithium-sulfur batteries. With the nanoscale interfacial engineering approach, various kinds of advanced thin films will be introduced to overcome the issues related to dendritic growth, reactive surface, and virtually “infinite” volume expansion of lithium metal anode.

Project Impact. The cycling life and stability of lithium metal anode will be dramatically increased. The success of this project, together with breakthroughs of sulfur cathode, will significantly increase the specific capacity of lithium batteries and decrease the cost as well, therefore stimulating the popularity of electric vehicles.

Out-Year Goals. Along with suppressing dendrite growth, the cycle life, Coulombic efficiency, as well as the current density of lithium metal anode will be greatly improved (no dendrite growth for current density up to 3.0 mA/cm², with Coulombic efficiency >99.5%) by choosing the appropriate interfacial nanomaterial.

Milestones

1. Fabrication of interconnected carbon hollow spheres with various sizes. (3/31/2015 – Complete)
2. Synthesize of layered hexagonal boron nitride and graphene with different thicknesses and defect levels. (3/31/2015 – Complete)
3. Demonstrate the guiding effect of polymer nanofibers for improved lithium metal cycling performance. (6/30/2015 – Complete)
4. Demonstrate the improved cycling life and Coulombic efficiency of lithium metal anode with nanoscale interfacial engineering. (9/30/2015 – Ongoing)
5. Demonstrate the improved cycling performance of lithium metal anode with different current density and areal capacity. (9/30/2015 – Ongoing)

Progress Report

Inspired by our previous knowledge that nanomaterials could enable stable lithium metal anodes, we continued to explore alternative nanomaterials beyond carbon nanospheres and ultrathin, two-dimensional layered materials. Electrospun polyacrylonitrile (PAN) nanofibers emerged as a suitable choice especially because of the potential interaction between lithium ion and surface polar groups. Through electrospinning and post treatment, large-scale fabrication of cross-linked PAN nanofibers is enabled, resulting in a polymer nanofiber mat with porosity up to 85%. Rather than the dendritic growth in the free situation, lithium tends to fill the pore space during its electroplating, arising from the specific interactions between lithium and polar groups, including $-OH$ and $=O$ on cross-linked PAN nanofibers. As a result, uniform lithium deposition was realized with minimum surface exposed to ether-based electrolyte.

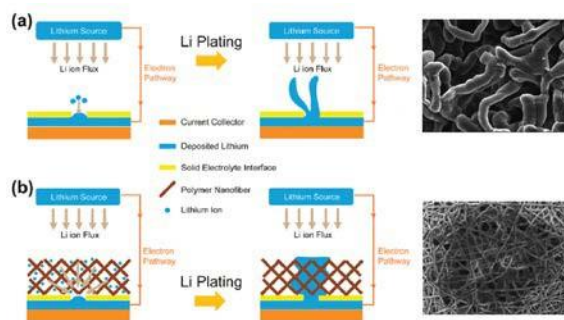


Figure 67. Guided deposition of lithium metal by polymer nanofibers. (a) Formation of dendritic lithium metal when no guiding nanofiber mat existed. (b) When nanofiber mat is applied, lithium metal deposition is guided by the mat, due to the polymer surface where polar groups are affiliated by lithium metal deposition.

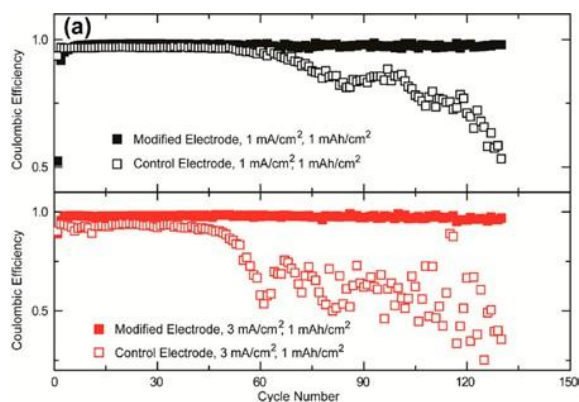


Figure 68. Stable cycling of lithium metal anode enabled by electrospun nanofibers. Average Coulombic efficiency of 97.4% was achieved for more than 120 cycles, with areal capacity and current density up to 3 mAh/cm² and 3 mA/cm², respectively.

Resulting from the stable intrinsic SEI layer in ether-based electrolyte, and more importantly, the flat surface morphology, stable cycling of lithium metal is realized. Average Coulombic efficiency, as high as 97.9% for 120 cycles, was realized with areal capacity and current of 1 mAh/cm² and 1 mA/cm². Moreover, even at a practical value of 3 mAh/cm² and 3 mA/cm², stable cycling with Coulombic efficiency of 97.4% was still achieved for more than 120 cycles. The stratagem of using specially designed 3D polymer nanofiber mat to address the uncontrolled Li dendrite growth problem definitely provided us with new insight into energy storage technologies based on Li metal.

Patents/Publications/Presentations

Liang, Z., and G. Zheng, C. Liu, N. Liu, W. Li, K. Yan, H. Yao, P.-C. Hsu, S. Chu, and Y. Cui. "Polymer Nanofiber-Guided Uniform Lithium Deposition for Battery Electrodes." *Nano Letters* 15 (2015): 2910-2916.

Task 7.6 – Lithium Dendrite Suppression for Lithium-Ion Batteries (Wu Xu and Ji-Guang Zhang, Pacific Northwest National Laboratory)

Project Objective. The objective of this project is to prevent lithium (Li) dendrite formation on Li-metal anode used in Li- metal batteries and to prevent Li dendrite formation on carbon anodes used in Li-ion batteries during extreme charge conditions such as overcharge, fast charge and charge at low temperatures. We will further explore various factors that affect the morphology of Li deposition, especially at high current density conditions. These factors include solvent-cation reaction, Li-ion additive cation interaction, etc. The long-term stability of these additives also will be investigated. Novel additives will be combined with common electrolytes used in state-of-the-art Li-ion batteries to prevent Li dendrite growth in these batteries, especially when they are operated under extreme conditions.

Project Impact. Li metal is an ideal anode material for rechargeable batteries. Unfortunately, uncontrollable dendritic Li growth and limited Coulombic efficiency during Li deposition/stripping inherent in these batteries have prevented their practical applications. This work will explore the new electrolyte additives that can lead to dendrite-free Li deposition with high Coulombic efficiency. The success of this work will increase energy density of Li and Li-ion batteries and accelerate market acceptance of electrical vehicles (EV), especially for plug-in hybrid electrical vehicles (PHEV) required by the EV Everywhere Grand Challenge proposed by the DOE/EERE.

Out-Year Goals. The long-term goal of the work is to enable Li and Li-ion batteries with >120 Wh/kg (for PHEVs), 1000 deep-discharge cycles, a 10-year calendar life, improved abuse tolerance, and less than 20% capacity fade over a 10-year period.

COLLABORATIONS. This project engages in collaboration with the following:

- Bryant Polzin (ANL) – NCA, NMC and graphite electrodes
- Chongmin Wang (PNNL) – Characterization by TEM/SEM
- Kang Xu (ARL) – ESI-MS studies on cation-solvent interactions in electrolytes
- Vincent Battaglia (LBNL) – LFP electrode

Milestones

1. Develop electrolytes to suppress Li dendrite growth on Li metal and graphite anode and to maintain Li Coulombic efficiency over 98%. (12/31/2014 – Complete)
2. Protect graphite electrode in PC-EC-based carbonate electrolytes with electrolyte additives. (3/31/2015 – Complete)
3. Demonstrate over 300 cycles for 4-V Li-metal batteries without internal short circuiting, through optimized electrolyte formulation(6/30/2015 – Complete)
4. Achieve over 500 cycles for 4-V Li-metal batteries without internal short circuiting, through optimized electrolyte formulation. (9/30/2015 – Ongoing)

Progress Report

This quarter, the cycling stability of Li|LiNi_{0.4}Mn_{0.4}Co_{0.2}O₂ (i.e., Li|NMC442) coin cells was investigated with 11 electrolytes containing 1.0 M LiPF₆ and 0.05 M CsPF₆ in EC/PC/EMC at different ratios. NMC-442 was used as the cathode because of its good structural stability and thermal stability. After two formation cycles at C/20 rate, the cells were charged at C/3 rate and discharged at 1C rate in the voltage range of 2.7 to 4.3 V. It is seen that all tested electrolytes have nearly the same first cycle charge/discharge voltage profiles (Figure 69a), and 9 of 11 electrolytes show stable cycling for 300 cycles before the capacity retention reaches 80% (Figure 69b).

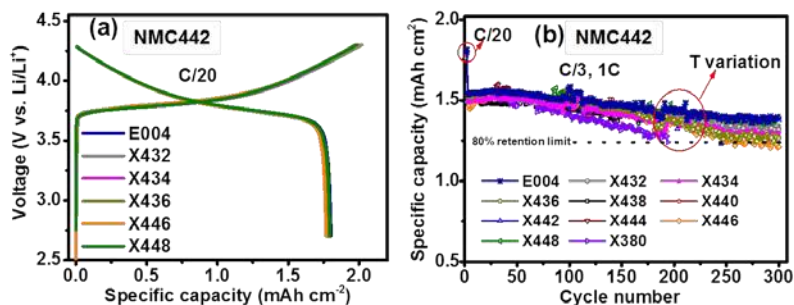


Figure 69. (a) Charge/discharge voltage profiles of selected electrolytes, and (b) cycling stability of Li|NMC-442 coin cells at RT.

The possible Li metal deposition on MAG-10 graphite anode from ANL(A-AGen2) during fast charging and overcharging conditions was further investigated. The electrolytes were 1.0 M LiPF₆ and 0.05 M CsPF₆ in EC/PC/EMC. After two formation cycles of Li|MAG-10 cells at C/20 rate in the voltage range of 0.005 to 1.5 V at RT, the cells were charged at four different current densities of 0.2, 0.5, 1.0 and 2.0 mA/cm². When charge capacity is cut off at 1.25 mAh/cm² of the graphite anode, that is, about 83.3% of the theoretical areal capacity (1.53 mAh/cm²), no deposited Li metal is found on the surface and inner side of the graphite anode (Figure 70b-c), even though the deposition curves show the voltage reached below 0 V for the charging at 0.5-2.0 mA/cm² (Figure 70a). The possible reason is that there is still limited Li metal formed, but it quickly reacts with electrolyte to form SEI. However, when the charge capacity is cut off at 2.0 mAh/cm² of the graphite anode, i.e., about 130.7% of the theoretical areal capacity or 30.7% overcharge, all the deposition curves show the voltage reached below 0 V for the charging at 0.2-2.0 mA/cm² (Figure 71a) Li metal is found at the surface of graphite anodes for charging at 0.5-2.0 mA/cm²; more Li metal deposits out when the charging current density increases (Figure 71b-c). It is indicated that Li metal still forms when the electrode is slightly overcharged especially at relatively high current densities. More tests are under way.

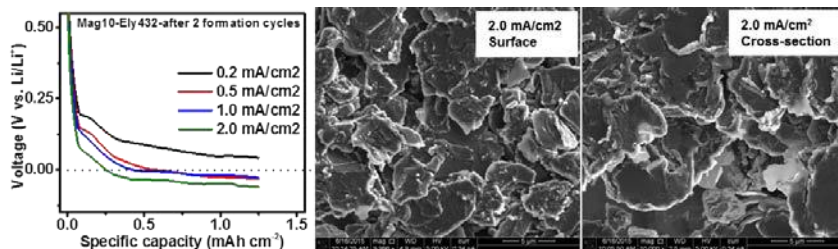


Figure 70. (a) Voltage curves of graphite charging or Li deposition on graphite anode at four charging current densities. (b, c) SME images of graphite anode charged at 2.0 mA/cm² and cutoff at 1.25 mAh/cm².

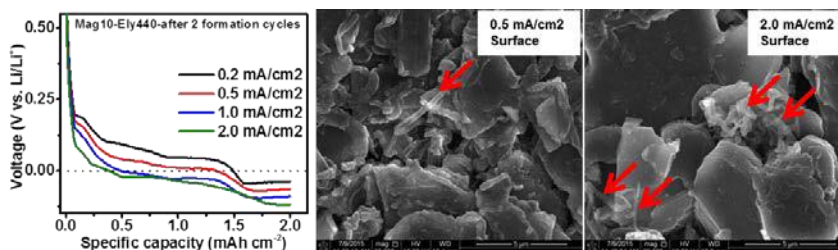


Figure 71. (a) Voltage curves of graphite charging or Li deposition on graphite anode at four charging current densities. (b, c) SME images of graphite anode charged at 0.5 and 2.0 mA/cm² and cutoff at 2.0 mAh/cm².

Patents/Publications/Presentations

1. Xiao, Liang, and Xilin Chen, Ruiguo Cao, Jiangfeng Qian, Hongfa Xiang, Jianming Zheng, Ji-Guang Zhang*, and Wu Xu*. “Enhanced Performance of $\text{Li}_2\text{LiFePO}_4$ Cells Using CsPF_6 as an Electrolyte Additive.” *Journal of Power Sources*, 293 (2015): 1062-1067.
2. Xiang, Hongfa, and Donghai Mei, Pengfei Yan, Priyanka Bhattacharya, Sarah D. Burton, Arthur V. Cresce, Ruiguo Cao, Mark H. Engelhard, Mark E. Bowden, Zihua Zhu, Bryant J. Polzin, Chongmin Wang, Kang Xu, Ji-Guang Zhang, and Wu Xu. “The Role of Cesium Cation in Directing Interphasial Chemistry on Graphite Anode in Propylene Carbonate-Rich Electrolytes.” *ACS Applied Materials & Interfaces*, under review.

TASK 8 – LITHIUM SULFUR BATTERIES

Summary and Highlights

Advances in Li-ion technology thus far have been stymied by challenges facing the development of high reversible capacity cathodes and stable anodes. Hence, there is a critical need for the development of alternate battery technologies with superior energy densities and cycling capabilities. Lithium-sulfur (Li-S) batteries in this regard have been identified as the next flagship technology, holding much promise due to the attractive theoretical specific energy densities of 2,567 Wh/kg. Moreover, realization of the high theoretical specific capacity of 1,675 mAh/g corresponding to the formation of Li_2S utilizing earth-abundant sulfur renders the system highly promising compared to other hitherto available cathode systems. The current research focus has thus shifted toward the development of lithium sulfur (Li-S) batteries. This system, however, suffers from major drawbacks, as elucidated below.

- Limited inherent electronic conductivity of sulfur and sulfur compound based cathodes.
- Volumetric expansion and contraction of both the sulfur cathode and lithium anode.
- Soluble polysulfide formation/dissolution and sluggish kinetics of subsequent conversion of polysulfides to Li_2S resulting in poor cycling life.
- Particle fracture and delamination as a result of the repeated volumetric expansion and contraction.
- Irreversible loss of lithium at the sulfur cathode, resulting in poor Coulombic efficiency.
- High diffusivity of polysulfides in the electrolyte, resulting in plating at the anode and consequent loss of driving force (that is, drop in cell voltage).

These major issues cause sulfur loss from the cathode, leading to mechanical disintegration. Additionally, surface passivation of anode and cathode systems results in a decrease in the overall specific capacity and Coulombic efficiency (CE) upon cycling. As a result, the battery becomes inactive within the first few charge-discharge cycles. Achievement of stable high capacity in Li-S batteries requires execution of fundamental studies to understand the degradation mechanisms in conjunction with engineered solutions. Task 8 of the BMR program addresses both aspects with execution of esoteric, fundamental *in situ* x-ray spectroscopy (XAS) and *in situ* electron paramagnetic resonance (EPR) studies juxtaposed with applied research comprising use of suitable additives, coatings, and exploration of composite morphologies. Both ANL and LBNL use x-ray based techniques to study phase evolution and loss of CE in Se_8 during lithiation/delithiation, while understanding polysulfide formation in sulfur and polysulfides (PSL) in oligomeric polyethylene oxide (PEO) solvent, respectively. Work from PNNL, U Pitts, and Stanford demonstrates high areal capacity electrodes in excess of 2 mAh/cm². Following loading studies reported in the first quarter, PNNL has performed *in situ* EPR to study reaction pathways mediated by sulfur radical formation. Coating/encapsulation approaches adopted by U Pitts and Stanford comprise flexible sulfur wire (FSW) electrodes coated with Li-ion conductors, and TiS_2 encapsulation of Li_2S in the latter, both ensuring polysulfide retention at sulfur cathodes. BNL work has focused on benchmarking of pouch cell testing by optimization of the voltage window and study of additives such as LiI and LiNO_3 . *Ab-initio* studies at Stanford and U Pitts involving calculation of binding energies and reaction pathways, respectively, augment the experimental results. *Ab-initio* molecular dynamics (AIMD) simulations performed at TAMU reveal multiple details regarding electrolyte decomposition reactions and the role of soluble polysulfides (PS) on such reactions. Using Kinetic Monte-Carlo (KMC) simulations, electrode morphology evolution and mesostructured transport interaction studies were also executed. Each of these projects has a collaborative team of experts with the required skill set needed to address the EV Everywhere Grand Challenge of 350 Wh/kg and 750 Wh/l, and cycle life of at least 1000 cycles.

Task 8.1 – New Lamination and Doping Concepts for Enhanced Li – S Battery Performance (Prashant N. Kumta, University of Pittsburgh)

Project Objective. To successfully demonstrate generation of novel sulfur cathodes for Li-S batteries meeting the targeted gravimetric energy densities ≥ 350 Wh/kg and ≥ 750 Wh/l with a cost target \$125/kWh and cycle life of at least 1000 cycles for meeting the EV Everywhere blueprint. The proposed approach will yield sulfur cathodes with specific capacity ≥ 1400 mAh/g, at ≥ 2.2 V, generating ~ 460 Wh/kg energy density higher than the target. Full cells meeting the required deliverables will also be made.

Project Impact. Identification of new laminated Sulfur cathode based systems displaying higher gravimetric and volumetric energy densities than conventional lithium ion batteries will likely result in new commercial battery systems that are more robust, capable of delivering better energy and power densities, and more lightweight than current Li-ion battery packs. Strategies and configurations based on new lithium-ion conductor (LIC)-coated sulfur cathodes will also lead to more compact battery designs for the same energy and power density specifications as current Li-ion systems. Commercialization of these new S cathode based Li-ion battery packs will represent, fundamentally, a major hallmark contribution of the DOE-OVT Program and the battery community.

Out-Year Goals. This is multi-year project comprises three major phases to be successfully completed in three years. Phase 1 (Year 1): Synthesis, Characterization, and Scale up of suitable LIC matrix materials and multilayer composite sulfur cathodes. This phase is ongoing. Phase 2 (Year 2): Development of LIC coated sulfur nanoparticles, scale up of high-capacity engineered LIC-coated multilayer composite electrodes, and doping strategies for improving electronic conductivity of sulfur. Phase 3 (Year 3): Advanced high energy density, high-rate, extremely cyclable cell development.

Collaborations. The project collaborates with the following members with the corresponding expertise:

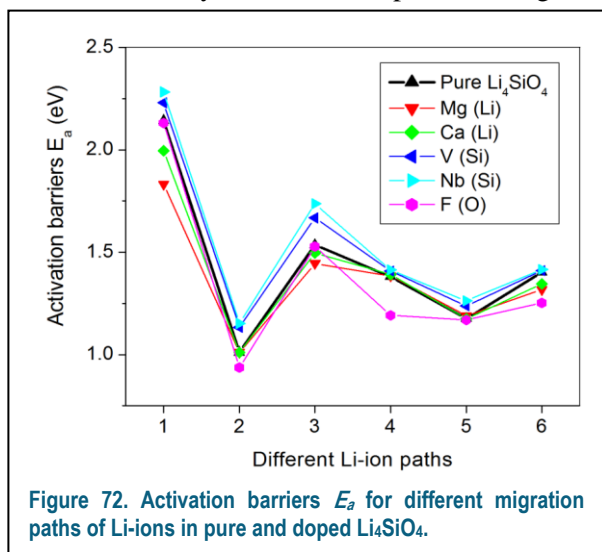
- Dr. Moni Datta (University of Pittsburgh): for experimental generation of nanoscale composites;
- Dr. Oleg Velikokhatnyi (University of Pittsburgh): for theoretical and computational studies;
- Dr. Spandan Maiti (University of Pittsburgh): for mechanical stability and multi-scale modeling;
- Dr. A. Manivannan (NETL): for x-ray photoelectron spectroscopy (XPS) for surface characterization;
- Dr. D. Krishnan Achary (University of Pittsburgh): for solid-state nuclear magnetic resonance (MAS-NMR) characterization.

Milestones

1. Demonstrate synthesis of finely dispersed nanoparticles of sulfur. (December 2014 – Complete)
2. Develop novel lithium-ion conducting membrane systems using *ab-initio* methods displaying impermeability to sulfur diffusion. (December 2014 – Complete)
3. Demonstrate capabilities for generation of novel sulfur 1D, 2D, and 3D morphologies exhibiting superior stability and capacity. (June 2015 – Complete)
4. Identification and synthesis of LIC materials for use as coatings for sulfur cathodes. (June 2015 – Complete)
5. Novel encapsulation and sheathing techniques, and exploration of unique architectures and generation of 3D composites displaying superior Li-ion conduction, reversible capacity, and stability. (June 2015 – Complete)
6. *Go/No-Go*: Decision will be based on the ability to demonstrate improvement in cycling upon use of the LIC coating. (October 2015 – Ongoing)

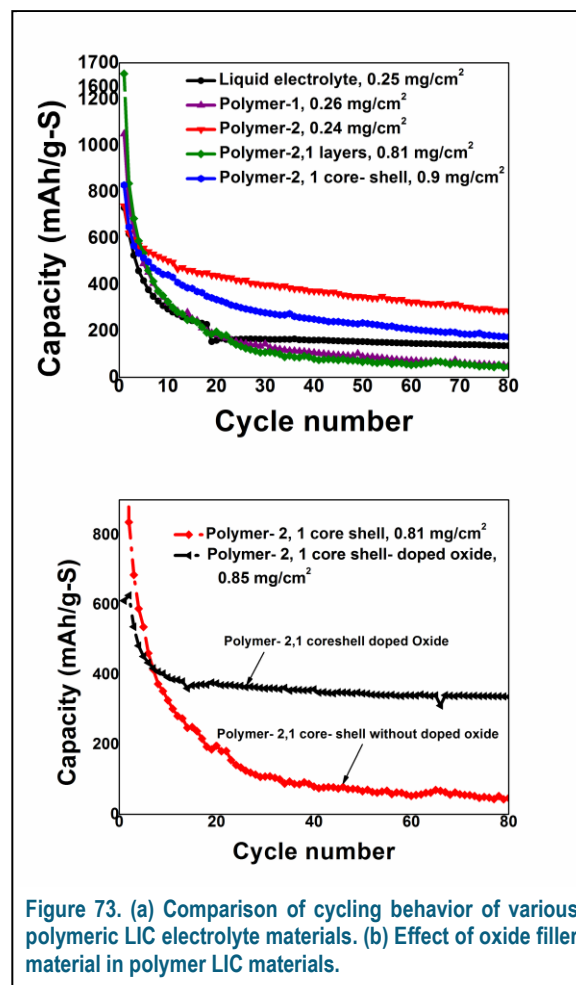
Progress Report

Work last quarter involved preparing polymer-flexible sulfur (FSW) composite electrodes coated with a LIC coating (FSW pellet-LIC) indicating stable capacity of ~650 mAh/g over 60 cycles and FSW electrodes with ~450 mAh/g over 135 cycles (fade rate~0.003%/cycle). Optimization of LIC thickness and ionic conductivity is vital in tandem with optimization of the polymer composition that is under way. This quarter, ionic conductivity of Li_4SiO_4 doped with Mg, Ca, V, Nb, and F has been theoretically studied. Using the nudged elastic band method implemented in VASP, the activation barrier, the E_a for various Li^+ migration pathways has been calculated. Results (Figure 72) show Mg and Ca on Li and also F on O sites decrease E_a for all corresponding Li-ion pathways, in contrast to pure Li_4SiO_4 . However, V and Nb on Si sites slightly increase E_a due to the larger ionic radii of V^{5+} and Nb^{5+} vs. Si^{4+} . Nevertheless, overall Li-ion conductivity is expected to improve due to Li^+ -vacancy formation



favoring Li-ion lattice hopping. Calculated cohesive energies of pure and doped Li_4SiO_4 indicate that V and Nb slightly decrease the structural and chemical stability, while Mg, Ca, and F cause no change, which indicates their efficacy for improved conductivity and stability of Li_4SiO_4 . Experimental system validation continues.

Polymer LIC (gel-polymer electrolytes (GPE) containing LIC (GPE-LIC)) systems were also explored. Polymeric LICs were used to replace traditional polymeric separators. Figure 73a depicts improvement in cycling stability of creating composite polymeric core-shell and layer-by-layer composites. Figure 73b shows further improvement in stability due to doped nanoparticle fillers (NF) in the polymer with stable capacity of ~400 mAh/g for 80 cycles. The electrolyte with NF acts as polysulfide filters and retainers, ensuring stability. Optimization involving a combination of FSW-LIC with doped inorganic and GPE-LIC continues and will be described in future reports.



Patents/Publications/Presentations

Presentations

- The Electrochemical Society, Chicago (Spring 2015): “Novel Flexible Sulfur Wire Fabrics (FSF) for Lithium-Sulfur Batteries”; P. H. Jampani, P. M. Shanthi, B. Gattu, and P. N. Kumta.
- The Electrochemical Society, Chicago (Spring 2015): “Effect of Coating and Particle Properties on the Cycling Stability of Li-Ion Conductor (LIC) Coated Sulfur Cathodes”; P. M. Shanthi, P. H. Jampani, B. Gattu, O. I. Velikokhatnyi, and P. N. Kumta.

Task 8.2 – Simulations and X-ray Spectroscopy of Li-S Chemistry (Nitash Balsara, Lawrence Berkeley National Laboratory)

Project Objective. Lithium-sulfur cells are attractive targets for energy storage applications as their theoretical specific energy of 2600 Wh/kg is much greater than the theoretical specific energy of current lithium-ion batteries. Unfortunately, the cycle-life of lithium-sulfur cells is limited due to migration of species generated at the sulfur cathode. These species, collectively known as polysulfides, can transform spontaneously, depending on the environment, and it has thus proven difficult to determine the nature of redox reactions that occur at the sulfur electrode. The objective of this project is to use x-ray spectroscopy to track species formation and consumption during charge-discharge reactions in a lithium-sulfur cell. Molecular simulations will be used to obtain x-ray spectroscopy signatures of different polysulfide species, and to determine reaction pathways and diffusion in the sulfur cathode. The long-term objective of this project is to use the mechanistic information to build high specific energy lithium-sulfur cells.

Project Impact. Enabling rechargeable lithium-sulfur cells has the potential to change the landscape of rechargeable batteries for large-scale applications beyond personal electronics due to: (1) high specific energy, (2) simplicity and low cost of cathode (the most expensive component of current lithium-ion batteries), and (3) earth abundance of sulfur. The proposed diagnostic approach also has significant potential impact as it represents a new path for determining the species that form during charge-discharge reactions in a battery electrode

Out-Year Goals. Year 1: Simulations of sulfur and polysulfides (PSL) in oligomeric polyethylene oxide (PEO) solvent. Prediction of x-ray spectroscopy signatures of PSL/PEO mixtures. Measurement of x-ray spectroscopy signatures PSL/PEO mixtures. Year 2: Use comparisons between theory and experiment to refine simulation parameters. Determine speciation in PSL/PEO mixtures without resorting to adhoc assumptions. Year 3: Build an all-solid lithium-sulfur cell that enables measurement of x-ray spectra *in situ*. Conduct simulations of reduction of sulfur cathode. Year 4: Use comparisons between theory and experiment to determine the mechanism of sulfur reduction and Li₂S oxidation in all-solid lithium-sulfur cell. Use this information to build lithium-sulfur cells with improved life-time.

Collaborations. This project collaborates with Tsu-Chien Weng, Dimosthenis Sokaras, and Dennis Nordlund at Stanford Synchrotron Radiation Lightsource, SLAC National Accelerator Laboratory in Stanford, California.

Milestones

1. Extend theoretical calculations of XAS to finite polysulfide concentrations. (12/1/14 – Complete)
2. Experimental study of the effect of polysulfide concentration on XAS spectra. (2/15/15 – Complete)
3. Quantitative comparison of experimental and theoretical XAS spectra. (5/20/15 – Complete)
4. Build and test cell for *in situ* XAS analysis. (8/23/15 – On Schedule)

Progress Report

Milestone 1 has been completed.

Milestone 2 has been completed. Experimental XAS of Li_2S_4 and Li_2S_8 dissolved in PEO were obtained at a range of temperatures (a) and concentrations (b). The XAS below show that the distribution of polysulfide present does not vary as temperature and concentration increases. We have also obtained XAS for Li_2S_x ($x = 4, 6$, and 8) dissolved in dimethylformamide (c), which is known to stabilize polysulfide radical anions. The $x = 4$ and $x = 6$ spectra have a lower energy feature near 2469.2 eV that we have previously shown to be attributed to polysulfide radical anions. Interestingly, this feature is not detectable in the $x = 8$ solution. Using our computational approach, we are working to understand why $x = 8$ solutions may not contain radical anions and what implications this may have for the battery.

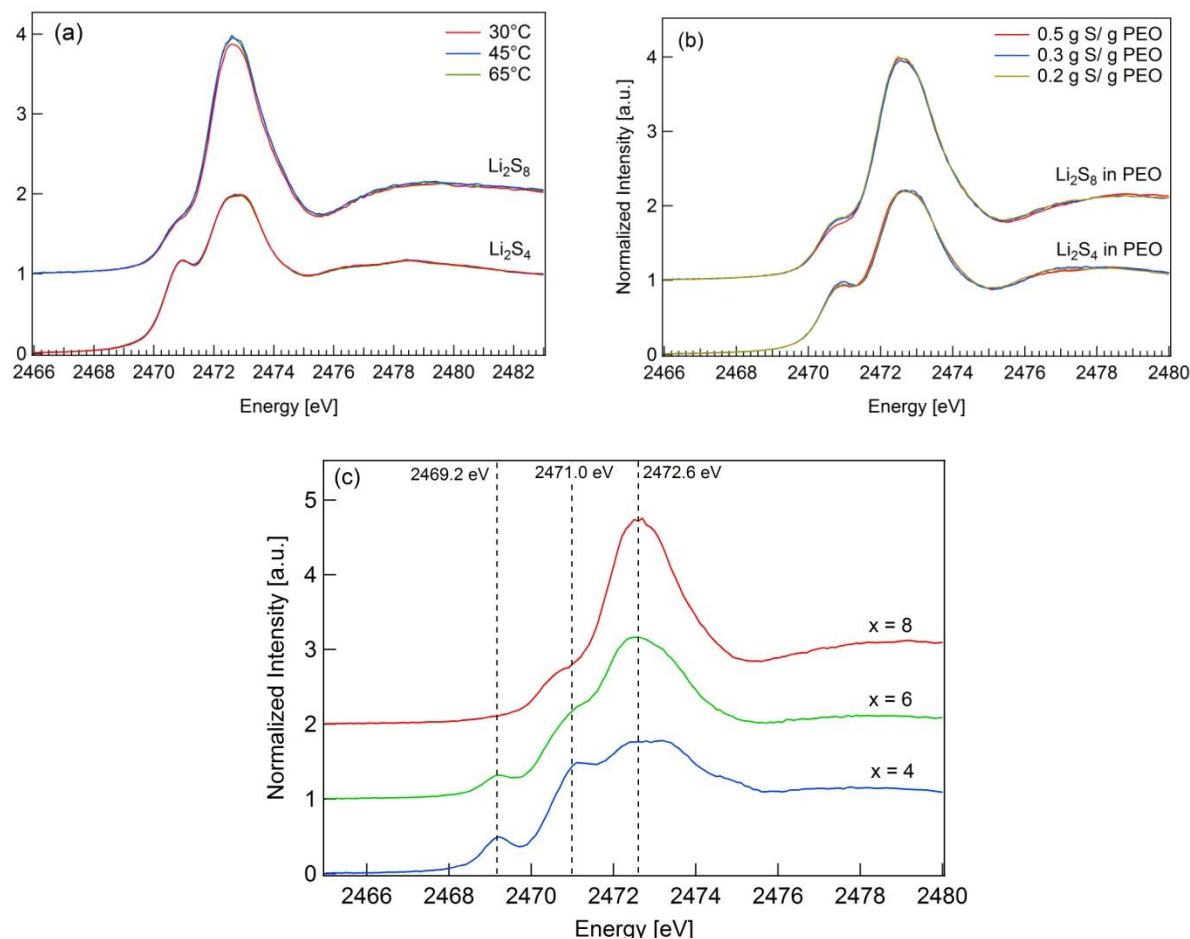


Figure 74. Experimental XAS data of Li_2S_4 and Li_2S_8 dissolved in PEO were obtained at a range of temperatures (a) and concentrations (b); XAS data were also obtained for Li_2S_x ($x = 4, 6$, and 8) dissolved in DMF (c).

Milestone 3 has been completed. Theoretical XAS spectra for lithium polysulfide species dissolved in dimethylformamide (DMF) are being calculated. These spectra will be used to analyze the above experimental XAS data of polysulfides dissolved in DMF.

Milestone 4 is in progress. Numerous Li-S pouch cells adapted for *in situ* soft x-ray XAS have been designed and tested. Heating stages for XAS at beamlines 9.3.1 of ALS and 4-3 of SSRL have also been built and tested with Li-S cells and are ready for use. We are now waiting on beam time to perform *in situ* studies of Li-S chemistry.

Patents/Publications/Presentations

Wujcik, K., and T. Pascal, C. D. Pemmaraju, D. Devaux, N. P. Balsara, and D. Prendergast. “Characterization of Polysulfide Radicals Present in an Ether-Based Electrolyte of a Lithium–Sulfur Battery During Initial Discharge Using *In situ* X-Ray Absorption Spectroscopy Experiments and First-Principles Calculations.” *Advanced Energy Materials*, accepted.

Task 8.3 – Novel Chemistry: Lithium Selenium and Selenium Sulfur Couple (Khalil Amine, Argonne National Laboratory)

Project Objective: The objective of this project is to develop a novel SeS_x cathode material for rechargeable lithium batteries with high energy density, long life, low cost, and high safety.

Project Impact: Development of a new battery chemistry is promising to support the goal of PHEV and EV applications.

Approach: Embedding Se_xS_y in a porous carbon matrix to suppress the dissolution of lithium polysulfide and to enhance the life of batteries using such electrode. Impact of stoichiometric and the porous structure of carbon matrix will be investigated in detail.

Out-Year Goals: When this new cathode is optimized, the following result can be achieved:

- A cell with nominal voltage of 2 V and energy density of 600 Wh/kg.
- A battery capable of operating for 500 cycles with low capacity fade.

Collaborations: This project engages in collaboration with the following:

- Prof. Chunsheng Wang of University of Maryland
- Dr. Yang Ren and Dr. Chengjun Sun of APS at ANL

Milestones

1. Synchrotron probe study of charge storage mechanism of Li/S batteries. (Q1 – Complete)
2. Study of stability of Li/Se batteries in carbonate-based electrolyte. (Q2 – Complete)
3. Investigation of the phase diagram of Se_xS_y system. (Q3 – Ongoing)

Progress Report

To study the phase stability of Se_xS_y against the chemical composition of final compound, a series of samples was synthesized to establish the S-Se phase diagram. Raman spectroscopy (see Figure 75) clearly shows signature of a new compound that was formed by mixing S and a proper amount of Se. XRD data also showed that the new compound had a different crystal structure from either S or Se. Two samples of great interest are SeS and Se_2S_5 . The former, SeS, was selected because it shows amorphous as synthesized; the latter was picked because it has broad diffraction peaks, indicating nano-crystallinity. At the same time, Se_2S_5 has more S than SeS; hence, Se_2S_5 is expected to have a higher reversible capacity than SeS. Therefore, Se_2S_5 was selected for detailed study, and investigation on SeS will be carried out for the coming quarter.

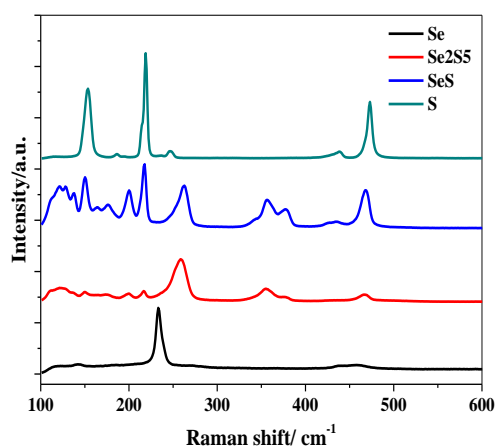


Figure 75. Raman spectroscopies of typical Se_xS_y samples.

Figure 76a shows the evolution of x-ray absorption near edge spectroscopy of Se_2S_5 material during the charge/discharge process. The absorbance of the material was color-coded in the contour plot; a red pixel means a high absorbance at the specific time and x-ray energy, while a blue pixel means a low absorbance. The peak at 12655 eV indicates the absorbance of Se, while the peak at 12720 eV is the absorbance of Li_2Se . This figure shows that Se was fully converted into Li_2Se during the initial discharge process, but only part of Li_2Se was reversed back to Se during the following charge process. It is believed that that trapped Li_2Se after the initial discharge is the primary contributor to the initial drop of reversible capacity of battery using Se_2S_5 cathode (see Figure 76b). Therefore, it is believed that the reversible capacity can be further improved by using an alternative impregnation process to enhance utilization of Li_2Se .

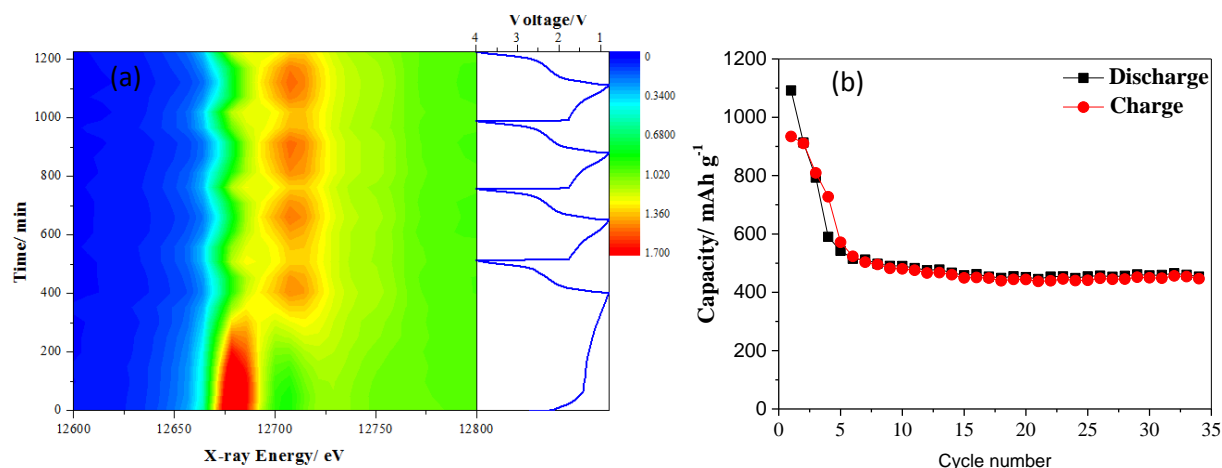


Figure 76. (a) *In situ* XANES of Li/ Se_2S_5 battery using a carbonate-based electrolyte. (b) Capacity retention of Li/ Se_2S_5 battery using a carbonate-based electrolyte.

Task 8.4 – Multi-Functional Cathode Additives (MFCA) for Li-S Battery Technology (Hong Gan, Brookhaven National Laboratory; and Co-PI Esther Takeuchi, Brookhaven National Laboratory and Stony Brook University)

Project Objective. Develop a low-cost battery technology for PEV application utilizing Li-S electrochemical system by incorporating multifunctional cathode additives (MFCA), consistent with the long-term goals of the DOE EV Everywhere Blueprint.

Project Impact. The Li-S battery system has gained significant interest due to its low material cost potential (35% cathode cost reduction over Li-ion) and its attractive 2.8x (volumetric) to 6.4x (gravimetric) higher theoretical energy density compared to conventional Li-ion benchmark systems. Commercialization of this technology requires overcoming several technical challenges. This effort will focus on improving the cathode energy density, power capability and cycling stability by introducing multifunctional cathode additives (MFCA). The primary deliverable of this project is to identify and characterize the best MFCA for Li-S cell technology development.

Approach. Transition metal sulfides are evaluated as cathode additives in sulfur cathode due to their high electronic conductivity and chemical compatibility to the sulfur cell system. Electrochemically active additives will also be selected for this investigation to further improve the energy density of the sulfur cell system. In the first year, the team will evaluate the transition metal sulfide cathode cells and sulfur cathode cells individually to establish the baseline. Then the interaction between transition metal sulfide additives and the sulfur electrode will be investigated. In parallel, commercially unavailable selected additives will be synthesized for electrochemical cell interaction studies.

Out-Year Goals. This multi-year project comprises two major phases to be successfully completed in three years. Phase 1 includes cathode and MFCA investigation; Phase 2 will include cell component interaction studies and full cell optimization. The work scope for year 1 will focus on the cathode and cathode additive studies. The proof of concept and feasibility studies will be completed for the Multi Functional Cathode Additives. By year-end, multiple types of additives will be identified and prepared, including the synthesis of the non-commercially available additives. The electrochemical testing of all selected MFCA will be initiated.

Collaborations. This project collaborates with Ke Sun, Dong Su, and Can Erdonmez at BNL, along with Amy Marschilok and Kenneth Takeuchi at SBU.

Milestones

1. Baseline Li/MFCA cell demonstration with selected transition metal sulfides. (Q1 – Complete)
2. Baseline Li/S cell demonstration with sulfur and/or Li₂S cathode. (Q2 – Complete)
3. Li/sulfur-MFCA concept cell demonstration for cathode-MFCA interaction. (Q3 – Complete)
4. Synthesis of selected non-commercial MFCA. (Q4 – Initiated)

Progress Report

MFCA Concept Cell Demonstration: The task objective is to demonstrate the interaction between sulfur cathode and transition metal sulfides. For this task, commercially available metal sulfides (Cu_2S , FeS , and TiS_2) were used as additives in sulfur cathode. Interactions between transition metal sulfides and sulfur within the hybrid cathode are examined with material phase transformation detected. Coin cells are tested to determine the effect of these additives on sulfur cathode cycling performance.

While interaction between Cu_2S and Li_2S only happens after cell cycling, Cu_2S and sulfur interact strongly to form nano-flake shaped crystalline CuS (SEM in Figure 77) during electrode preparation. With excess mole% of Cu_2S vs. sulfur in hybrid cathode, up to 100% sulfur utilization for the first discharge under C/10 rate was observed (Figure 77), indicating the complete conversion of sulfur into CuS , since Cu_2S is electrochemically non-active at above 1.8-V cut off. Figure 78 shows the coin cell cycling capacity based on sulfur loading. For hybrid cathode with $\text{Cu}_2\text{S}:\text{S} < 1:1$, dissolution of copper ions in the electrolyte was found to be detrimental to the cell cycle life.

Unlike Cu_2S , XRD showed no material phase change by just physically mixing FeS and sulfur, which is consistent with literature [*Journal of the Electrochemical Society* 160, no. 8 (2013): A1009]. However, a new FeS_2 phase was detected by TEM electron diffraction after just one discharge/charge cycle of [$\text{FeS}+\text{S}$] coin cell (Figure 79), which provides direct evidence for the electrochemical initiated material phase transition.

The effect of electrochemically active and chemically stable TiS_2 additive was also investigated in hybrid cathode with weight ratio $\text{S}:\text{TiS}_2 = 3:1$, in which TiS_2 contributing to ~4.5% of the total cathode theoretically capacity. Relative to control sulfur electrode, the hybrid electrode exhibited additional sloped voltage plateau at below 2.0 V, indicating the participation of TiS_2 in cathode discharge. Although the hybrid cathode has lower initial capacity densities (mAh/g, total electrode) vs. the control, capacity crossover happened after 10 cycles due to the lower capacity fade rate of hybrid cathode cells (Figure 80).

The above examples demonstrate complex mechanisms of transition metal sulfide and sulfur interaction. Depending on the types of transition metal sulfide, either chemical (Cu_2S) or electrochemical (FeS) induced material conversion can happen under the cathode preparation and the cell electrochemical testing conditions. The beneficial effect on coin cell cycle life by using the chemically stable and electrochemically active TiS_2 additive in sulfur cathode is also demonstrated.

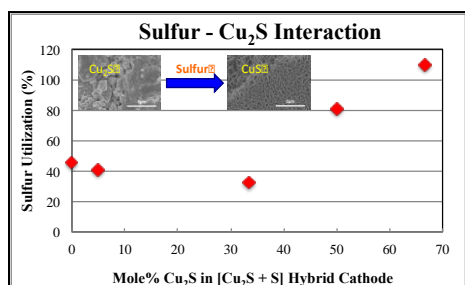


Figure 77. Nano-CuS from $\text{Cu}_2\text{S}+\text{Sulfur}$

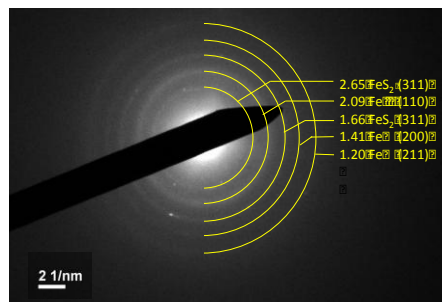


Figure 79. Conversion of FeS to FeS_2

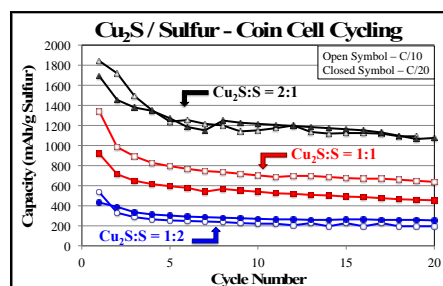


Figure 78. $\text{S}:\text{Cu}_2\text{S}$ Coin Cell Cycling

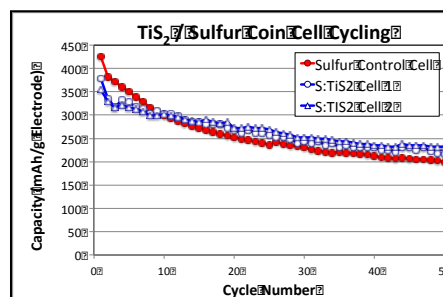


Figure 80. TiS_2+S vs. S Control Cycling

Task 8.5 – Development of High-Energy Lithium-Sulfur Batteries (Jie Xiao and Jun Liu, Pacific Northwest National Laboratory)

Project Objective. The project objective is to develop high-energy, low-cost lithium sulfur (Li-S) batteries with long lifespan. All proposed work will employ thick sulfur cathode (≥ 2 mAh/cm² of sulfur) at a relevant scale for practical applications. The diffusion process of soluble polysulfide out of the thick cathode will be revisited to investigate the cell failure mechanism at different cycling. Alternative anode will be explored to address the lithium anode issue. The fundamental reaction mechanism of polysulfide under the electrical field will be explored by applying advanced characterization techniques to accelerate the development of Li-S battery technology.

Project Impact. The theoretical specific energy of Li-S batteries is ~2300 Wh/kg, which is almost three times higher than that of state-of-the-art Li-ion batteries. The major challenge for Li-S batteries is polysulfide shuttle reactions, which initiate a series of chain reactions that significantly shorten battery life. The proposed work will design novel approaches to enable Li-S battery technology and accelerate market acceptance of long-range electrical vehicles (EV) required by the EV Everywhere Grand Challenge proposed by the DOE/EERE.

Out-Year Goals. This project has the following out-year goals:

- Fabricate Li-S pouch cells with thick electrodes to understand sulfur chemistry/electrochemistry in the environments similar to the real application.
- Leverage the Li-metal protection project funded by DOE and PNNL advanced characterization facilities to accelerate development of Li-S battery technology.
- Develop Li-S batteries with a specific energy of 400 Wh/kg at cell level, 1000 deep-discharge cycles, improved abuse tolerance, and less than 20% capacity fade over a 10-year period to accelerate commercialization of electrical vehicles.

Collaborations. This project engages in collaboration with the following:

- Dr. Xiao-Qing Yang (LBNL) – *In situ* characterization
- Dr. Bryant Polzin (ANL) – electrode fabrication
- Dr. Xingcheng Xiao (GM) – materials testing

Milestones

1. Optimization of sulfur loading to reach 3-4 mAh/cm² areal specific capacity on the cathode. (12/31/2014 – Complete)
2. Complete the investigation on the fundamental reaction mechanism of Li-S batteries. (3/31/2015 – Complete).
3. Identify alternative anode to stabilize the interface reactions on the anode side (6/30/2014 – Complete).
4. Demonstrate the stable cycling of sulfur batteries (2-4 mAh/cm²) with less than 20% degradation for 200 cycles. (9/30/2015 – Ongoing)

Progress Report

The third quarter milestone was completed this period. Previous study revealed when thick sulfur cathode was coupled with lithium anode, the cell failure was largely determined by the anode side. An alternative and more stable anode was graphite. However, graphite only works well in the presence of ethylene carbonate (EC), which is incompatible with polysulfides and their derived sulfur radicals. A new electrolyte recipe was identified this quarter to enable stable cycling of graphite in an EC-free environment; this led to demonstration of a Li-ion sulfur battery prototype employing intercalation chemistry.

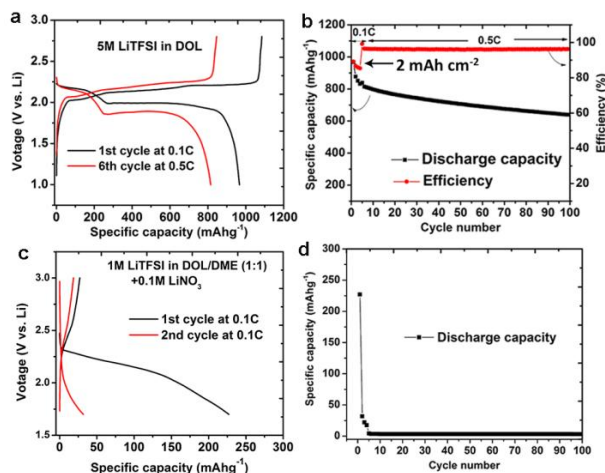


Figure 81. (a) Charge/discharge curves of lithiated graphite/sulfur (LG/S) full cell at different C rates in 5M LiTFSI/DOL electrolyte without any additive and (b) their corresponding cycling stability and Coulombic efficiency. (c) Charge/discharge curves of LG/S full cell at 0.1 C in 1M LiTFSI/DOL/DME with 0.1M LiNO₃ as additive and (d) their corresponding cycling performance. Areal capacity of cathode (limiting electrode) is 2 mAh/cm².

Lithiated graphite was coupled with a sulfur cathode to construct a full cell by using electrolyte comprised of 5M LiTFSI in pure DOL. At a low rate of 0.1 C, the LG/S cell exhibited a high capacity of 980 mAh g⁻¹ (2 mAh cm⁻²) with two flat discharge plateaus at 2.2 and 2.0 V (Figure 81a). This means sulfur in the LG/S full cell experienced similar reaction pathways as those in conventional Li-S cells. In the first charging process, a capacity around 1080 mAh g⁻¹ was obtained, delivering a high Coulombic efficiency of 90.7% without any additive in the electrolyte. When the rate was elevated to 0.5 C after the first 5 cycles, a capacity as high as 815 mAh g⁻¹ was delivered, indicating the good kinetics of Li⁺ across the electrolyte, electrodes and their interfaces. After around 100 cycles (Figure 81b), a high capacity retention rate of 81.3% was achieved at 0.5 C with a Coulombic efficiency above 97%. Of note, the cycling performance of full cells also largely depended on the mass balance of cathode and anode. More systematic optimization is in progress to further improve capacity retention.

As a comparison, LG/S full cell was also tested in traditional electrolyte such as 1M LiTFSI in DOL/DME (1:1 v:v). Only a small capacity of 220 mAh g⁻¹ was obtained with a sloped discharge curve during the first cycle, which is quite different than that of conventional Li-S cells. In the subsequent charging process, there was almost no capacity (Figure 81c), indicating the exfoliation of graphite upon Li⁺ intercalation. With repeated cycling, the discharge capacity quickly faded to almost zero after only five cycles (Figure 81d).

The increased LiTFSI concentration and the removal of DME in the electrolyte both contributed to stable cycling of graphite anode in the absence of EC solvent. The detailed functioning mechanism of this new electrolyte is still being investigated and will be reported later.

Patents/Publications/Presentations

1. Lv, D., and P. Yan, Y. Shao, Q. Li, S. Ferrara, H. Pan, G. L. Graff, B. Polzin, C. Wang, J.-G. Zhang, J. Liu, and J. Xiao. *Chem. Commun.*, (2015): In Press.
2. Presentation at Beyond Lithium Ion VIII, Oak Ridge, Tennessee (June 2015): “Alternative Binder and Anode for Lithium-Sulfur Batteries”; D. Lv, Q. Li, P. Yan, S. Ferrara, Y. Wang, M. H. Engelhard, C. Wang, J.-G. Zhang, J. Liu, and J. Xiao.

Task 8.6 – Nanostructured Design of Sulfur Cathodes for High Energy Lithium-Sulfur Batteries (Yi Cui, Stanford University)

Project Objective. The charge capacity limitations of conventional transition metal oxide cathodes are overcome by designing optimized nano-architected sulfur cathodes.

This study aims to enable sulfur cathodes with high capacity and long cycle life by developing sulfur cathodes from the perspective of nanostructured materials design, which will be used to combine with lithium metal anodes to generate high-energy lithium-sulfur batteries. Novel sulfur nanostructures as well as multifunctional coatings will be designed and fabricated to overcome issues related to volume expansion, polysulfide dissolution, and the insulating nature of sulfur.

Project Impact. The capacity and the cycling stability of sulfur cathode will be dramatically increased. This project's success will make lithium-sulfur batteries to power electric vehicles and decrease the high cost of batteries.

Out-Year Goals. The cycle life, capacity retention, and capacity loading of sulfur cathodes will be greatly improved (200 cycles with 80% capacity retention, >0.3 mAh/cm² capacity loading) by optimizing material design, synthesis and electrode assembly.

Collaborations. This project engages in collaboration with the following:

- BMR program principal investigators
- SLAC: *In situ* x-ray, Dr. Michael Toney
- Stanford: Prof. Nix, mechanics; Prof. Bao, materials

Milestones

1. Demonstrate synthesis to generate monodisperse sulfur nanoparticles with/without hollow space. (October 2013 – Complete)
2. Develop surface coating with one type of polymers and one type of inorganic materials. (January 2014 – Complete)
3. Develop surface coating with several types of polymers; Understand amphiphilic interaction of sulfur and sulfide species. (April 2014 – Complete)
4. Demonstrate sulfur cathodes with 200 cycles with 80% capacity retention and 0.3mAh/cm² capacity loading. (July 2014 – Complete)
5. Demonstrate Li₂S cathodes capped by layered metal disulfides. (December 2014 – Complete)
6. Identify the interaction mechanism between sulfur species and different types of sulfides/oxides/metals, and find the optimal material to improve the capacity and cycling of sulfur cathode. (July 2015 – On Track)

Progress Report

Previously, we demonstrated that conductive metal oxides, such as tin-doped indium oxide (ITO) and magnéli phase Ti_4O_7 can function as a highly effective matrix to bind with sulfur species, and thus can suppress the lithium polysulfide shuttle effect and enable the controlled deposition of Li_2S . However, the detailed mechanism and the corresponding selection criteria of the metal oxides are still lacking. We are investigating the interaction mechanism between sulfur species and different types of materials, including metal oxides and metal sulfides, and trying to identify the optimal material to improve capacity and cycling stability of sulfur cathode.

We have studied the absorption of lithium polysulfides on the surfaces of various oxide materials, including CeO_2 , Al_2O_3 , La_2O_3 , MgO and CaO , as shown in Figure 82. Figure 82a shows the digital image of the adsorption test of lithium polysulfide (Li_2S_8) using different mass of oxide samples with same total surface area. The color of the solution containing Al_2O_3 and CeO_2 is lighter than others, indicating better adsorption performance of these two metal oxide nanoparticles. To better understand the absorption mechanism, DFT calculation was performed to reveal the corresponding adsorption energy and sites, as shown in Figure 82c. The adsorption energy of Li_2S on $\text{CeO}_2(111)$, $\text{Al}_2\text{O}_3(110)$, $\text{La}_2\text{O}_3(001)$, $\text{MgO}(100)$ and $\text{CaO}(100)$ surfaces is -6.33, -7.12, -5.85, -5.71, and -5.49 eV, respectively. The calculation is consistent with the experimental observation, in which the materials with higher absorption energy exhibited stronger absorption performance. We are studying the binding mechanism and testing the electrochemical properties of sulfur cathodes incorporated with these materials.

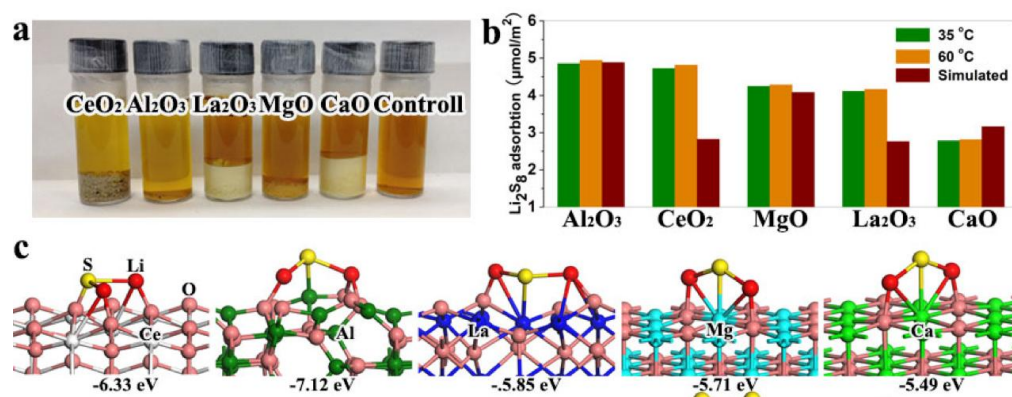


Figure 82. (a) Digital images of the Li_2S_8 trapping by the metal oxide nanoparticles in 1,3-dioxolane (DOL) and dimethoxyethane (DME) (1:1, v:v) solution. (b) Experimental and simulated adsorption amount of Li_2S_8 on different metal oxides. (c) Optimized geometries of most stable Li_2S on $\text{CeO}_2(111)$, $\text{Al}_2\text{O}_3(110)$, $\text{La}_2\text{O}_3(001)$, $\text{MgO}(100)$, and $\text{CaO}(100)$ surfaces.

Task 8.7 – Addressing Internal “Shuttle” Effect: Electrolyte Design and Cathode Morphology Evolution in Li-S Batteries (Perla Balbuena, Texas A&M University)

Project Objective. The project objective is to overcome the lithium-metal anode deterioration issues through advanced Li-anode protection/stabilization strategies including (i) *in situ* chemical formation of a protective passivation layer and (ii) alleviation of the “aggressiveness” of the environment at the anode by minimizing the polysulfide shuttle with advanced cathode structure design.

Project Impact. Through formulation of alternative electrolyte chemistries as well as design, fabrication, and test of improved cathode architectures, it is expected that this project will deliver Li/S cells operating for 500 cycles at efficiency greater than 80%.

Approach. A mesoscale model including different realizations of electrode mesoporous structures generated based on a stochastic reconstruction method will allow virtual screening of the cathode microstructural features and the corresponding effects on electronic/ionic conductivity and morphological evolution. Interfacial reactions at the anode due to the presence of polysulfide species will be characterized with *ab initio* methods. For the cathode interfacial reactions, data and detailed structural and energetic information obtained from atomistic-level studies will be used in a mesoscopic-level analysis. A novel sonochemical fabrication method is expected to generate controlled cathode mesoporous structures that will be tested along with new electrolyte formulations based on the knowledge gained from the mesoscale and atomistic modeling efforts.

Out-Year Goals. By determining reasons for successes or failures of specific electrolyte chemistries, and assessing relative effects of composite cathode microstructure and internal shuttle chemistry vs. that of electrolyte chemistry on cell performance, expected results are : (1) develop an improved understanding of the Li/S chemistry and ways to control it; (2) develop electrolyte formulations able to stabilize the Li anode; (3) develop new composite cathode microstructures with enhanced cathode performance; and (4) develop a Li/S cell operating for 500 cycles at an efficiency > 80%.

Collaborations. This is a collaborative work combining first-principles modelling (Perla Balbuena, Texas A&M University), mesoscopic level modelling (Partha Mukherjee, Texas A&M University), and synthesis, fabrication, and test of Li/S materials and cells (Vilas Pol, Purdue University).

Milestones

1. Synthesis of the C/S cathode hybrid materials: Develop lab-scale Li-S composite. (December 14 – Complete); Perform advanced characterization. (March 2015 – Complete)
2. Determination of the structure of the PS/Li Interface: Characterization of thermodynamics of nucleation and growth of PS deposits on the Li surface. (March 2015 – Complete)
3. Determination of the chemistry of the C/S composite cathode: Characterize dissolution, reduction, and lithiation of S in the composite cathode microstructure. (June 2015 – Complete)
4. Study of electrode morphology evolution and mesostructure transport interaction: Study cathode mesostructure impact on product formation and deposition. *Go/No-Go*: Comparative analysis of the mesoscale model and experimental characterization. (September 2015 – In Progress)

Progress Report

Reactions at the cathode/electrolyte surface. Density functional theory (DFT) and *ab initio* molecular dynamics (AIMD) simulations revealed multiple details regarding sulfur reduction reactions and the solubility of short-chain polysulfides (PS). Simulations were done with 1M solution of LiTFSI in pure solvents (DME and DOL). It was found that Li_2S precipitation may be induced by defects or uncoordinated sites on carbon. Once molecular adsorption starts, various structures similar to the (110) and (111) of Li_2S can grow over graphene (representing a carbon basal plane). Figure 83 illustrates that increasing Li_2S coverage favors the formation of the Li_2S (111) structure. On the other hand, the carbon surface may facilitate unwanted PS dissolution, especially inside of nanopores < 1.5 nm. New studies are being conducted to detect effective materials to control PS dissolution. So far two materials have been identified, and they are being tested computationally for sulfur reduction. Detailed DFT and AIMD analyses have elucidated the sulfur lithiation and species found as a function of time, which is equivalent to lithiation capacity. Current studies focus on the effect of current rate.

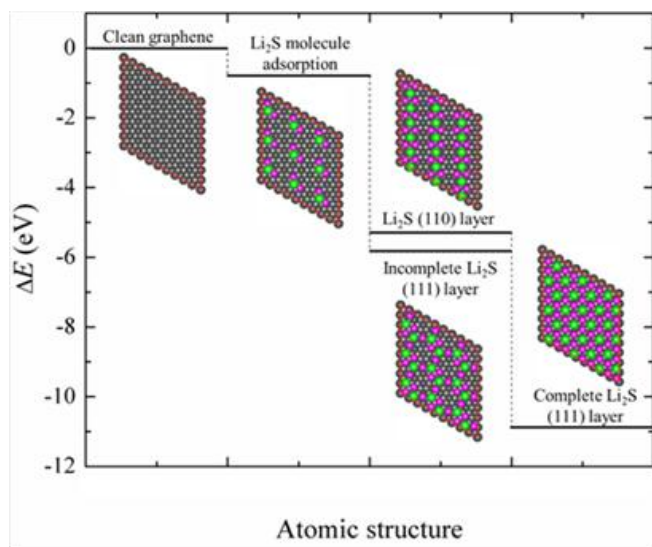


Figure 83. Energy profile of Li_2S (111) layer formation on graphene calculated with DFT/vdW-D3 approach. Green, violet and grey spheres represent S, Li and C atoms, respectively.

Experimental. Sulfur amounts in S-C composite fabricated via sonochemical power were varied and optimized. The composites were characterized with morphological (SEM), compositional (EDS), and structural (XRD). It is confirmed that most of the nanosulfur is loaded in the carbon cavities. Electrochemical performance was tested on newly prepared electrolyte composed of 1 M solution of LiTFSI in organic solvent of equal parts DOL/ D_2 . Due to the hygroscopic nature of salts and impurities in the solvents, the new electrolyte did not perform well. Namely, most of the Li-S batteries showed low capacity and significant fade. Other tests using industrial (Arkema Inc.) electrolyte, also showed poor electrochemical performance in most of the cells. After several trials, a protocol was developed to dry solvents and salt that started showing promise. Currently, multiple cells are cycling at various currents for the new C/S composite employing 1M LiTFSI salt in 50% DOL/50% D_2 and addition of minor additive (LiNO_3) as well as glass fiber separator. A small fraction of graphene is used in the carbon-sulfur composite to enhance electrode conductivity.

Mesoscale modeling. The approach has been extended to predict the influence of cathode microstructure – precipitation – transport interaction on performance. It was found that at the cathode microstructure level, the porosity and microstructural changes (due to morphological variations in shapes of solid products) affect transport in the electrolyte and also the interfacial reactions. The information from the coarse-grained KMC simulation (for discharge product formation, developed in the second quarter) at the electrode microstructural scale and the coverage of electrochemically active area and its relation to the fraction of surface area available for electrochemical reactions was incorporated into the macrohomogeneous model for cell performance based on the “porous electrode theory.” Preliminary performance predictions show two different discharge regimes for the cell voltage similar to that observed experimentally.

Patents/Publications/Presentations

Liu, Z., and D. Hubble, P. B. Balbuena, and P. P. Mukherjee. “Adsorption of Insoluble Polysulfides Li_2S_x ($x = 1, 2$) on Li_2S Surfaces.” *Phys. Chem. Chem. Phys.* 17 (2015): 9032-9039.

TASK 9 – LI-AIR BATTERIES

Summary and Highlights

High-density energy storage systems are critical for electric vehicles (EV) required by the EV Everywhere Grand Challenge proposed by the DOE/EERE. Conventional Li-ion batteries still cannot fully satisfy the ever-increasing needs because of their limited energy density, high cost, and safety concerns. As an alternative, the rechargeable Li-O₂ battery has the potential to be used for long range EVs. The practical energy density of a Li-O₂ battery is expected to be ~ 800 Wh kg⁻¹. The advantages of Li-O₂ batteries come from their open structure; that is, they can absorb the active cathode material (oxygen) from the surrounding environment instead of carrying it within the batteries. However, the open structure of Li-O₂ batteries also leads to several disadvantages. The energy density of Li-O₂ batteries will be much lower if oxygen has to be provided by an onboard container. Although significant progress has been made in recent years on the fundamental properties of Li-O₂ batteries, the research in this field is still in an early stage and many barriers must be overcome before practical applications. The main barriers include:

- Instability of electrolytes. Superoxide species generated during discharge or O₂ reduction process is highly reactive with electrolyte and other components in the battery. Electrolyte decomposition during charge or O₂ evolution process is also significant due to high over-potentials.
- Instability of air electrode (dominated by carbonaceous materials) and other battery components (such as separators and binders) during charge/discharge processes in an oxygen-rich environment.
- Limited cyclability of the battery associated with instability of the electrolyte and other components of the batteries.
- Low energy efficiency associated with large over-potential and poor cyclability of Li-O₂ batteries.
- Low power rate capability due to electrode blocking by the reaction products.
- Absence of a low cost, high efficiency oxygen supply system (such as oxygen selective membrane).

The main goal of the PNNL Task is to provide a better understanding on the fundamental reaction mechanisms of Li-O₂ batteries and identify the required components (especially electrolytes and electrodes) for stable operation of Li-O₂ batteries. The PNNL researchers will investigate stable electrolytes and oxygen evolution reaction (OER) catalysts to reduce the charging overvoltage of Li-O₂ batteries and improve their cycling stability. New electrolytes will be combined with stable air electrodes to ensure their stability during Li-O₂ reaction. Considering the difficulties in maintaining the stability of conventional liquid electrolyte, the Liox team will explore the use of a nonvolatile, inorganic molten salt comprising nitrate anions and operating Li-O₂ cells at elevated temperature (>80°C). It is expected that these Li-O₂ cells will have a long cycle life, low over potential, and improved robustness under ambient air compared to current Li-air batteries. At Argonne National Laboratory, new cathode materials and electrolytes for lithium-air batteries will be developed for Li-O₂ batteries with long cycle life, high capacity, and high efficiency. The state-of-the-art characterization techniques and computational methodologies will be used to understand the charge and discharge chemistries. UMass/BNL team will investigate the root causes of the major obstacles of the air cathode in the Li-air batteries. Special attention will be paid to optimizing high-surface carbon material used in the gas diffusion electrode, catalysts, electrolyte, and additives stable in Li-air system and with capability to dissolve Li oxide and peroxide. Success of this project will establish a solid foundation for further development of Li-O₂ batteries toward practical applications for long-range EVs. The fundamental understanding and breakthrough in Li-O₂ batteries may also provide insight on improving the performance of Li-S batteries and other energy storage systems based on chemical conversion processes.

Task 9.1 – Rechargeable Lithium-Air Batteries (Ji-Guang Zhang and Wu Xu, PNNL)

Project Objective. The objective of this work is to develop stable electrolyte and oxygen evolution reaction (OER) catalysts to reduce the charging overvoltage of lithium (Li)-air batteries and improve the cycling stability of rechargeable Li-air batteries. New catalysts will be synthesized to improve the capacity and cycling stability of Li-O₂ batteries. New electrolytes will be investigated to ensure their oxygen-stability during Li-O₂ reaction.

Project Impact. Li-air batteries have a theoretical specific energy that is more than five times that of state-of-the-art Li-ion batteries and are potential candidates for use in next-generation, long-range electric vehicles (EV). Unfortunately, the poor cycling stability and low Coulombic efficiency of Li-air batteries have prevented practical application to date. This work will explore a new electrolyte and electrode that could lead to long cyclability and high Coulombic efficiencies in Li-air batteries that can be used in the next generation EVs required by the EV Everywhere Grand Challenge proposed by the DOE/EERE.

Out-Year Goals. The long-term goal of the proposed work is to enable rechargeable Li-air batteries with a specific energy of 800 Wh/kg at cell level, 1000 deep-discharge cycles, improved abuse tolerance, and less than 20% capacity fade over a 10-year period to accelerate commercialization of long-range EVs.

Collaborations. This project engages in collaboration with the following:

- Yangchuan (Chad) Xing (University of Missouri) – Metal oxide coated glassy carbon electrode
- Chunmei Ben (NREL) – Metal oxide coated glassy carbon electrode
- Chongmin Wang (PNNL) – Characterization of cycled air electrodes by TEM/SEM

Milestones

1. Synthesize and characterize the modified glyme solvent and the dual transition metal oxide catalyst. (12/31/2014 – Complete)
2. Improve the stability of solvent using conventional carbon air. (3/31/2015 – Complete)
3. Identify the solvent to be stable for at least 50 cycles on modified air electrode. (6/30/2015 –Complete)
4. Integrate the new electrolyte and modified air electrode to assemble Li-O₂ batteries with at least 120 cycles stable operation. (9/30/2015 – Ongoing)

Progress Report

This quarter, the effects of salt concentration in electrolytes on the cycling performance of Li-O₂ batteries with CNTs/PVDF/carbon paper air electrodes were investigated. Three LiTFSI-DME electrolytes with 1 M, 2 M, and 3 M salt concentrations were tested between 2 – 4.5 V. In the cells with 1 M and 2 M electrolytes, the discharge capacities can maintain at 1000 mAh g⁻¹ for only 2 and 8 cycles, respectively, and quickly decrease to below 100 mAh g⁻¹ after 20 and 35 cycles. In contrast, in the cells with 3 M electrolyte, the capacity can be maintained at a discharge capacity of 1000 mAh g⁻¹ for 55 cycle life (Figure 84d), although the charge capacity starts to decrease after the 40th cycle (Figure 84c). In addition, cell resistance decreases with increasing salt concentration.

SEM images (Figure 85) of the morphologies of the cycled air electrodes and Li metal anodes in the three electrolytes indicate that discharged products (Li₂O₂ and others) remain in the air electrodes and cannot be decomposed during charging, and that the Li anodes have been severely corroded. However, the 3 M electrolyte results in the network architectures composed of numerous carbon nanotubes, nearly no Li₂O₂, and a lower level of electrolyte decomposition products leftover, along with a well protected Li metal anode. DFT calculations (Figure 86) indicate that the Li⁺-(DME)₂ and Li⁺-(DME)₃ solvates present in the 3 M electrolyte have much higher Gibbs activation energy barriers than the pure DME molecule by the attack of superoxide radical anion. It is demonstrated that the highly concentrated electrolyte is more stable against reduced oxygen species, leading to less electrolyte decomposition and more ionic conductive layer on the CNTs air-electrodes, along with a well protected Li metal anode. These results verified a simple but effective way to develop stable electrolytes for rechargeable Li-O₂ batteries.

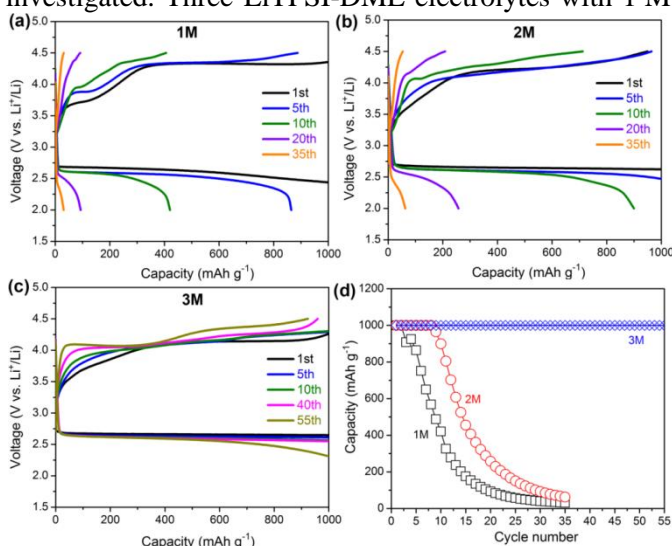


Figure 84. Voltage profiles of selected cycles for Li-O₂ cells with (a) 1 M, (b) 2 M and (c) 3 M electrolytes cycled at a discharge capacity limited (100 mAh g⁻¹) protocol between 2.0 and 4.5 V at a current density of 0.1 mA cm⁻². (d) Comparison of cycling stability performance.

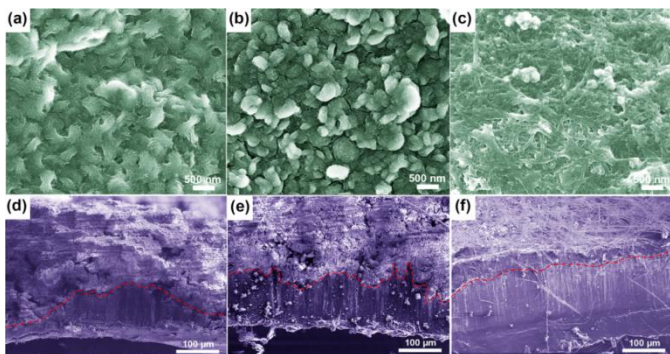


Figure 85. SEM images of air-electrodes at the charged state (a-c) and Li metal anodes (d-f) after 40 full discharge/charge cycles from LiTFSI-DME electrolytes of 1 M (a,d), 2 M (b,e), and 3 M (c,f).

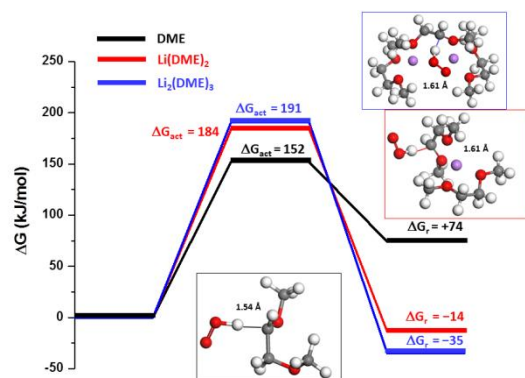


Figure 86. DFT calculations of the Gibbs activation barriers for the C-H bond scission from CH₂ groups in DME, Li⁺-(DME)₂, and Li⁺-(DME)₃ by the attack of superoxide radical anion (O₂^{•-}).

Patents/Publications/Presentations

Liu, B., and W. Xu,* P. Yan, P. Bhattacharya, R. Cao, M. E. Bowden, M. H. Engelhard, C. Wang, and J.-G. Zhang*. “ ZnCo_2O_4 as a High-Performance Bifunctional Catalyst for Rechargeable Lithium-Oxygen Batteries.” Under review.

Task 9.2 – Efficient Rechargeable Li/O₂ Batteries Utilizing Stable Inorganic Molten Salt Electrolytes (Vincent Giordani, Liox)

Project Objective. The project objective is to develop high specific energy, rechargeable Li-air batteries having lower overpotential and improved robustness under ambient air compared to current Li-air batteries. The technical approach involves replacing traditional organic and aqueous electrolytes with a nonvolatile, inorganic molten salt comprising nitrate anions and operating the cell at elevated temperature (>80°C). The research methodology includes powerful *in situ* spectroscopic techniques coupled to electrochemical measurements (for example, electrochemical mass spectrometry) designed to provide quantitative information about the nature of chemical and electrochemical reactions occurring in the air electrode.

Project Impact. If successful, this project will solve particularly intractable problems relating to air electrode efficiency, stability and tolerance to the ambient environment. Furthermore, these solutions may translate into reduced complexity in the design of a Li-air stack and system, which in turn may improve prospects for use of Li-air batteries in EVs. Additionally, the project will provide materials and technical concepts relevant for development of other medium temperature molten salt Li battery systems of high specific energy, which may also have attractive features for EVs.

Out-Year Goals. The long-term goal of this project is to develop Li-air batteries comprising inorganic molten salt electrolytes and protected Li anodes that demonstrate high (>500 Wh/kg) specific energy and efficient cycleability in ambient air. By the end of the project, it is anticipated that problems hindering use of both the Li anode and air electrode will be overcome due to materials advances and strategies enabled within the intermediate (>80 °C) operating temperature range of the system under development.

Collaborations. This project engages in collaboration with the following:

- Bryan McCloskey (LBNL): Analysis of air electrode and electrolyte
- Julia Greer (Caltech): Design of air electrode materials and structures

Milestones

1. Demonstrate eutectic compositions having eutectic points below 120°C. (December 2014 – Complete)
2. Measure ionic conductivity and Li⁺ transference number in eutectic compositions. (December 2014 – Complete)
3. Measure diffusion coefficients and solubilities of O₂, Li₂O₂, and Li₂O. (March 2015 – Complete)
4. Synthesize oxidation-resistant carbons. (March 2015 – Complete)
5. *Go/No-Go*: Demonstrate suitability of analytical approach for elevated temperature molten salt metal-O₂ cells. Criteria: Quantify Li₂O₂ yield, e⁻/O₂, and OER/ORR ratios for baseline carbon air electrodes. (June 2015 – Complete)
6. Quantify Li₂O₂ yield, e⁻/O₂, and OER/ORR ratios for oxidation-resistant carbon air electrodes. (June 2015 – Complete)
7. Measure diffusion coefficients and solubilities of H₂O, CO₂, LiOH, and Li₂CO₃. (September 2015 – Ongoing)
8. Synthesize metals and metal alloys of high air electrode stability and/or catalytic activity. (September 2015 – Ongoing)

Progress Report

The Go/No-Go decision condition for this quarter has been satisfied. Criteria included quantification of lithium peroxide yield, e^-/O_2 and OER/ORR molar ratios for our baseline carbon-based cathode (Super P). Boron-doped carbon nanotubes were synthesized last quarter, and the electrochemical parameters mentioned above were determined this quarter.

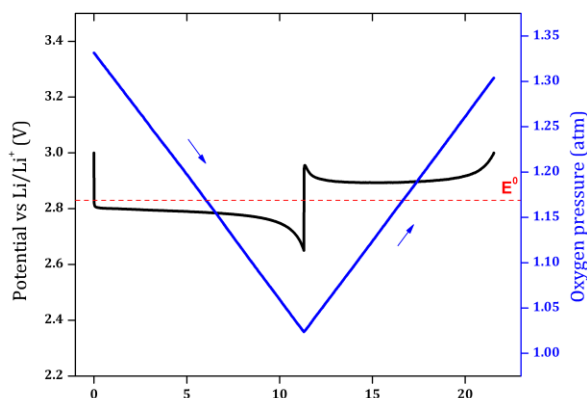


Figure 87. Voltage/Pressure profile for a Li-O₂ cell cycling at 150°C using Super P carbon cathode and LiNO₃-KNO₃ eutectic. 0.25 mA (100 mA per gr of carbon) constant current discharge/charge with 2.65 and 3 V voltage cutoff. E° based of 2 Li + O₂ ⇌ Li₂O₂ equilibrium at 150°C.

Table 6. Molten Salt Li-O₂ cell characteristics: e^-/O_2 and OER/ORR ratios. Analysis done on 1st cycle in (Li/K)NO₃ melt cycling at 150°C.

O ₂ cathode	Super P carbon	B-doped CNT
e^-/O_2 discharge	1.99	2.02
e^-/O_2 charge	2.12	2.37
OER/ORR	0.730	0.491

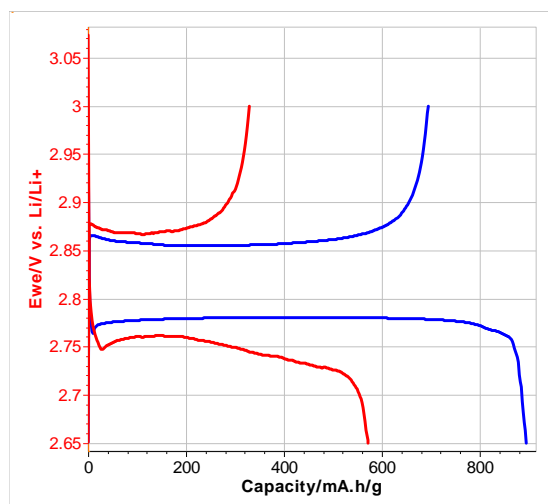


Figure 88. Voltage profile comparison between (a) B-doped CNT cathode and (b) Super P carbon cathode. T=150°C in LiNO₃-KNO₃ eutectic. 100 mA per gr of carbon constant current discharge/charge with 2.65 and 3 V voltage cutoff. C loading ~4 mg/cm²

A Li₂O₂ titration developed for nonaqueous Li-air batteries was employed to study quantitative yield of Li₂O₂ during discharge in the molten eutectic nitrate salts. The titration is accomplished by extracting discharged cathodes from batteries, immersing them in ultrapure water, and titrating formed H₂O₂. An implicit assumption, bolstered by numerous control studies, in our yield calculation for nonaqueous Li-O₂ batteries is that Li₂O₂ formed during discharge forms a stoichiometric equivalent of H₂O₂ when immersed in water. It is found instead that high concentrations of LiNO₃ in solution, which are necessarily transferred to the aqueous phase by nitrates left in the cathode after extraction, form a complex peroxide/nitrate/nitrite equilibrium that results in lower calculated Li₂O₂ yields than is physically possible given more reliable *in situ* O₂ consumption/evolution measurements. We are working to understand this equilibrium and hope to be able to apply an appropriate correction factor to our titrations that will accurately predict the Li₂O₂ yield from molten nitrate cells in the future. Meanwhile, e^-/O_2 and OER/ORR molar ratios were determined using pressure analysis and electrochemical mass spectrometry (Figure 87 and Table 6). Results indicate that B-doped CNTs behave poorly in the molten Li-O₂ system. Consistent with low OER/ORR ratio, voltage profile for B-doped CNT cathode shows poor Coulombic efficiency (~55%) and greater voltage hysteresis (Figure 88a) compared to Super P. This study will be extended to other types of carbon materials such as boron-doped diamond, graphitic carbons, Vulcan XC 72R carbon black, and B-doped CNTs with various degrees of doping. Based on e^-/O_2 , OER/ORR, and electrochemical performance (Coulombic efficiency, voltage hysteresis, and discharge capacity), Super P carbon remains the best candidate. OER/ORR<1 is consistent with build-up of Li₂CO₃ in these cells, and non-carbonaceous O₂ cathode materials are being tested to understand the origin of Li₂CO₃ side product formation.

Patents/Publications/Presentations

Presentation: Annual Merit Review in Arlington, Virginia (June 2015); Vincent Giordani.

Task 9.3 – Li-Air Batteries (Khalil Amine, ANL)

Project Objective. The project objectives are as follows:

- Develop new cathode materials and electrolytes for lithium-air batteries for long cycle life, high capacity, and high efficiency.
- Use state-of-the-art characterization techniques to understand the charge and discharge chemistries.
- Use state-of-the-art computational methodologies to understand and design new materials and electrolytes for Li-air batteries.

Project Impact. This project anticipates the following impacts:

- New electrolytes that are stable and increase cycle life.
- New cathode materials that increase cycle life and reduce overpotentials.
- Increased cycle life.

Out-Year Goals. The out-year goals of this work are to find catalysts that promote discharge product morphologies that reduce charge potentials and to find electrolytes for long cycle life through testing and design.

Collaborations. This project engages in collaboration with Professor Yang-Kook Sun at Hanyang University, and Professor Yiying Wu at Ohio State University.

Milestones

1. Characterize stability of the LiO_2 component of the activated carbon cathode using Raman techniques. Use DFT calculations to model the stability of the LiO_2 component of the activated carbon cathode to explain the Raman results. (12/31/2014 – Complete)
2. Investigate the role of impurities in the performance of activated carbon and how they can promote the formation and stability of LiO_2 and reduce charge overpotentials. Use DFT calculations to help understand how the impurities affect the morphologies. (3/31/2015 – Complete)
3. Investigate addition of metal nanoparticle catalysts to high surface area carbons such as reduced graphene oxides to promote growth of morphologies with higher LiO_2 contents to reduce charge overpotentials. Use DFT calculations to model the nanoparticle catalysts. (6/30/2015 – Ongoing)
4. Use one of the metal catalyst/carbon systems with good performance to start investigations of how electrolytes can be used to improve the performance (cycle life) of the Li-air battery. Use DFT calculations to help design new electrolytes for the Li-air batteries. (9/30/2015 – Ongoing)

Progress Report

Although lithium-oxygen batteries are attracting considerable attention because of potential for extremely high energy density, their practical use has been restricted due to low energy efficiency and poor cycle life compared to lithium-ion batteries. A nanostructured cathode based on molybdenum carbide nanoparticles (Mo_2C) dispersed on carbon nanotubes has been found to dramatically increase the electrical efficiency up to 88% and cycle life. It is found that the Mo_2C nanoparticle catalyst contributes to the formation of a well-dispersed lithium peroxide nanolayers (Li_2O_2) on the Mo_2C /carbon nanotubes with large contact area during oxygen reduction reaction (ORR). This Li_2O_2 structure can be decomposed at low potential upon oxygen evolution reaction (OER) by avoiding the energy loss associated with the decomposition of the typical Li_2O_2 discharge products due to its nanostructure.

The origin of the effectiveness of Mo_2C /carbon nanotube as a cathode in $\text{Li}-\text{O}_2$ batteries was investigated by DFT calculations. From DFT calculations, we found that the O_2 molecules tend to be reduced on Mo_2C (001) and (101) surfaces that are dominant on the Wulff shape of Mo_2C nanoparticles. For the two low-energy Mo-terminated equivalent surfaces [that is, (001)-Mo and (101)-Mo surfaces], the chemisorption of O_2 on the surfaces is exothermic. At both (001)-Mo and (101)-Mo surfaces, the decomposition of the O-O bond of chemisorbed O_2 molecules is exothermic and oxidizes the surface by forming new Mo-O bonds. For a near fully oxidized Mo_2C (101)-Mo surface, the top surface is dominated by the Mo-O bonds analogous to a MoO_3 bulk like layer shown in Figure 89. As shown in Figure 89, the surface chemistry and electronic properties of the oxidized Mo_2C are mainly dictated by the Mo 3d electronic states. The original metallic-like Mo_2C surface remains even after the surface is significantly oxidized.

For verification of the DFT predictions, XPS data were collected on a Mo_2C /carbon nanotube. It is found the surface of the as-received Mo_2C powder tends to be oxidized. Some MoO_2 is also present in the XPS data. To complement the surface-sensitive XPS data, the bulk-sensitive XRD data shows that the MoO_3 -like feature in the cathode is not a layered orthorhombic crystalline MoO_3 bulk, but rather a noncrystalline amorphous phase that is formed on the surface of the Mo_2C nanoparticles as a thin layer. From DFT calculations, the layered crystalline MoO_3 bulk is insulating (band gap ~ 2 eV), whereas the noncrystalline amorphous phase of MoO_3 bulk is metallic. Thus, we suspect that the formation of metallic noncrystalline MoO_3 -like layers on the Mo_2C nanoparticles along with the carbon nanotubes are good electrocatalysts and are responsible for the low charge overpotentials found for their use in $\text{Li}-\text{O}_2$ batteries.

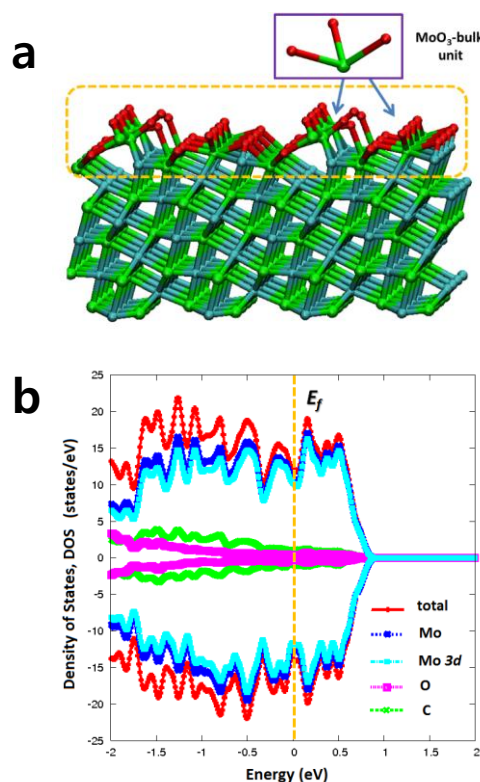


Figure 89. Results of DFT calculations: (a) The oxidized Mo_2C (101)-Mo surface with a MoO_3 -like portion (the highlighted region shows a MoO_3 -bulk unit-like configuration in the inset) on top surface layer after the adsorbed O_2 molecules dissociate. (b) The electronic density of states (e-DOS) around the Fermi-level (E_f). The light-blue region is the Mo 3d projected e-DOS that dominate the e-DOS around the Fermi-level.

Patents/Publications/Presentations

Kwak, Won-Jin, and Kah Chun Lau, Chang-Dae Shin, Khalil Amine, Larry A. Curtiss, and Yang-Kook Sun. “A Mo₂C/Carbon Nanotube Composite Cathode for Lithium–Oxygen Batteries with High Energy Efficiency and Long Cycle Life.” *ACS Nano* 9, no. 4 (2015): 4129–4137, DOI: 10.1021/acsnano.5b00267.

Task 9.4 – Overcome the Obstacles for the Rechargeable Li-air Batteries (Deyang Qu, University of Massachusetts – Boston; and Xiao-Qing Yang, Brookhaven National Laboratory)

Project Objective. The primary objective is to investigate the root causes of the major obstacles of the air cathode in the Li-air batteries, which impede the realization of high energy, high power, long cycle life Li-air batteries, and understand the mechanisms of such barriers and eventually overcome those obstacles. In this objective, special attention will be paid to the investigation of high surface carbon material use in the gas diffusion electrode (GDE), establishment of 2-phase interface on the GDE, catalysts, electrolyte and additives stable in Li-air system and with capability to dissolve Li oxide and peroxide. The electrolyte investigation and development will involve close collaboration with Brookhaven National Laboratory. The secondary objective is to engineer design of a Li-air battery with high energy, high rate, long cycle life, and high round-trip efficiency; special attention will be paid to Li-air flow cell.

Project Impact. Li-air chemistry represents the highest energy density among chemical energy systems. The successful implementation of the technology in the electric vehicles would not only reduce the cost of electrochemical energy storage system, but also provide long driving distance per charge by significantly increasing energy density. The attributes would enable cost effective market entry of electric vehicles for U.S. automakers.

One-Year Goals. The project research will focus on fundamental mechanisms of oxygen reduction in nonaqueous electrolytes and the re-oxidization of the soluble boron-peroxide complex; multiple boron complexes will be synthesized in BNL and tested in UMB. The impact of carbon surface structure on the O₂ reduction will be investigated. The unique flow-cell design will be further optimized by means of the inclusion of boron additives.

Collaborations. Principal investigator Deyang Qu is the Johnson Control Endowed Chair Professor; the UWM and BNL team closely collaborates with Johnson Control scientists and engineers. The collaboration enables the team to validate outcomes of fundamental research in pilot-scale cells. This team has been working closely with top scientists on new material synthesis at ANL, LBNL, and PNNL, with U.S. industrial collaborators at General Motors, Duracell, and Johnson Control. The team also works with international collaborators in Japan and South Korea. These collaborations will be strengthened and expanded to give this project a vision on both today's state-of-the-art technology and tomorrow's technology, with feedback from the material designer and synthesizers upstream as well as industrial end users downstream.

Milestones

1. Complete the studies of the impact of carbon surface structure on the O₂ reduction. (December 2014 – Complete)
2. Complete the kinetics studies of catalytic disproportionation of superoxide (determination of reaction order and reaction constant). (March 2015 – Complete)
3. Complete the test of the Li-air flow cell. (June 15 – Complete)
4. Complete *in situ* electrochemical study for the oxygen reduction in various boron additives. (September 2015 – In progress)

Progress Report

This quarter, the solvent effects on the oxygen reduction and evolution in nonaqueous electrolyte with Li salts was further investigated. The last report shows that solvation of Li cations with different solvent molecules would change the Lewis acidity of Li ions, thus having an impact on the redox reaction of O_2 . This quarter, the preferential solvation of Li^+ cations and the relative strength of interaction were determined. Not only does the solvation preference of Li^+ vary with different solvents, but also the solvent molecules in the solvation shell alter the Lewis acidity of the solvated Li^+ ions. The Li^+ exhibits low acidity if it is solvated with the solvent molecules that have a high strength of interaction with Li^+ . The differences in the acidity for the solvated Li^+ ions were demonstrated through the catalytic disproportionation of the O_2^- formed during the reduction of O_2 in the corresponding electrolyte.

Table 7. The relative strength of integration between Li ion and various solvents against DMSO.

Daughter ion	Relative Abundance	Daughter ion	Relative Abundance
$[DMSO+Li]^+$	100	$[Py+Li]^+$	3.6
$[DMSO+Li]^+$	100	$[ACN+Li]^+$	2.3
$[DMSO+Li]^+$	30.1	$[DME+Li]^+$	100
$[DMSO+Li]^+$	0.1	$[DMDME+Li]^+$	100
$[DMSO+Li]^+$	100	$[EC+Li]^+$	6.2
$[DMSO+Li]^+$	100	$[PC+Li]^+$	5.7
$[DMSO+Li]^+$	100	$[DMC+Li]^+$	6.2
$[DMSO+Li]^+$	100	$[DEC+Li]^+$	9.6
$[DMSO+Li]^+$	100	$[DMF+Li]^+$	51.6
$[DMSO+Li]^+$	100	$[GBL+Li]^+$	8.0
$[DMSO+Li]^+$	94	$[DMSO^{d6}+Li]^+$	100

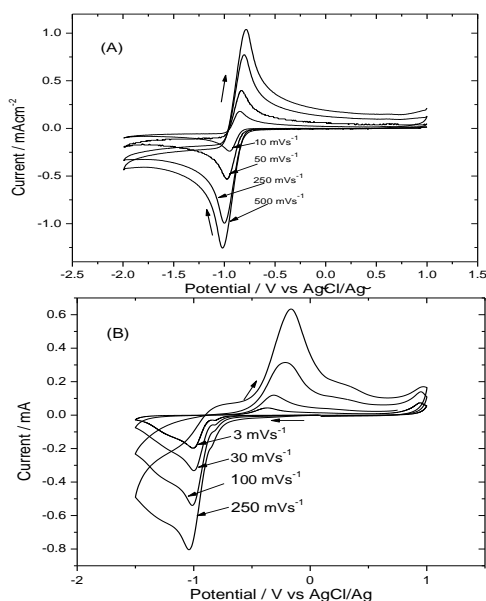


Figure 90. Cyclic voltammograms at various scan rates in 1 M TEABF₄ DMSO electrolyte (A) and 1 M LiBF₄ DMSO electrolyte (B) saturated with O_2 on a glassy carbon-disc electrode.

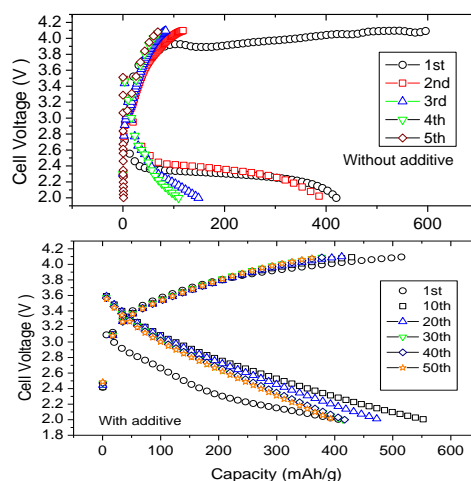


Figure 91. First 50 cycles for a Li-air flow cell with and without B additive.

The impact of the additive of strong boron based Lewis acid in combination with the flow cell design was further investigated. A lab flow cell was made and the preliminary tests of cycling were done. The results are shown in Figure 91. Clearly, the capacity of the cell without the additive decreased very rapidly while the efficiency was low; both the capacity and efficiency improved significantly when the additive was added. We believe the strong Lewis acid additive, on one hand, accelerate the superoxide disproportionation rate which minimized its chemical interaction with the electrolyte; one the other hand, make the Li_2O_2 more soluble which delayed the cathode passivation due to solid precipitation.

Patents/Publications/Presentations

Zheng, Dong, and Xuran Zhang, Deyu Qu, Xiao-Qing Yang, Hung-Sui Lee, and Deyang Qu. “Investigation of the Electrocatalytic Oxygen Reduction and Evolution Reactions in Lithium-Oxygen Batteries.” *J. Power Sources* 288 (2015):9-12.

TASK 10 – NA-ION BATTERIES

Summary and Highlights

To meet the challenges of powering the PHEV, the next generation of rechargeable battery systems with higher energy and power density, lower cost, better safety characteristics, and longer calendar and cycle life (beyond lithium-ion batteries, which represent today's state-of-the-art technology) must be developed. Recently, Na-ion battery systems have attracted increasing attention due to the more abundant and less expensive nature of the Na resource. The issue is not insufficient lithium on a global scale, but what fraction can be used in an economically effective manner. Most untapped lithium reserves occur in remote or politically sensitive areas. Scale-up will require a long lead time, involve heavy capital investment in mining, and may require the extraction and processing of lower quality resources, which could drive extraction costs higher. Currently, high costs remain a critical barrier to the widespread scale-up of battery energy storage. Recent computational studies on voltage, stability, and diffusion barriers of Na-ion and Li-ion materials indicate that Na-ion systems can be competitive with Li-ion systems.

The primary barriers and limitations of current state-of-the-art of Na-ion systems are as follows:

- Building a sodium battery requires redesigning battery technology to accommodate the chemical reactivity and larger size of sodium ions.
- Lithium batteries pack more energy than sodium batteries per unit mass. Therefore, for sodium batteries to reach energy densities similar to lithium batteries, the positive electrodes in the sodium battery need to hold more ions.
- Since Na-ion batteries are an emerging technology, new materials to enable Na electrochemistry and the discovery of new redox couples along with the diagnostic studies of these new materials and redox couples are quite important.
- In sodium electrochemical systems, the greatest technical hurdles to overcome are the lack of high-performance electrode and electrolyte materials that are easy to synthesize, safe, and non-toxic, with long calendar and cycling life and low cost.
- Furthermore, fundamental scientific questions need to be elucidated, including (1) the difference in transport and kinetic behaviors between Na and Li in analogous electrodes; (2) Na insertion/extraction mechanism; (3) solid electrolyte interphase (SEI) layer on the electrodes from different electrolyte systems; and (4) charge transfer in the electrolyte–electrode interface and Na⁺ ion transport through the SEI layer.

This task will use the synchrotron based *in situ* x-ray techniques and other diagnostic tools to evaluate new materials and redox couples, to explore fundamental understanding of the mechanisms governing the performance of these materials and provide guidance for new material developments. This task will also be focused on developing advanced diagnostic characterization techniques to investigate these issues, providing solutions and guidance for the problems. The synchrotron based *in situ* x-ray techniques (x-ray diffraction and hard and soft x-ray absorption) will be combined with other imaging and spectroscopic tools such as high resolution transmission electron microscopy (HRTEM), mass spectroscopy (MS), and transmission x-ray microscopy (TXM).

Task 10.1 – Exploratory Studies of Novel Sodium-Ion Battery Systems (Xiao-Qing Yang and Xiqian Yu, Brookhaven National Laboratory)

Project Objective: The primary objective of this proposed project is to develop new advanced *in situ* material characterization techniques and to apply these techniques to explore the potentials, challenges, and feasibility of new rechargeable battery systems beyond the lithium-ion batteries (LIBs), namely the sodium-ion battery systems for plug-in hybrid electric vehicles (PHEV). To meet the challenges of powering the PHEV, new rechargeable battery systems with high energy and power density, low cost, good abuse tolerance, and long calendar and cycle life must be developed. This project will use the synchrotron based *in situ* x-ray diagnostic tools developed at BNL to evaluate the new materials and redox couples, exploring the fundamental understanding of the mechanisms governing the performance of these materials.

Project Impact. The Multi Year Program Plan (MYPP) of Vehicle Technology Program (VTP) describes the goals for battery: “Specifically, lower-cost, abuse-tolerant batteries with higher energy density, higher power, better low-temperature operation, and longer lifetimes are needed for the development of the next-generation of HEVs, PHEVs, and EVs.” If this project succeeds, the knowledge gained from diagnostic studies and collaborations with U.S. industries and international research institutions will help U.S. industries develop new materials and processes for a new generation of rechargeable battery systems beyond lithium-ion batteries, such as Na-ion battery systems in their efforts to reach these VTP goals.

Approach. This project will use the synchrotron based *in situ* x-ray diagnostic tools developed at BNL to evaluate the new materials and redox couples to enable a fundamental understanding of the mechanisms governing the performance of these materials and to provide guidance for new material and new technology development regarding Na-ion battery systems.

Out-Year Goals. Complete the *in situ* x-ray diffraction and absorption studies of sodium iron ferrocyanide (Prussian Blue Analogous) as cathode materials for Na-ion batteries during charge-discharge cycling.

Collaborations. The BNL team has been working closely with top scientists on new material synthesis at ANL, LBNL, and PNNL, with U.S. industrial collaborators at General Motors, Duracell, and Johnson Control along with international collaborators in Japan and South Korea. These collaborations will be strengthened and expanded to give this project a vision on both today’s state-of-the-art technology and tomorrow’s technology being developed, with feedback from the material designer and synthesizers upstream and from industrial end users downstream.

Milestones

1. Complete the particle size effects on kinetic properties of $\text{Li}_4\text{Ti}_5\text{O}_{12}$ as anode materials for Na-ion batteries using synchrotron based *in situ* x-ray diffraction. (December 2014 – Complete)
2. Complete the *in situ* x-ray diffraction studies of sodium iron ferrocyanide (Prussian Blue Analogous) as cathode materials for Na-ion batteries during charge-discharge cycling. (March 2015 – Complete)
3. Complete the *in situ* x-ray diffraction studies of NaCrO_2 during electrochemical chemical de-sodiation. NaCrO_2 is considered as a potential cathode material for Na-ion batteries. (June 2015 – Complete)
4. Complete the x-ray absorption studies of NaCrO_2 at different sodiation levels. (September 2015 – In Progress)

Progress Report

This quarter, the second milestones for FY15 were completed.

BNL has been focused on studies of a new cathode material for sodium-ion batteries. Structure evolution of layered NaCrO_2 cathode for sodium-ion batteries during charge was investigated using synchrotron-based *in situ* x-ray diffraction and *ex-situ* x-ray absorption spectroscopy. Three solid solution phases with expanding 'c' and contracting 'a'/'b' lattice parameters were observed. The coordination changes of Cr and Na during sodium extraction were also studied. Figure 92 shows the *in situ* XRD patterns along with the first charge curve. At the beginning of the charge, (003) peak continuously shifted to the lower two-theta angles, indicating that a solid solution reaction was involved with c-axis expansion. When $x = 0.08$ was reached, a new (003) peak emerged from the left side of the original (003) peak with increasing intensity with further charging. As we know, the (003) peak is a single-fold peak. Thus, every new (003) peak is a fingerprint for the formation of a new phase. In the range of $0.08 < x < 0.2$, two-phase coexistence could be observed. The intensity of (003) peak for the second phase increased with further charging in expense of that for the first one, while the position of (003) peak of the second phase shifted to lower two theta angles. When $x = \sim 0.25$ was reached, the second phase dominated the structure while the first phase disappeared. When $x = 0.3$ was reached, another (003) peak appeared, and the (003) peak of the second phase became broader indicating the formation of the third phase. When $x = 0.4$ was reached, only the third phase could be observed. In the range of $0.4 < 0.48$, the (003) peak of the third phase shifted to lower angles but shifting two theta angle range for the third phase was smaller than the second phase.

The peak at 62.4° in the first pattern corresponds to (110) reflection of the O_3 -type structure. The position changes of this peak represent the structure changes of the *a-b* plane. During charge, the original sharp (110) peak decreased in intensity and became broader and broader in peak shape, indicating some lattice distortion in the *a-b* plane. The (110) peak shifting to the higher two theta angles indicates the contraction of the 'a' and 'b' lattice parameters. Based on the variation of all Bragg peaks, it can be concluded that the structure evolution took place through phase transitions of three solid-solution phases with two two-phase coexistence regions.

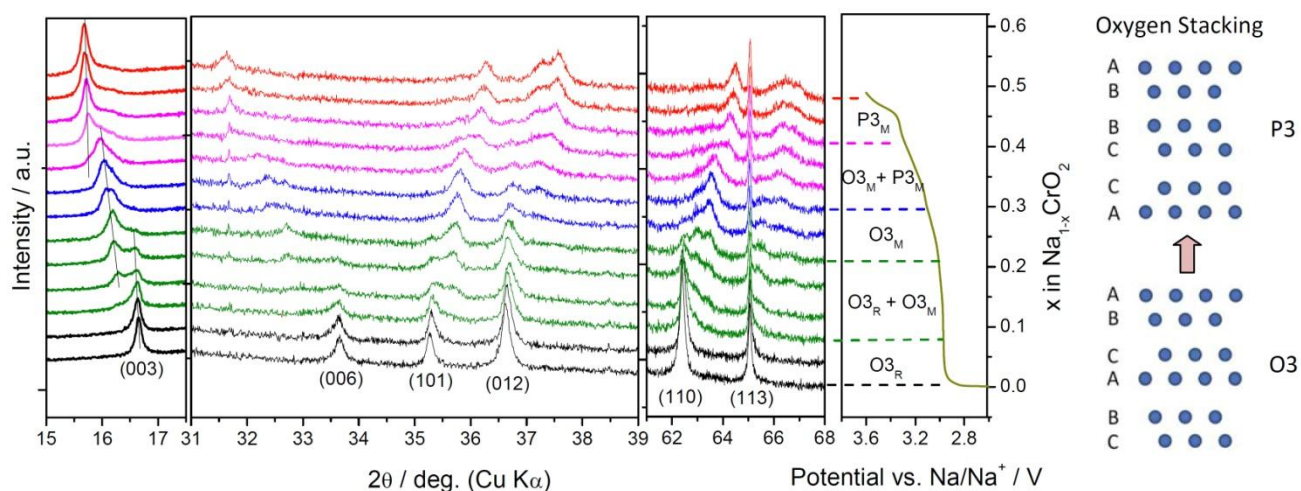


Figure 92. *In situ* x-ray diffraction patterns collected during the first charge (up to 3.6 V at C/12 rate) for a NaCrO_2/Na cell (The 2θ angles are calculated to corresponding angles for $\lambda=1.54 \text{ \AA}$ for $\text{Cu-K}\alpha$ from the real $\lambda=0.7747 \text{ \AA}$ wavelength used for synchrotron XRD experiment). Corresponding voltage-composition profile is given on the right of XRD patterns. Oxygen stacking of O_3 and P_3 structure is given on the right.

Patents/Publications/Presentations

1. Wang, Yuesheng, and Jue Liu, Byungju Lee, Ruimin Qiao, Zhenzhong Yang, Shuyin Xu, Xiqian Yu, et al. “Ti-substituted tunnel-type $\text{Na}_{0.44}\text{MnO}_2$ oxide as a negative electrode for aqueous sodium-ion batteries.” *Nature Communications* 6 (2015).
2. Presentation at the MRS 2015 Spring Meeting, San Francisco (April 8, 2015): “Synchrotron-Based X-Ray Characterization on the Thermal Decomposition Mechanism of Charged Cathode Materials for Na-Ion Batteries”; Seongmin Bak, Enyuan Hu, Yongning Zhou, Xiqian Yu, Xiao-Qing Yang,* and Kyung-Wan Nam*.